National Defence
Research and Development Branch

Défense nationale
Bureau de recherche et développement

TECHNICAL MEMORANDUM 97/203
November 1996

VALIDATION OF SHIPMO7 AND PRECAL WITH A WARSHIP MODEL

Dann L. Chow — Kevin A. McTaggart

Defence Research Establisnment Atlantic

Centre de Recherches pour la Défense Atlantique

Canada

DEFENCE RESEARCH ESTABLISHMENT ATLANTIC

9 GROVE STREET
P.O. BOX 1012
DARTMOUTH, N.S.
B2Y 3Z7

TELEPHONE
(902) 426-3100

CENTRE DE RECHERCHES POUR LA DÉFENSE ATLANTIQUE

9 GROVE STREET
C.P. BOX 1012
DARTMOUTH, N.É.
B2Y 3Z7

National Defence
Research and Development Branch

Défense nationale
Bureau de recherche et développement

VALIDATION OF SHIPMO7 AND PRECAL WITH A WARSHIP MODEL

Dann L. Chow — Kevin A. McTaggart

November 1996

Approved by R.W. Graham: _____
Head/Hydronautics Section

TECHNICAL MEMORANDUM 97/203

Defence Research Establishment Atlantic

Centre de Recherches pour la Défense Atlantique

Canada

Abstract

This technical memorandum describes a validation study of SHIPMO7 and PRECAL, two frequency domain codes for predicting ship motions and sea loads in waves. SHIPMO7 is a strip theory code while PRECAL is a three-dimensional panel code. Results from the two codes are compared with non-proprietary experimental data for a warship model. In general, SHIPMO7 gives good agreement with motions and sea loads, while PRECAL is slightly inferior. The consistently better results for SHIPMO7 in the lateral plane are likely due to its careful treatment of appendage and viscous forces. Neglecting rudder autopilot motions does not appear to influence significantly predictions from either code. A proposed approximate method for predicting sectional gyradii leads to satisfactory predictions of torsional moment.

Résumé

Cette note technique décrit une étude de validation de SHIPMO7 et de PRECAL, deux codes du domaine des fréquences pour prédire les mouvements des navires et les chargements hydrodynamiques dans les vagues. SHIPMO7 est un code de la théorie des bandes alors que PRECAL est un code de facettes tridimensionnel. Les résultats des deux codes sont comparés à des expériences non brevetées avec un modèle pour navires de guerre. En général, le SHIPMO7 correspond bien aux mouvements et aux chargments hydrodynamiques, alors que le PRECAL est légèrement inférieur. Les résultats du SHIPMO7 sont toujours meilleurs dans le plan latéral à cause de la prise en compte détaillée des appendices et des efforts visqueux. L'absense de prise en compte des mouvements du gouvernail ne semble pas influer de façon importante sur les prédictions du SHIPMO7 et du PRECAL. On propose une méthode approximative de prédiction des rayons de giration des sections que permet de prédire de façon satisfaisante le moment de torsion.

DREA TM/97/203

VALIDATION OF SHIPMO7 AND PRECAL WITH A WARSHIP MODEL

by

Dann Chow and Kevin McTaggart

EXECUTIVE SUMMARY

Introduction

SHIPMO7, the latest version of DREA's strip theory ship motion program, can now predict sea loads, including forces from appendages. PRECAL, which has been developed by the Cooperative Research Ships organization, is another tool available to DND for predicting ship motions and sea loads. Because PRECAL is a fully three-dimensional code, it should give more accurate results than the strip theory code SHIPMO, particularly for low L/B hull forms. This technical memorandum compares motion and load predictions for SHIPMO7 and PRECAL with experimental data for a warship model. Because the experimental data are non-proprietary, DND is able to distribute this validation study to other organizations considering using SHIPMO7 or PRECAL. The present validation study was an integral part of the SHIPMO7 development process, and helped to ensure proper implementation of the underlying theory.

Principal Results

Both SHIPMO7 and PRECAL give generally good motion and sea load predictions for the warship model. As expected, vertical plane predictions are better than lateral plane predictions and motion predictions are better than sea load predictions. Despite the limitations of strip theory, SHIPMO7 gives better results than PRECAL, particularly for lateral plane motions and sea loads. Problems with PRECAL roll damping predictions required that roll damping coefficients from SHIPMO7 be used as input for PRECAL. Torsion predictions differ significantly between SHIPMO7 and PRECAL because PRECAL assumes constant metacentric height for all ship sections while SHIPMO7 correctly considers the longitudinal variation of roll restoring forces. It appears that neglecting rudder motions does not introduce significant errors to motion and load predictions. A proposed method for approximating sectional roll gyradii gives consistency between motion and load roll inertial properties and leads to satisfactory torsion predictions.

Significance of Results

SHIPMO7 motion and sea load predictions appear to be sufficiently accurate for design of naval frigates. PRECAL, which requires significantly greater computational resources because it is fully three-dimensional, gives accuracy similar to SHIPMO in the vertical plane but is less accurate in the lateral plane. The present version of PRECAL does not correctly predict roll damping; thus, the user must provide roll damping coefficients as input. For slender ships such as narrow stern naval frigates, the only advantage of PRECAL relative to SHIPMO7 is that it can provide hull pressures.

Future Plans

It is recommended that DND adopt SHIPMO7 for predictions of motions and sea loads in ship design. If hull hydrodynamic pressures are required or a low L/B hull form is under consideration, then PRECAL should be used. Hopefully, future versions of PRECAL will be able to predict roll damping satisfactorily. The proposed method for approximating sectional roll gyradii will likely be used for predicting torsional loads on DND ships.

Contents

Notation

a	wave amplitude
AP	aft perpendicular
B	beam
CG	center of gravity
Fn	Froude number
FP	forward perpendicular
g	gravitational acceleration
I_{xx}	roll moment of inertia for entire vessel
I_{xx-i}	roll moment of inertia of section i (about local CG)
k_r	proportionality constant for calculating sectional roll gyradii
$\overline{KG}$	vertical location of centre of gravity (above baseline)
L	ship length between perpendiculars
l_i	length of section i
m_i	mass of section i
N_s	number of ship sections
r_{xx}	roll radius of gyration
r_{xx-i}	roll radius of gyration of section i (about local CG)
V_i	load amplitude for mode i
z_i	height of CG of section i above ship CG
β_s	incident sea direction (relative to ship speed)
ζ_i	motion amplitude for mode i
λ	wavelength
ρ	water density
ω	wave frequency
ω_e	encounter frequency
$\triangle$	ship mass displacement

1 Introduction

The ability to predict ship responses at sea accurately is a problem of great interest to naval architects. This report describes a validation study of the ship motions and sea loads of a warship model predicted by two codes, SHIPMO7 and PRECAL. The warship model was developed by Lloyd et al. [1, 2] and tested at Admiralty Marine Technology Establishment, Haslar. Experiments were conducted in regular waves at two ship speeds and seven headings. SHIPMO7 is an updated version of DREA's ship motion code SHIPMO [3], a strip theory program suitable for evaluating seakeeping of slender ships in moderate seas. PRECAL is a suite of programs developed through the Netherlands Ship Model Basin (NSMB) Cooperative Research Ships (CRS) PRECAL Working Group and is based on three-dimensional panel theory. Both programs are designed to predict ship motions in regular waves, and in uni-directional and multi-directional irregular seas.

Validation studies of previous SHIPMO versions have shown that predictions for ship motions are in good agreement with experimental data, whereas predictions for sea loads are generally not as accurate [4, 5]. It was postulated that the new version of SHIPMO could give superior load predictions if all forces acting on the ship were treated consistently for both motion and load calculations. The present validation study was done concurrently with the development of SHIPMO7 to ensure correct implementation of load predictions.

This report begins by providing a description of SHIPMO7 and PRECAL and their capabilities. A brief discussion of their theoretical backgrounds and code designs is also included. A short description of the warship experiments is provided, followed by a discussion of relevant inputs for SHIPMO7 and PRECAL. Finally, comparisons of the predictions with the experimental data are presented, accompanied by an analysis of the results and conclusions based on this validation study.

2 SHIPMO7 Strip Theory Program

SHIPMO7 is the newest version of DREA's ship motion program SHIPMO, a strip theory program that is suitable for evaluating seakeeping of slender ships in moderate seas. SHIPMO predicts ship motions for six degrees of freedom, in both regular and irregular waves. From responses for the six basis degrees of freedom, SHIPMO can calculate sea loads, local accelerations, slamming, deck wetness, ship-referenced forces, and motion-induced interruptions. The main advantages of SHIPMO relative to many other seakeeping codes are its relatively simple input specification, fast computational time, and robustness.

SHIPMO is a typical frequency domain strip theory code, and is based largely on the theory of Salvesen, Tuck, and Faltinsen [6]. In addition to this linear potential theory basis, SHIPMO includes extensions described by Schmitke [7] to include viscous roll damping and the effects of ship appendages. The program is expected to give reliable results within the limitations of strip theory, that is for slender ships ($L/B > 4$) operating in moderate sea conditions (e.g. up to sea state 7 for naval frigates) [3].

Strip theory requires the user to divide the ship into a large number of two-dimensional sections in the vertical $y - z$ plane (i.e. a large number of "strips"). The potential flow around each section is determined. Velocity potentials and hydrodynamic coefficients are then calculated for each section and integrated along the ship length to obtain hydrodynamic coefficients for

the entire ship. Using computed hydrodynamic forces, SHIPMO computes motions in regular waves. For lateral plane motions, an iterative process is used to determine amplitude-dependent roll damping and the subsequent ship responses. After motions in regular waves are computed, SHIPMO can compute motions in irregular seas using linear superposition.

SHIPMO7 introduces several features that were either not present in the previous versions or have been significantly improved [3]:

1. elimination of irregular frequencies,
2. consistent integration of forces for motion and load predictions,
3. inclusion of all appendage and viscous forces in load predictions,
4. prediction of added resistance in waves.

The resulting code appears to be sufficiently robust for routine engineering computations.

3 PRECAL Program Suite

PRECAL is a suite of programs that predict motions, sea loads, and the pressure distribution on a ship hull in waves. The programs were developed through three CRS Working Groups and are intended to be suitable for most ship types. The three core programs of PRECAL that were used in this validation study are as follows:

- HYDMES: generates the hydrodynamic mesh and calculates the hydrostatic and mass inertia terms.
- HYDCAL: calculates the velocity potentials, source strengths, and flow velocities for the hydrodynamic mesh.
- RESCAL: determines the global ship motion responses and resulting sea loads.

A program to post-process RESCAL results for use in finite element meshes is available but was not required for this study. For further details concerning PRECAL's code design and theory, consult References 8 and 9.

Although similar to SHIPMO7, PRECAL predictions are based on three-dimensional panel theory rather than two-dimensional strip theory. For this reason, it was expected that PRECAL predictions for ship loads would demonstrate slightly better agreement with experimental results than SHIPMO7.

PRECAL allows the user to choose either the zero-speed Green function or the forward-speed Green function for use in its analysis. In this validation study, the less complicated and more computationally stable [10, 11] zero-speed Green function is used throughout. In addition, the automatic panel generation option that PRECAL offers is also used.

The current CRS-distributed version of PRECAL (version 1.0) still contains several coding problems. Only one of these errors affects this study directly. The roll damping contributed by fin lift forces, eddy damping, and viscous hull effects are not calculated accurately. To circumvent this problem, roll damping coefficients calculated by SHIPMO7 were used as input for the RESCAL response calculation program.

4 Description of Model and Experiments

The experiments reported by Lloyd et al. are perhaps the most comprehensive set of non-proprietary data for ship motions and sea loads in regular waves. To assist with validation of seakeeping codes, References 1 and 2 include complete descriptions of the warship model and experimental conditions.

The warship model is representative of a typical narrow stern naval destroyer. The model was constructed using four segments that were joined at stations 5, 10, and 13 (SHIPMO convention, described below). Strain gauge dynamometers were attached at the segment joints to measure the loads acting on the ship. Motions were measured with accelerometers.

All tests were conducted in regular waves at a wave steepness (wave height/wavelength) of 1/50 at wave headings of 0, 30, 60, 90, 120, 150, and 180 degrees, where 180 degrees represents head seas. The tests were conducted at nominal Froude numbers of 0.21 and 0.29 based on power in calm water, with actual speeds in waves estimated to be within 10 percent of the nominal values. A full set of experimental results exists for the lower ship speed, but some cases for the higher speed were not completed.

5 Ship Input Parameters for SHIPMO7 and PRECAL

It is essential that the input parameters describing the warship model are accurate in order to present a valid comparison between the ship motion and sea load predictions and the experimental results. Among the most vital of these parameters are the mass distribution and the sectional roll properties. Sample input files are presented in Appendix A for SHIPMO and in Appendix B for PRECAL. The PRECAL computations used 160 panels on half the hull surface.

The sectional mass distribution of the warship model is provided by Lloyd et al. (Reference 1, Table II). Although 21 equally-spaced stations are used in References 1 and 2 and in both prediction codes, the station numbering convention varies. Lloyd et al. use stations 1 to 21, with 1 being the FP and 21 being the AP. SHIPMO7 uses stations 0 to 20, with 0 being the FP and 20 being the AP. PRECAL uses stations 0 to 10, and reverses the order by making 0 the AP and 10 the FP. For the current validation study, the sea load analysis is performed at stations 5, 10, and 13 according to the SHIPMO7 convention.

Sectional masses are assumed to be uniformly distributed between mid-stations (e.g., stations 0.5 and 1.5) except at the bow and stern. The mass for station 0 is assumed to be evenly distributed between stations 0 and 0.5, while the mass for station 20 is assumed to be evenly distributed between stations 19.5 and 20. Provisions for bow and stern overhang masses are available in both SHIPMO7 and PRECAL but are not required for the warship model. The resulting sectional mass distribution is shown in Figure 1.

To verify the input sectional mass distribution of Figure 1, masses were evaluated for each of the four warship segments and compared with actual segment masses given in Reference 1. Figure 2 indicates that the computed segment masses are in excellent agreement with the actual values.

For each ship section on a given model segment, the section $\overline{KG}$ value is assumed to be equal to the segment $\overline{KG}$ value. For a section that spans two segments, the section $\overline{KG}$ value is a weighted average. Figure 3 shows the resulting section $\overline{KG}$ values for computations.

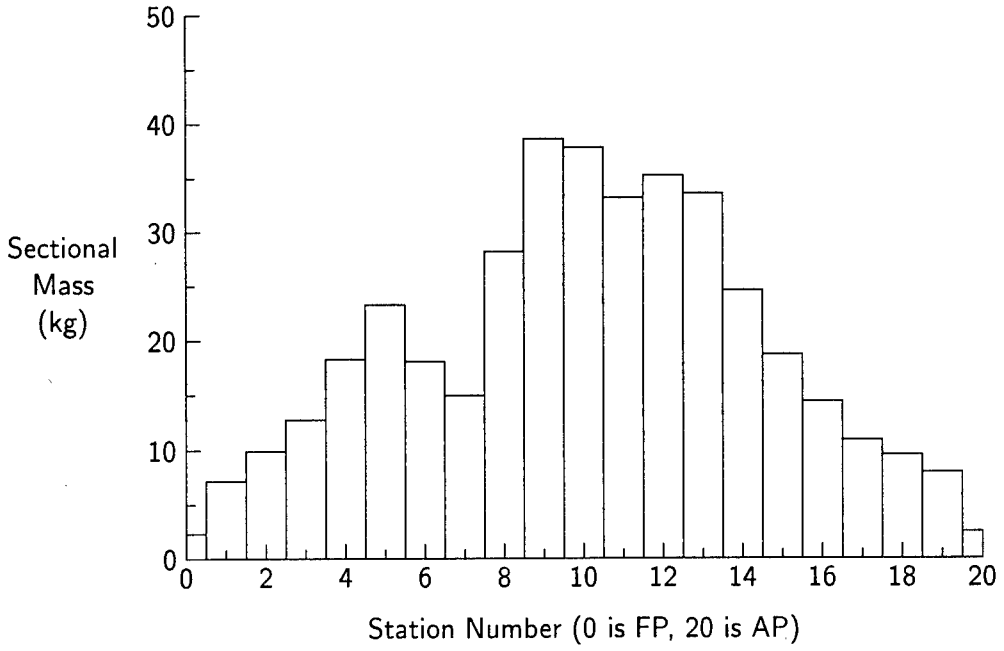

Figure 1: Input Sectional Mass Distribution for Warship Model

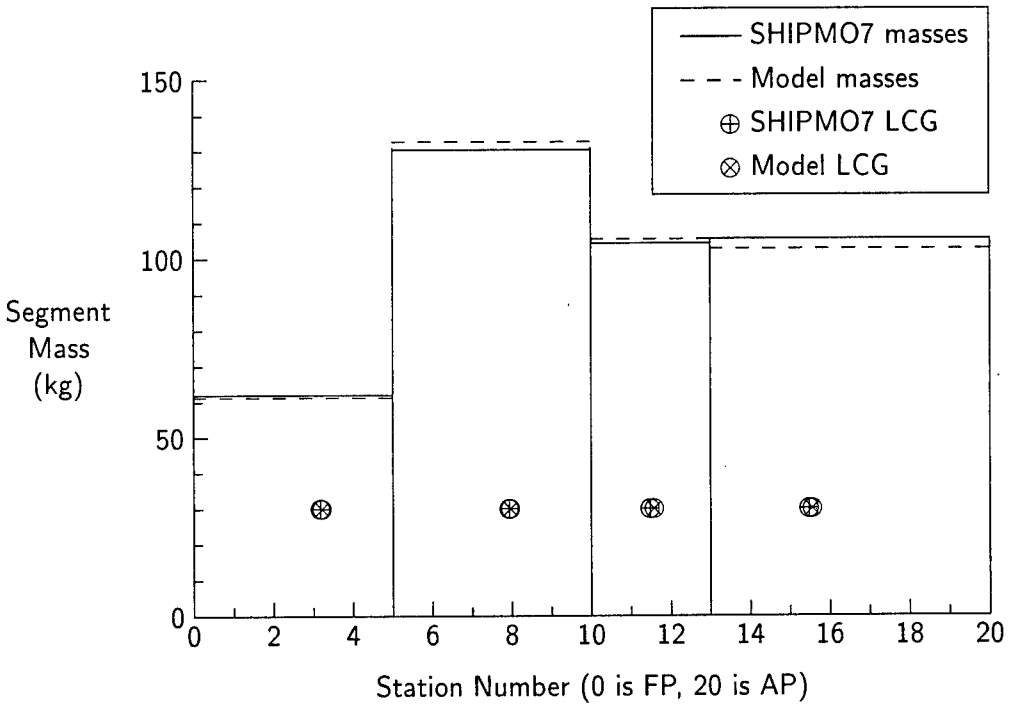

Figure 2: Segment Mass Distribution for Warship Model

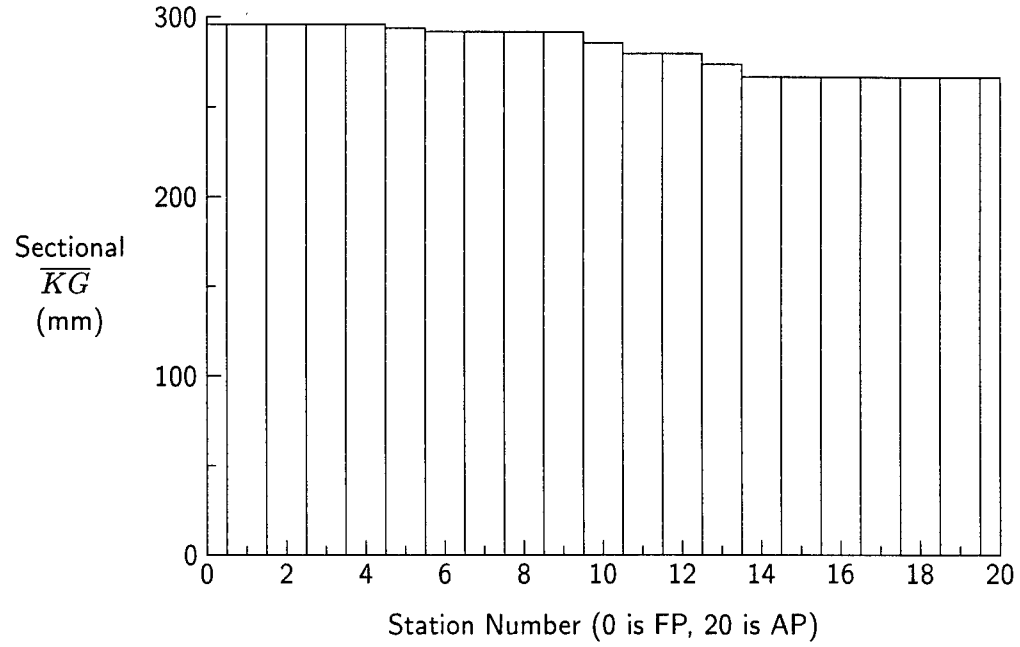

Figure 3: Assumed Sectional $\overline{KG}$ Values for Computations

The warship roll gyradius based on properties of the four model segments is equal to 182 mm; however, Lloyd et al. report that the actual dry ship gyradius based on the model roll natural frequency is 198 mm. They indicate that the value of 182 mm based on the four model segments is likely incorrect because of inaccuracies in the measured gyradii of the segments. Using an input dry gyradius of 198 mm, SHIPMO7 calculates the roll natural frequency at zero speed to be 2.29 rad/s, which is considered to be acceptably close to the value of 2.37 rad/s reported in Reference 1.

For predicting torsional loads, SHIPMO7 and PRECAL required input sectional roll gyradii. The input sectional gyradii must be consistent with the ship roll gyradius used for motion computations. Given the absence of measured sectional gyradii, the following procedure was used to obtain estimates of sectional gyradii that were consistent with the ship gyradius:

1. Calculate roll moment of inertia I_{xx} for the entire vessel using the roll radius of gyration r_{xx} value of 198 mm reported for the entire ship:

$$I_{xx} = \triangle r_{xx}^2 \tag{5.1}$$

2. Assume that the local roll gyradius r_{xx-i} about the sectional CG is directly proportional to the square root of the mass per unit length m_i/l_i of the section. This assumption is based on the premise that the mass for each section can be modelled as a circular cylinder, with density being constant along the entire ship length but with a different radius for each ship section. A single proportionality constant k_r is applicable along the length of the ship.

$$r_{xx-i} = k_r \sqrt{\frac{m_i}{l_i}} \tag{5.2}$$

3. Solve for the proportionality constant k_r. The following equation gives the total roll inertia of the ship:

$$I_{xx} = \sum_{i=1}^{N_s} \left(k_r^2 \frac{m_i}{l_i} + z_i^2 \right) m_i \tag{5.3}$$

where N_s is the number of ship sections and z_i is the sectional CG elevation relative to the ship CG. Using the above equation, the constant k_r is solved as follows:

$$k_r = \sqrt{\frac{I_{xx} - \sum_{i=1}^{N_s} m_i z_i^2}{\sum_{i=1}^{N_s} \frac{m_i^2}{l_i}}} \tag{5.4}$$

4. Compute the sectional roll gyradii using Equation (5.2).

This method provides reasonable estimates of sectional roll gyradii which are consistent with the ship inertia properties.

As mentioned earlier, the current version of PRECAL has problems computing roll damping; thus, roll damping coefficient based on SHIPMO7 calculations were used as input to PRECAL. For each combination of ship speed and heading, SHIPMO7 roll damping coefficients exhibited relatively little variation with wave frequency. Because of the importance of roll damping during roll resonance, the SHIPMO7 roll damping at a wave encounter frequency corresponding to the ship roll natural frequency was considered suitable for all wave frequencies. Further examination of SHIPMO7 roll damping coefficients indicated that roll damping showed little variation with ship heading and could be modelled as a function of only ship speed. The high ship speeds and low roll motion amplitudes of the warship model cause lift forces to dominate roll damping, with the resulting dependence on ship speed. The PRECAL computations use roll damping coefficients of 0.19 and 0.24 for the Froude numbers of 0.21 and 0.29 respectively.

Although the warship model was steered by autopilot during the experiments, it was assumed that rudder deflections were zero in the SHIPMO7 and PRECAL runs because of insufficient data regarding the autopilot properties.

6 Validation Study Results

This section presents the comparison plots between numerical predictions and the experimental results for the warship model. Predictions from SHIPMO7 and PRECAL are shown for every test case, whereas experimental results are shown whenever available. Non-dimensionalized bending moments and shear forces have been multiplied by a factor of 100, except for torsional moment which is multiplied by 1000, as is done in References 1 and 2.

Comparison plots are presented in Appendix C.1 for ship motions and in Appendix C.2 for sea loads. The order of presentation is shown in Table 1. For each speed/heading combination, the following motions and loads were considered: roll, heave, pitch, yaw, vertical bending moment, horizontal bending moment, torsional moment, and vertical shear force. All loads are analyzed at three locations: stations 5, 10 and 13 (SHIPMO convention). Motions and loads which were deemed insignificant by Lloyd et al., such as the roll motion in head and following seas, are not presented. Horizontal shear force, which is significant for oblique seas, was not considered by

Lloyd et al. and is consequently ignored in this study. All motion and load RAOs are presented as a function of wavelength/ship length (λ/L), as is done in References 1 and 2.

Table 1: Presentation Order of Validation Study Results

Motion or Load Type	**Fn**	**Figure Numbers**	**Headings**
Heave	0.21	Figures 4-10	0, 30, 60, 90, 120, 150, 180
	0.29	Figures 11-17	0, 30, 60, 90, 120, 150, 180
Pitch	0.21	Figures 18-23	0, 30, 60, 120, 150, 180
	0.29	Figures 24-29	0, 30, 60, 120, 150, 180
Roll	0.21	Figures 30-34	30, 60, 90, 120, 150
	0.29	Figures 35-39	30, 60, 90, 120, 150
Yaw	0.21	Figures 40-43	30, 60, 120, 150
	0.29	Figures 44-47	30, 60, 120, 150
Vertical Bending Moment	0.21	Figures 48-65	0, 30, 60, 120, 150, 180
	0.29	Figures 66-83	0, 30, 60, 120, 150, 180
Horizontal Bending Moment	0.21	Figures 84-95	30, 60, 120, 150
	0.29	Figures 96-107	30, 60, 120, 150
Torsional Moment	0.21	Figures 108-122	30, 60, 90, 120, 150
	0.29	Figures 123-137	30, 60, 90, 120, 150
Vertical Shear Force	0.21	Figures 138-158	0, 30, 60, 120, 150, 180
	0.29	Figures 159-179	0, 30, 60, 120, 150, 180

7 Discussion of Results

When considering the results presented in Appendices C.1 and C.2, it is important to recall the limitations of the input data for the numerical predictions. Because insufficient autopilot data are available, the numerical predictions assume zero rudder deflection. This assumption introduces errors in motion and load predictions for the lateral plane, with the greatest errors likely occurring for yaw motions. Uncertainties related to input sectional gyradii introduce errors in torsion predictions; however, the input gyradius for the entire ship is considered to be quite accurate and should not degrade roll predictions.

7.1 Ship Motions

The comparisons for heave and pitch motions indicate that both SHIPMO7 and PRECAL give very good agreement with the experiments. This result is expected because the relevant input parameters are known to good accuracy and the hydrodynamic forces can be accurately predicted using potential flow theory for the given experimental conditions. In spite of the

limitations of strip theory, SHIPMO7 predictions do not appear to deteriorate at the higher ship speed.

For roll motions, SHIPMO7 gives good predictions even though rudder motions are neglected. PRECAL has a tendency to underpredict roll motions. The superior performance of SHIPMO7 is likely because great development effort has been devoted to prediction of lateral plane forces, including appendage and viscous forces.

For yaw motions, experimental data are available only for a Froude number of 0.21 at headings of 30 and 60 degrees. SHIPMO7 gives good agreement with the experiments even though the autopilot is not modelled. PRECAL appears to underpredict the yaw motions. In Figure 44, PRECAL yaw predictions exhibit an anomaly at $\lambda/L \approx 0.4$ due to a very low encounter frequency. SHIPMO7 uses approximations based on other wavelengths to avoid such anomalies at low encounter frequencies.

7.2 Sea Loads

For vertical bending moment, SHIPMO7 and PRECAL give very good agreement with the experiments, with SHIPMO7 giving somewhat more consistent results. The most striking contrasts between SHIPMO7 and PRECAL predictions occur at a heading of 60 degrees for both Froude numbers, with SHIPMO7 giving good predictions while PRECAL significantly underpredicts bending moments.

Even though the autopilot is not modelled, SHIPMO7 gives good results for horizontal bending moment while PRECAL tends to underpredict. For torsion, SHIPMO7 gives acceptable results, suggesting that the method described in Section 5 gives reasonable values for sectional gyradii. The poor torsion predictions by PRECAL are attributed to its assumption that the metacentric height of each ship section is equal to the ship metacentric height. In contrast, SHIPMO7 correctly considers the variation of sectional metacentric heights along the ship length.

Experimental data for vertical shear are available only for stations 5 and 13 in head seas at a Froude number of 0.21. Based on these two cases, SHIPMO7 appears to give good results while PRECAL underpredicts vertical shear. At a Froude number of 0.29 and heading of 60 degrees, SHIPMO predictions in Figures 166 and 167 are unexpectedly high at short wavelengths, while PRECAL predictions appear to be more reasonable. Unfortunately, there are no experimental data available for comparison. The cause of this result is unknown given that the encounter frequency appears to be sufficiently high for good predictions from SHIPMO7 and PRECAL.

8 Conclusions

Both SHIPMO7 and PRECAL give generally good motion and sea load predictions for the warship model. As expected, vertical plane predictions tend to be better than lateral plane predictions and motion predictions tend to be better than sea load predictions. Despite the limitations of strip theory, SHIPMO7 gives better results than PRECAL, particularly for lateral plane motions and sea loads. Problems with PRECAL roll damping predictions required that roll damping coefficients from SHIPMO7 be used as input for PRECAL. It appears that the neglect of rudder motions does not introduce significant errors to motion and load predictions. A proposed method for approximating sectional roll gyradii gives consistency between motion and load roll inertial properties and leads to satisfactory torsion predictions from SHIPMO7. Poor

torsion predictions from PRECAL are likely due to its assumption that sectional metacentric height is constant along the ship length.

A SHIPMO7 Sample Input File

```
Lloyd Warship, offsets, inertia based on mass distribution       <----- Title
METRIC   METRIC  FRESH  SPEEDCOR  NOSWELLCOR  MODAMP  OUTPPR     <----- Options
warship.ppr                                  <----- Post-processing file name
LOAD  NORAW                                  <----- Options
2.2 6.0 0.1                                  <----- Wave frequency min, max, increment
WRITEHY  BOUND2D  LATLONG HVCOR              <----- Hydrodynamic coefficient flags
warship.hy                                   <----- Hydrodynamic coefficient file
1. 16. 0.75                                  <----- Encounter frequency min, max, increment
REGULAR                                      <----- Wave spectrum
7 0.0                                        <----- Number of sea directions, spreading angle
0.  30.  60.  90.  120.  150.  180.          <----- Sea directions
1                                            <----- Number of seaways
0.02                                         <----- Wave steepness
2    3.17 4.38                                <----- Number of speeds, speed array
6.157  0.283  1.355                          <----- Ship length, KG, pitch RG
GMCOMP   DRYROLLRG                           <----- GM and roll RG flags
0.198                                        <----- Dry roll RG
OFFSETS                                      <----- Hull form definition flag
21 21 1. 1.                                  <----- Stations, scaling factors
     0                                       <----- Offset data
     3
 0.000 0.008 0.009
 0.204 0.207 0.233
     1
    11
 0.000 0.010 0.017 0.024 0.029 0.033 0.037 0.041 0.045 0.049 0.053
 0.000 0.000 0.026 0.052 0.078 0.103 0.129 0.155 0.181 0.207 0.233
     2
    11
 0.000 0.014 0.034 0.048 0.059 0.068 0.075 0.081 0.087 0.093 0.100
 0.000 0.000 0.026 0.052 0.078 0.103 0.129 0.155 0.181 0.207 0.233
     3
    11
 0.000 0.017 0.053 0.076 0.093 0.105 0.114 0.123 0.131 0.139 0.147
 0.000 0.000 0.026 0.052 0.078 0.103 0.129 0.155 0.181 0.207 0.233
     4
    11
 0.000 0.019 0.072 0.106 0.127 0.143 0.155 0.166 0.175 0.184 0.192
 0.000 0.000 0.026 0.052 0.078 0.103 0.129 0.155 0.181 0.207 0.233
     5
    11
 0.000 0.021 0.098 0.138 0.163 0.182 0.196 0.207 0.217 0.225 0.233
 0.000 0.000 0.026 0.052 0.078 0.103 0.129 0.155 0.181 0.207 0.233
     6
    11
 0.000 0.023 0.123 0.173 0.201 0.220 0.234 0.245 0.254 0.261 0.267
 0.000 0.000 0.026 0.052 0.078 0.103 0.129 0.155 0.181 0.207 0.233
```

```
     7
    11
 0.000 0.024 0.154 0.209 0.238 0.257 0.269 0.278 0.285 0.289 0.293
 0.000 0.000 0.026 0.052 0.078 0.103 0.129 0.155 0.181 0.207 0.233
     8
    11
 0.000 0.025 0.182 0.239 0.267 0.285 0.295 0.302 0.307 0.310 0.312
 0.000 0.000 0.026 0.052 0.078 0.103 0.129 0.155 0.181 0.207 0.233
     9
    11
 0.000 0.025 0.200 0.259 0.286 0.301 0.310 0.316 0.320 0.322 0.323
 0.000 0.000 0.026 0.052 0.078 0.103 0.129 0.155 0.181 0.207 0.233
    10
    11
 0.000 0.025 0.208 0.238 0.295 0.309 0.317 0.322 0.325 0.327 0.328
 0.000 0.000 0.026 0.052 0.078 0.103 0.129 0.155 0.181 0.207 0.233
    11
    11
 0.000 0.024 0.190 0.258 0.289 0.306 0.316 0.322 0.325 0.327 0.328
 0.000 0.000 0.026 0.052 0.078 0.103 0.129 0.155 0.181 0.207 0.233
    12
    11
 0.000 0.024 0.157 0.237 0.274 0.296 0.309 0.317 0.321 0.326 0.327
 0.000 0.000 0.026 0.052 0.078 0.103 0.129 0.155 0.181 0.207 0.233
    13
    11
 0.000 0.023 0.101 0.194 0.245 0.276 0.295 0.308 0.315 0.319 0.321
 0.000 0.000 0.026 0.052 0.078 0.103 0.129 0.155 0.181 0.207 0.233
    14
    11
 0.000 0.021 0.056 0.125 0.195 0.242 0.272 0.291 0.303 0.310 0.313
 0.000 0.000 0.026 0.052 0.078 0.103 0.129 0.155 0.181 0.207 0.233
    15
    11
 0.000 0.020 0.035 0.067 0.127 0.192 0.237 0.266 0.284 0.294 0.299
 0.000 0.000 0.026 0.052 0.078 0.103 0.129 0.155 0.181 0.207 0.233
    16
    10
 0.000 0.021 0.034 0.063 0.126 0.193 0.236 0.260 0.273 0.281
 0.005 0.026 0.052 0.078 0.103 0.129 0.155 0.181 0.207 0.233
    17
     8
 0.000 0.027 0.058 0.132 0.197 0.230 0.246 0.256
 0.059 0.078 0.103 0.129 0.155 0.181 0.207 0.233
    18
     7
 0.000 0.015 0.057 0.149 0.193 0.214 0.225
 0.100 0.103 0.129 0.155 0.181 0.207 0.233
```

```
   19
    5
0.000 0.081 0.151 0.173 0.181
0.134 0.155 0.181 0.207 0.233
   20
    3
0.000 0.049 0.083
0.204 0.207 0.233
DISP                    <----- Control flag for load waterline
0.4022  3.108           <----- Displacement, LCG
3                        <----- Number of stations for sea loads
5 10 13               <----- Station for sea loads
.00230 .00715 .00991 .01276 .01826 .02326 .01806 .01496
.02817 .03864 .03786 .03321 .03529 .03364 .02464 .01872
.01442 .01094 .00956 .00795 .00250                      <----- Sectional tonnages
0.296  0.296  0.296  0.296  0.296  0.294  0.292  0.292
0.292  0.292  0.286  0.280  0.280  0.274  0.267  0.267
0.267  0.267  0.267  0.267  0.267                      <----- Sectional KG values
0.083  0.104  0.122  0.139  0.166  0.188  0.165  0.150
0.206  0.242  0.239  0.224  0.231  0.226  0.193  0.168
0.148  0.129  0.120  0.110  0.087                      <----- Sectional RRG values
0.0 0.0 0.0 0.0 0.0                 <----- Bow mass distribution
0.0 0.0 0.0 0.0 0.0                 <----- Stern mass distribution
0  0. 0.                            <----- Number of seakeeping positions
5                                   <----- Number of bilge keel pairs
7 8                                 <----- Stations for bilge keel pairs
7.073 7.500 0.251 0.095 0.024
7.500 8.093 0.267 0.078 0.024
9 9
8.801 9.356 0.276 0.069 0.024
10 11
10.029 10.500 0.276 0.069 0.024
10.500 11.016 0.277 0.068 0.024
12 12
11.702 12.316 0.270 0.075 0.024
13 14
12.949 13.500 0.258 0.088 0.024
13.500 13.810 0.243 0.104 0.024
18. 0.07 0.924                      <----- Skeg station, breadth, length
19.5 0.10 0.13 0.127 0.134 0.098 0.0 1  <----- Rudder
0. 0. 0. 0. 0. 0. 0.                <----- Rudder roll gains
0. 0. 0.                            <----- Rudder yaw gains
4                                   <----- Number of pairs of stationary foils
17.0 0.15 0.10 0.100 0.021 0.021 0. -107.0 1.  <----- Outboard arm
17.0 0.07 0.09 0.100 0.021 0.021 0.  -47.0 1.  <----- Inboard arm
18.8 0.17 0.15 0.142 0.034 0.034 0. -100.0 1.  <----- Outboard arm
18.8 0.02 0.11 0.128 0.034 0.034 0.  -60.0 1.  <----- Inboard arm
```

```
FIN                  <----- Stabilization control flag
4                    <----- Number of fin pairs
 8.4 0.28 0.1 0.05 0.097 0.097 0. -43.5 1.    <----- Fin pair 1
 9.6 0.28 0.1 0.05 0.097 0.097 0. -43.5 1.    <----- Fin pair 2
11.3 0.28 0.1 0.05 0.097 0.097 0. -43.5 1.    <----- Fin pair 3
12.6 0.28 0.1 0.05 0.097 0.097 0. -43.5 1.    <----- Fin pair 4
0. 0. 0. 0. 0. 0.                             <----- Stabilizing fin roll gains
```

B PRECAL Sample Input Files

B.1 HYDMES Pre-processor Input File 1 - warship.hin

```
AUTOMATIC FACET GENERATION - SHIPMO7/PRECAL VALIDATION STUDY (June, 1997)
Lloyd Warship Model
MONOHULL
OPTION
OCAL
OINP
OOUT
OMAS
ENDOPT
CONSTS
CDEN 1.000
CACC 9.80665
ENDCON
SHIPDS
SDIM 6.157  6.157  0.653  0.203  -0.007
SGMS 15.511 0.027
SSYM Y=0
ENDSHI
#
# Mass Distribution Data
#    DM         XM         YM         ZM         Ixx        Iyy        Izz
MASSDI
0.00230    3.07850  0.00000  0.09300  0.00002  0.00000  0.00000
0.00715    2.77065  0.00000  0.09300  0.00008  0.00000  0.00000
0.00991    2.46280  0.00000  0.09300  0.00015  0.00000  0.00000
0.01276    2.15495  0.00000  0.09300  0.00025  0.00000  0.00000
0.01826    1.84710  0.00000  0.09300  0.00050  0.00000  0.00000
0.02326    1.53925  0.00000  0.09100  0.00082  0.00000  0.00000
0.01806    1.23140  0.00000  0.08900  0.00049  0.00000  0.00000
0.01496    0.92355  0.00000  0.08900  0.00034  0.00000  0.00000
0.02817    0.61570  0.00000  0.08900  0.00120  0.00000  0.00000
0.03864    0.30785  0.00000  0.08900  0.00226  0.00000  0.00000
0.03786    0.00000  0.00000  0.08300  0.00217  0.00000  0.00000
0.03321   -0.30785  0.00000  0.07700  0.00167  0.00000  0.00000
0.03529   -0.61570  0.00000  0.07700  0.00188  0.00000  0.00000
0.03364   -0.92355  0.00000  0.07100  0.00171  0.00000  0.00000
0.02464   -1.23140  0.00000  0.06400  0.00092  0.00000  0.00000
0.01872   -1.53925  0.00000  0.06400  0.00053  0.00000  0.00000
0.01442   -1.84710  0.00000  0.06400  0.00031  0.00000  0.00000
0.01094   -2.15495  0.00000  0.06400  0.00018  0.00000  0.00000
0.00956   -2.46280  0.00000  0.06400  0.00014  0.00000  0.00000
0.00795   -2.77065  0.00000  0.06400  0.00010  0.00000  0.00000
0.00250   -3.07850  0.00000  0.06400  0.00002  0.00000  0.00000
ENDMAS
```

```
AFTEND
TOTFAC
0.5 1.0 80
ENDTOT
ENDAFT
FOREND
TOTFAC
0.5 1.0 80
ENDTOT
ENDFOR
ENDFIL
```

B.2 HYDMES Pre-processor Input File 2 - warship.hul

```
Lloyd Warship Model
6.157  0.653  21
  0.0  4
 0.000 0.0245 0.049 0.083
 0.204 0.2055 0.207 0.233
  0.5  5
 0.000 0.081 0.151 0.173 0.181
 0.134 0.155 0.181 0.207 0.233
  1.0  7
 0.000 0.015 0.057 0.149 0.193 0.214 0.225
 0.100 0.103 0.129 0.155 0.181 0.207 0.233
 1.5  8
 0.000 0.027 0.058 0.132 0.197 0.230 0.246 0.256
 0.059 0.078 0.103 0.129 0.155 0.181 0.207 0.233
  2.0 10
 0.000 0.021 0.034 0.063 0.126 0.193 0.236 0.260 0.273 0.281
 0.005 0.026 0.052 0.078 0.103 0.129 0.155 0.181 0.207 0.233
  2.5 11
 0.000 0.020 0.035 0.067 0.127 0.192 0.237 0.266 0.284 0.294 0.299
 0.000 0.000 0.026 0.052 0.078 0.103 0.129 0.155 0.181 0.207 0.233
  3.0 11
 0.000 0.021 0.056 0.125 0.195 0.242 0.272 0.291 0.303 0.310 0.313
 0.000 0.000 0.026 0.052 0.078 0.103 0.129 0.155 0.181 0.207 0.233
  3.5 11
 0.000 0.023 0.101 0.194 0.245 0.276 0.295 0.308 0.315 0.319 0.321
 0.000 0.000 0.026 0.052 0.078 0.103 0.129 0.155 0.181 0.207 0.233
  4.0 11
 0.000 0.024 0.157 0.237 0.274 0.296 0.309 0.317 0.321 0.326 0.327
 0.000 0.000 0.026 0.052 0.078 0.103 0.129 0.155 0.181 0.207 0.233
  4.5 11
 0.000 0.024 0.190 0.258 0.289 0.306 0.316 0.322 0.325 0.327 0.328
 0.000 0.000 0.026 0.052 0.078 0.103 0.129 0.155 0.181 0.207 0.233
  5.0 11
 0.000 0.025 0.208 0.238 0.295 0.309 0.317 0.322 0.325 0.327 0.328
 0.000 0.000 0.026 0.052 0.078 0.103 0.129 0.155 0.181 0.207 0.233
  5.5 11
 0.000 0.025 0.200 0.259 0.286 0.301 0.310 0.316 0.320 0.322 0.323
 0.000 0.000 0.026 0.052 0.078 0.103 0.129 0.155 0.181 0.207 0.233
  6.0 11
 0.000 0.025 0.182 0.239 0.267 0.285 0.295 0.302 0.307 0.310 0.312
 0.000 0.000 0.026 0.052 0.078 0.103 0.129 0.155 0.181 0.207 0.233
  6.5 11
 0.000 0.024 0.154 0.209 0.238 0.257 0.269 0.278 0.285 0.289 0.293
 0.000 0.000 0.026 0.052 0.078 0.103 0.129 0.155 0.181 0.207 0.233
  7.0 11
 0.000 0.023 0.123 0.173 0.201 0.220 0.234 0.245 0.254 0.261 0.267
 0.000 0.000 0.026 0.052 0.078 0.103 0.129 0.155 0.181 0.207 0.233
```

```
 7.5 11
0.000 0.021 0.098 0.138 0.163 0.182 0.196 0.207 0.217 0.225 0.233
0.000 0.000 0.026 0.052 0.078 0.103 0.129 0.155 0.181 0.207 0.233
 8.0 11
0.000 0.019 0.072 0.106 0.127 0.143 0.155 0.166 0.175 0.184 0.192
0.000 0.000 0.026 0.052 0.078 0.103 0.129 0.155 0.181 0.207 0.233
8.5 11
0.000 0.017 0.053 0.076 0.093 0.105 0.114 0.123 0.131 0.139 0.147
0.000 0.000 0.026 0.052 0.078 0.103 0.129 0.155 0.181 0.207 0.233
 9.0 11
0.000 0.014 0.034 0.048 0.059 0.068 0.075 0.081 0.087 0.093 0.100
0.000 0.000 0.026 0.052 0.078 0.103 0.129 0.155 0.181 0.207 0.233
 9.5 11
0.000 0.010 0.017 0.024 0.029 0.033 0.037 0.041 0.045 0.049 0.053
0.000 0.000 0.026 0.052 0.078 0.103 0.129 0.155 0.181 0.207 0.233
10.0  3
0.000 0.008 0.009
0.204 0.207 0.233
```

B.3 HYDCAL Input File - warship.cnd

```
HYDCAL RUN AT FR = 0.21, May 1997
Lloyd Warship Model
MONOHULL
OPTION
OKTS
OFSP
ENDOPT
CONDNS
SPED  3.17
HEAD  0 30 60 90 120 150 180.0
FREQ  2.20 2.40 2.60 2.80 3.00
      3.20 3.40 3.60 3.80 4.00
      4.20 4.40 4.60 4.80 5.00
ENDCON
FSPANS
2
ENDFSP
ENDFIL
```

B.4 RESCAL Input File - warship.inp

```
RESCAL: FR = 0.21, ROLL DAMPING = 0.19 FROM SHIPMO (June 1997)
Lloyd Warship Model
MONOHULL
#
OPTION
OMOT
OPRE
OLOA
ENDOPT
#
ROLLIN
DAMP 0.190
ENDROL
#
#  LOAD POSITION - Long. loads are calculated at SHIPMO7 stations 5.0,
#                  10.0, 13.0 (PRECAL convention - 0.0 at AP, 1.0 at FP)
LOPOSN
LONGI
0.750
0.500
0.350
ENDLOP
#
ENDFIL
```

C Validation Study Results

C.1 Ship Motions

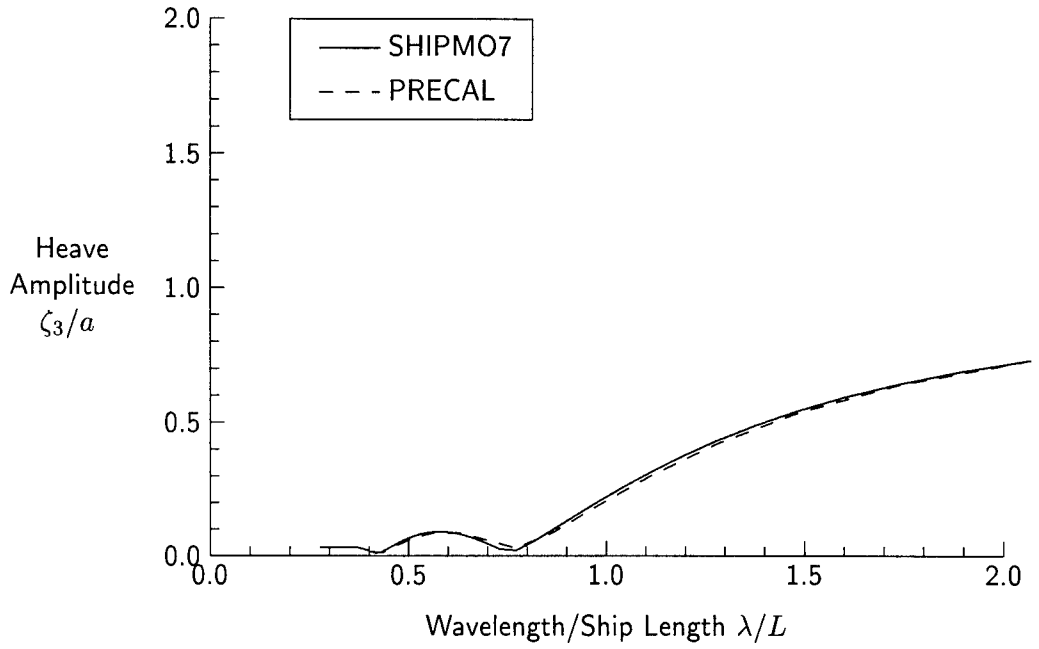

Figure 4: Heave, $Fn = 0.21$, $\beta = 0$ degrees

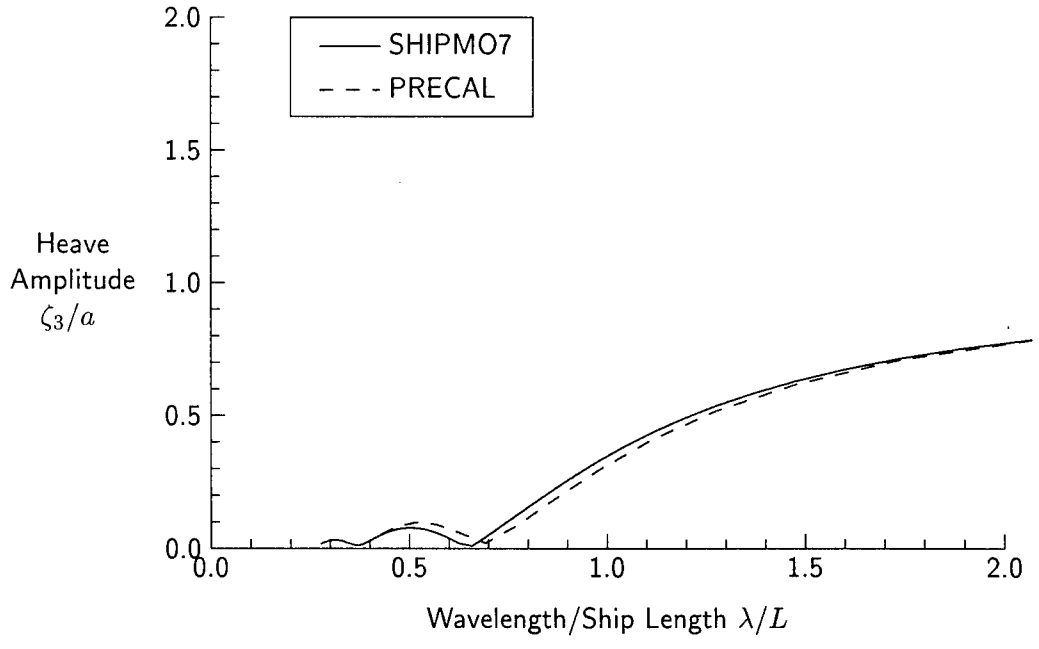

Figure 5: Heave, $Fn = 0.21$, $\beta = 30$ degrees

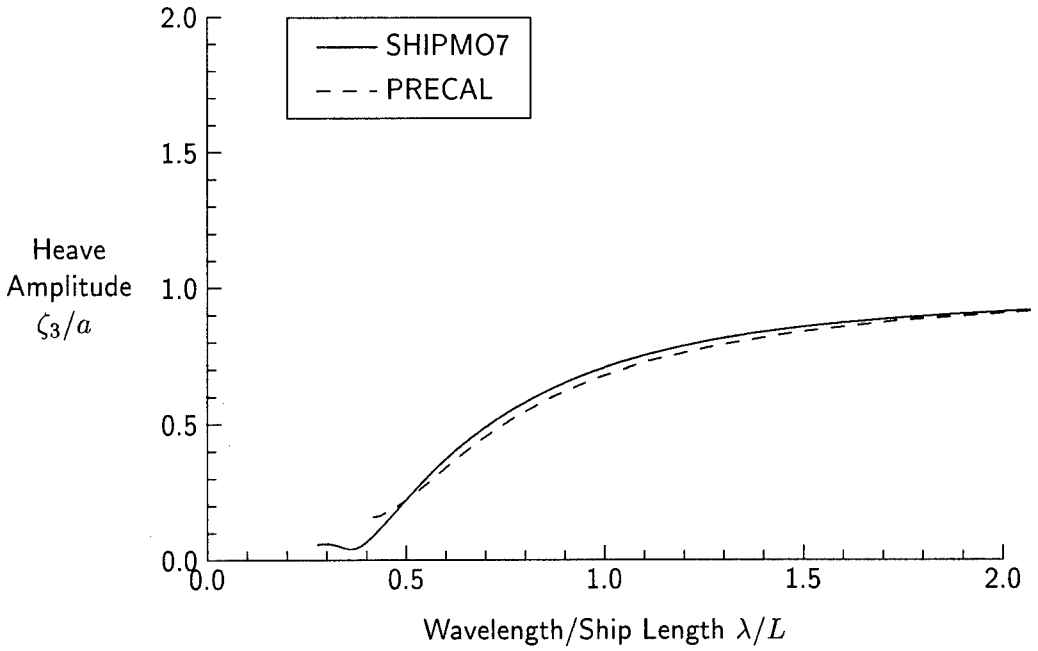

Figure 6: Heave, $Fn = 0.21$, $\beta = 60$ degrees

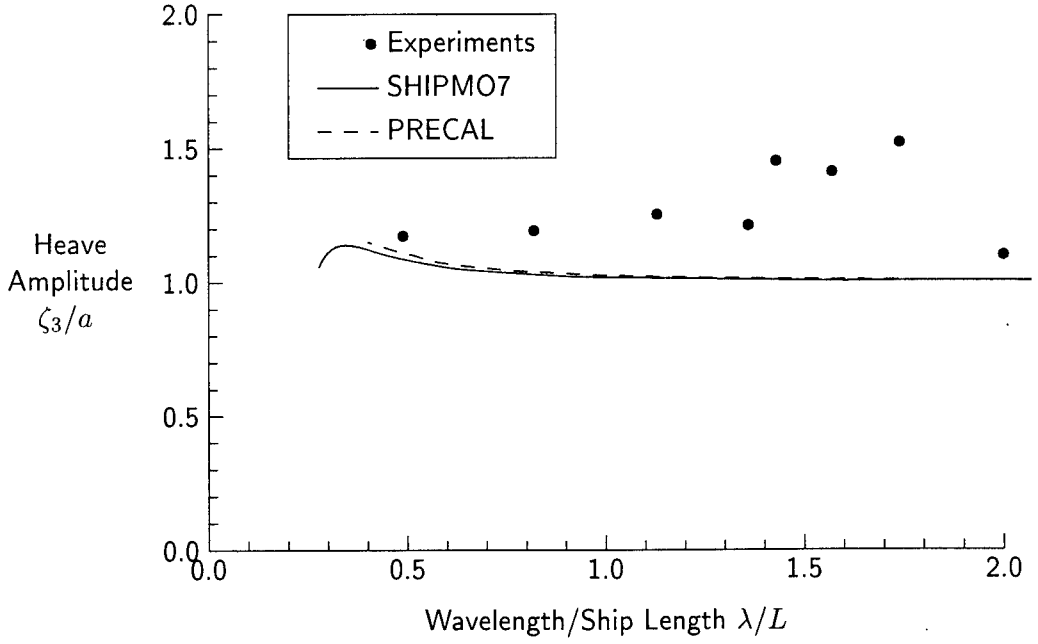

Figure 7: Heave, $Fn = 0.21$, $\beta = 90$ degrees

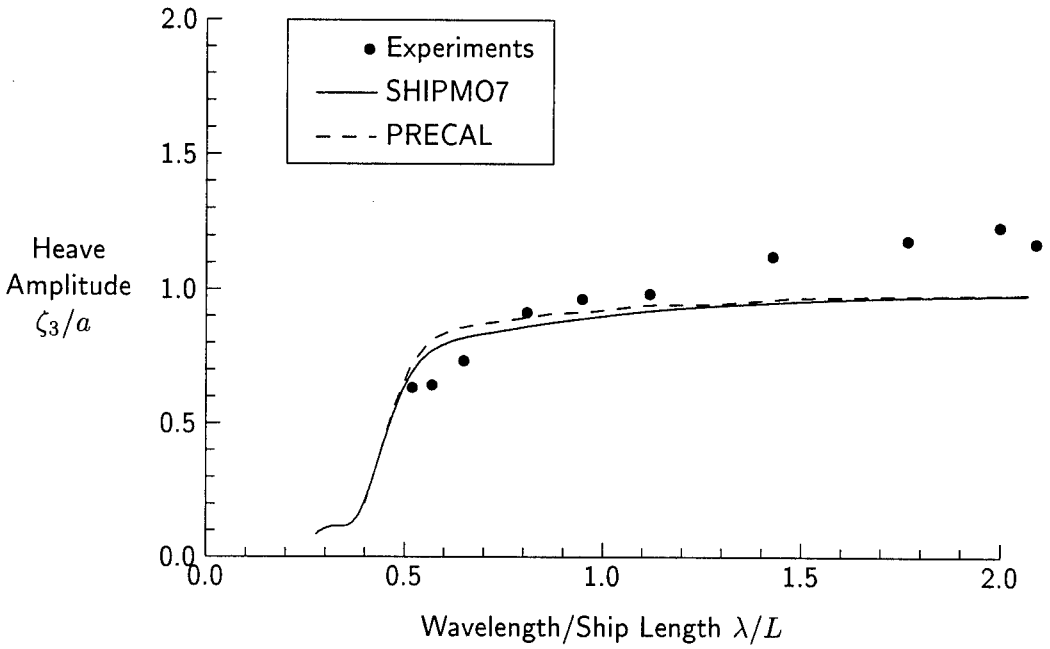

Figure 8: Heave, $Fn = 0.21$, $\beta = 120$ degrees

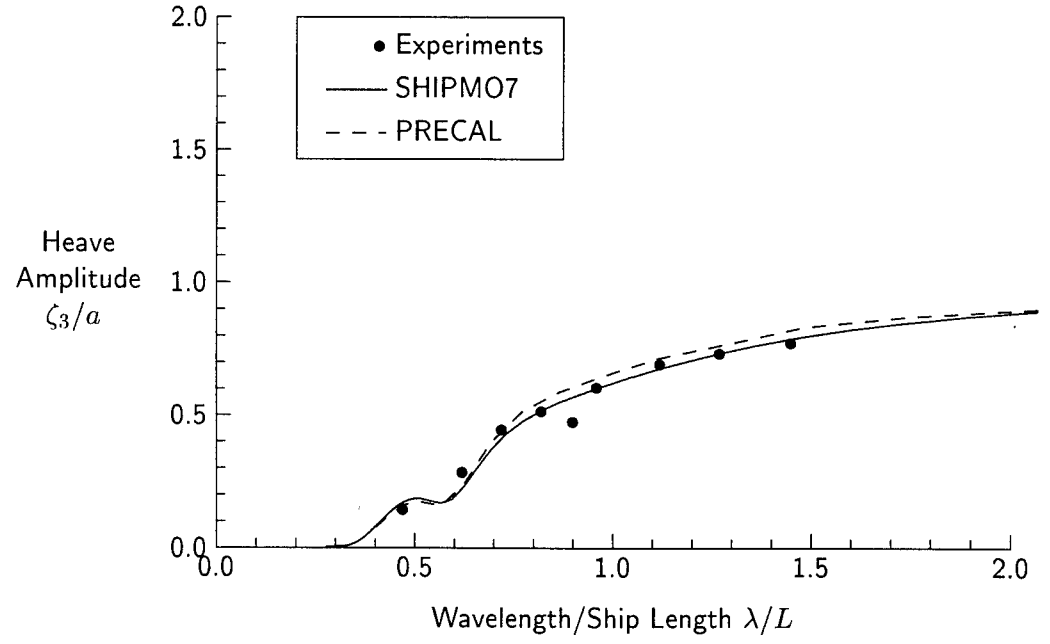

Figure 9: Heave, $Fn = 0.21$, $\beta = 150$ degrees

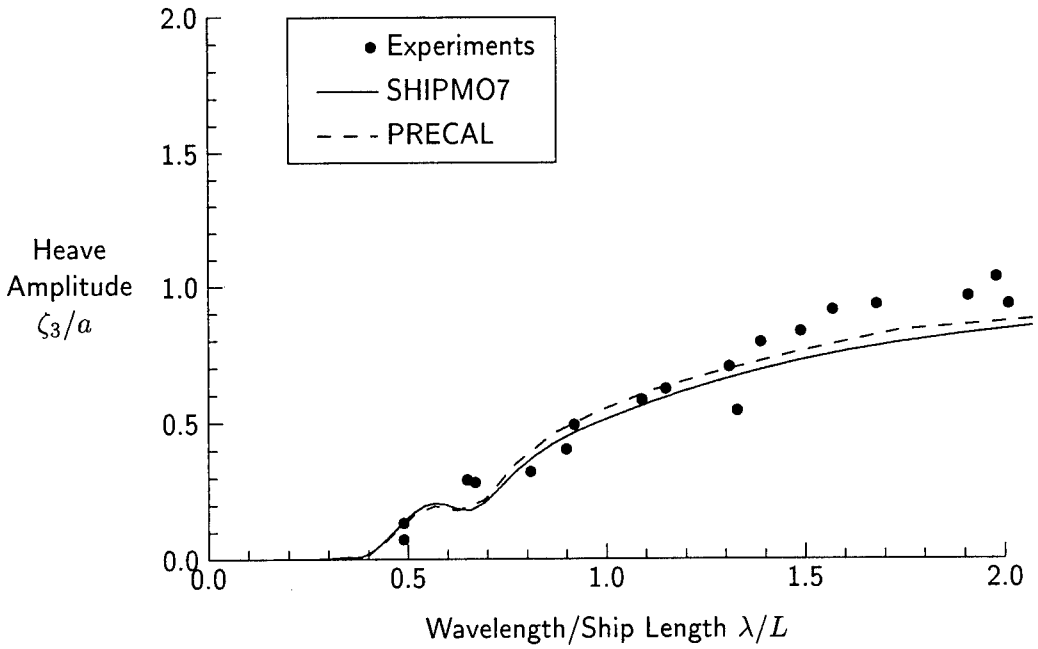

Figure 10: Heave, $Fn = 0.21$, $\beta = 180$ degrees

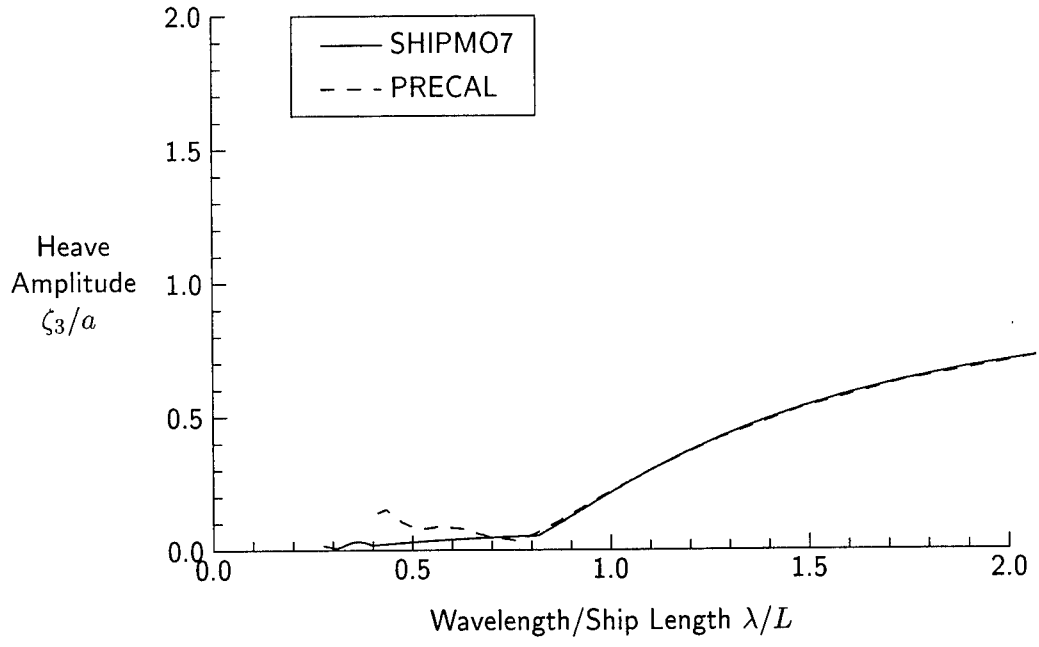

Figure 11: Heave, $Fn = 0.29$, $\beta = 0$ degrees

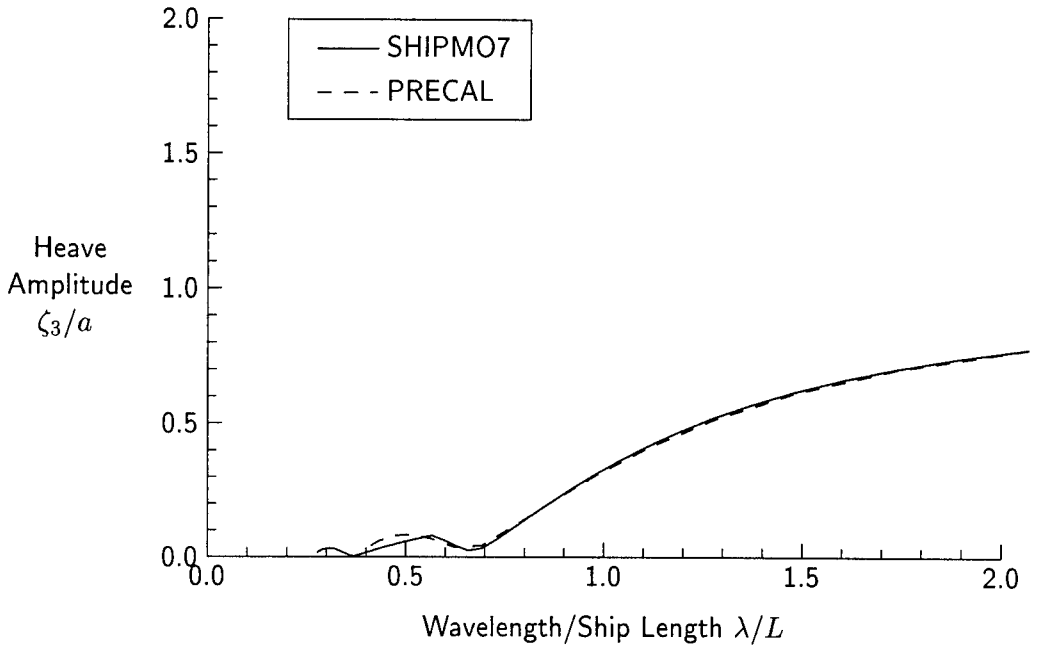

Figure 12: Heave, $Fn = 0.29$, $\beta = 30$ degrees

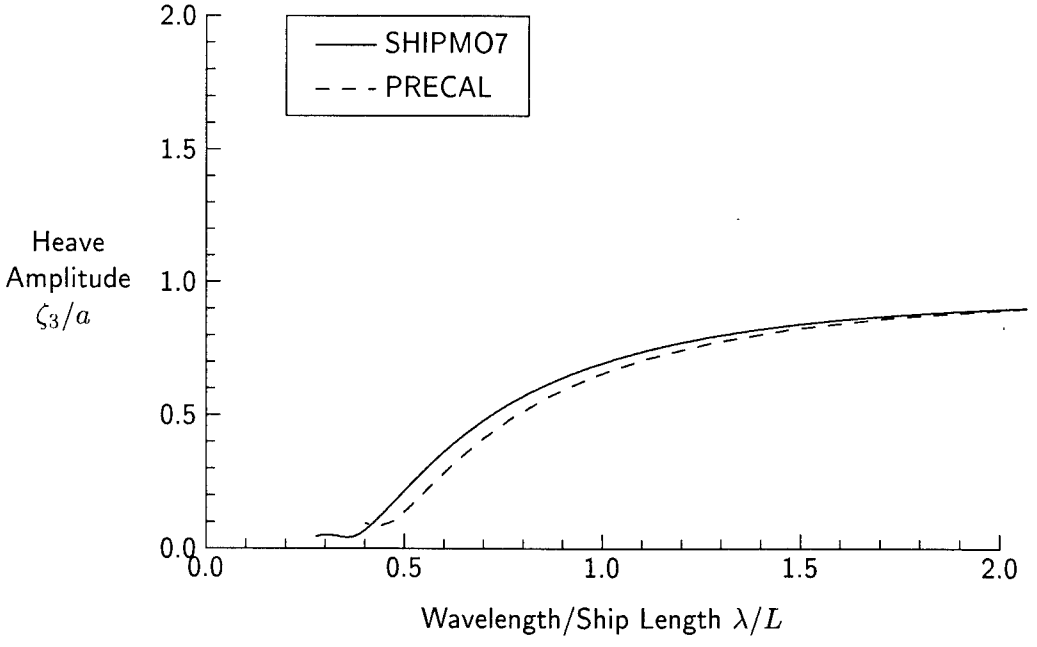

Figure 13: Heave, $Fn = 0.29$, $\beta = 60$ degrees

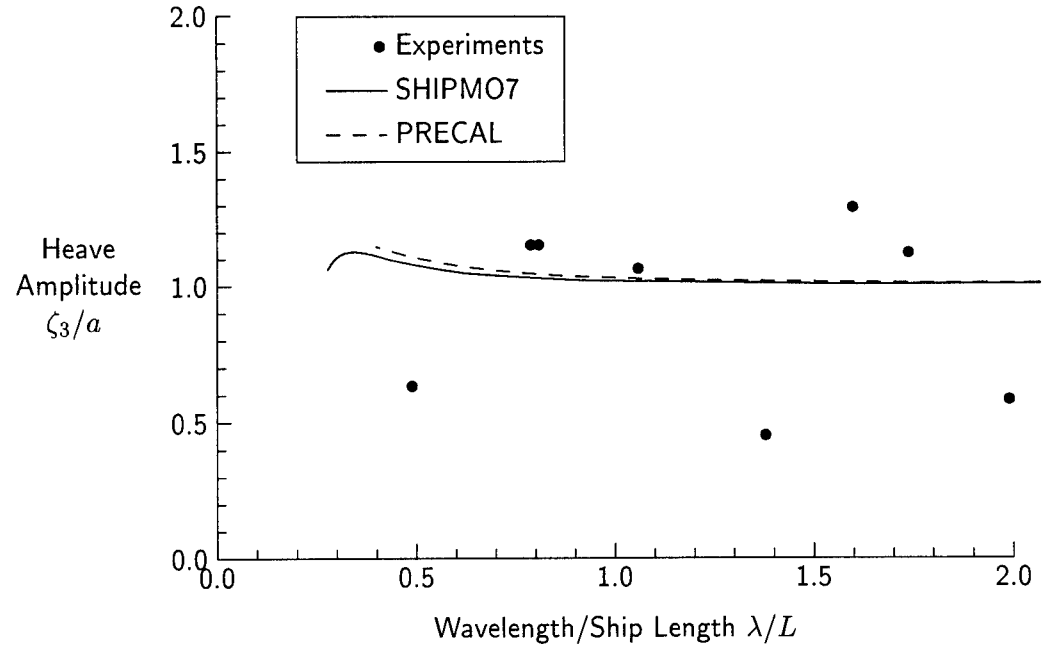

Figure 14: Heave, $Fn = 0.29$, $\beta = 90$ degrees

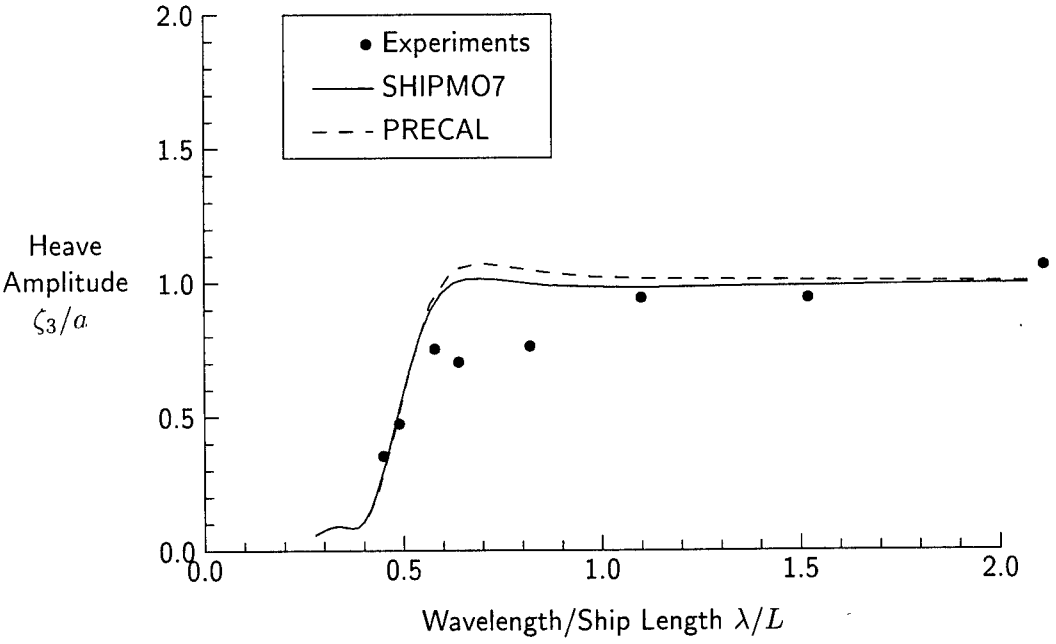

Figure 15: Heave, $Fn = 0.29$, $\beta = 120$ degrees

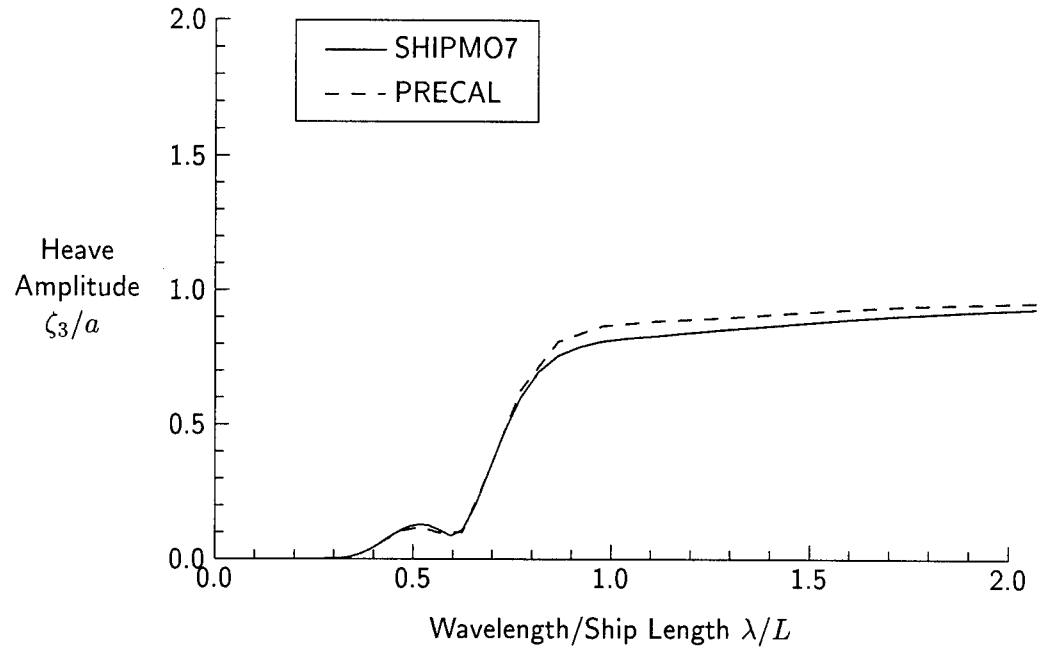

Figure 16: Heave, $Fn = 0.29$, $\beta = 150$ degrees

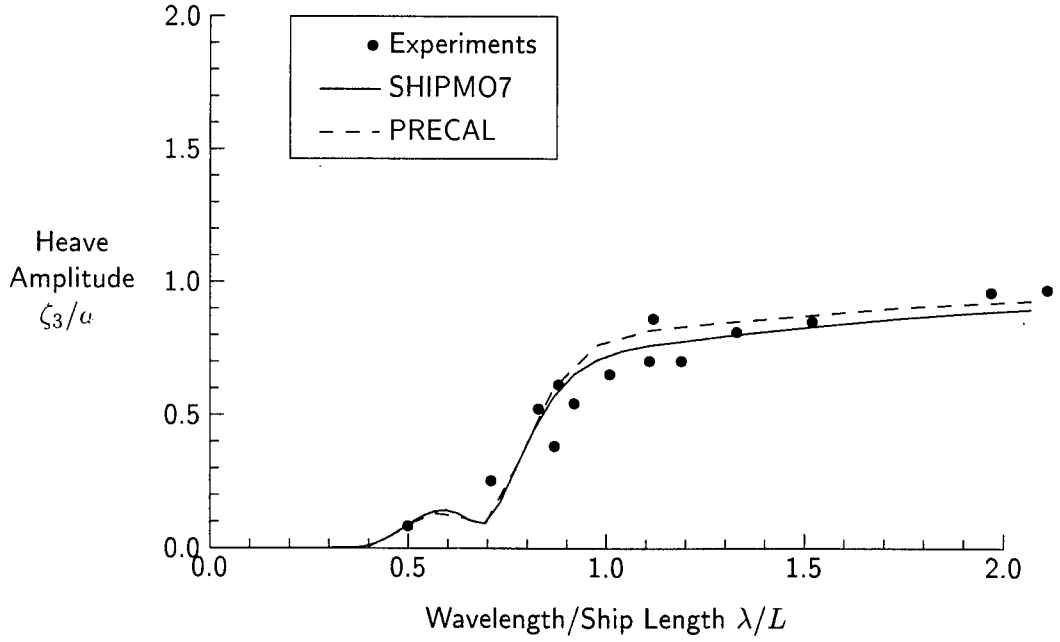

Figure 17: Heave, $Fn = 0.29$, $\beta = 180$ degrees

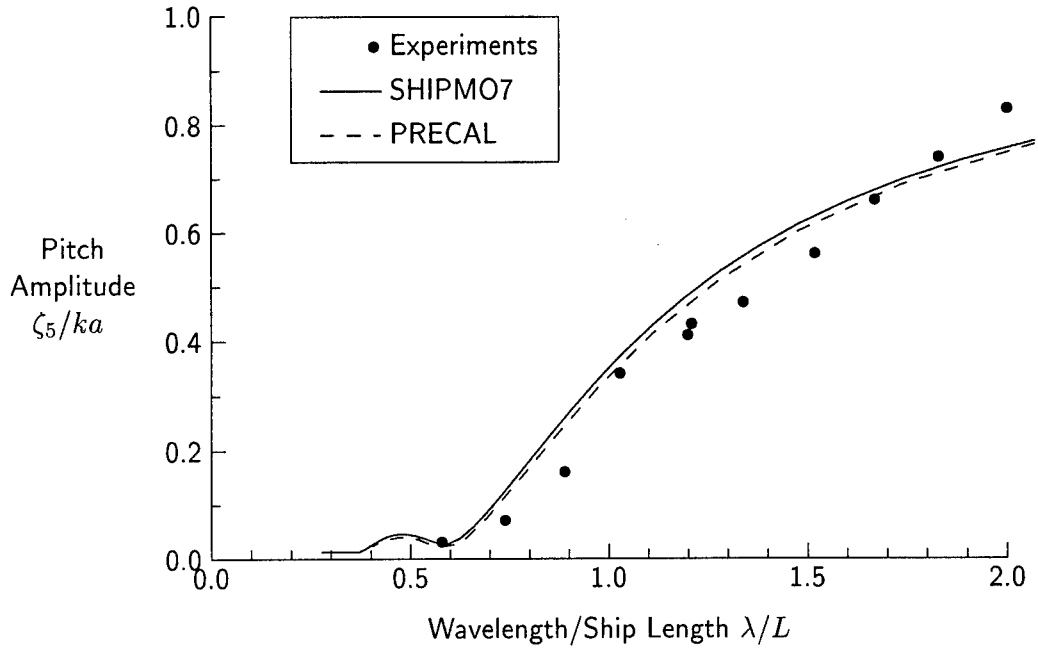

Figure 18: Pitch, $Fn = 0.21$, $\beta = 0$ degrees

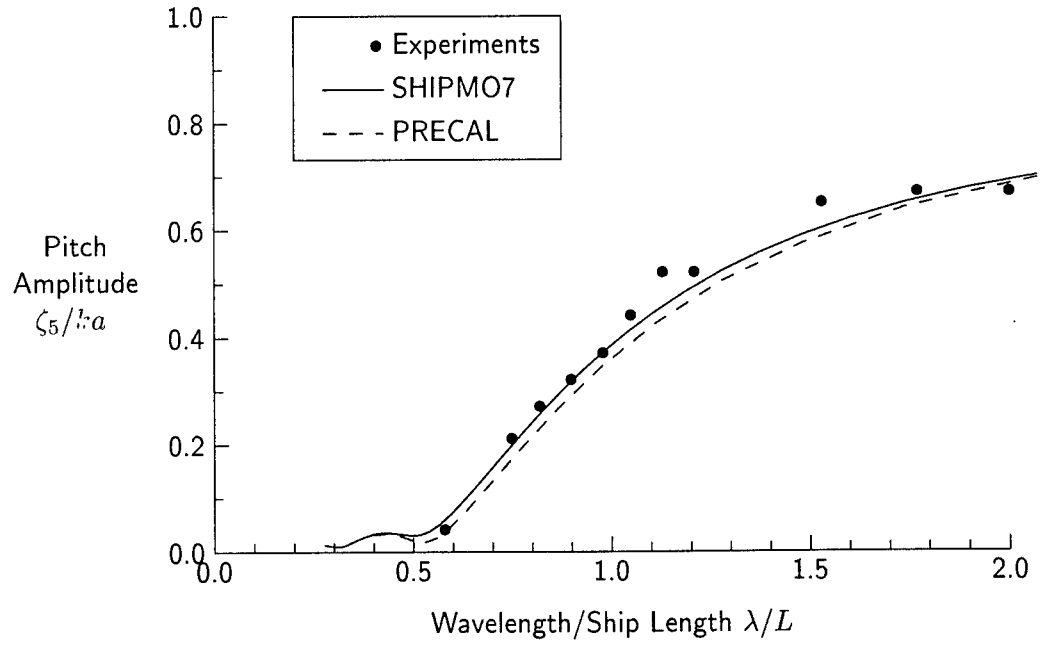

Figure 19: Pitch, $Fn = 0.21$, $\beta = 30$ degrees

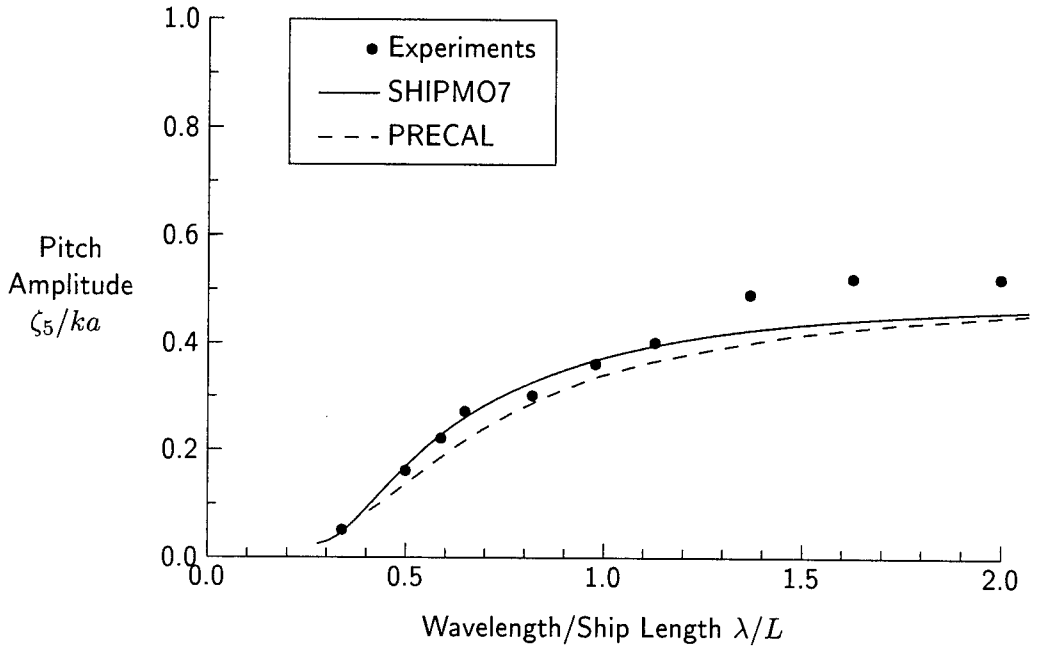

Figure 20: Pitch, $Fn = 0.21$, $\beta = 60$ degrees

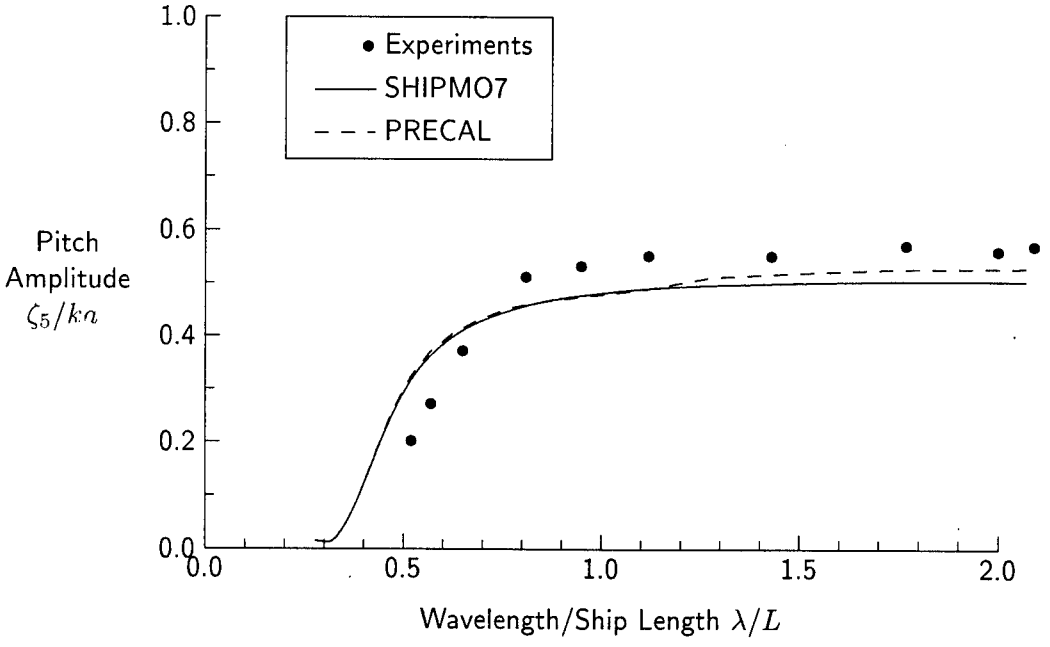

Figure 21: Pitch, $Fn = 0.21$, $\beta = 120$ degrees

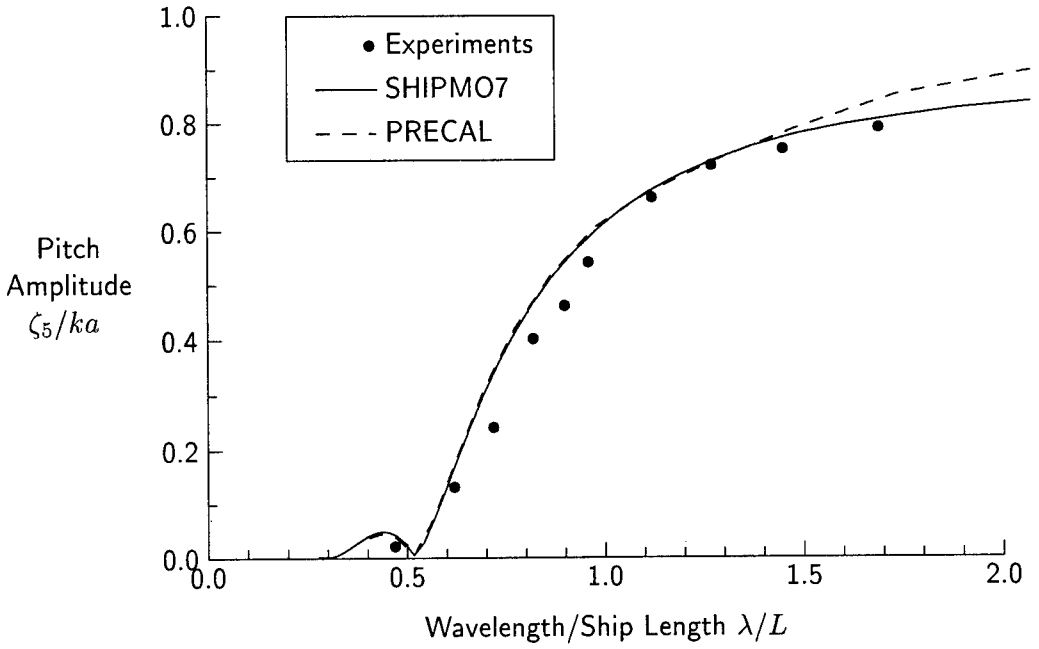

Figure 22: Pitch, $Fn = 0.21$, $\beta = 150$ degrees

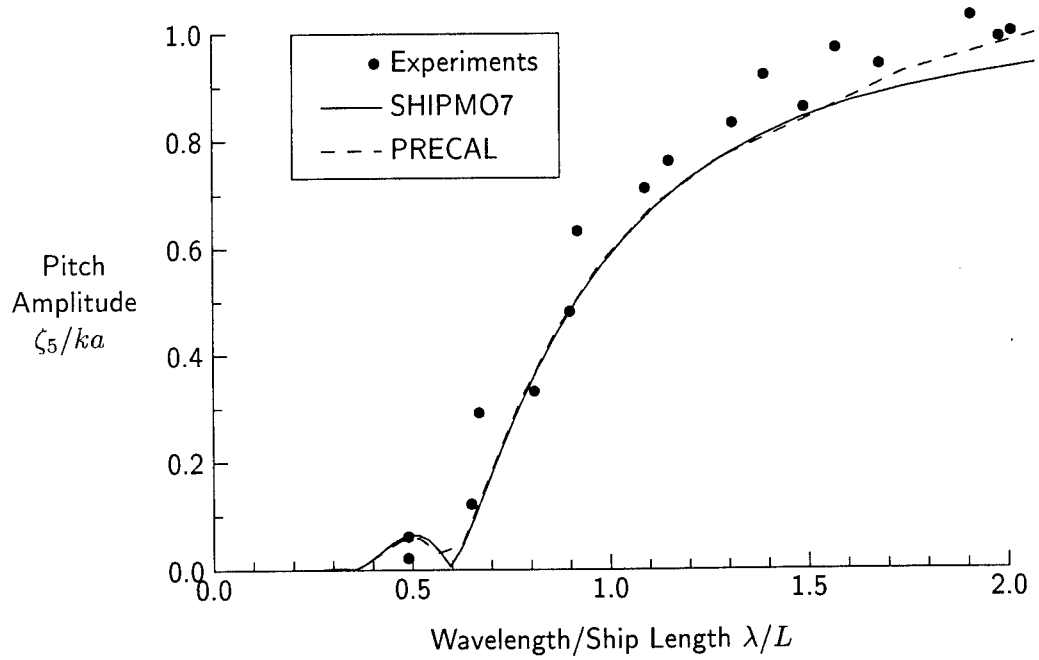

Figure 23: Pitch, $Fn = 0.21$, $\beta = 180$ degrees

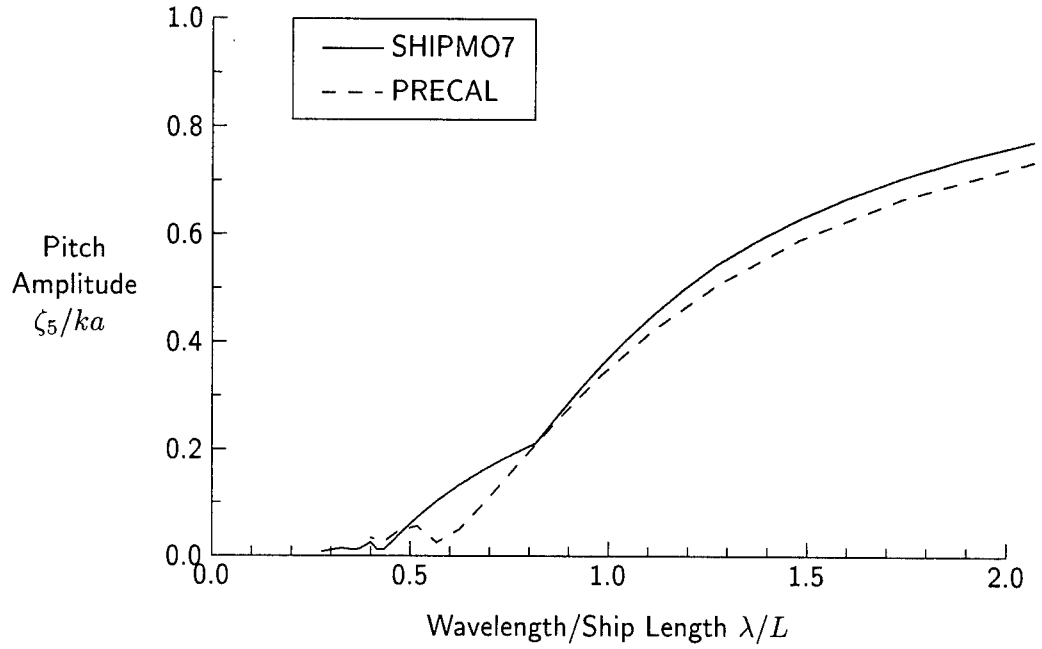

Figure 24: Pitch, $Fn = 0.29$, $\beta = 0$ degrees

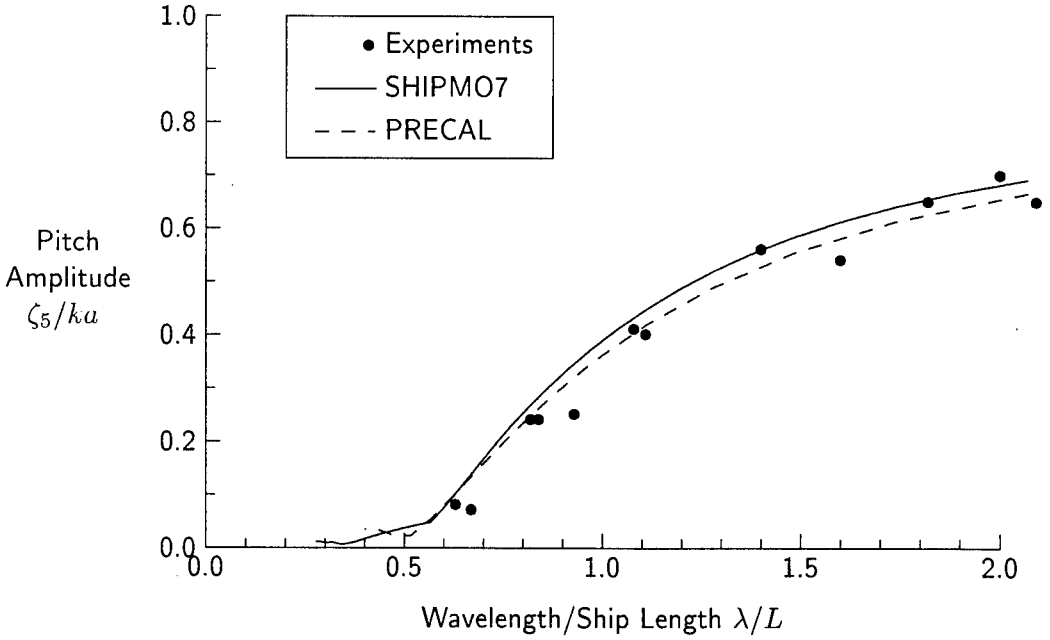

Figure 25: Pitch, $Fn = 0.29$, $\beta = 30$ degrees

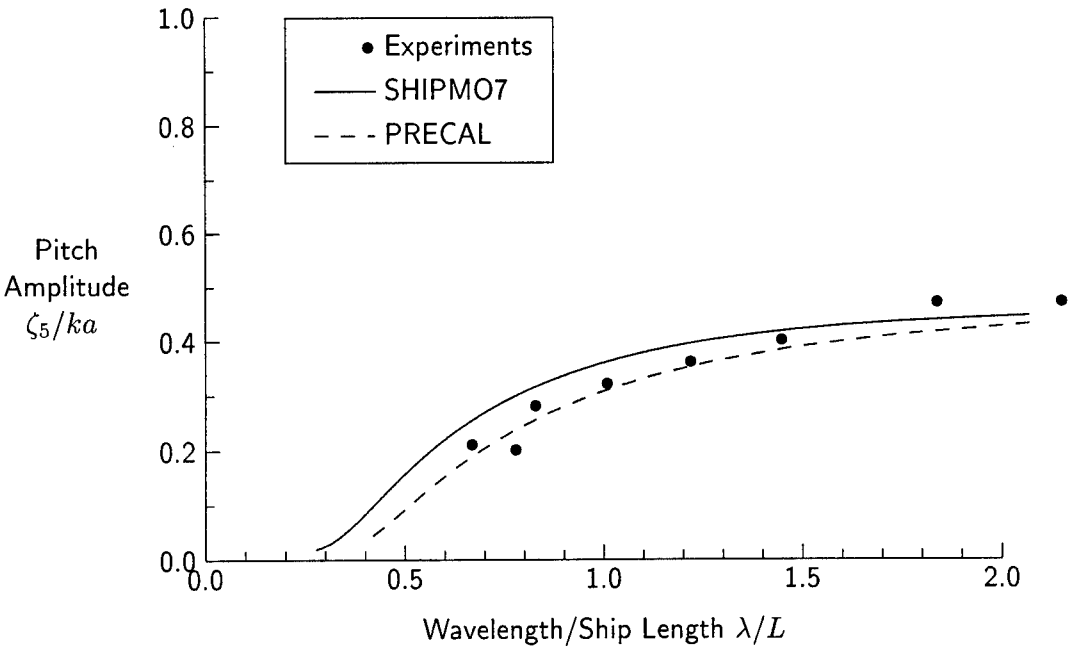

Figure 26: Pitch, $Fn = 0.29$, $\beta = 60$ degrees

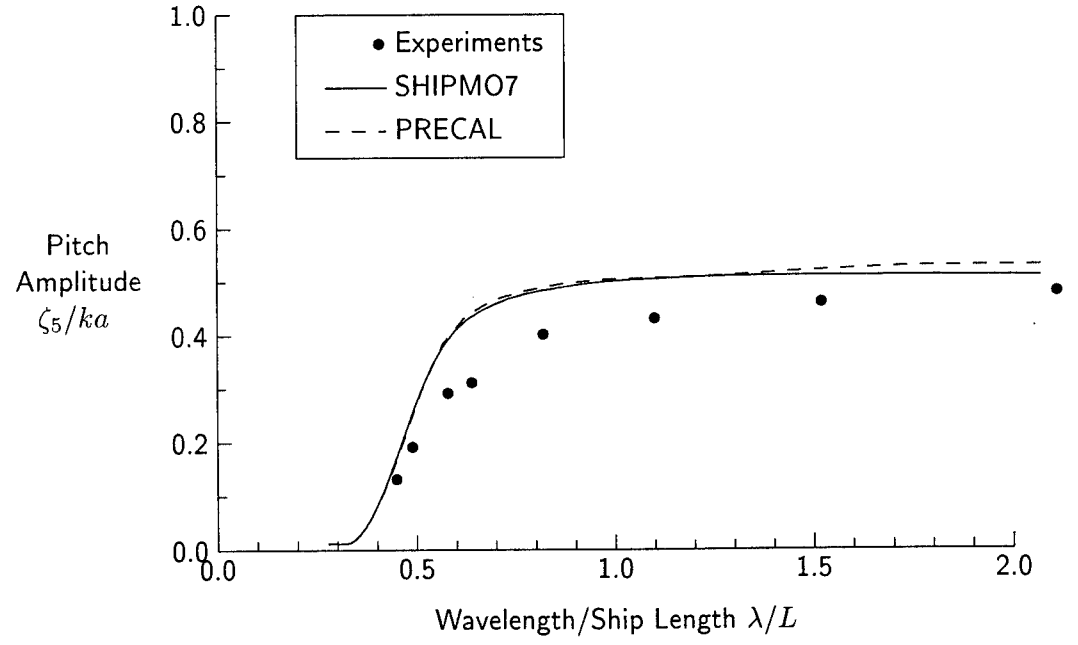

Figure 27: Pitch, $Fn = 0.29$, $\beta = 120$ degrees

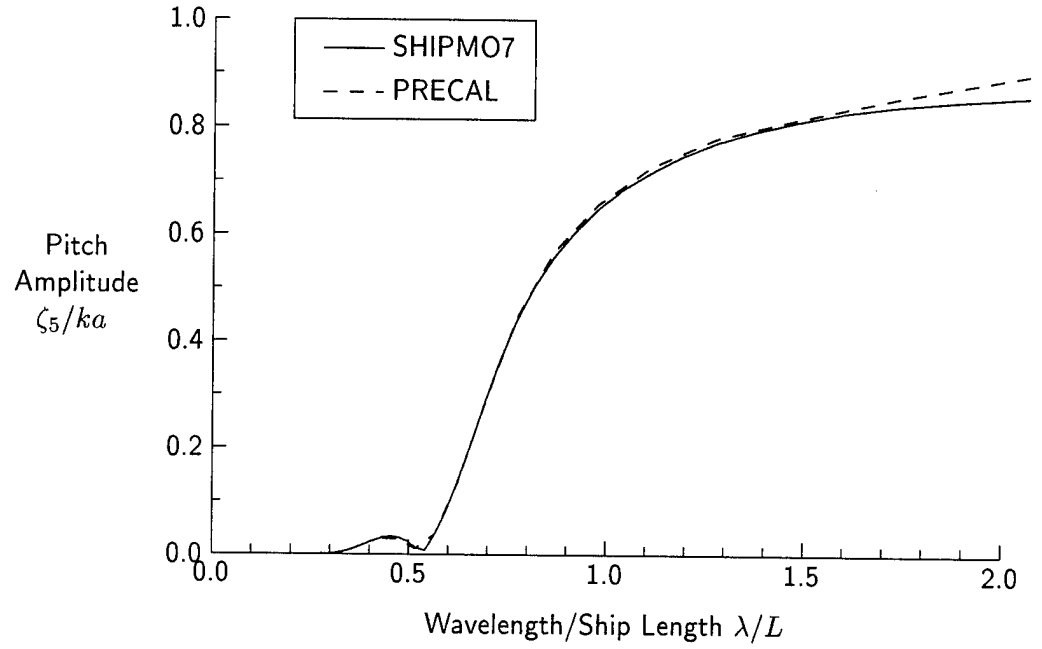

Figure 28: Pitch, $Fn = 0.29$, $\beta = 150$ degrees

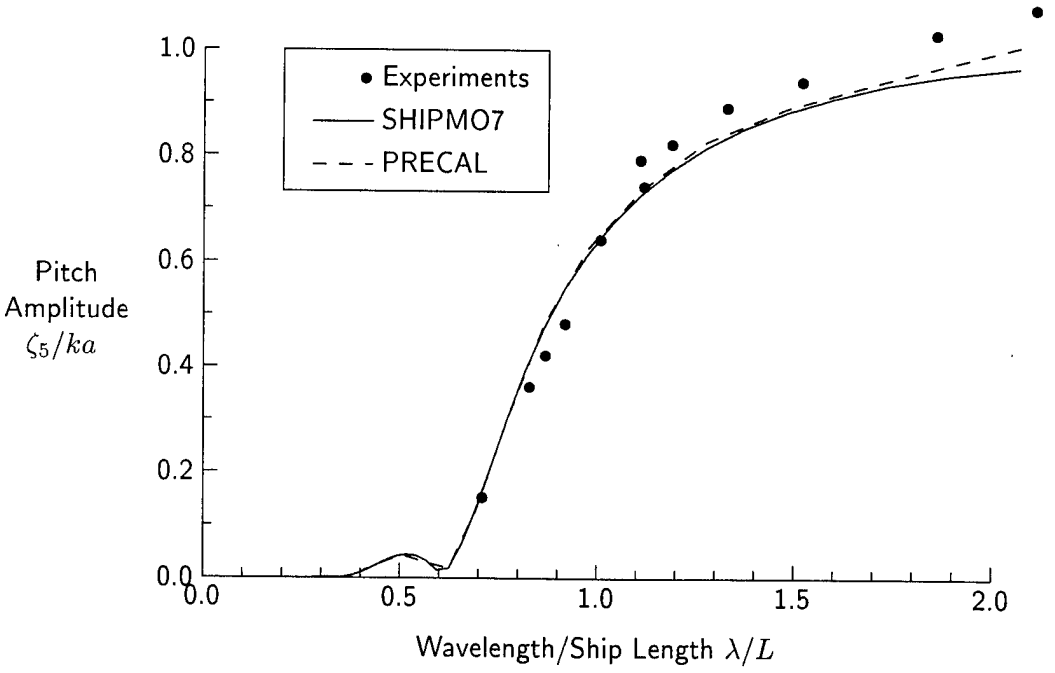

Figure 29: Pitch, $Fn = 0.29$, $\beta = 180$ degrees

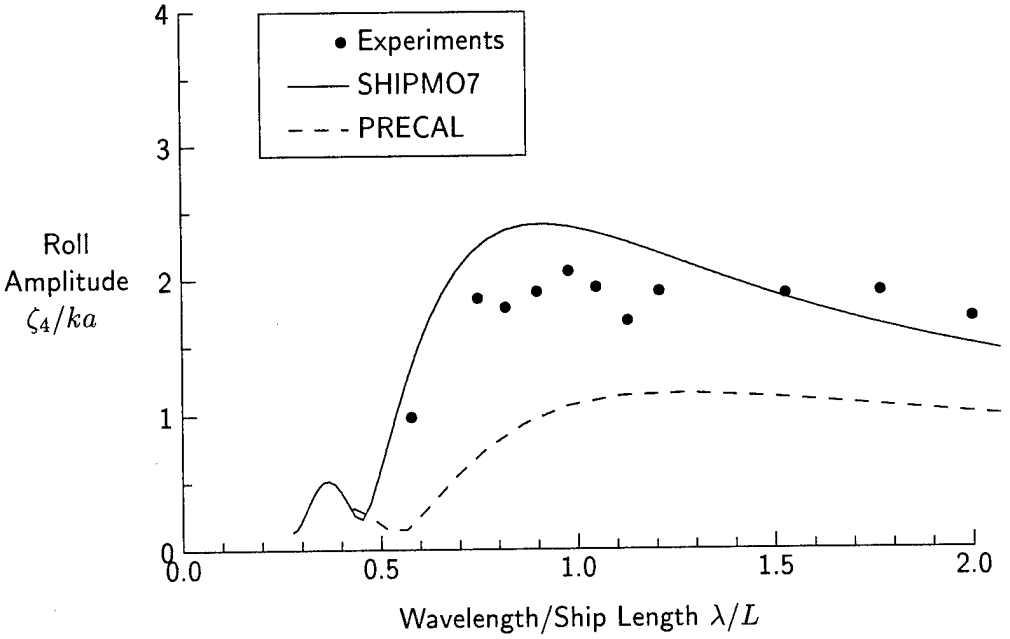

Figure 30: Roll, $Fn = 0.21$, $\beta = 30$ degrees

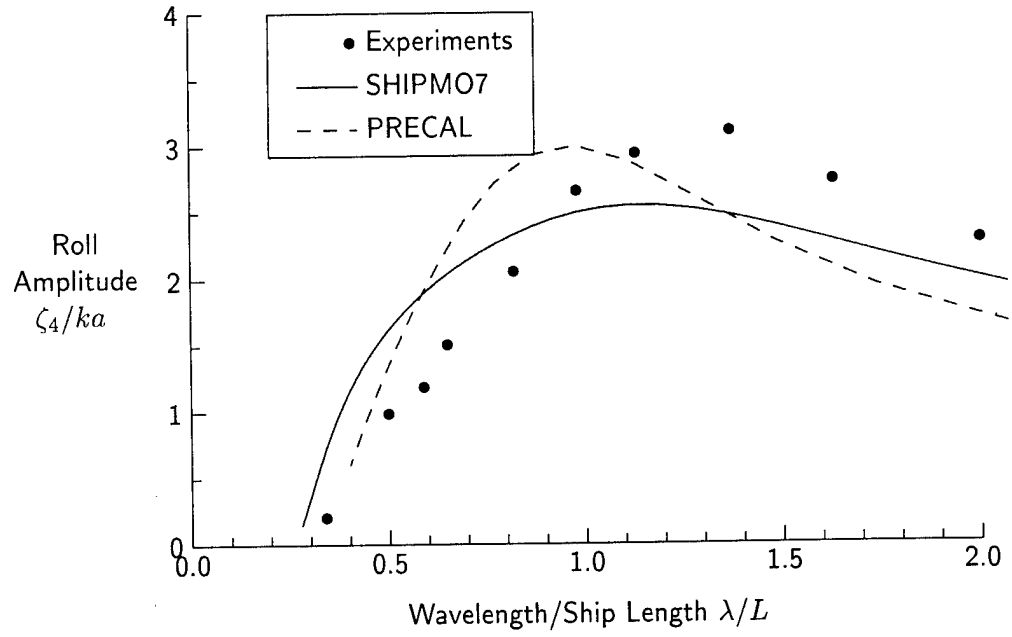

Figure 31: Roll, $Fn = 0.21$, $\beta = 60$ degrees

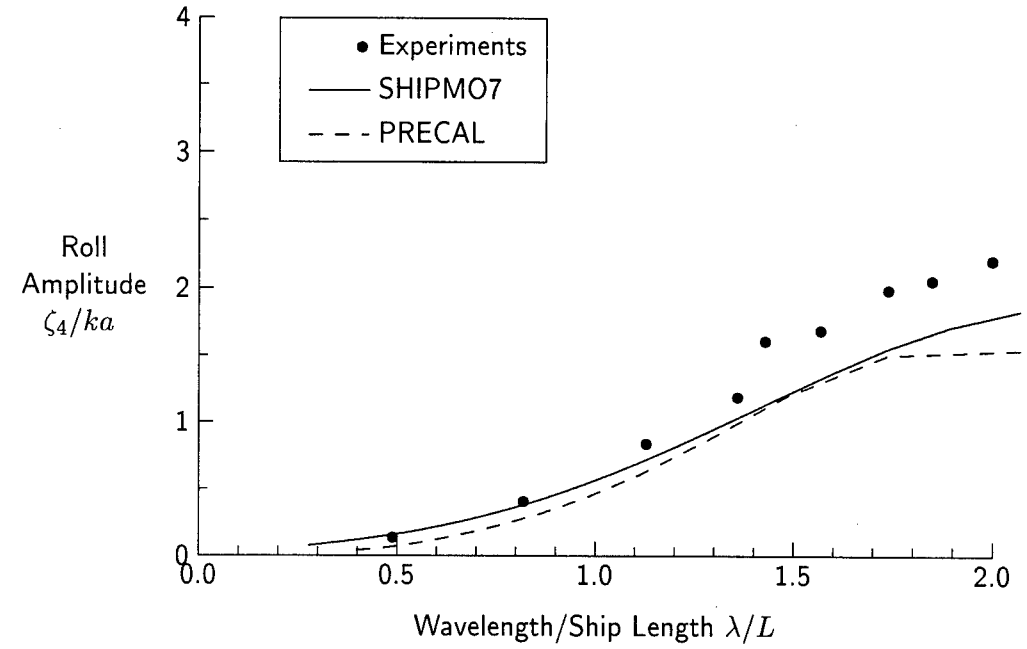

Figure 32: Roll, $Fn = 0.21$, $\beta = 90$ degrees

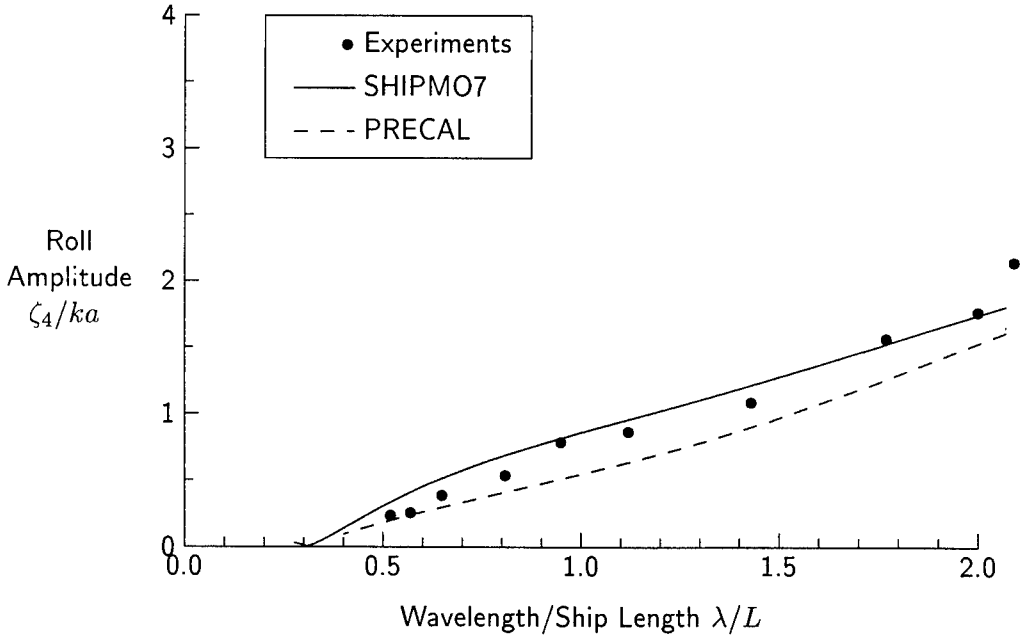

Figure 33: Roll, $Fn = 0.21$, $\beta = 120$ degrees

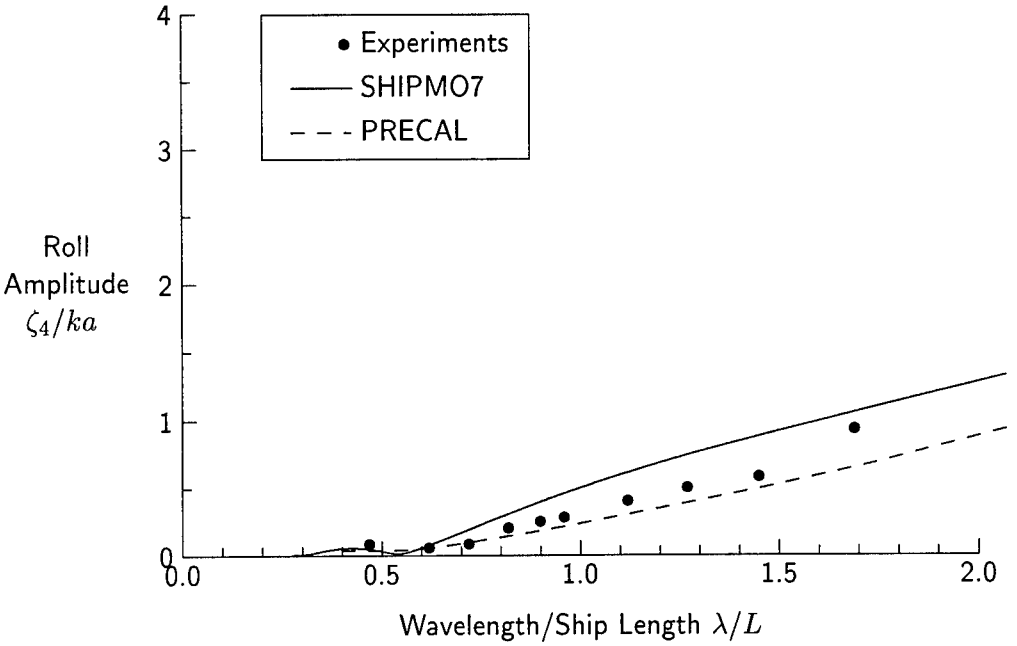

Figure 34: Roll, $Fn = 0.21$, $\beta = 150$ degrees

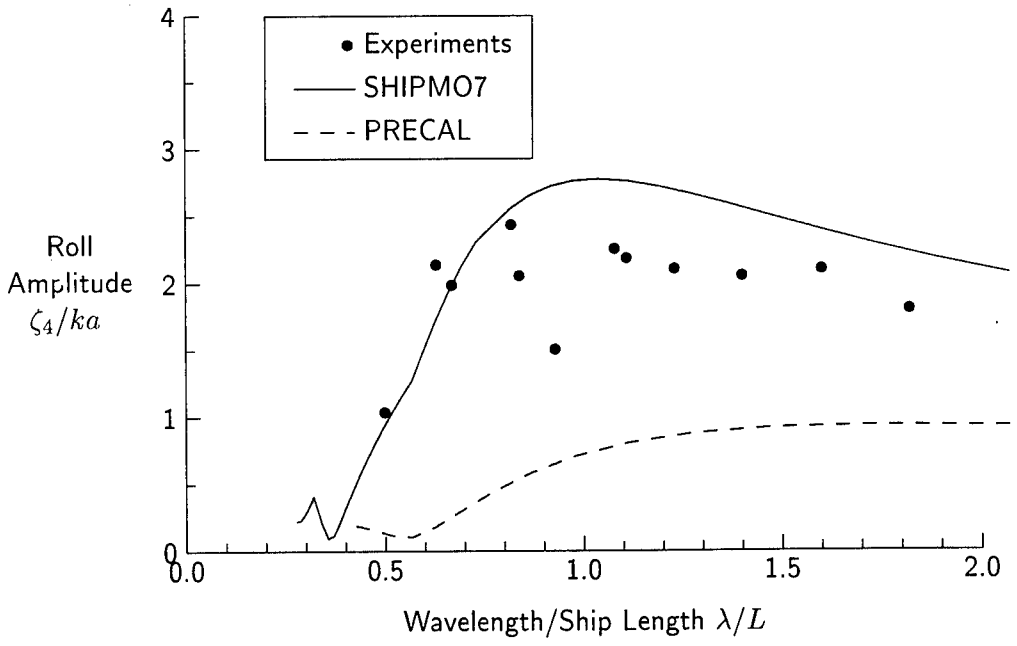

Figure 35: Roll, $Fn = 0.29$, $\beta = 30$ degrees

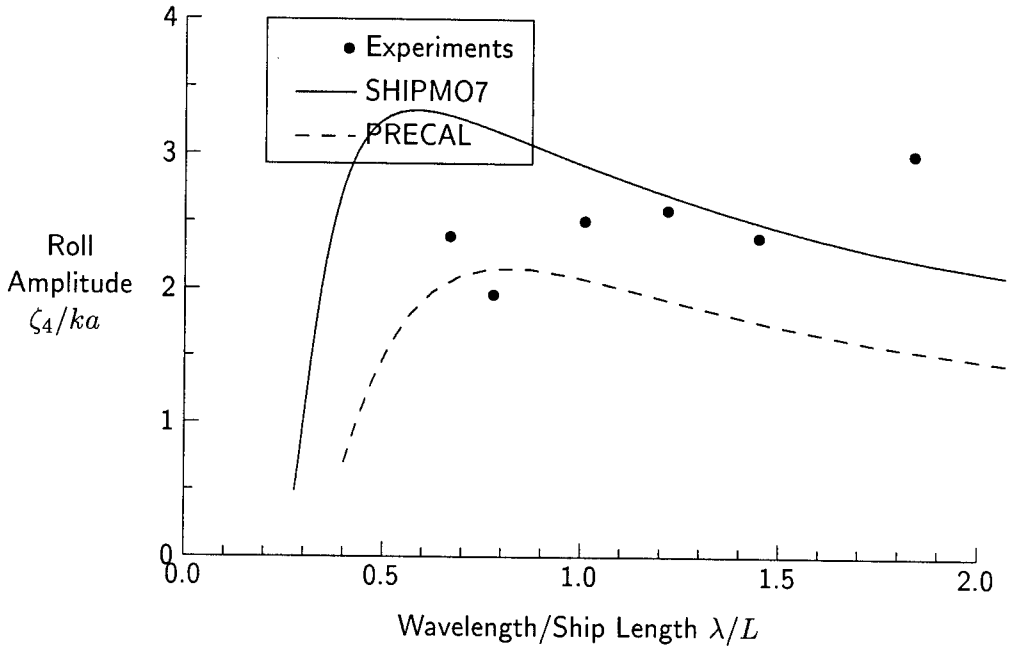

Figure 36: Roll, $Fn = 0.29$, $\beta = 60$ degrees

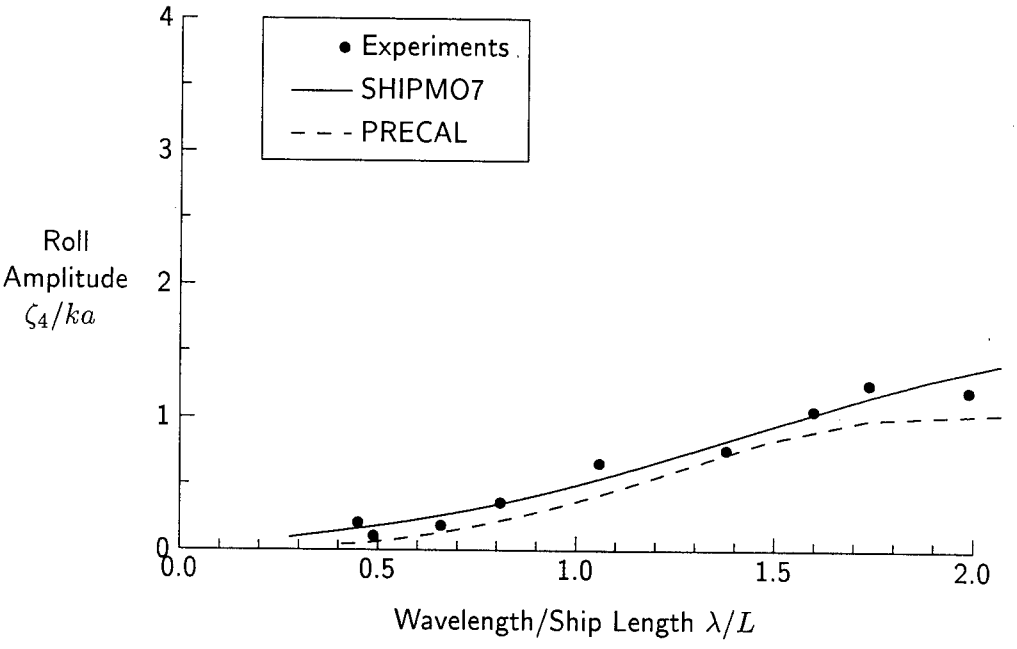

Figure 37: Roll, $Fn = 0.29$, $\beta = 90$ degrees

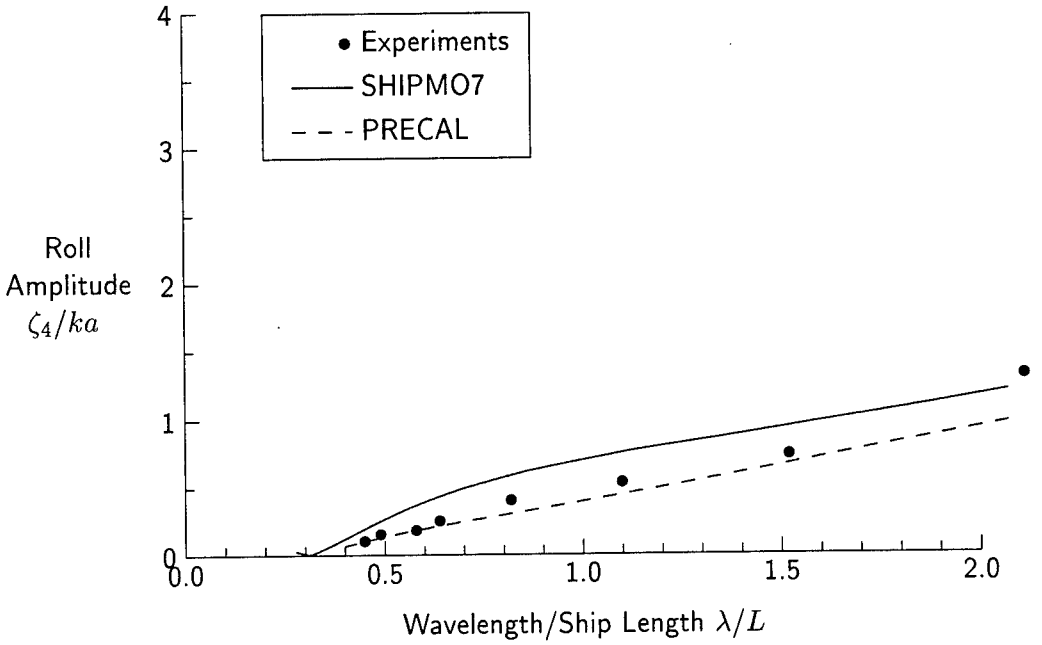

Figure 38: Roll, $Fn = 0.29$, $\beta = 120$ degrees

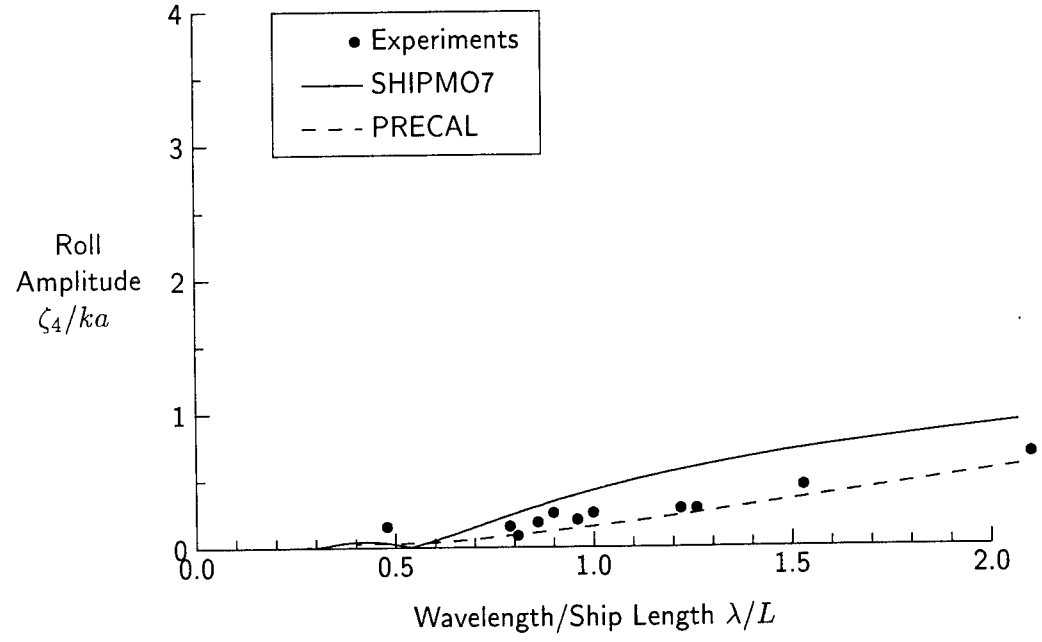

Figure 39: Roll, $Fn = 0.29$, $\beta = 150$ degrees

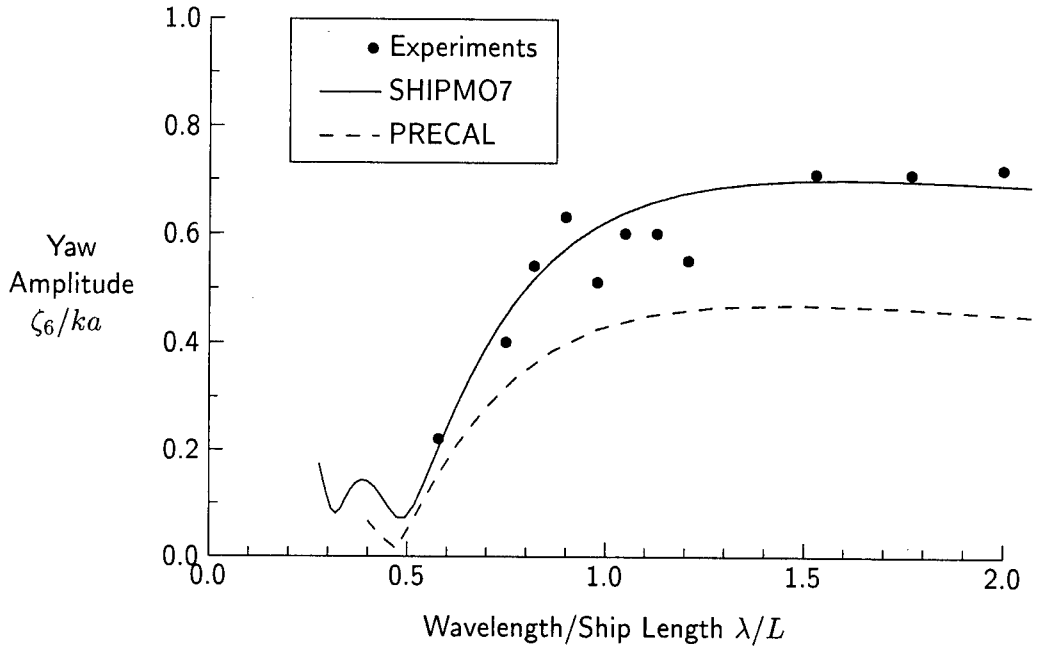

Figure 40: Yaw, $Fn = 0.21$, $\beta = 30$ degrees

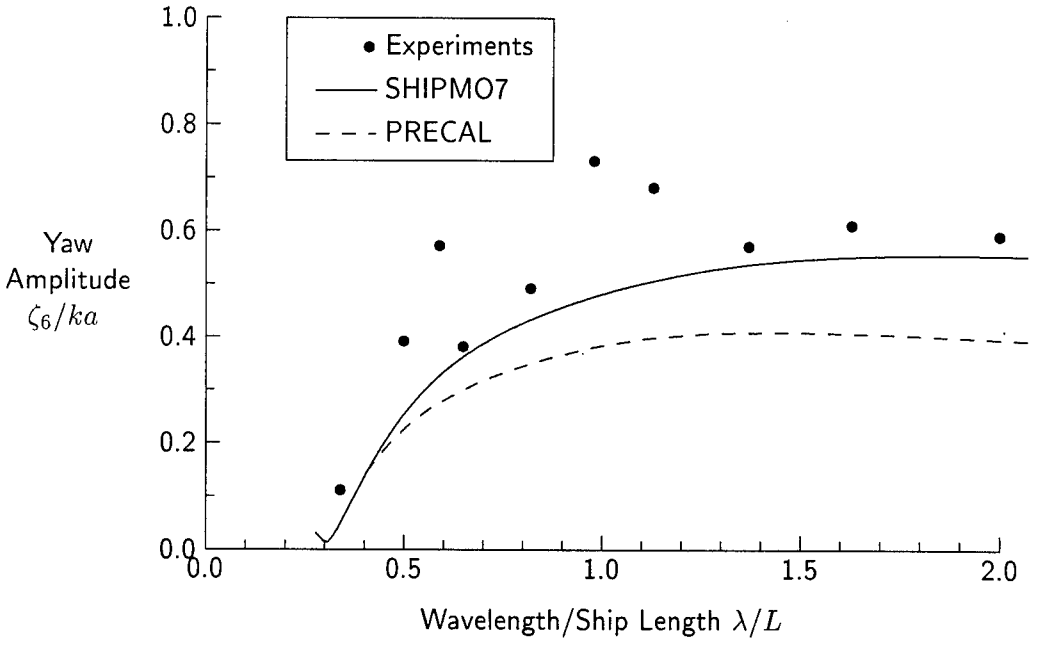

Figure 41: Yaw, $Fn = 0.21$, $\beta = 60$ degrees

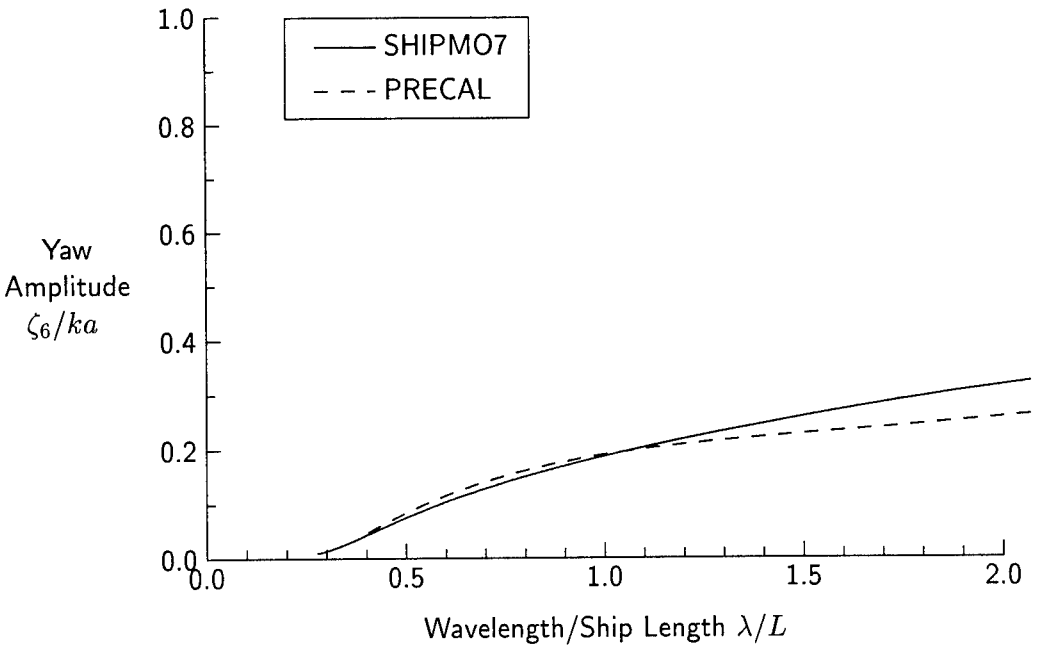

Figure 42: Yaw, $Fn = 0.21$, $\beta = 120$ degrees

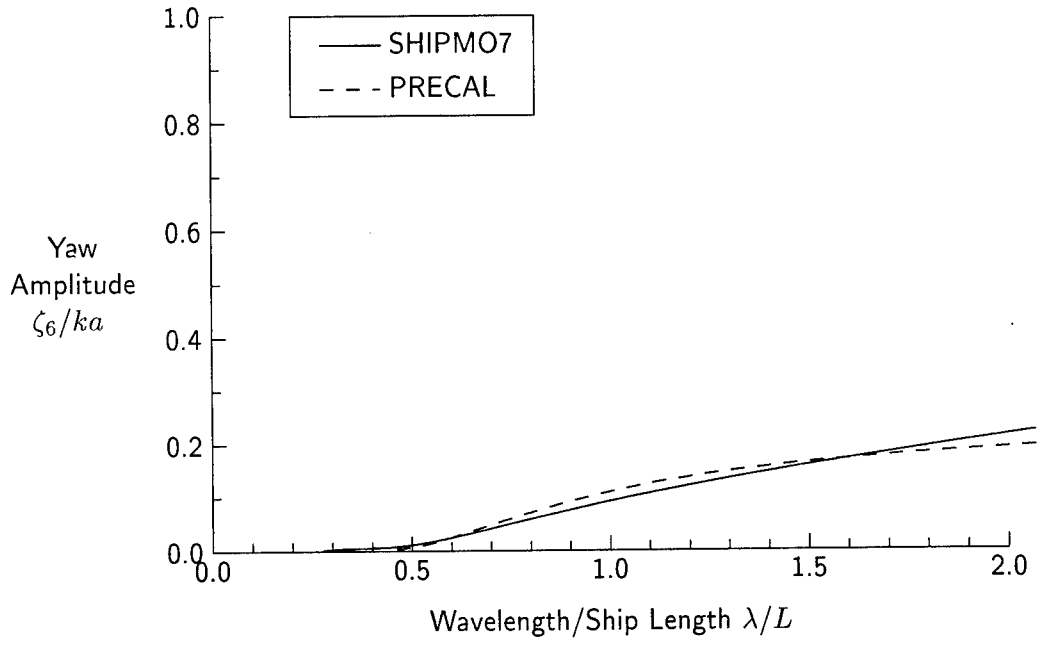

Figure 43: Yaw, $Fn = 0.21$, $\beta = 150$ degrees

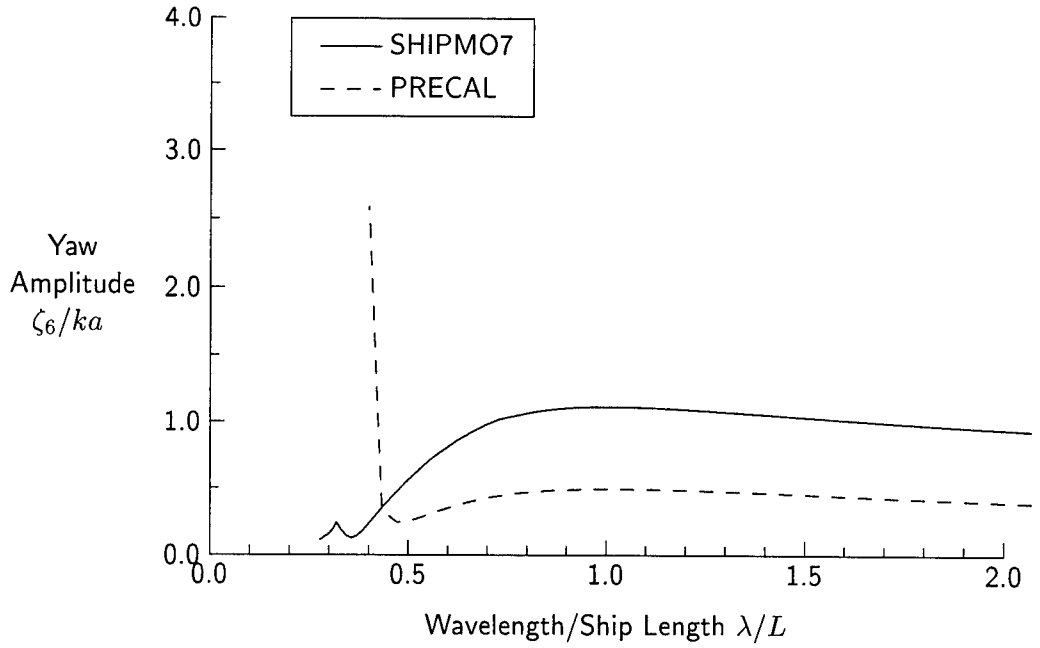

Figure 44: Yaw, $Fn = 0.29$, $\beta = 30$ degrees

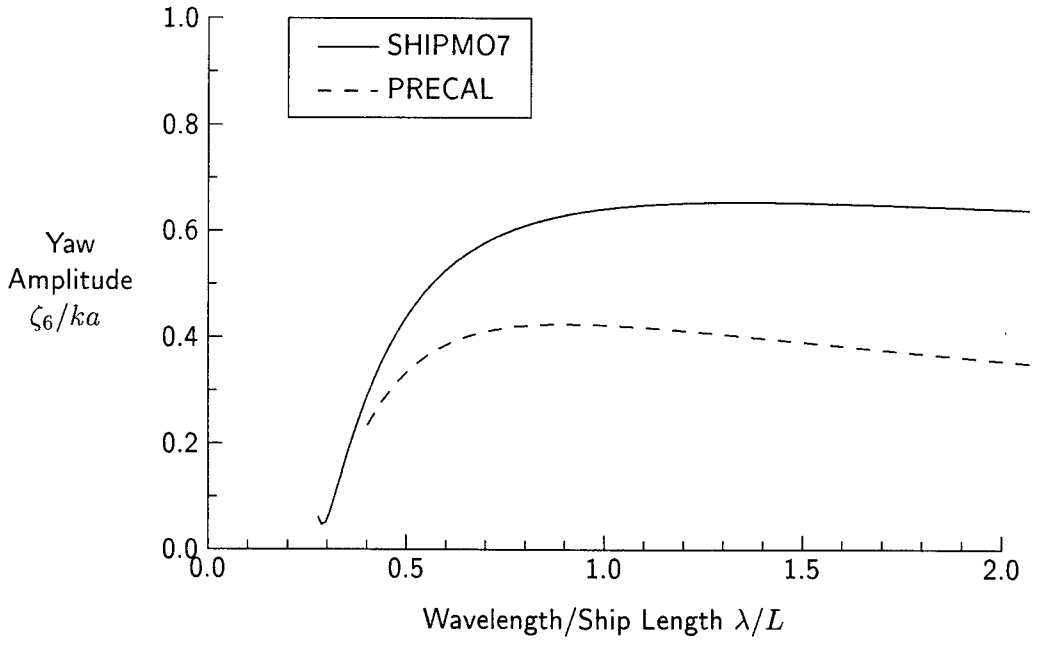

Figure 45: Yaw, $Fn = 0.29$, $\beta = 60$ degrees

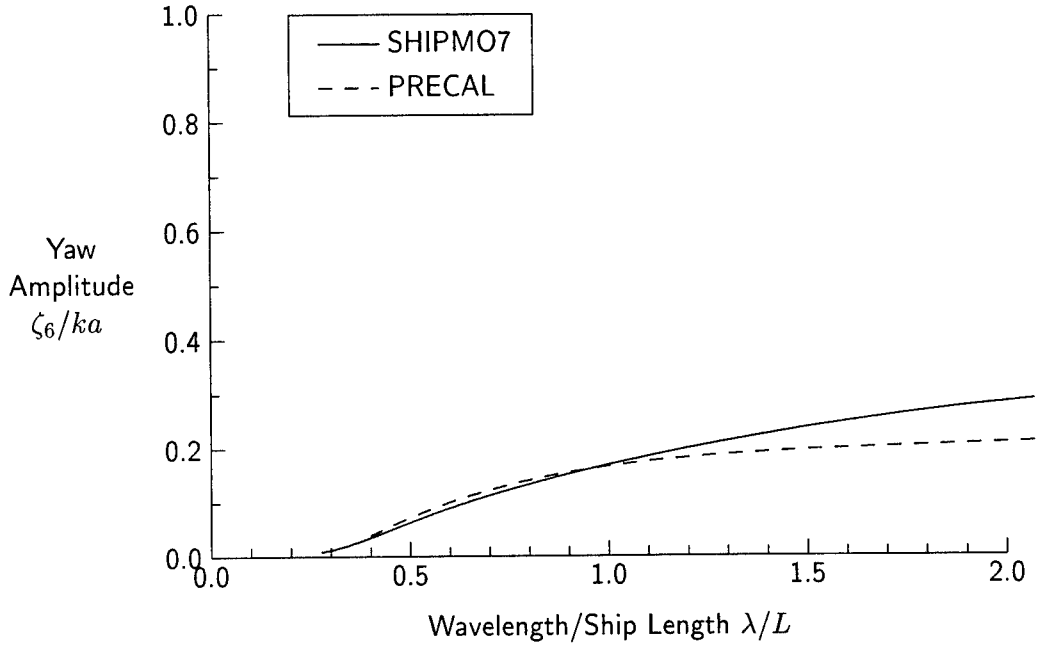

Figure 46: Yaw, $Fn = 0.29$, $\beta = 120$ degrees

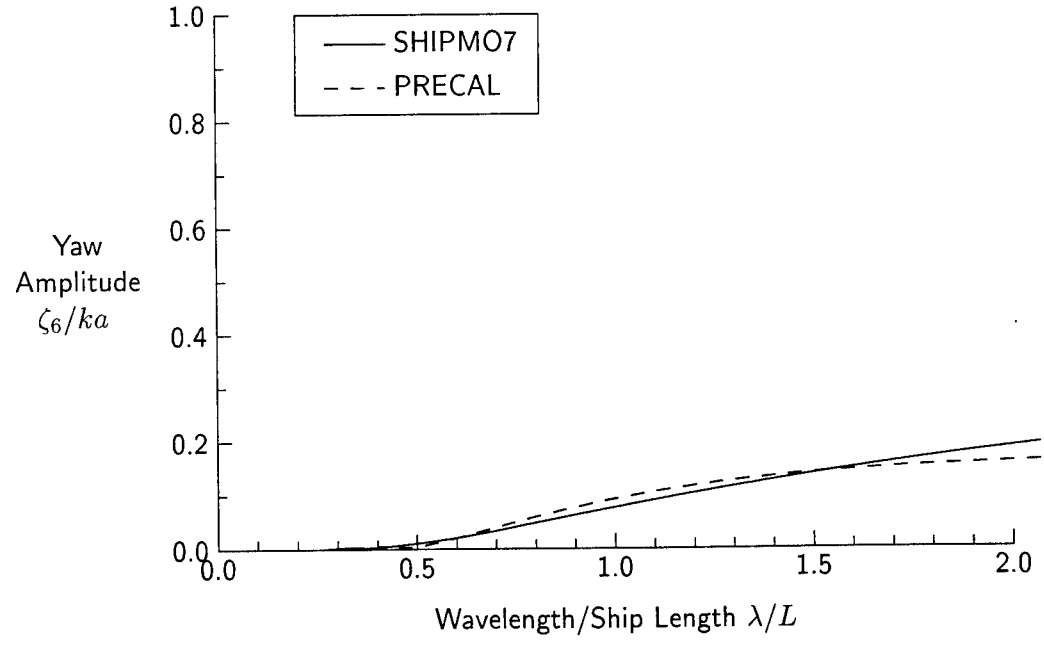

Figure 47: Yaw, $Fn = 0.29$, $\beta = 150$ degrees

C.2 Sea Loads

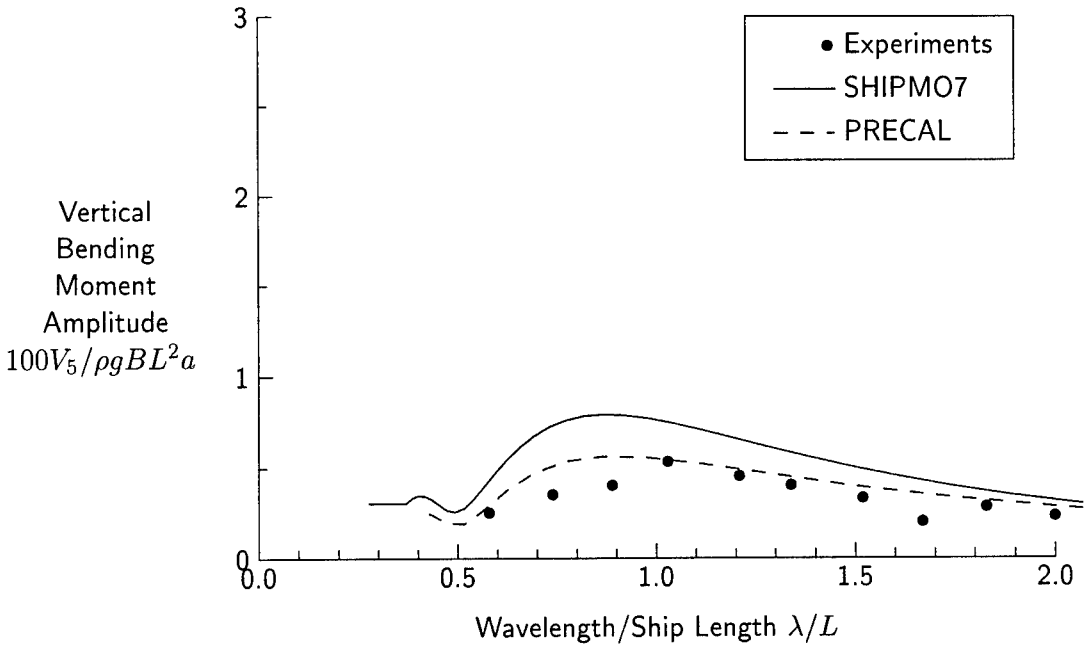

Figure 48: Vertical Bending Moment at Station 5, $Fn = 0.21$, $\beta = 0$ degrees

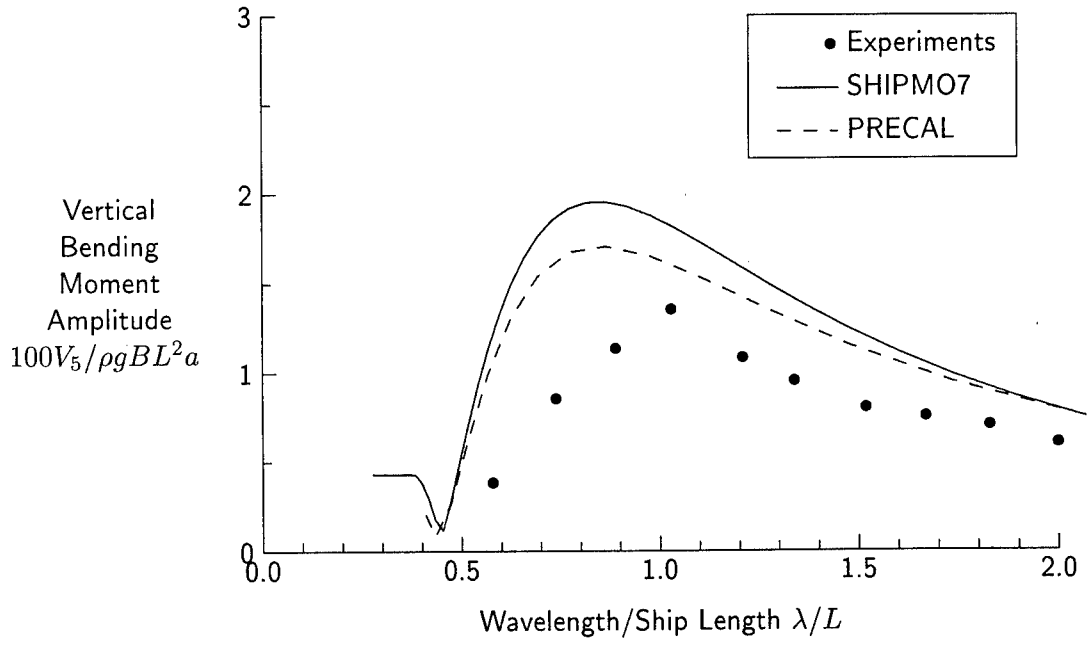

Figure 49: Vertical Bending Moment at Station 10, $Fn = 0.21$, $\beta = 0$ degrees

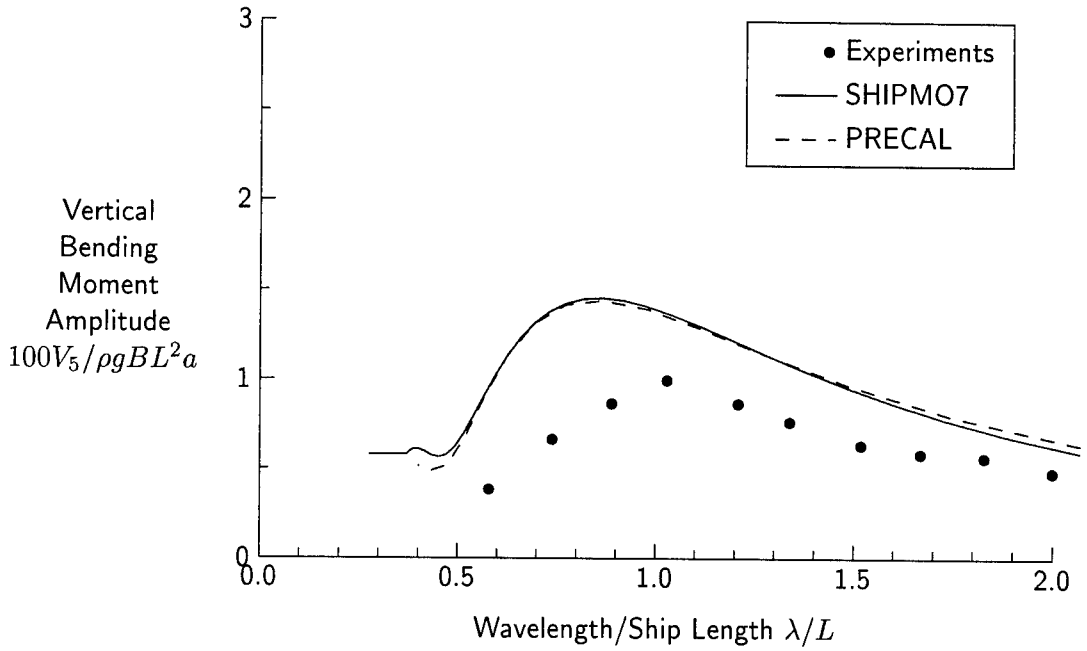

Figure 50: Vertical Bending Moment at Station 13, $Fn = 0.21$, $\beta = 0$ degrees

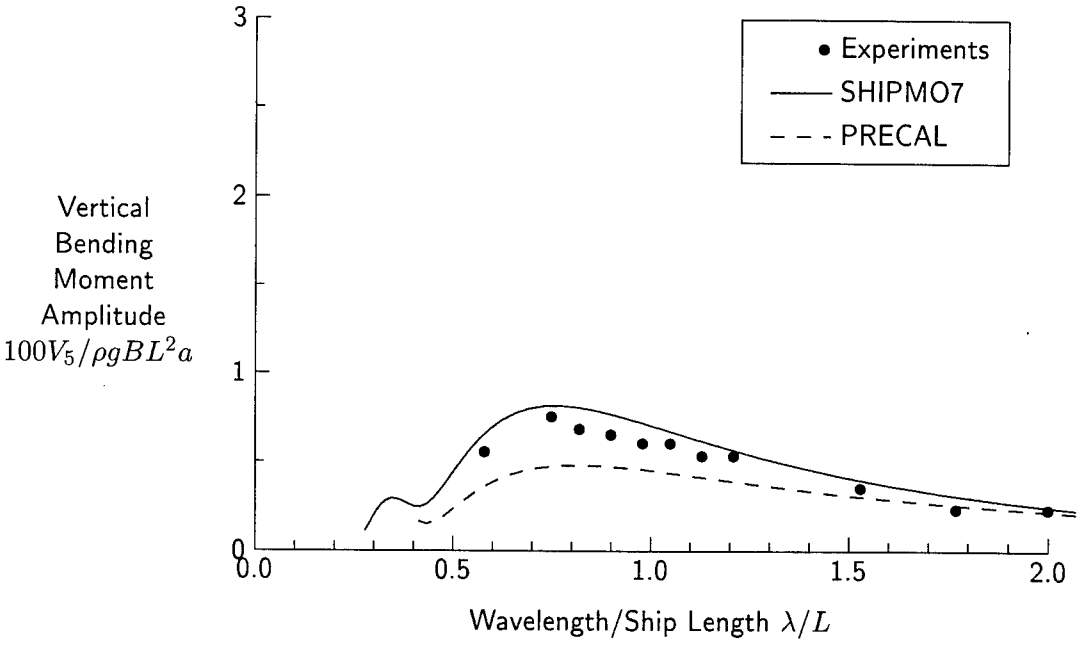

Figure 51: Vertical Bending Moment at Station 5, $Fn = 0.21$, $\beta = 30$ degrees

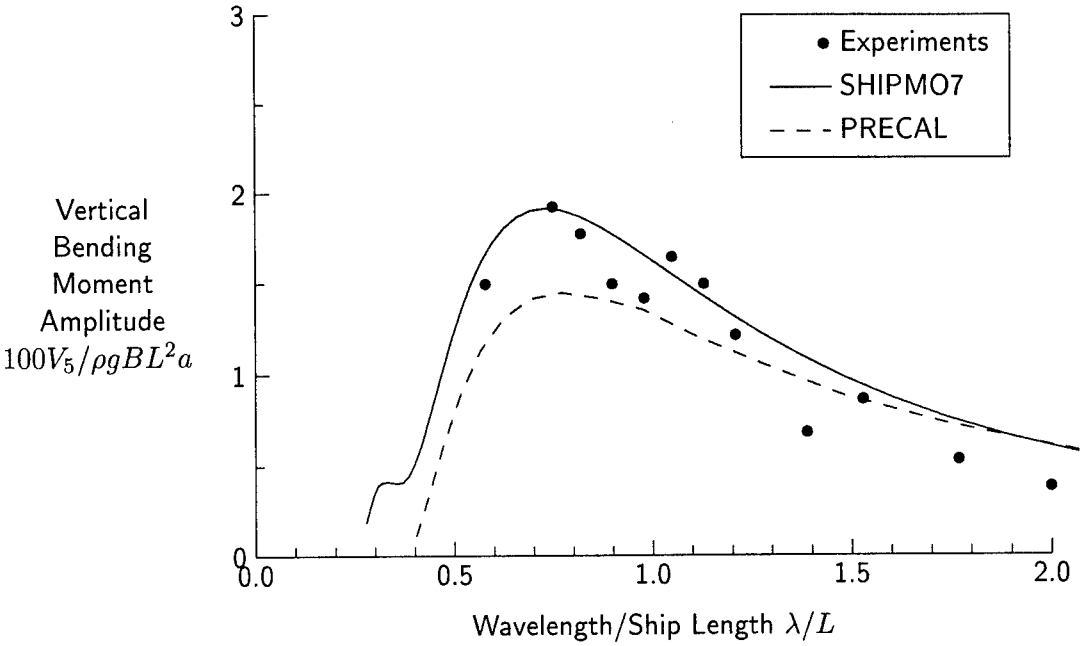

Figure 52: Vertical Bending Moment at Station 10, $Fn = 0.21$, $\beta = 30$ degrees

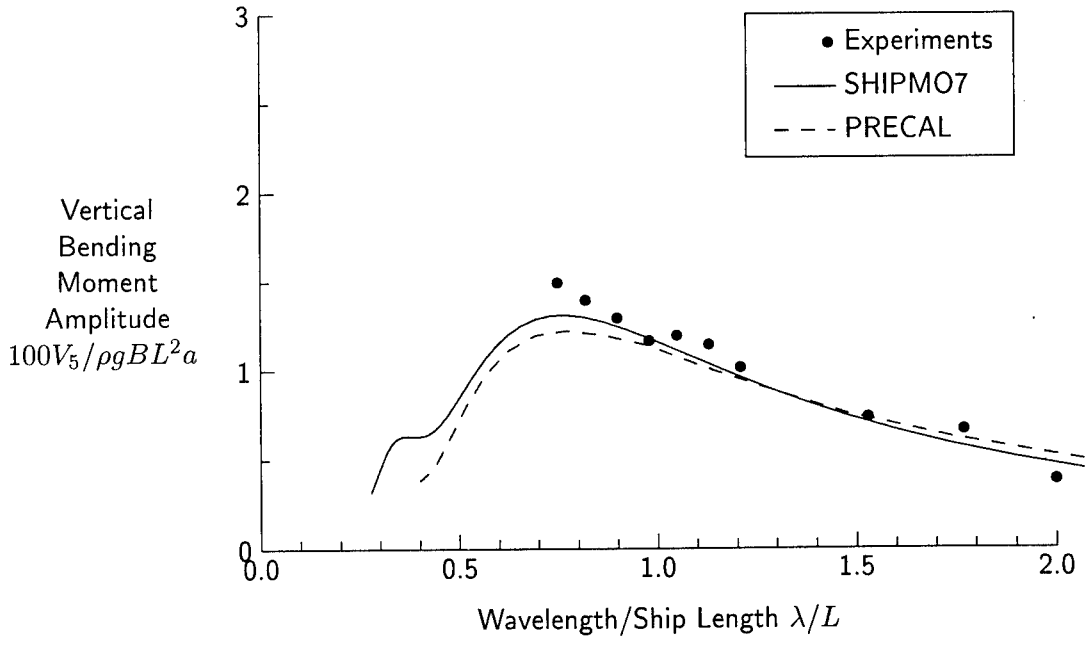

Figure 53: Vertical Bending Moment at Station 13, $Fn = 0.21$, $\beta = 30$ degrees

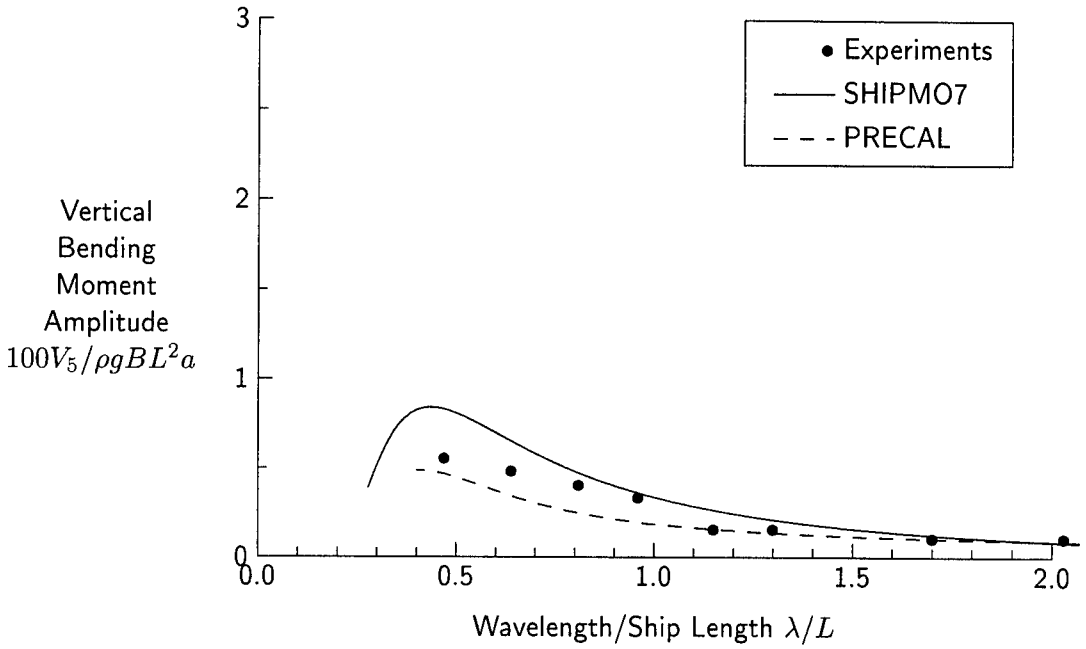

Figure 54: Vertical Bending Moment at Station 5, $Fn = 0.21$, $\beta = 60$ degrees

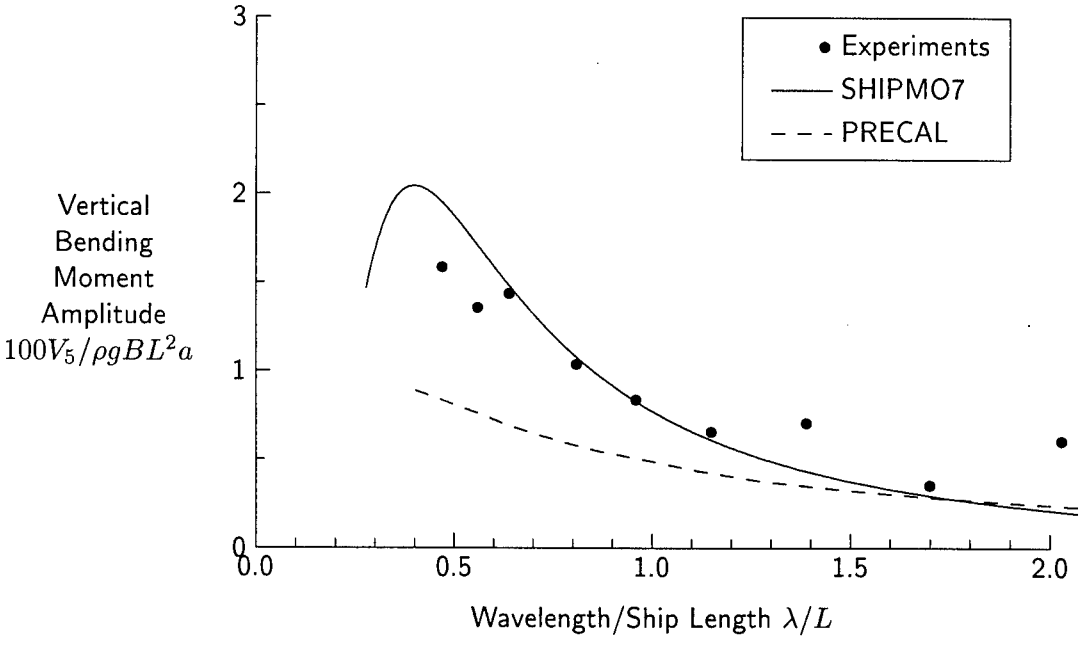

Figure 55: Vertical Bending Moment at Station 10, $Fn = 0.21$, $\beta = 60$ degrees

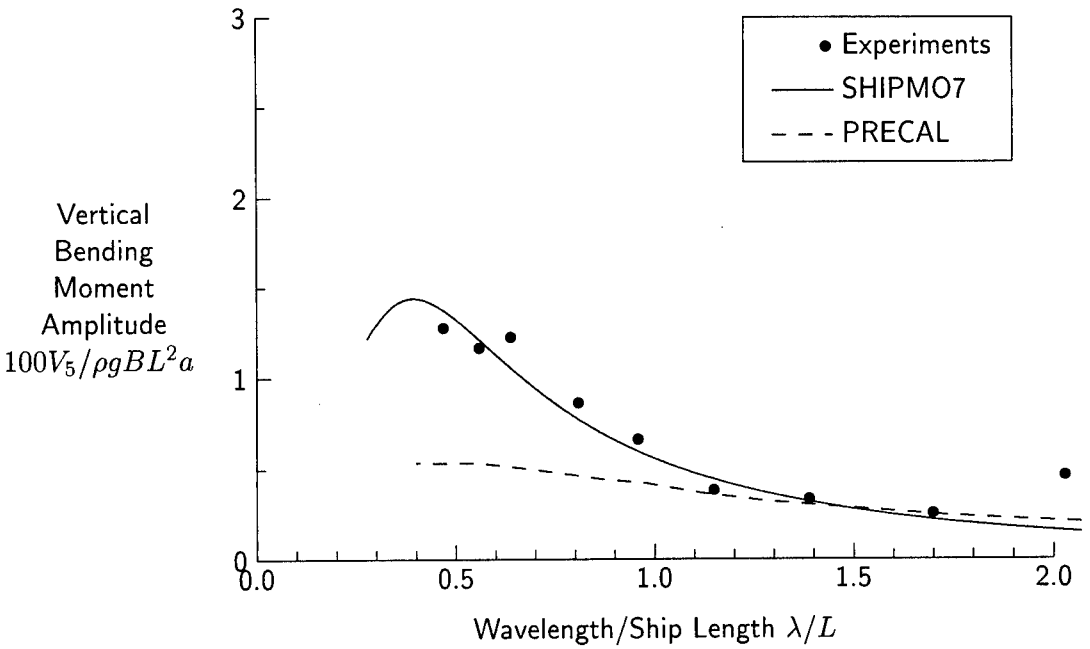

Figure 56: Vertical Bending Moment at Station 13, $Fn = 0.21$, $\beta = 60$ degrees

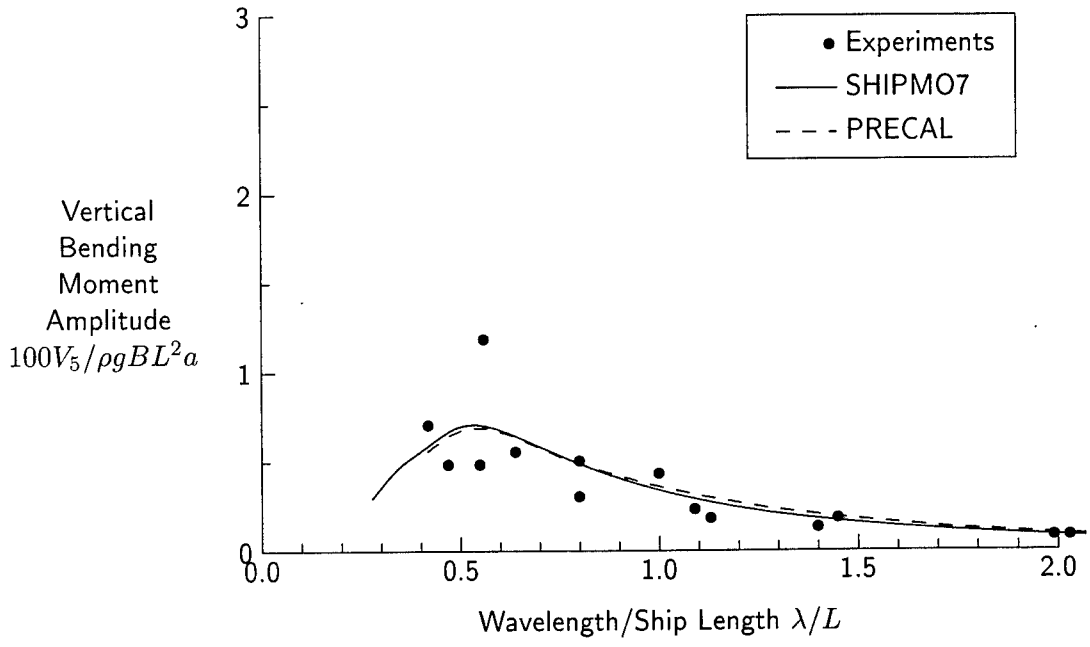

Figure 57: Vertical Bending Moment at Station 5, $Fn = 0.21$, $\beta = 120$ degrees

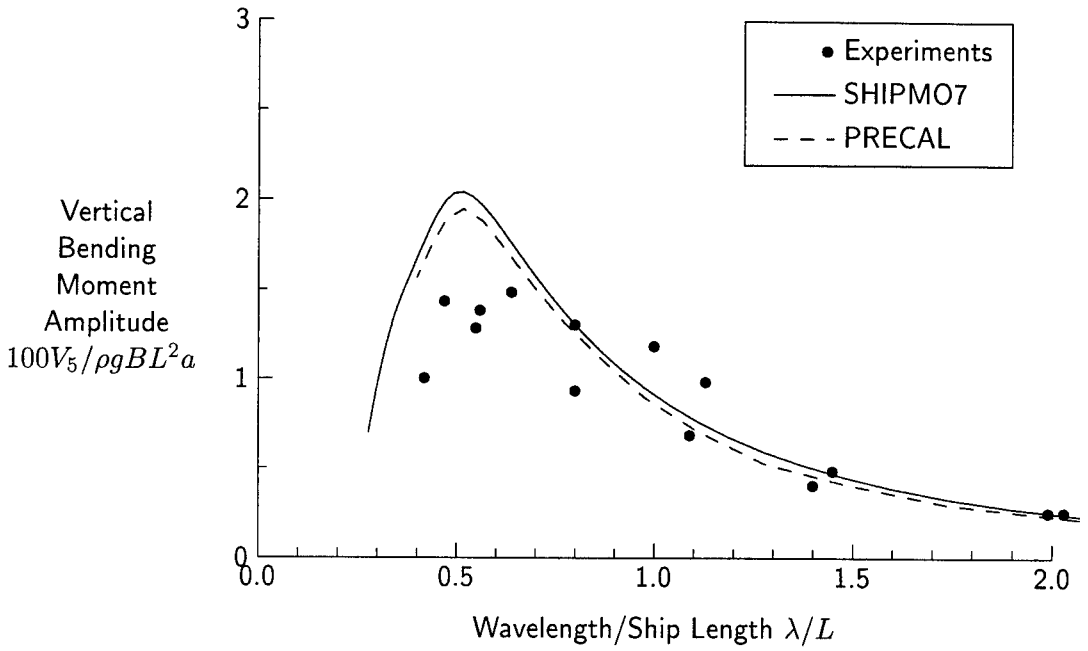

Figure 58: Vertical Bending Moment at Station 10, $Fn = 0.21$, $\beta = 120$ degrees

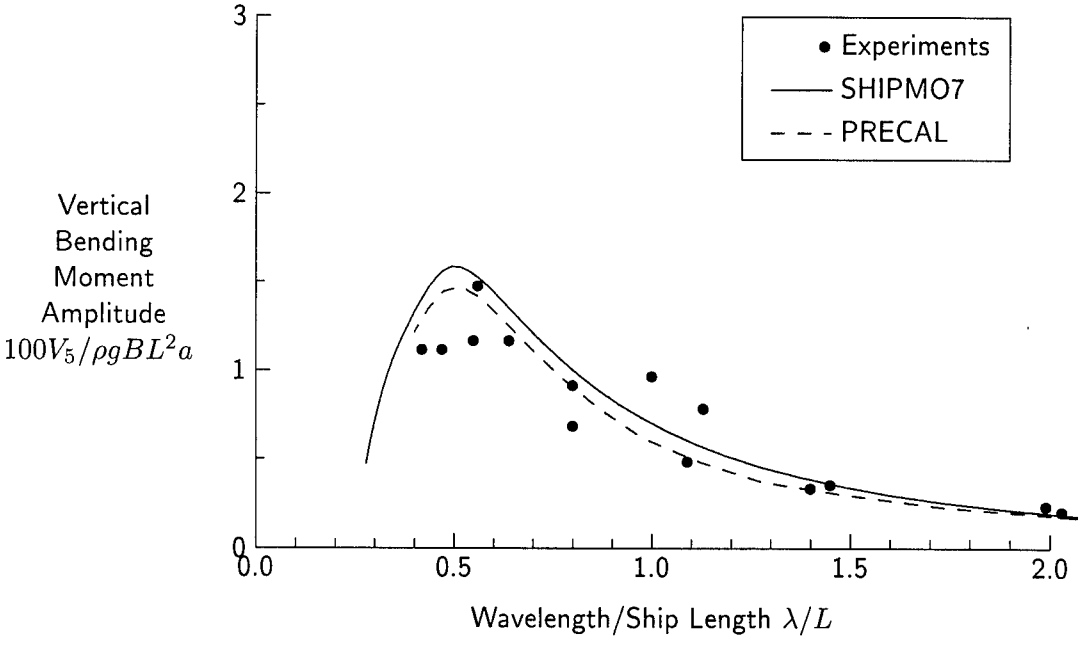

Figure 59: Vertical Bending Moment at Station 13, $Fn = 0.21$, $\beta = 120$ degrees

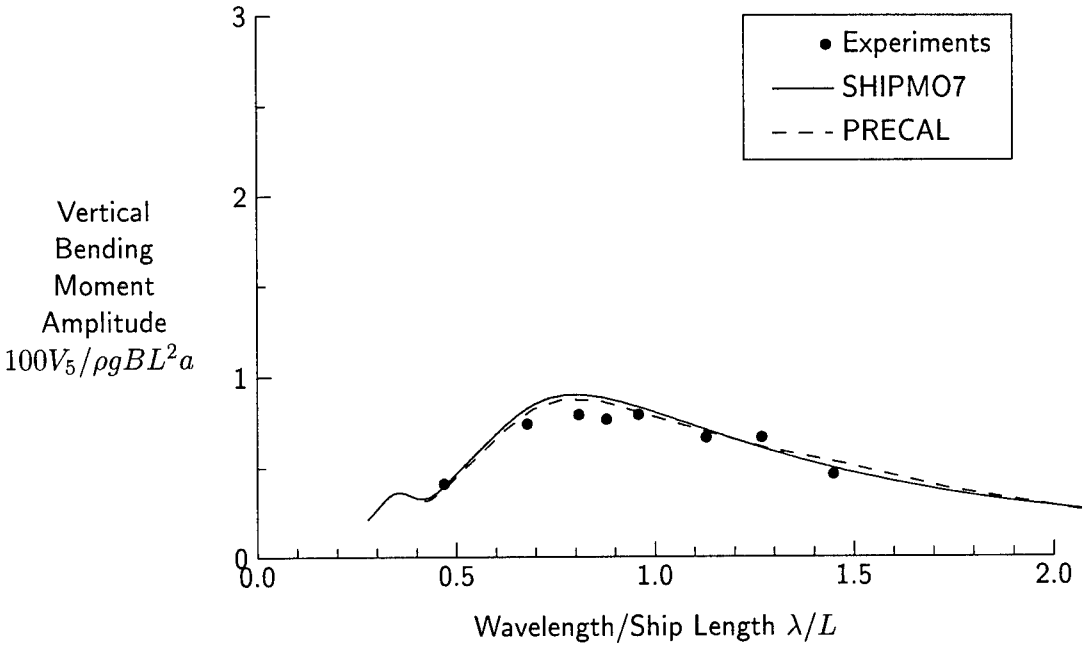

Figure 60: Vertical Bending Moment at Station 5, $Fn = 0.21$, $\beta = 150$ degrees

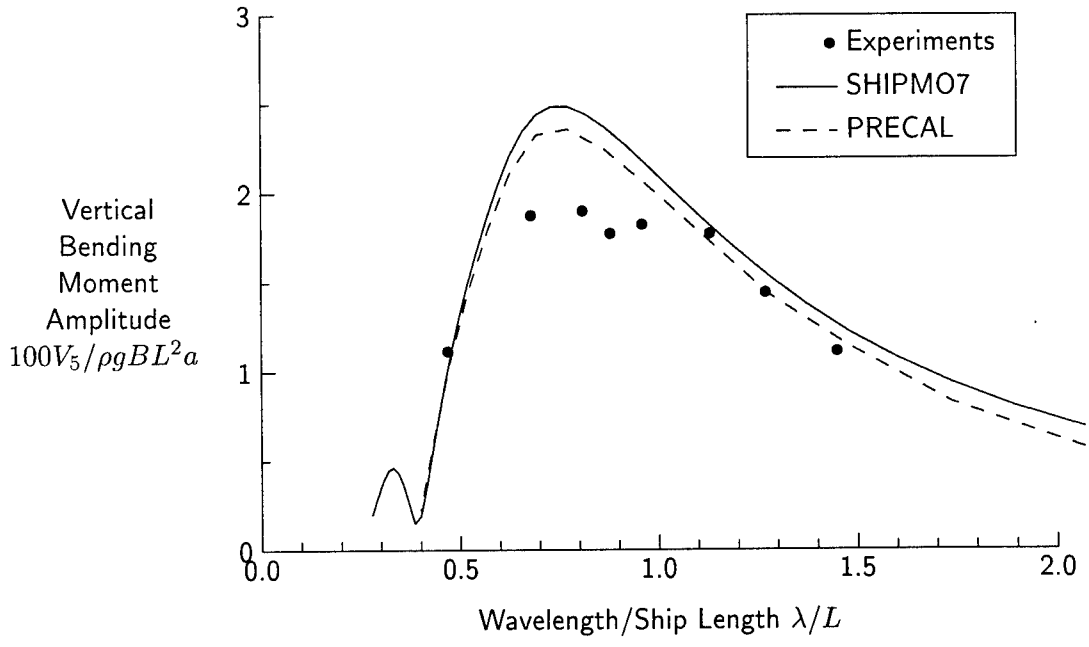

Figure 61: Vertical Bending Moment at Station 10, $Fn = 0.21$, $\beta = 150$ degrees

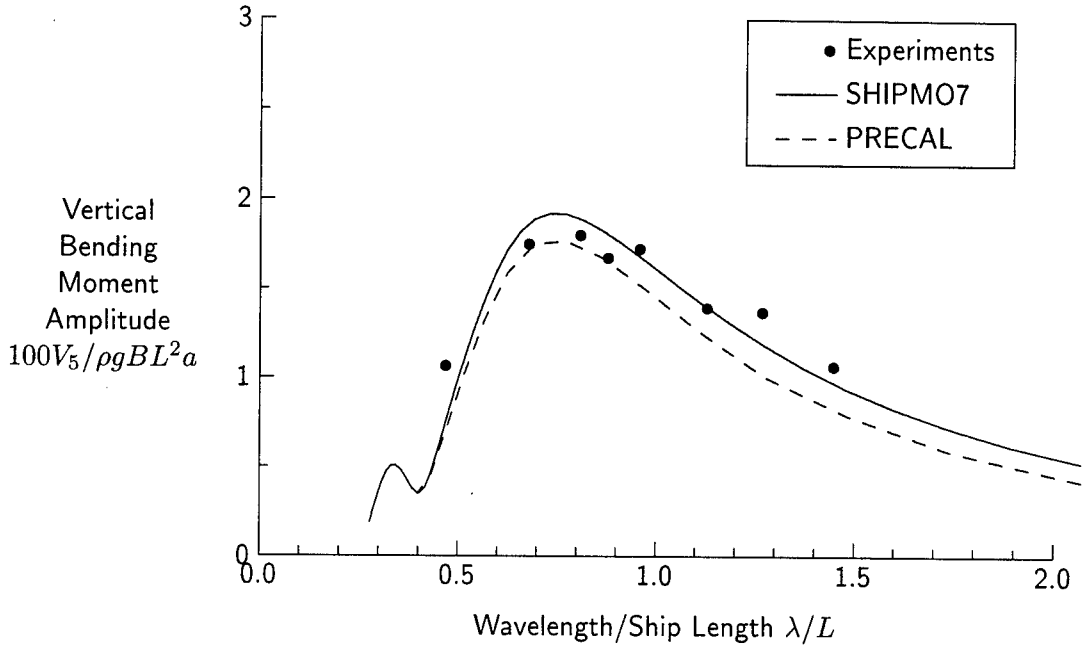

Figure 62: Vertical Bending Moment at Station 13, $Fn = 0.21$, $\beta = 150$ degrees

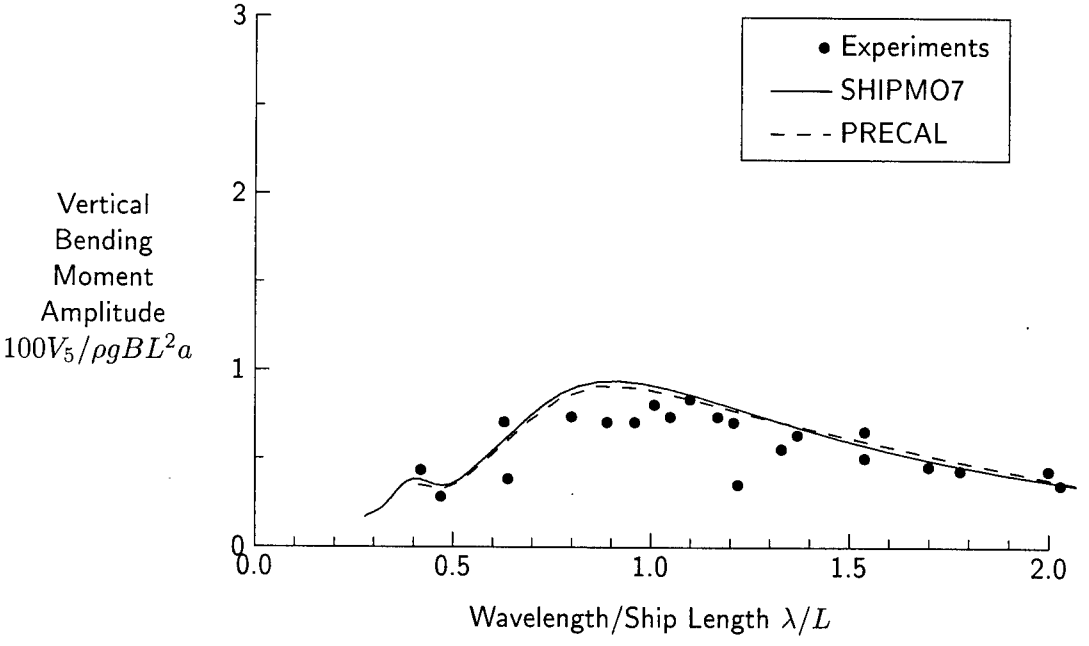

Figure 63: Vertical Bending Moment at Station 5, $Fn = 0.21$, $\beta = 180$ degrees

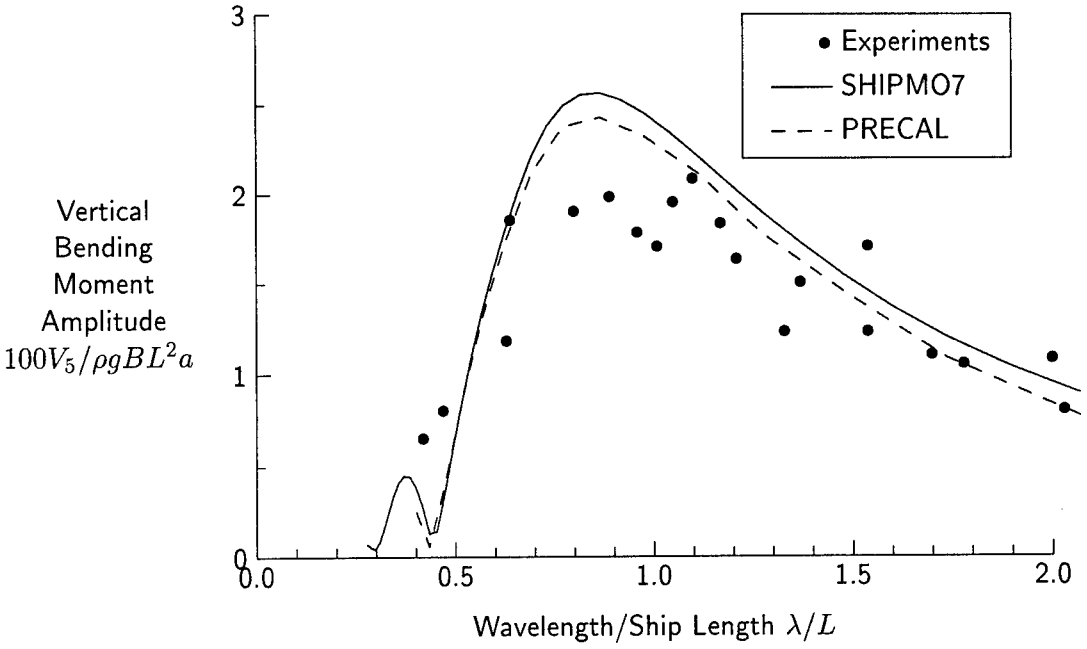

Figure 64: Vertical Bending Moment at Station 10, $Fn = 0.21$, $\beta = 180$ degrees

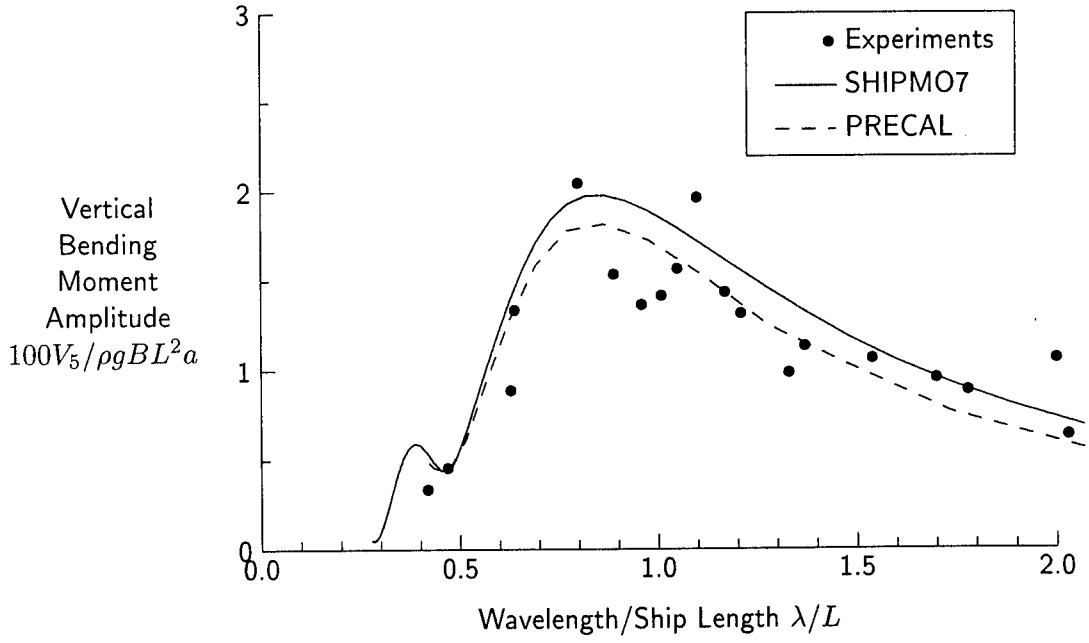

Figure 65: Vertical Bending Moment at Station 13, $Fn = 0.21$, $\beta = 180$ degrees

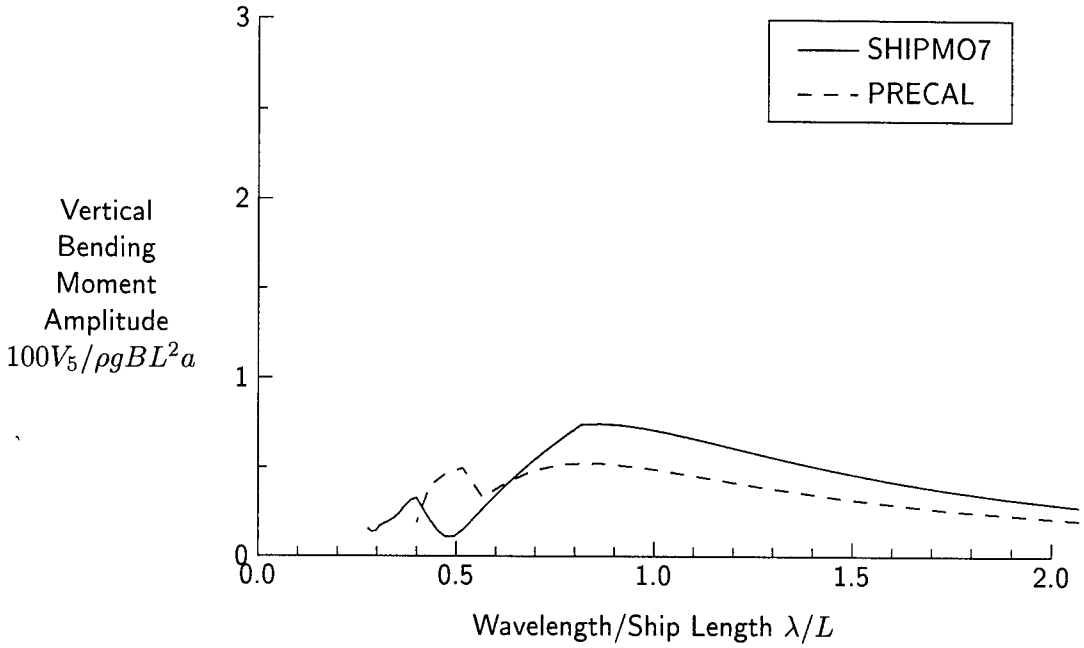

Figure 66: Vertical Bending Moment at Station 5, $Fn = 0.29$, $\beta = 0$ degrees

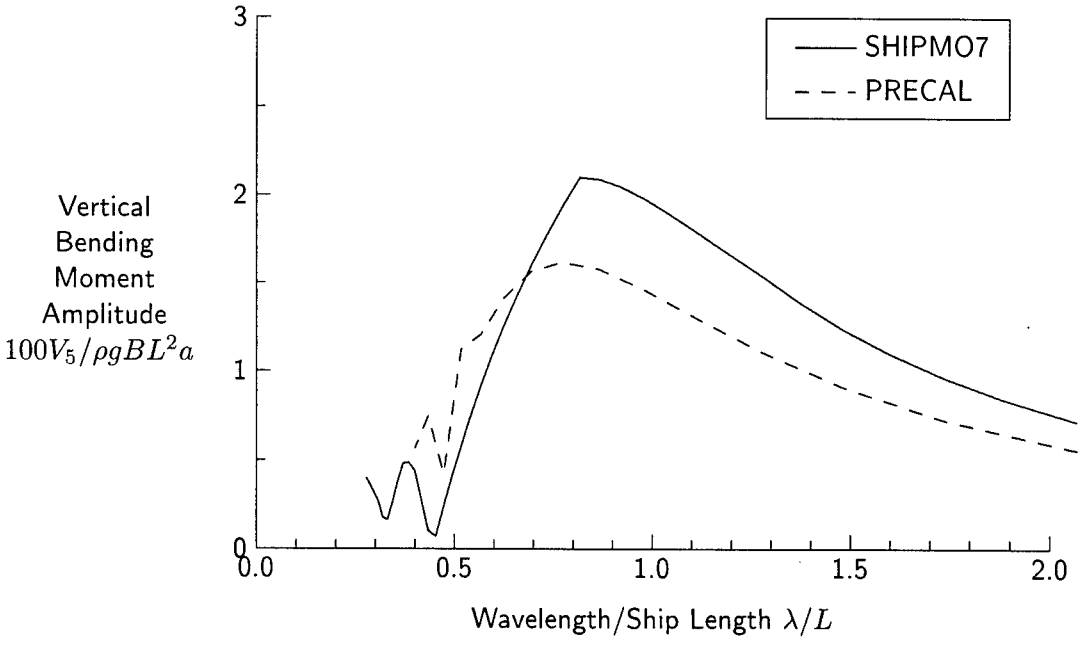

Figure 67: Vertical Bending Moment at Station 10, $Fn = 0.29$, $\beta = 0$ degrees

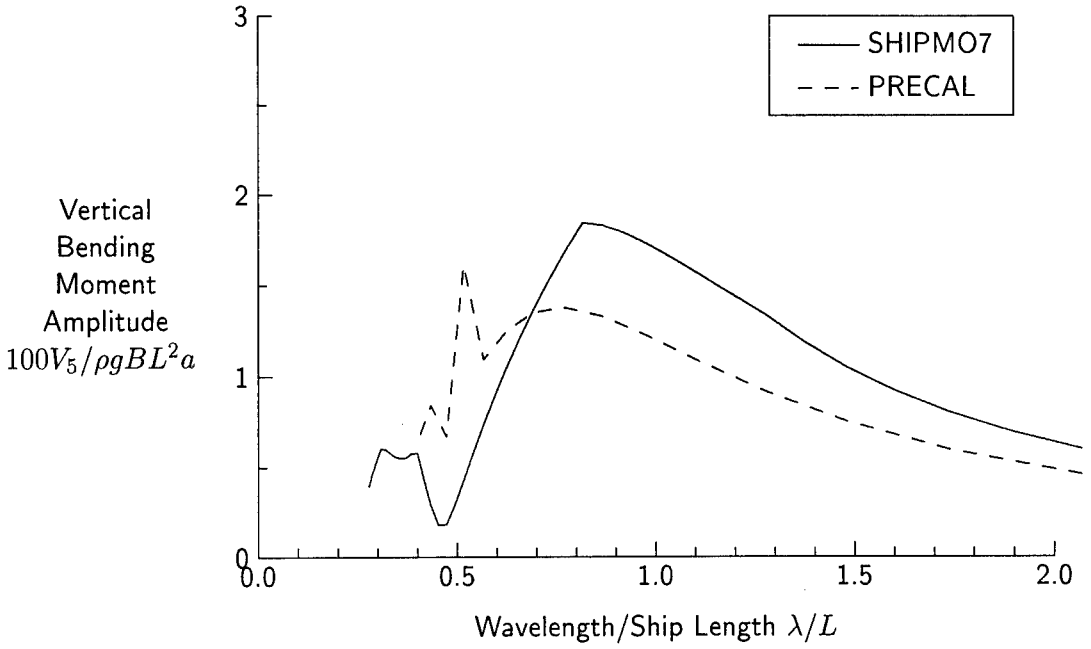

Figure 68: Vertical Bending Moment at Station 13, $Fn = 0.29$, $\beta = 0$ degrees

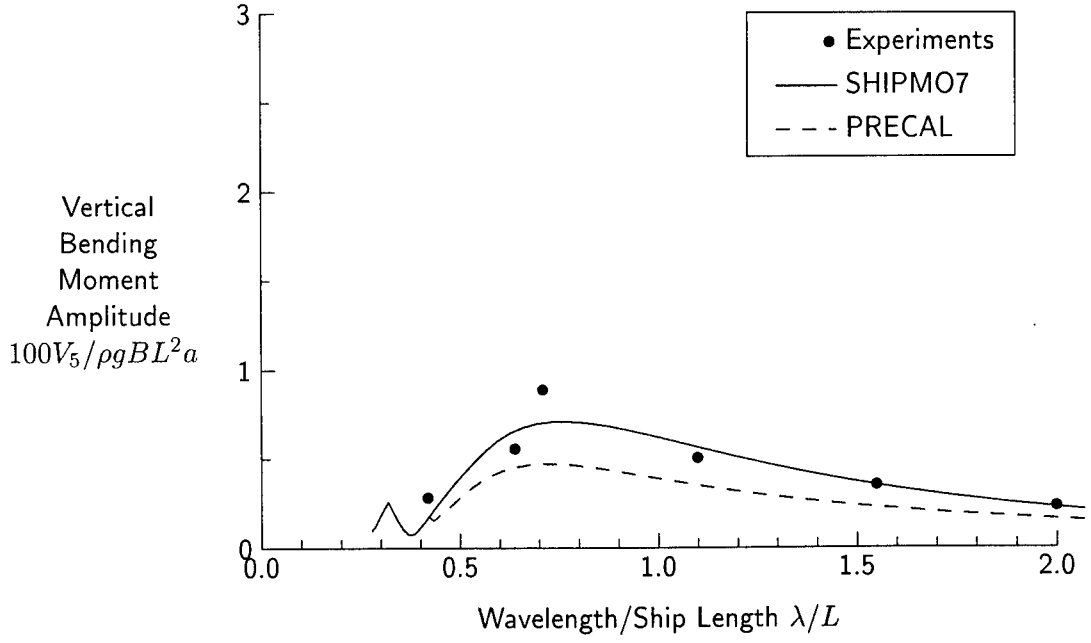

Figure 69: Vertical Bending Moment at Station 5, $Fn = 0.29$, $\beta = 30$ degrees

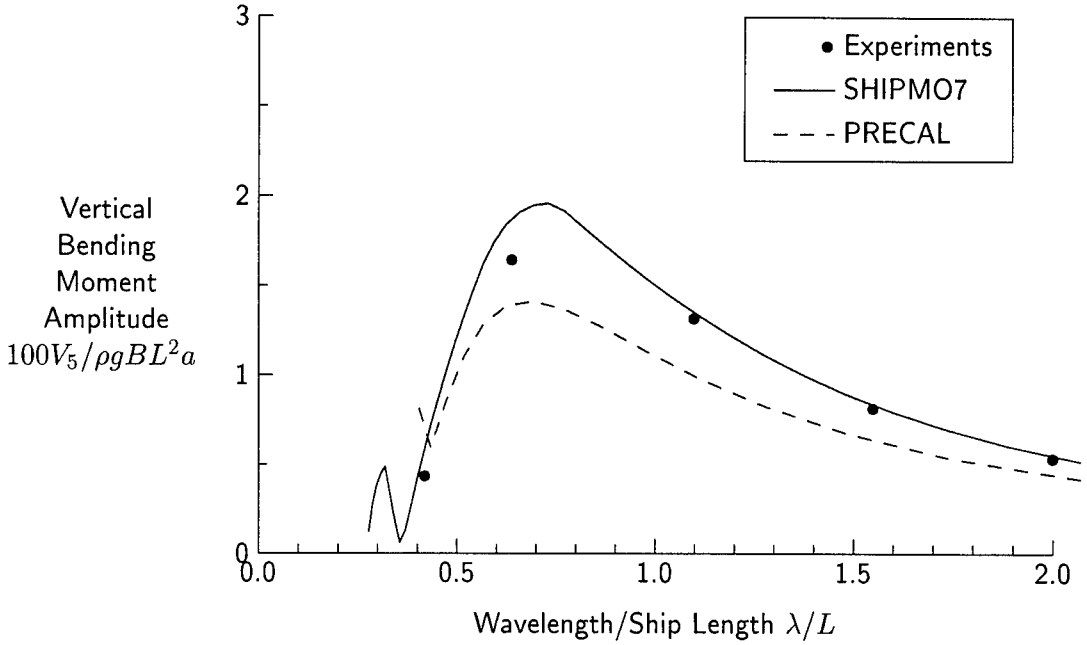

Figure 70: Vertical Bending Moment at Station 10, $Fn = 0.29$, $\beta = 30$ degrees

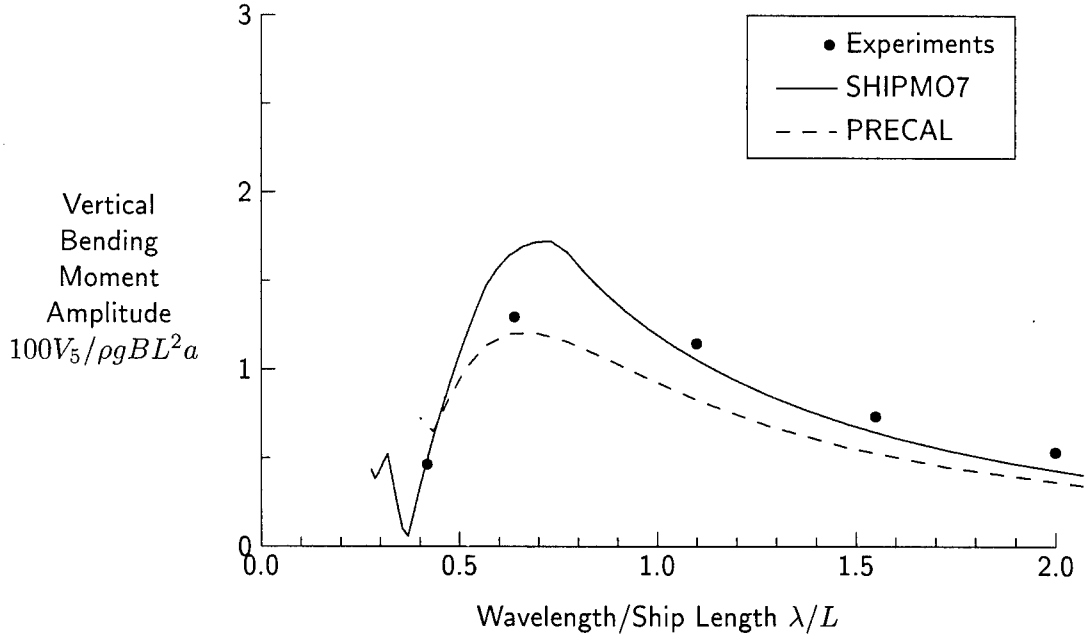

Figure 71: Vertical Bending Moment at Station 13, $Fn = 0.29$, $\beta = 30$ degrees

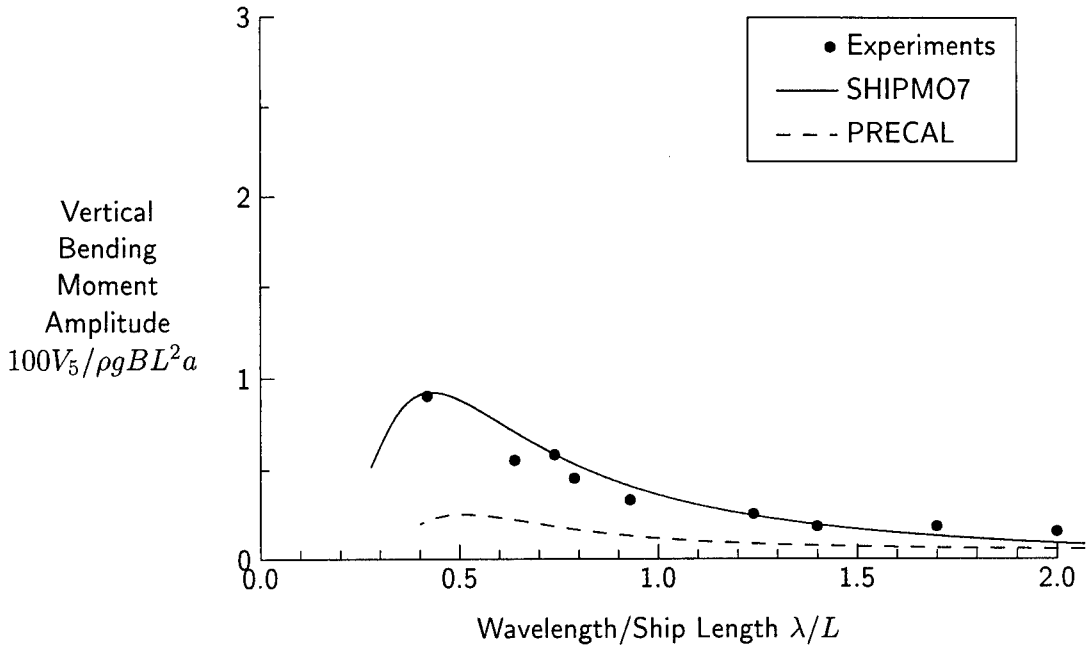

Figure 72: Vertical Bending Moment at Station 5, $Fn = 0.29$, $\beta = 60$ degrees

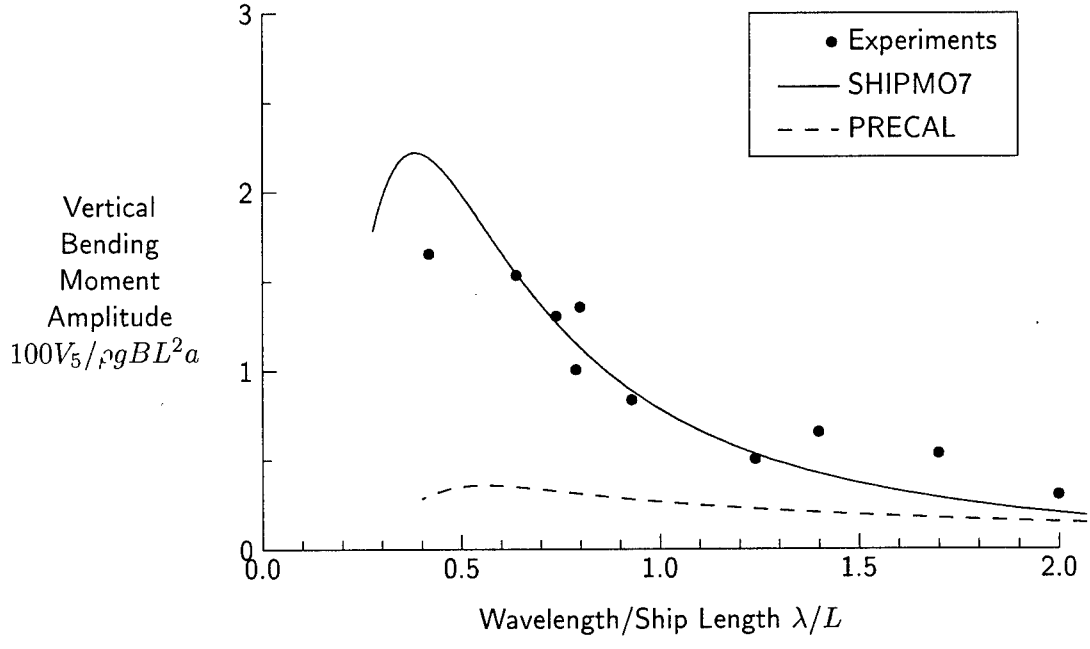

Figure 73: Vertical Bending Moment at Station 10, $Fn = 0.29$, $\beta = 60$ degrees

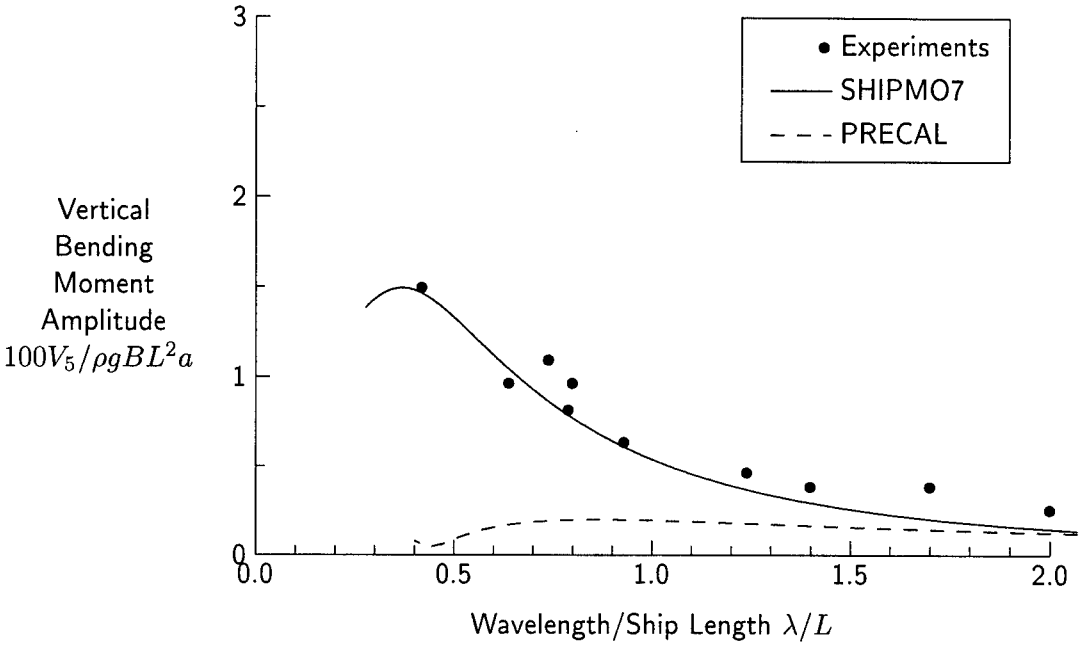

Figure 74: Vertical Bending Moment at Station 13, $Fn = 0.29$, $\beta = 60$ degrees

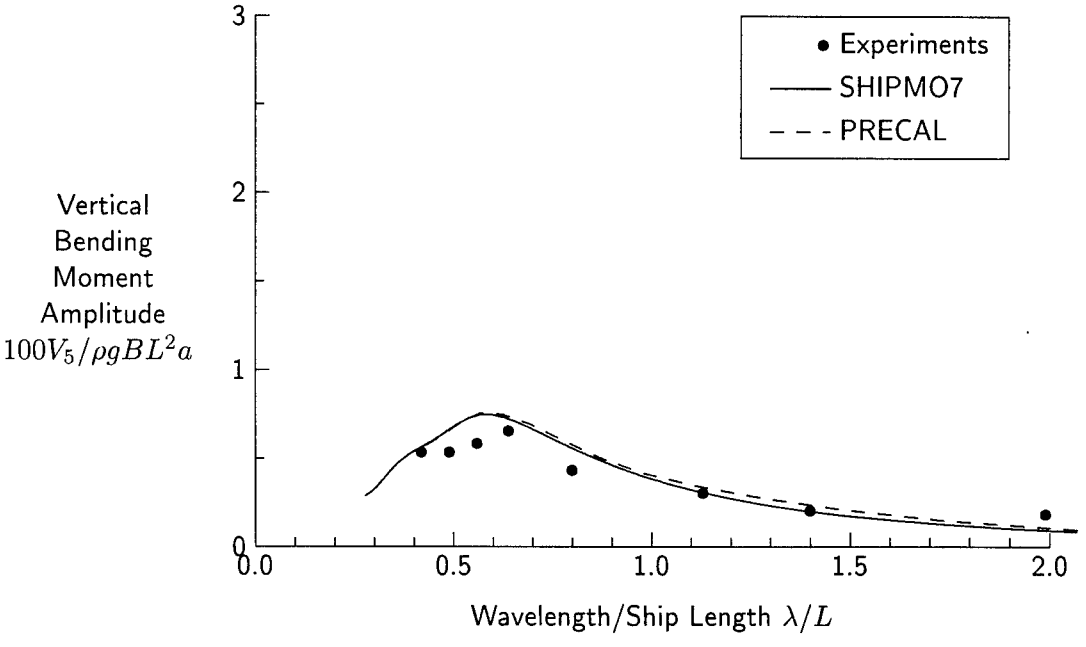

Figure 75: Vertical Bending Moment at Station 5, $Fn = 0.29$, $\beta = 120$ degrees

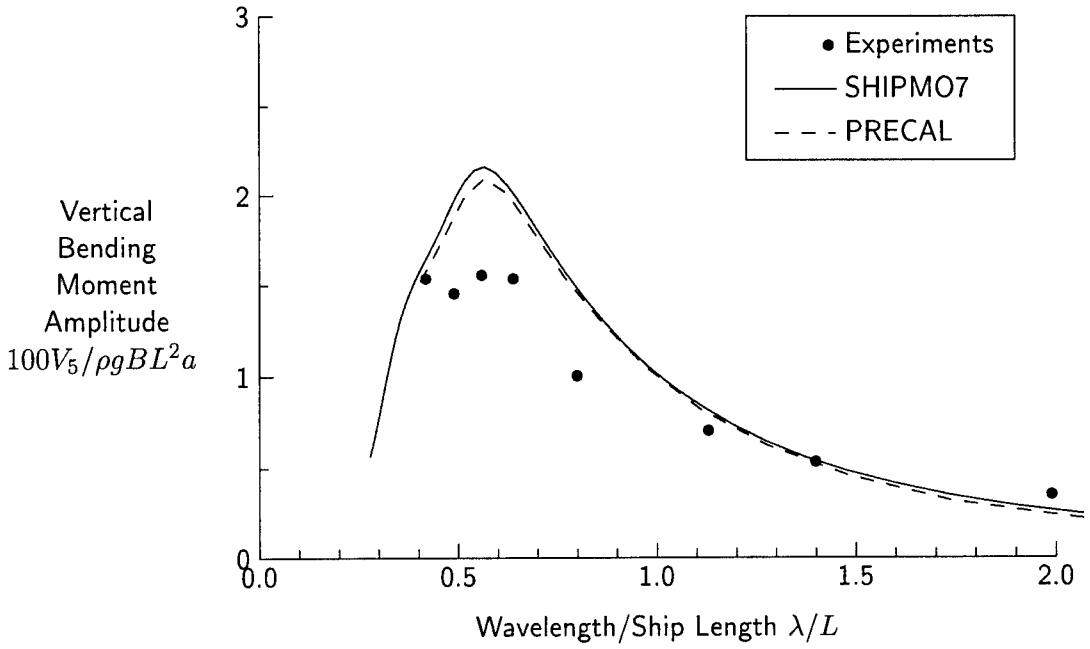

Figure 76: Vertical Bending Moment at Station 10, $Fn = 0.29$, $\beta = 120$ degrees

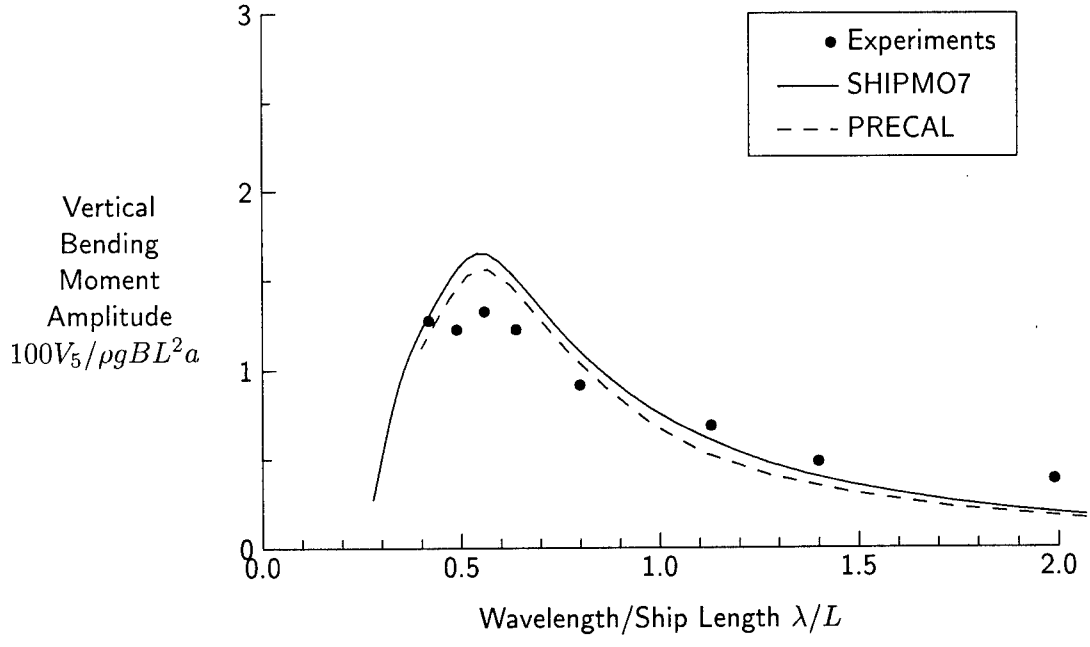

Figure 77: Vertical Bending Moment at Station 13, $Fn = 0.29$, $\beta = 120$ degrees

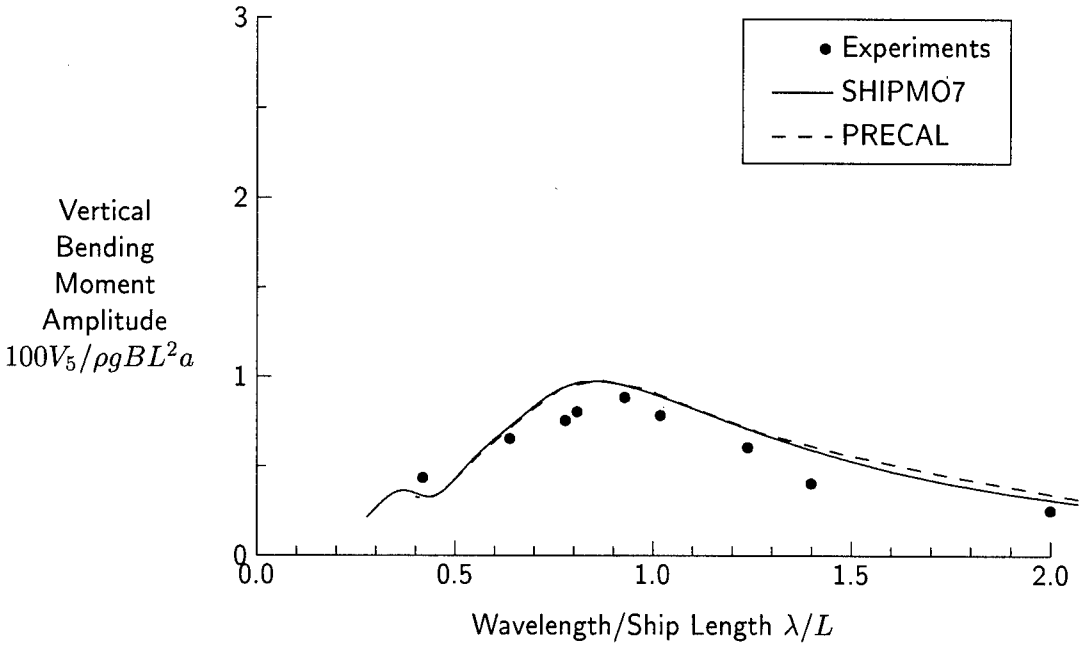

Figure 78: Vertical Bending Moment at Station 5, $Fn = 0.29$, $\beta = 150$ degrees

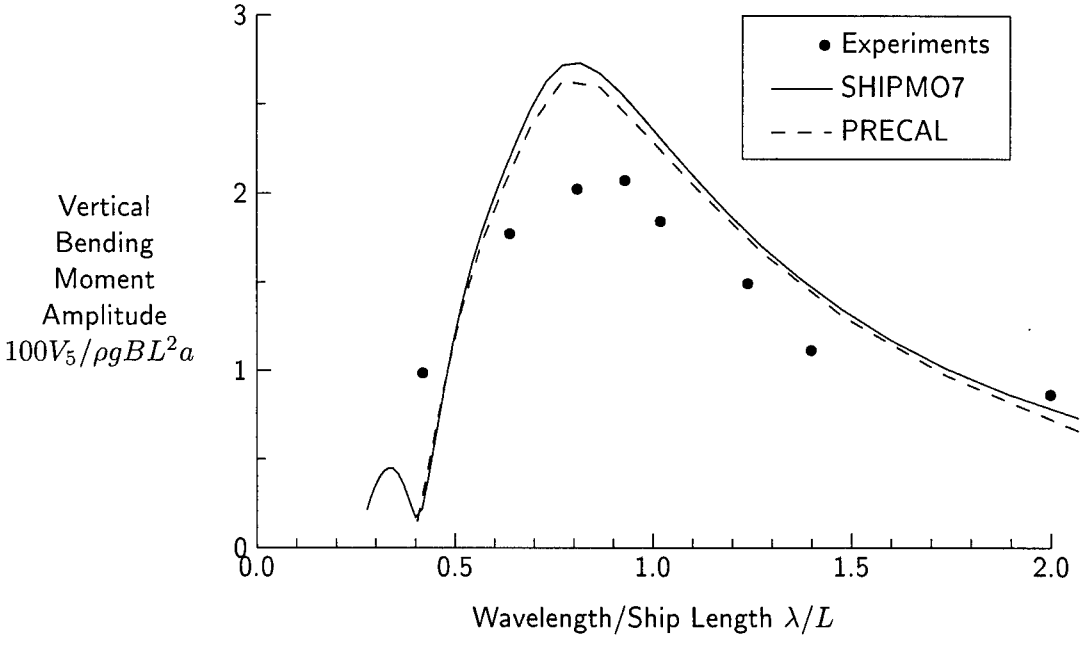

Figure 79: Vertical Bending Moment at Station 10, $Fn = 0.29$, $\beta = 150$ degrees

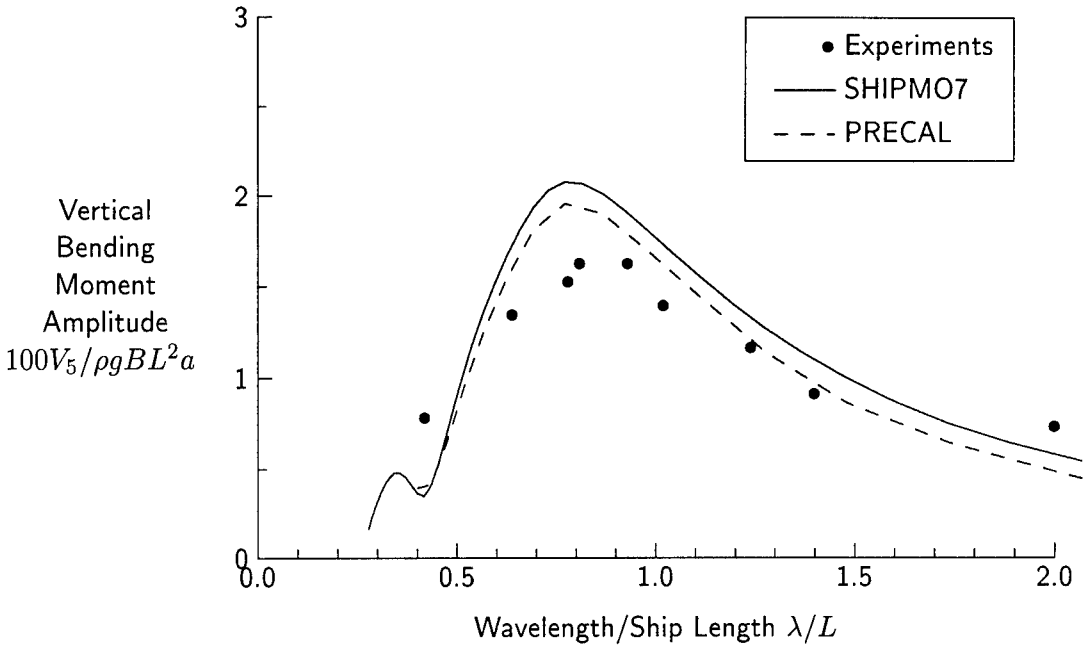

Figure 80: Vertical Bending Moment at Station 13, $Fn = 0.29$, $\beta = 150$ degrees

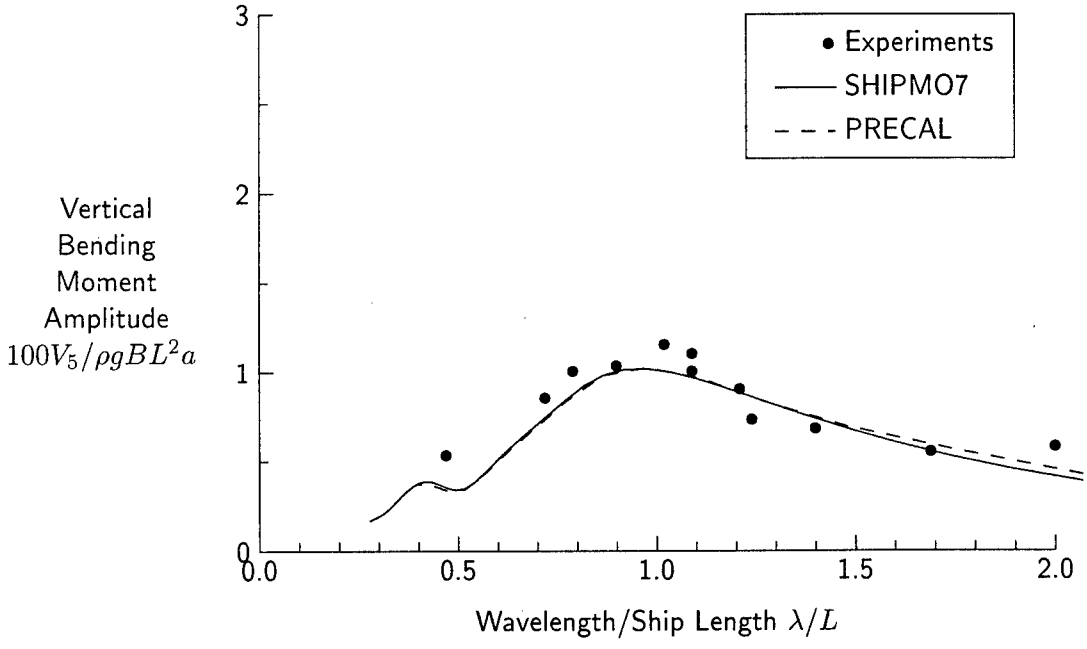

Figure 81: Vertical Bending Moment at Station 5, $Fn = 0.29$, $\beta = 180$ degrees

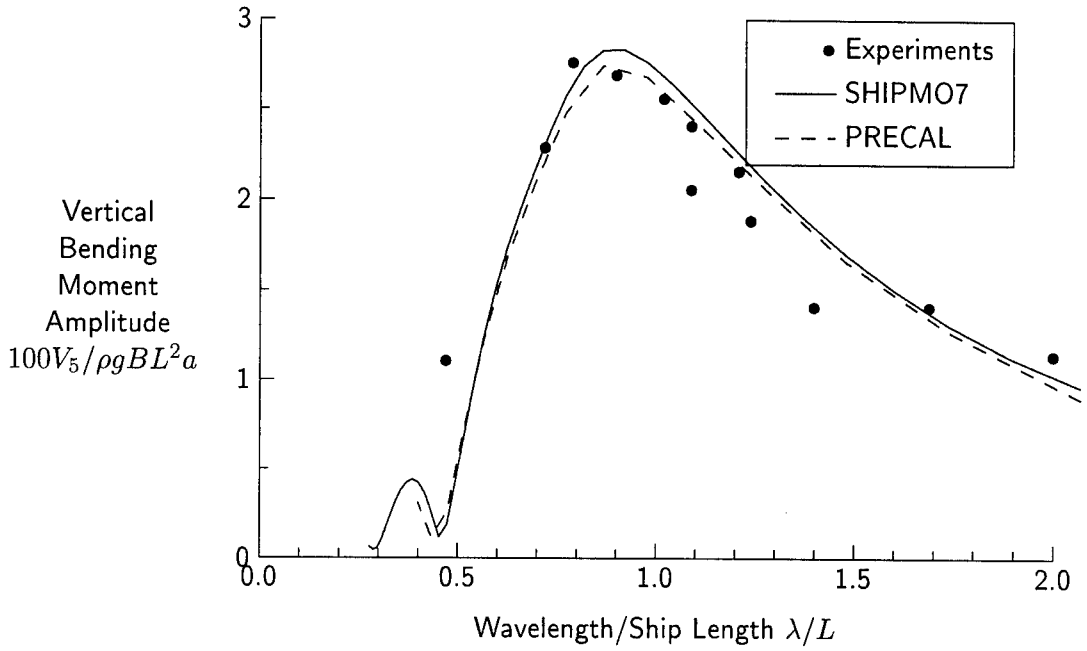

Figure 82: Vertical Bending Moment at Station 10, $Fn = 0.29$, $\beta = 180$ degrees

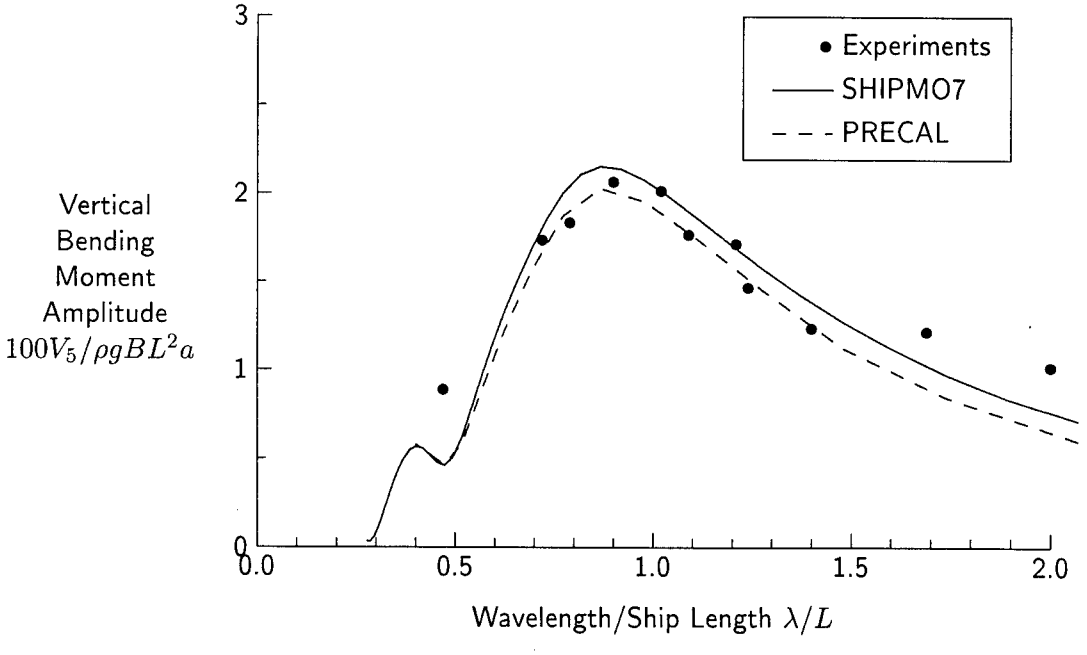

Figure 83: Vertical Bending Moment at Station 13, $Fn = 0.29$, $\beta = 180$ degrees

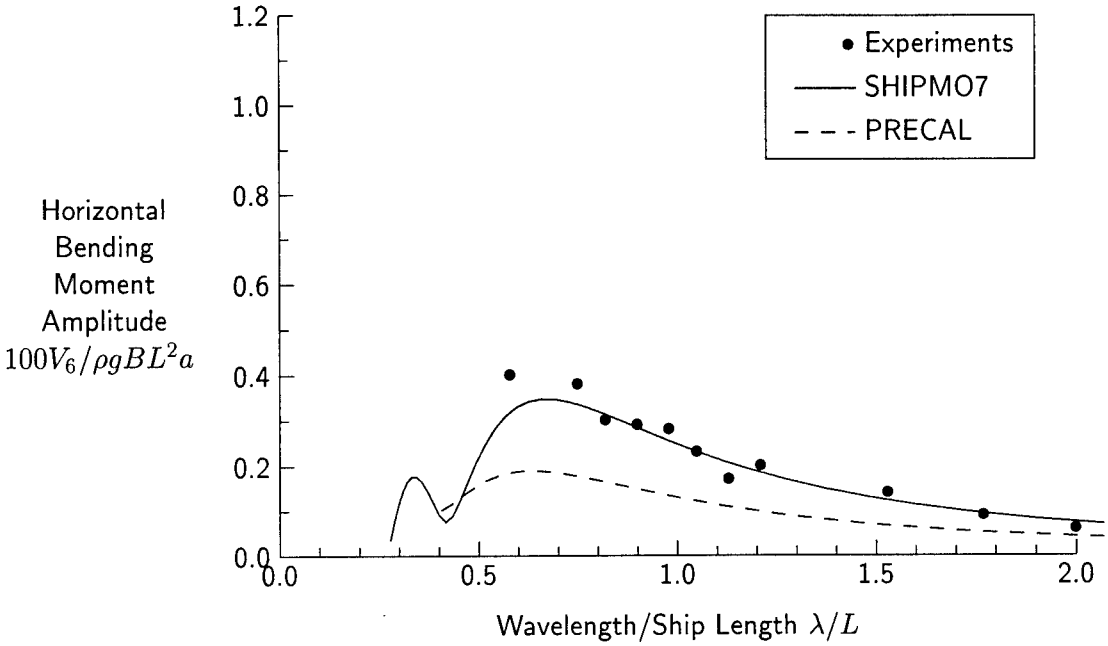

Figure 84: Horizontal Bending Moment at Station 5, $Fn = 0.21$, $\beta = 30$ degrees

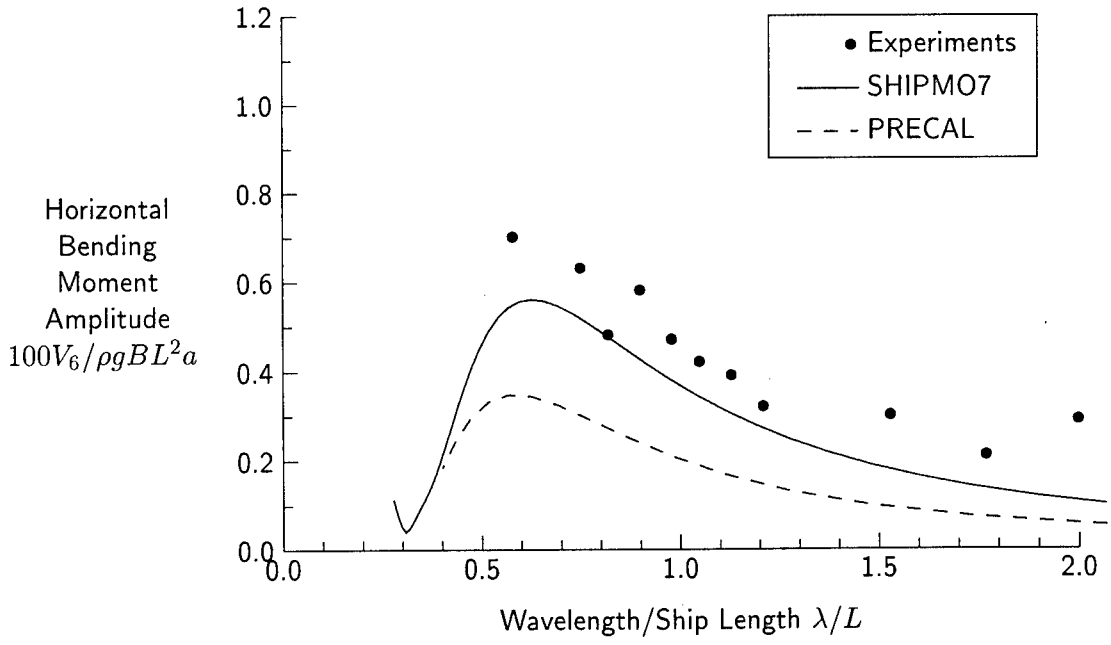

Figure 85: Horizontal Bending Moment at Station 10, $Fn = 0.21$, $\beta = 30$ degrees

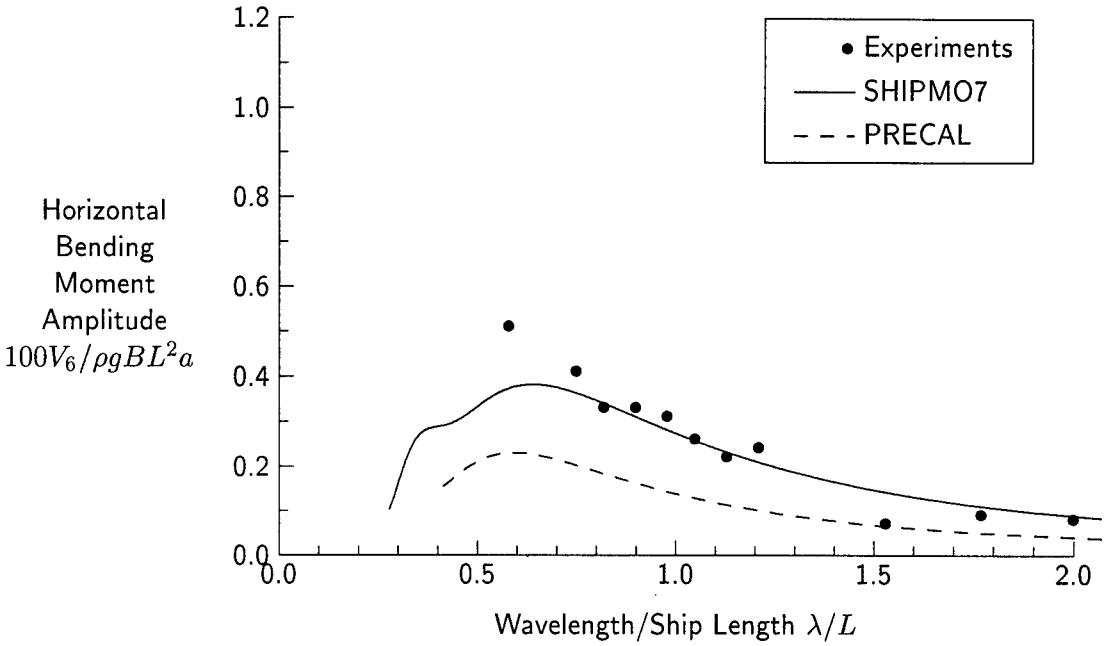

Figure 86: Horizontal Bending Moment at Station 13, $Fn = 0.21$, $\beta = 30$ degrees

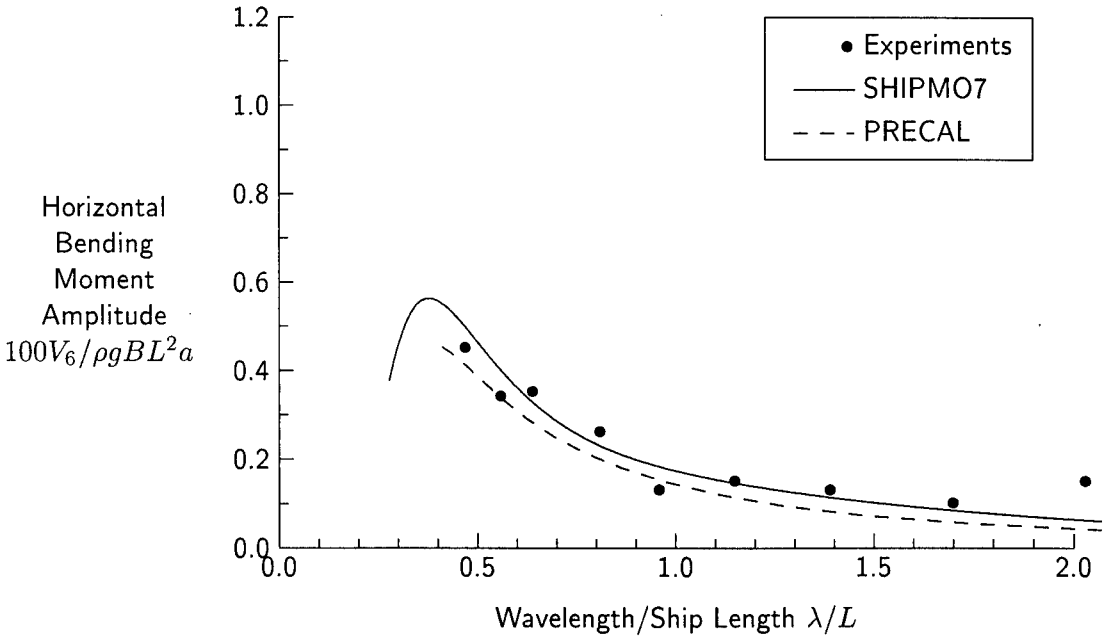

Figure 87: Horizontal Bending Moment at Station 5, $Fn = 0.21$, $\beta = 60$ degrees

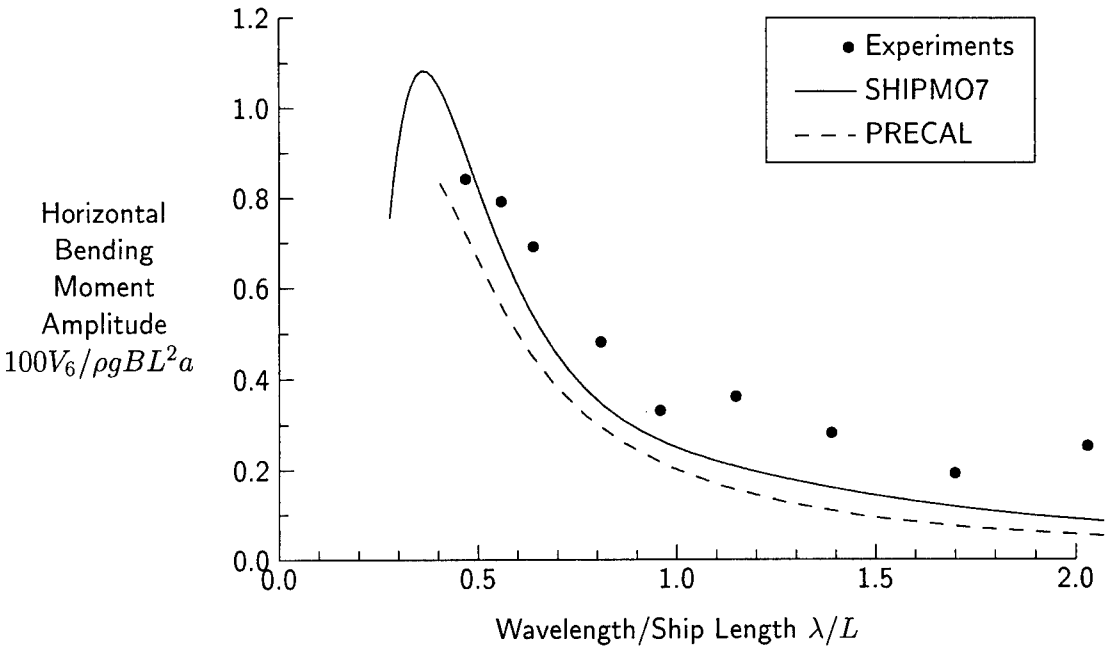

Figure 88: Horizontal Bending Moment at Station 10, $Fn = 0.21$, $\beta = 60$ degrees

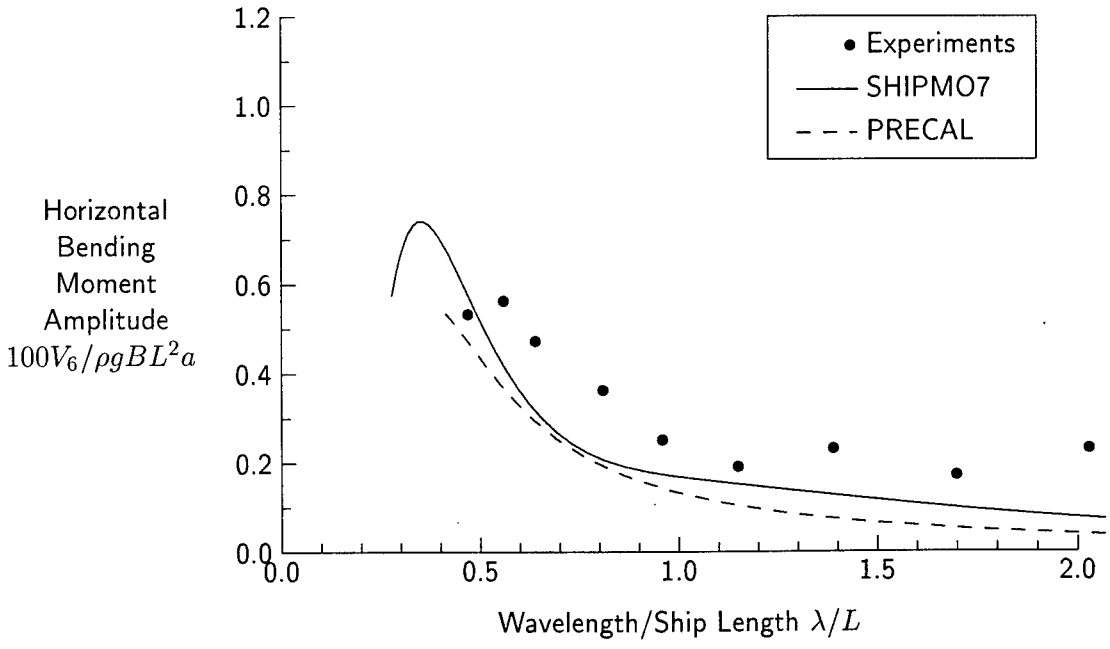

Figure 89: Horizontal Bending Moment at Station 13, $Fn = 0.21$, $\beta = 60$ degrees

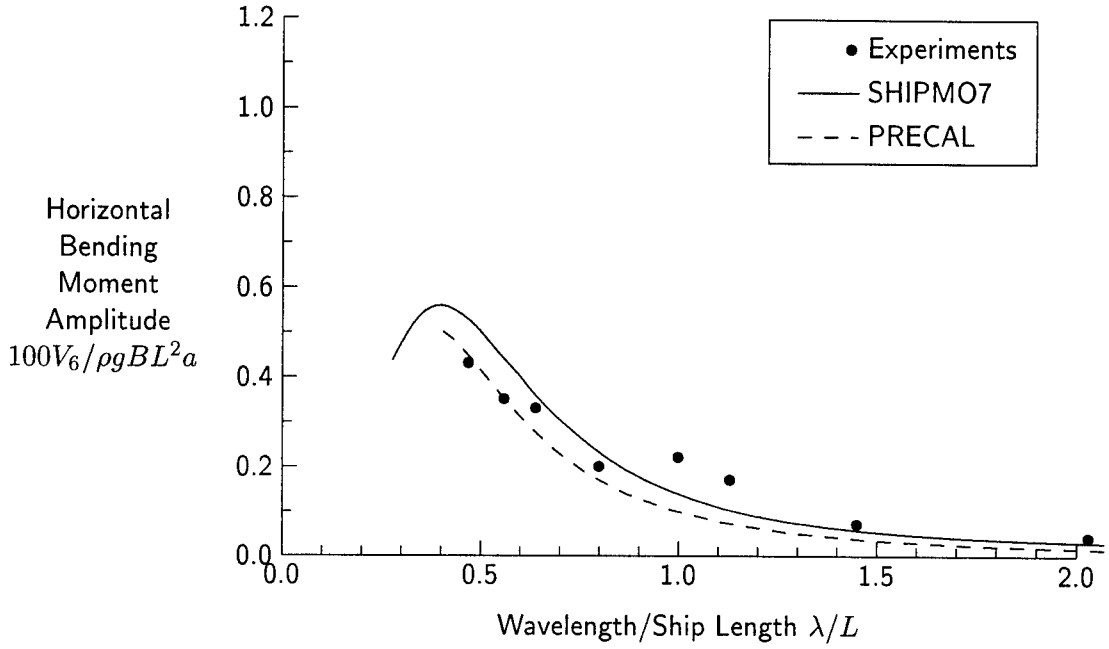

Figure 90: Horizontal Bending Moment at Station 5, $Fn = 0.21$, $\beta = 120$ degrees

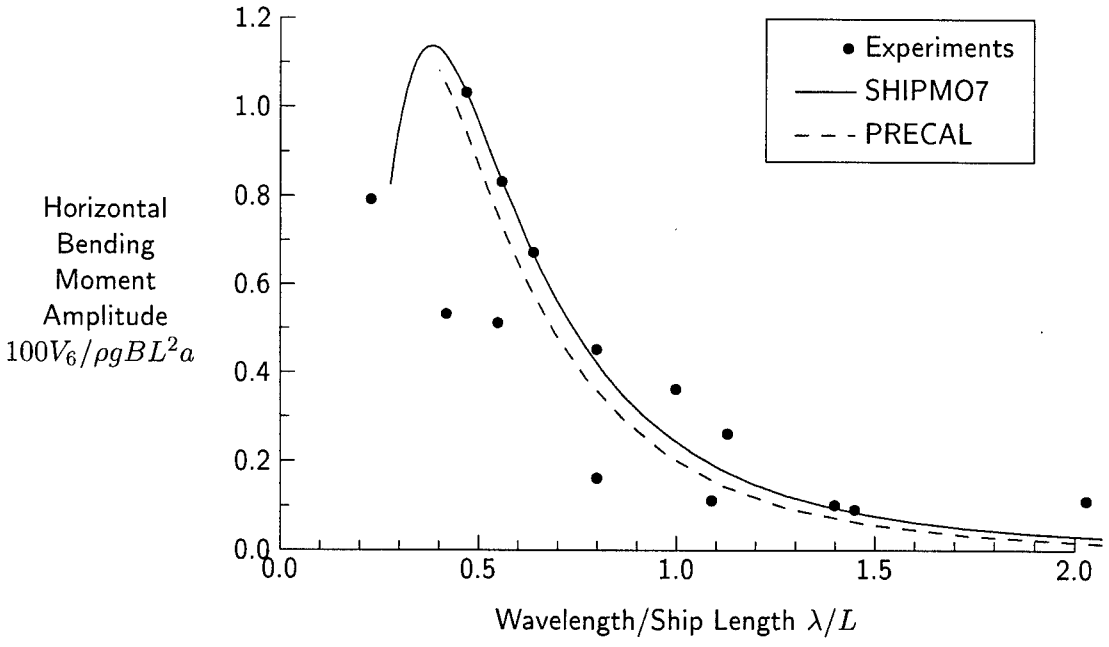

Figure 91: Horizontal Bending Moment at Station 10, $Fn = 0.21$, $\beta = 120$ degrees

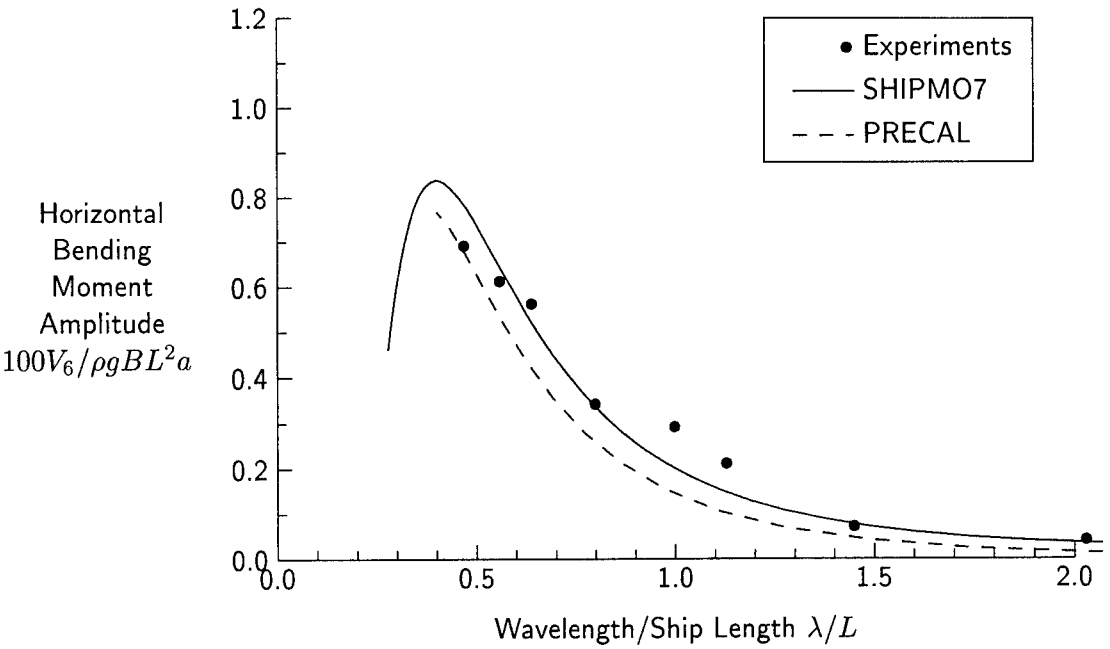

Figure 92: Horizontal Bending Moment at Station 13, $Fn = 0.21$, $\beta = 120$ degrees

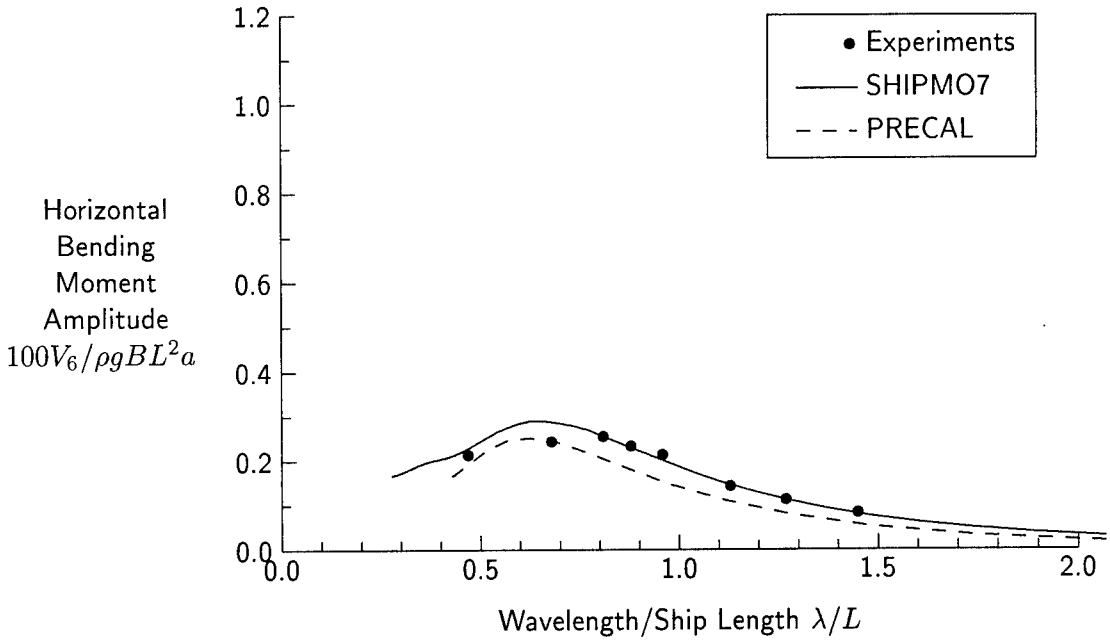

Figure 93: Horizontal Bending Moment at Station 5, $Fn = 0.21$, $\beta = 150$ degrees

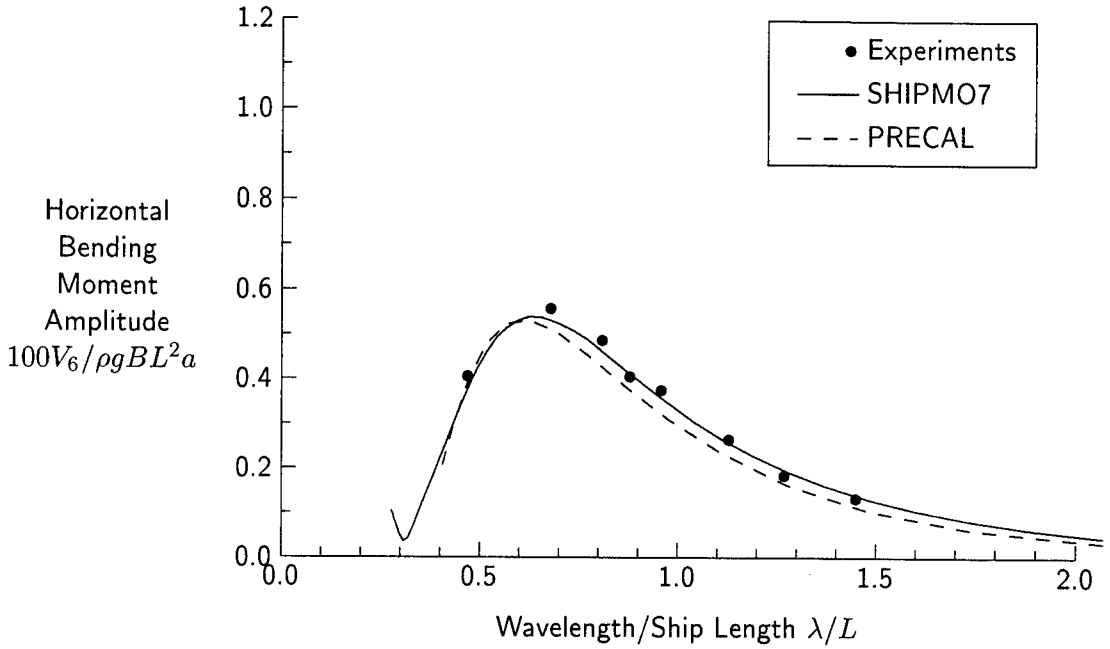

Figure 94: Horizontal Bending Moment at Station 10, $Fn = 0.21$, $\beta = 150$ degrees

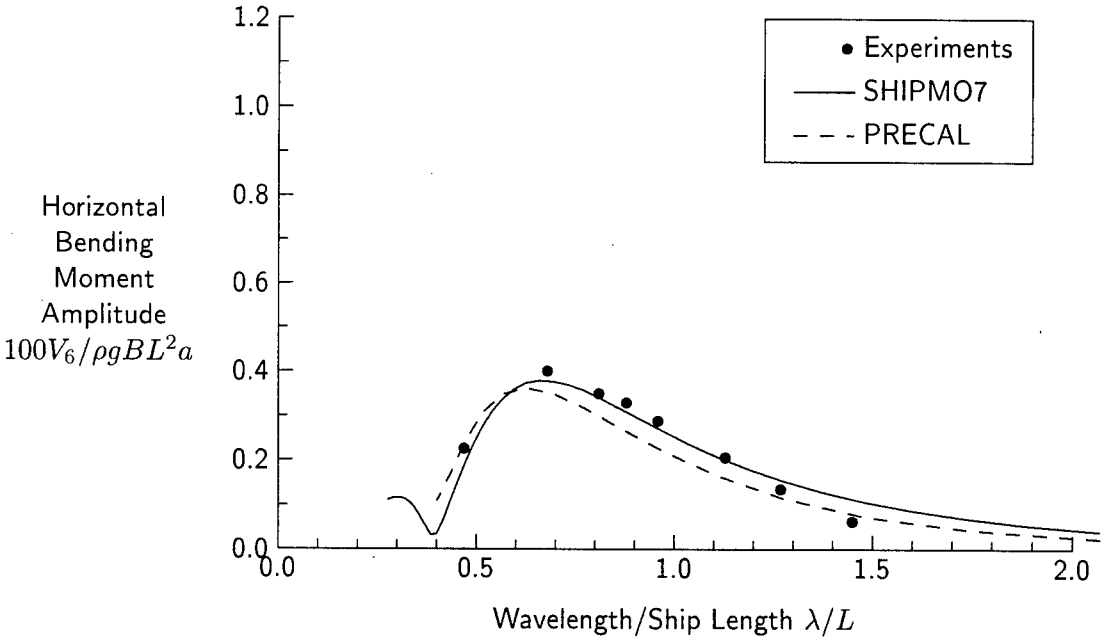

Figure 95: Horizontal Bending Moment at Station 13, $Fn = 0.21$, $\beta = 150$ degrees

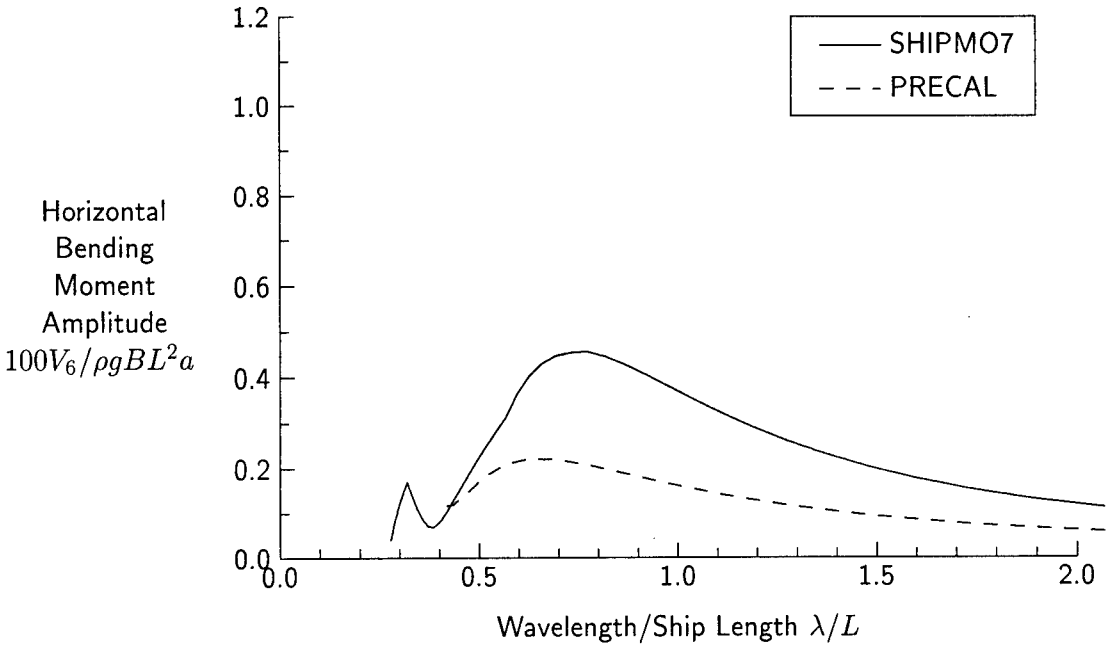

Figure 96: Horizontal Bending Moment at Station 5, $Fn = 0.29$, $\beta = 30$ degrees

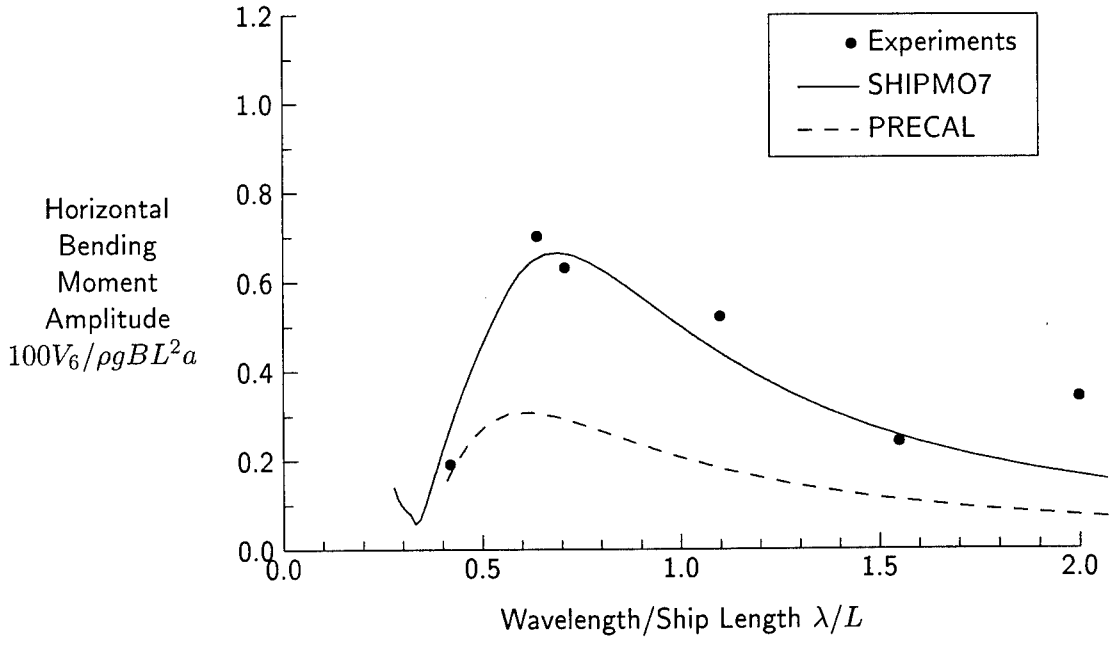

Figure 97: Horizontal Bending Moment at Station 10, $Fn = 0.29$, $\beta = 30$ degrees

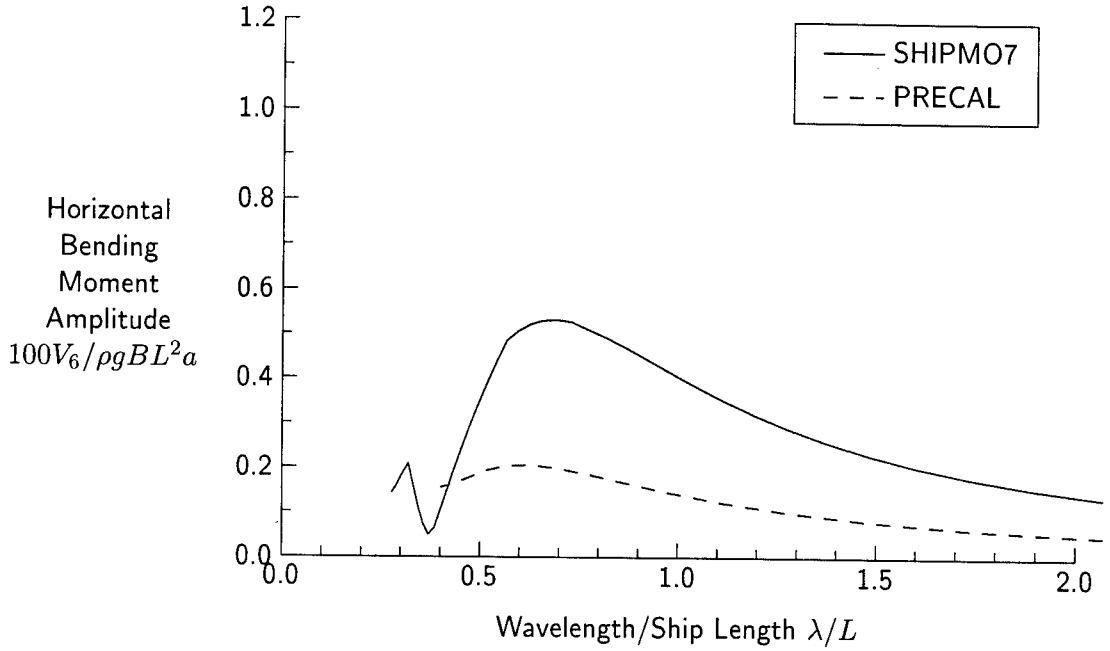

Figure 98: Horizontal Bending Moment at Station 13, $Fn = 0.29$, $\beta = 30$ degrees

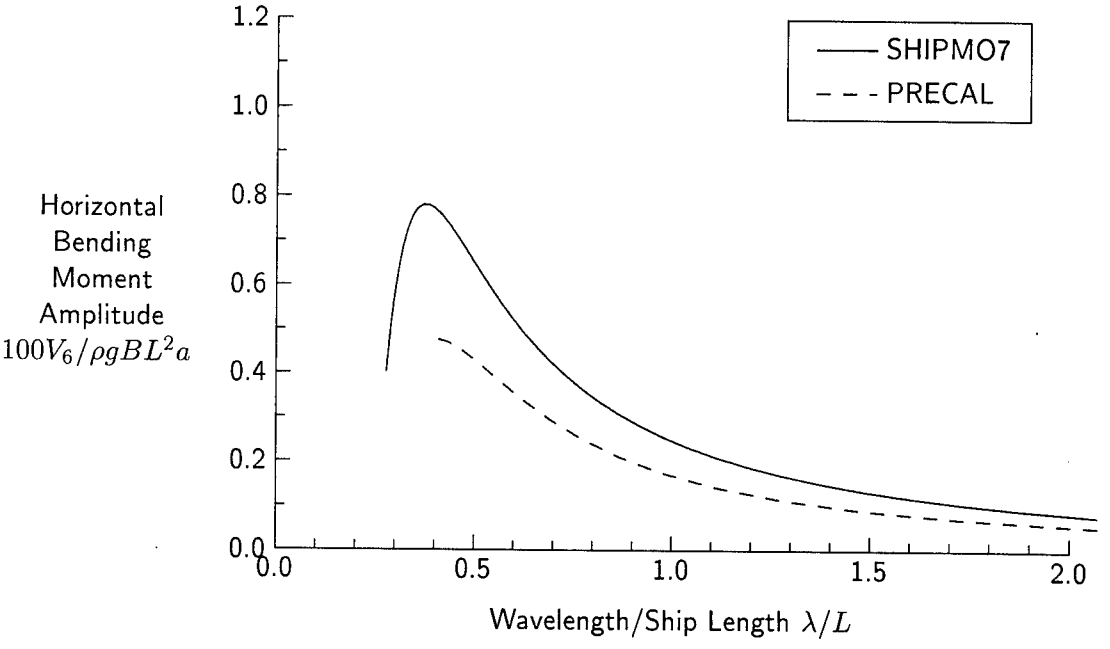

Figure 99: Horizontal Bending Moment at Station 5, $Fn = 0.29$, $\beta = 60$ degrees

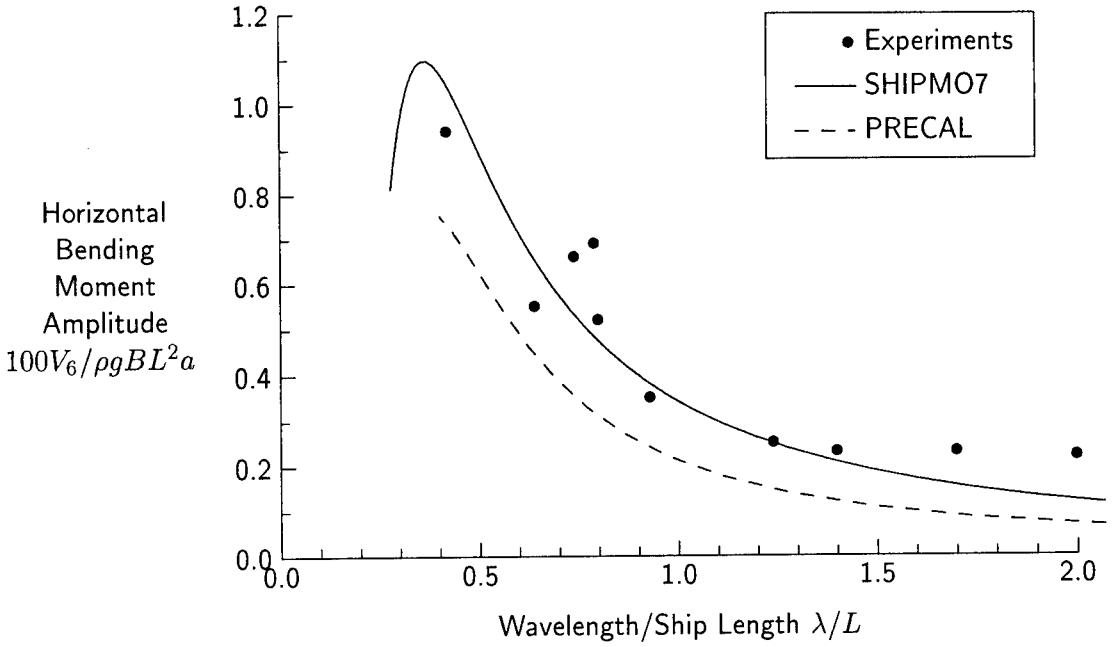

Figure 100: Horizontal Bending Moment at Station 10, $Fn = 0.29$, $\beta = 60$ degrees

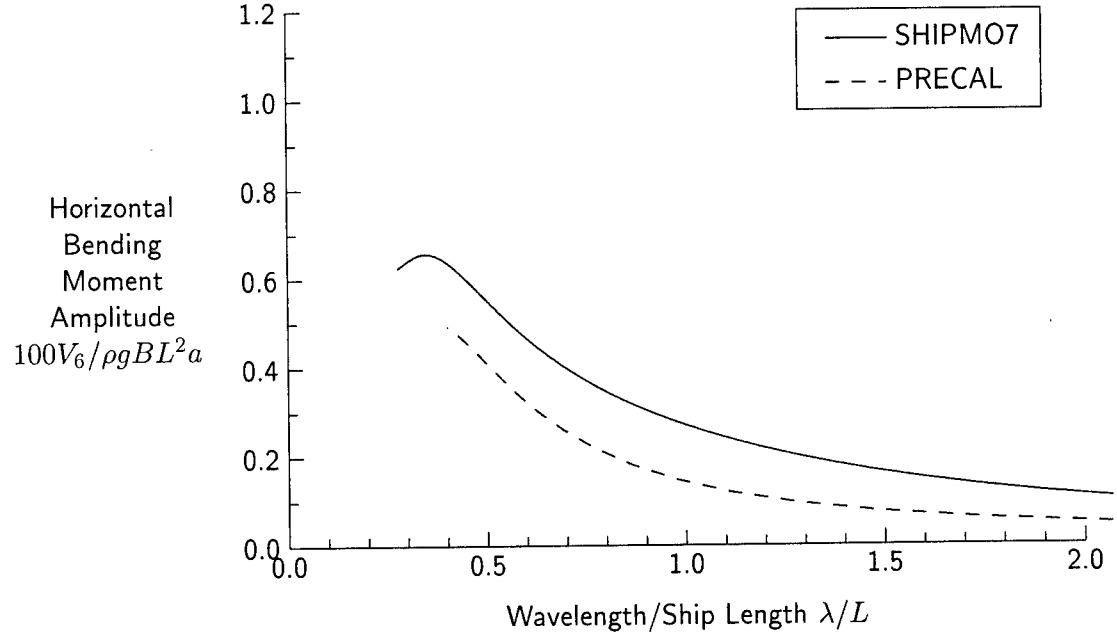

Figure 101: Horizontal Bending Moment at Station 13, $Fn = 0.29$, $\beta = 60$ degrees

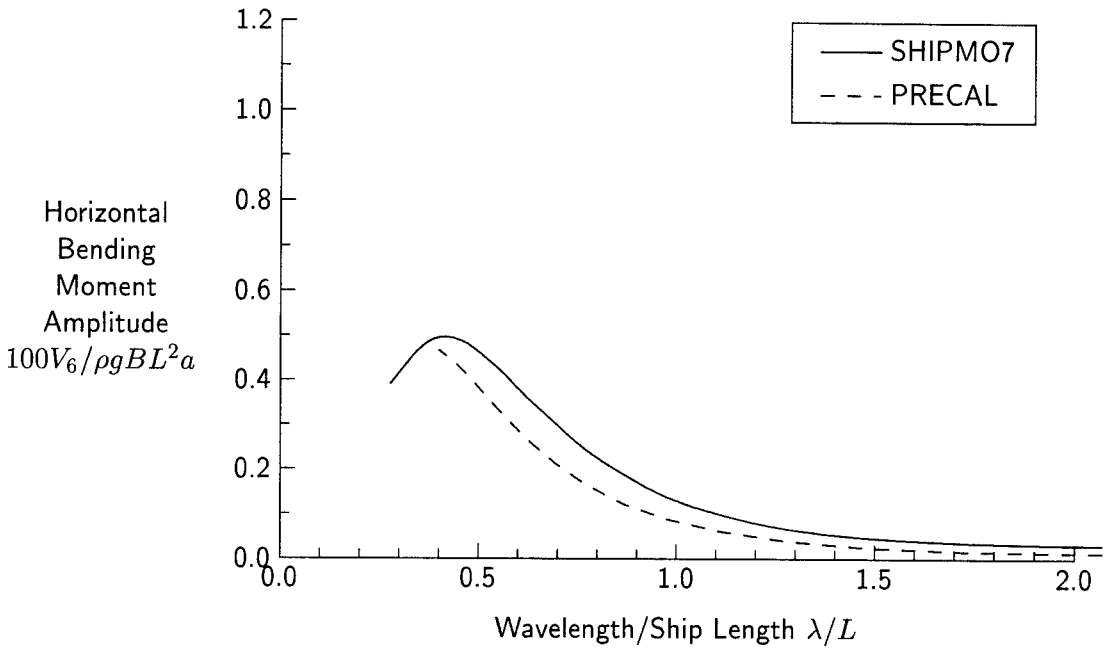

Figure 102: Horizontal Bending Moment at Station 5, $Fn = 0.29$, $\beta = 120$ degrees

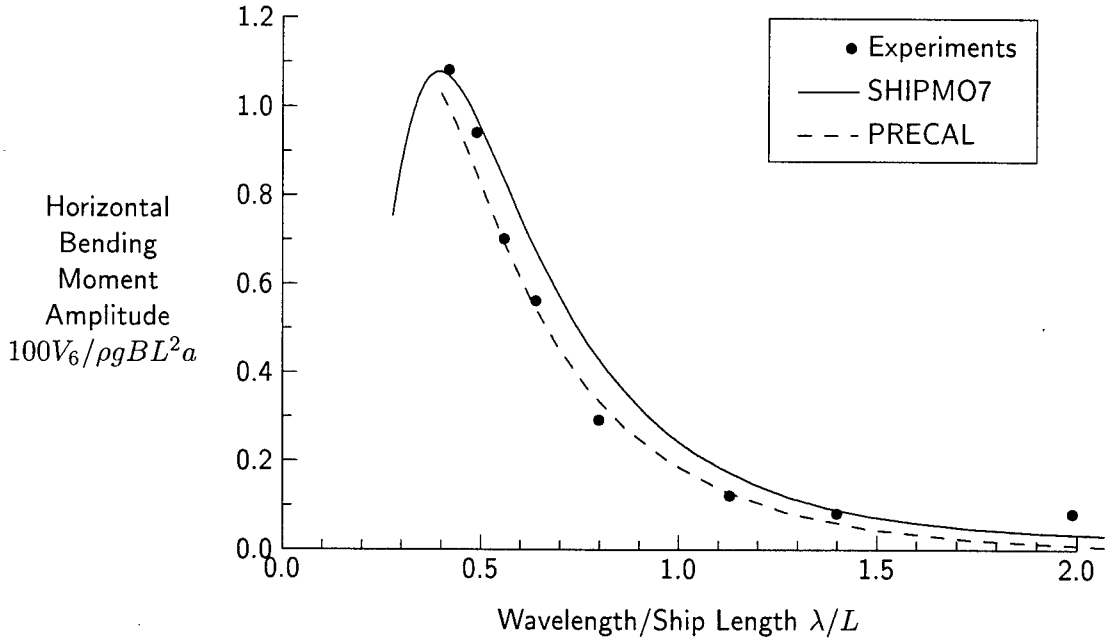

Figure 103: Horizontal Bending Moment at Station 10, $Fn = 0.29$, $\beta = 120$ degrees

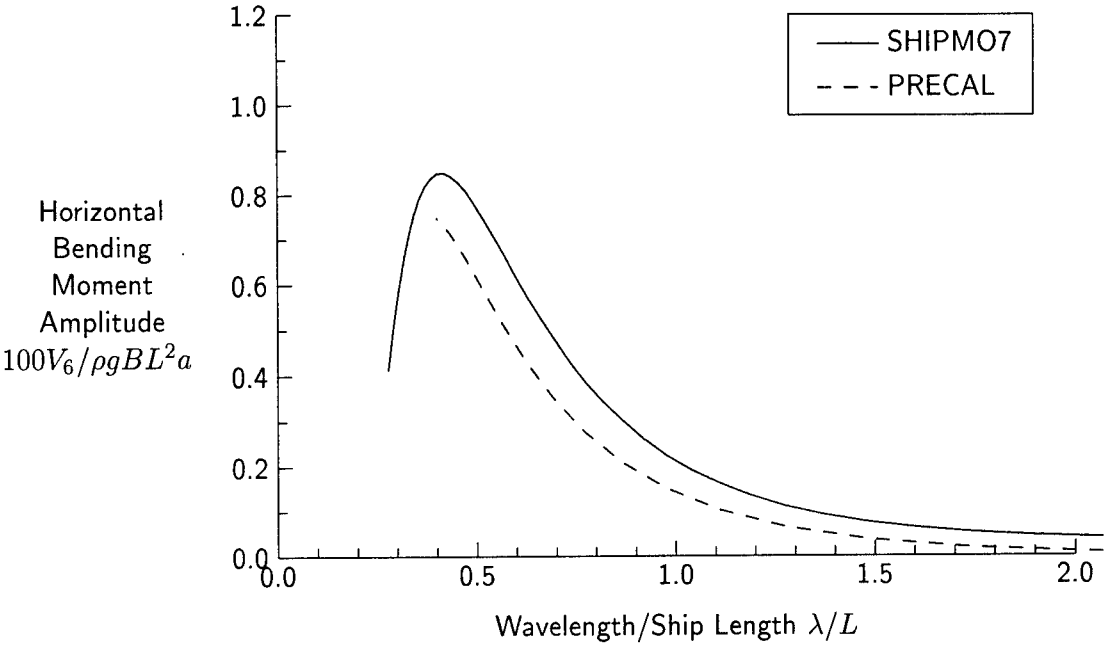

Figure 104: Horizontal Bending Moment at Station 13, $Fn = 0.29$, $\beta = 120$ degrees

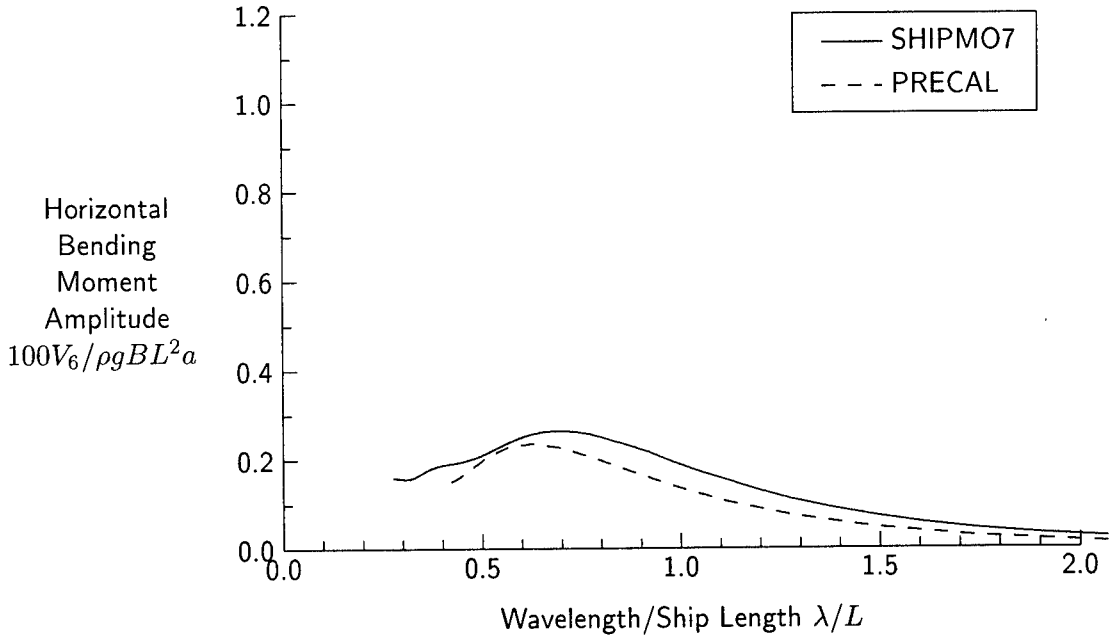

Figure 105: Horizontal Bending Moment at Station 5, $Fn = 0.29$, $\beta = 150$ degrees

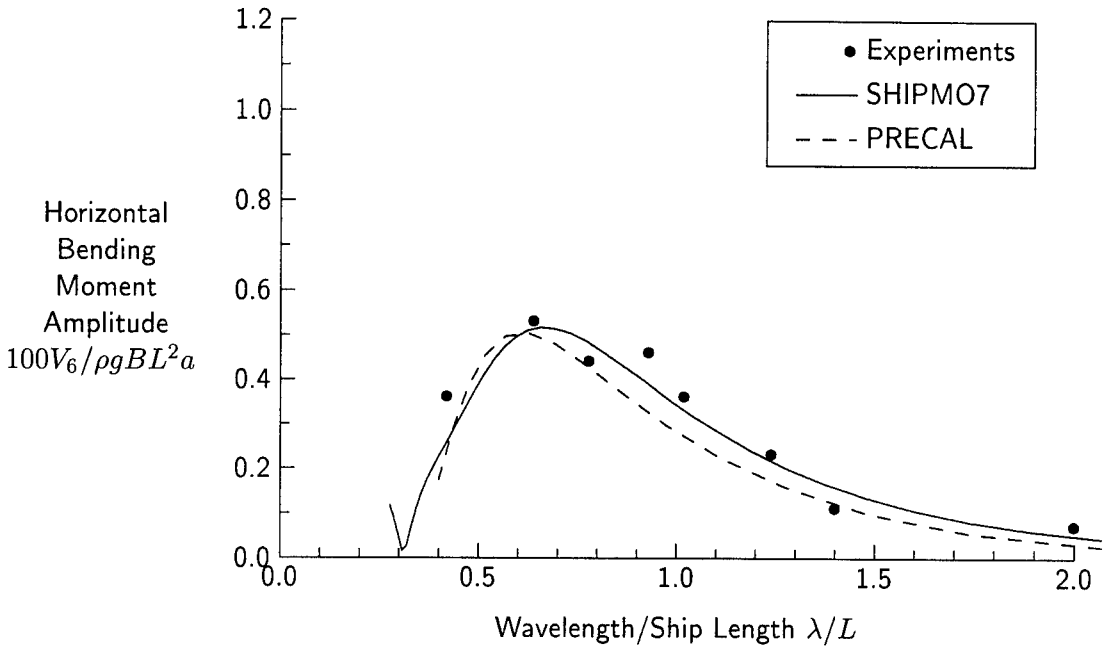

Figure 106: Horizontal Bending Moment at Station 10, $Fn = 0.29$, $\beta = 150$ degrees

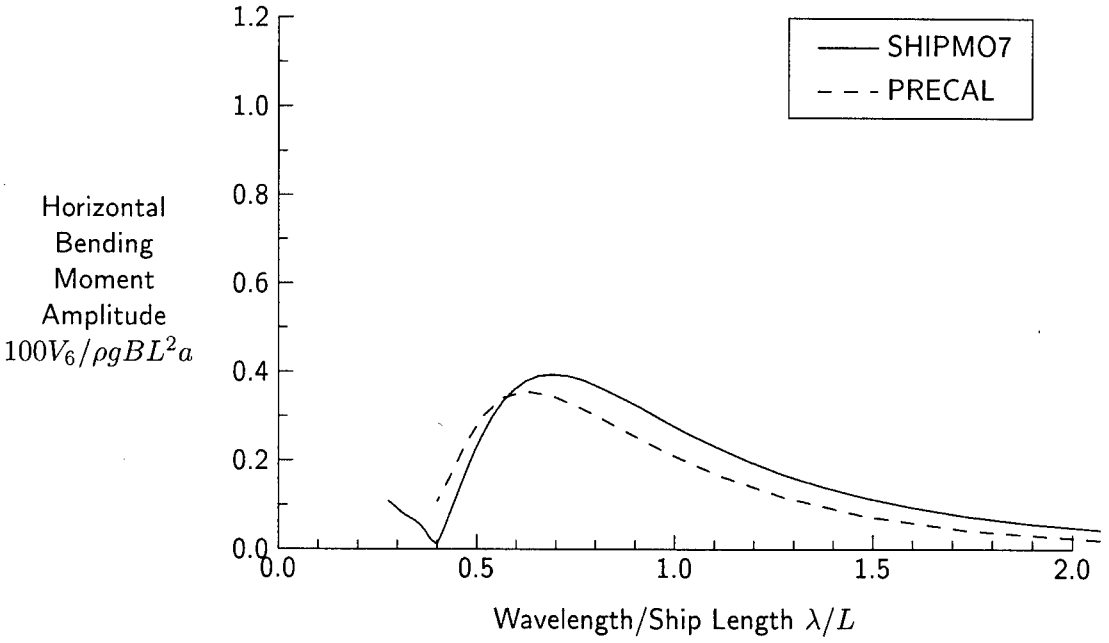

Figure 107: Horizontal Bending Moment at Station 13, $Fn = 0.29$, $\beta = 150$ degrees

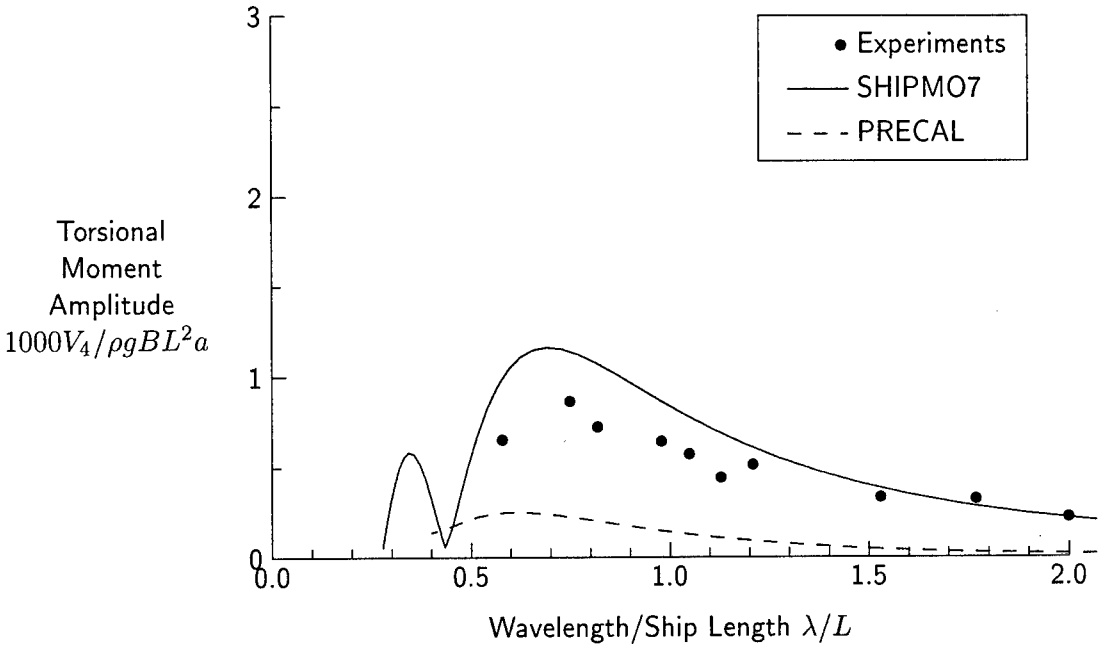

Figure 108: Torsional Moment at Station 5, $Fn = 0.21$, $\beta = 30$ degrees

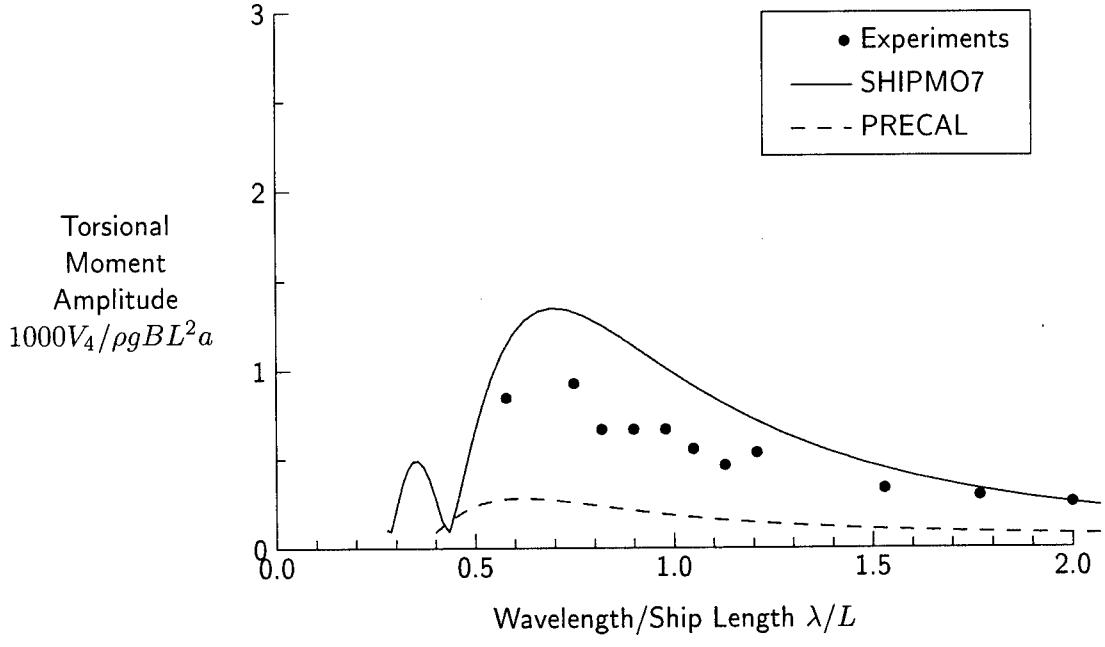

Figure 109: Torsional Moment at Station 10, $Fn = 0.21$, $\beta = 30$ degrees

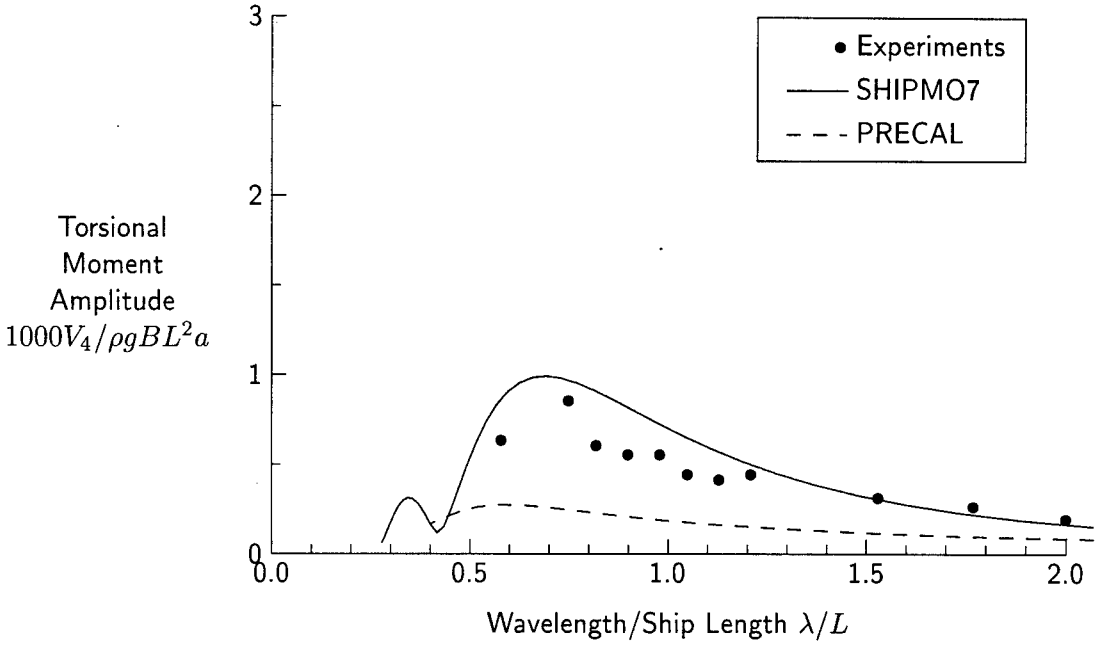

Figure 110: Torsional Moment at Station 13, $Fn = 0.21$, $\beta = 30$ degrees

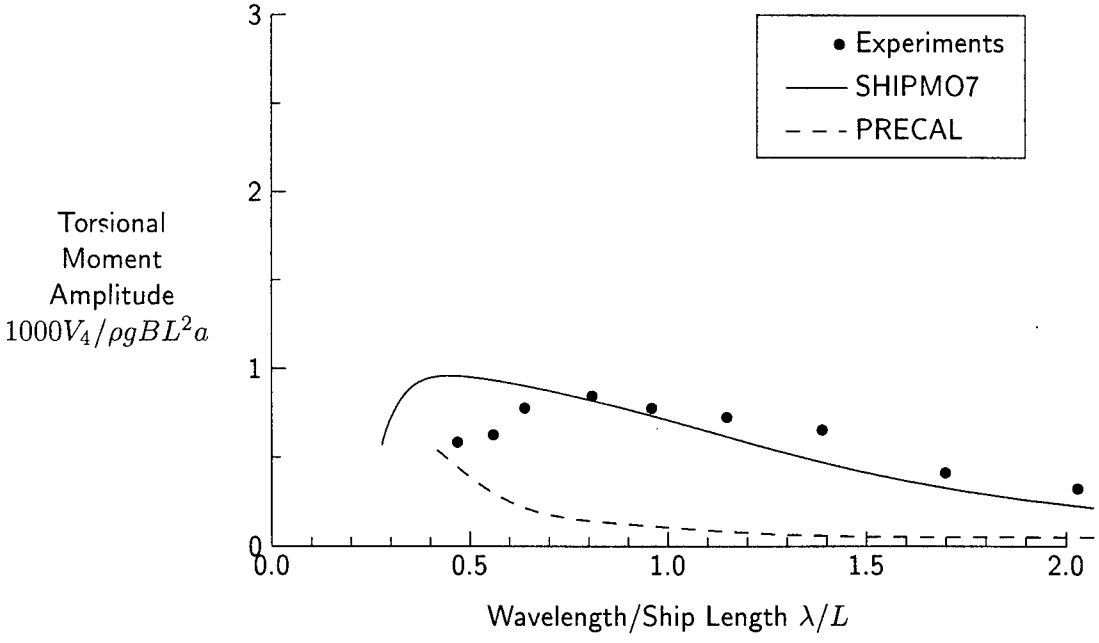

Figure 111: Torsional Moment at Station 5, $Fn = 0.21$, $\beta = 60$ degrees

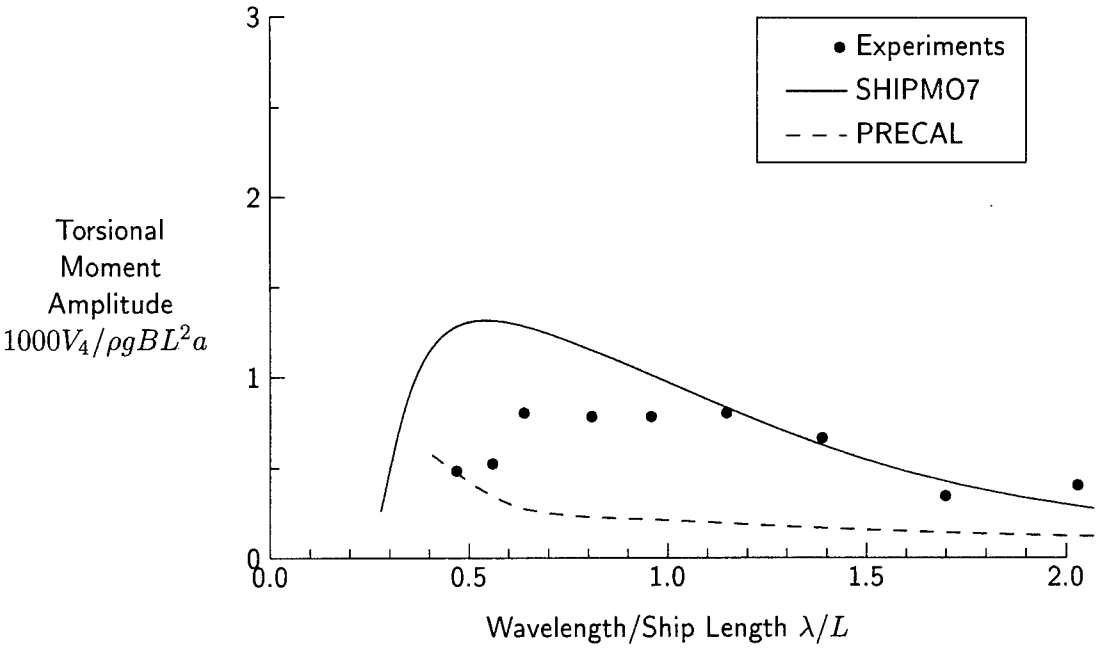

Figure 112: Torsional Moment at Station 10, $Fn = 0.21$, $\beta = 60$ degrees

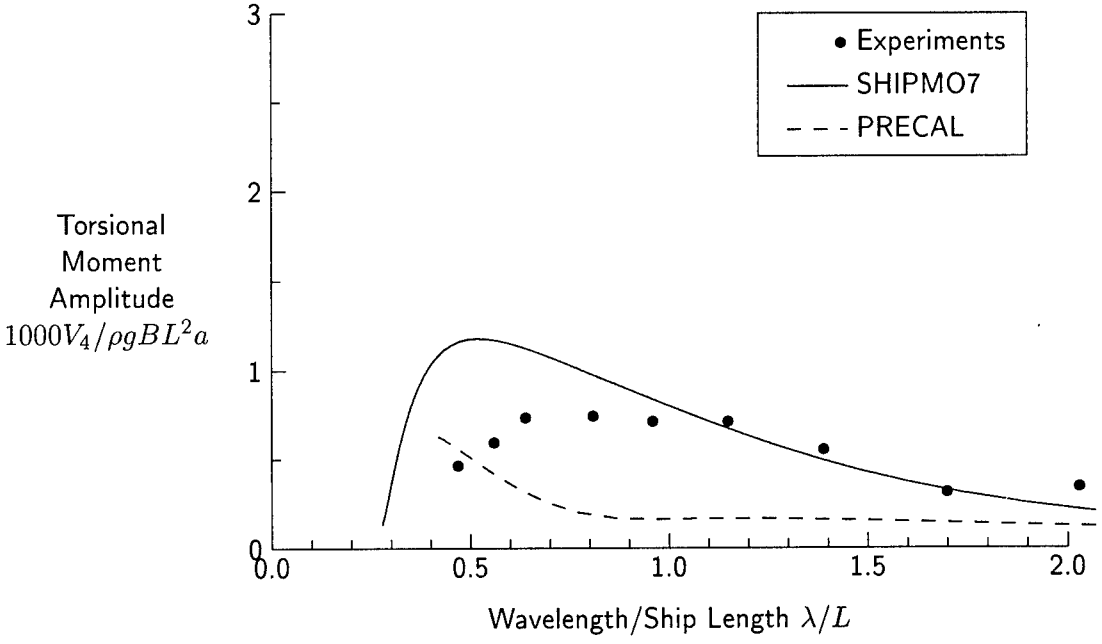

Figure 113: Torsional Moment at Station 13, $Fn = 0.21$, $\beta = 60$ degrees

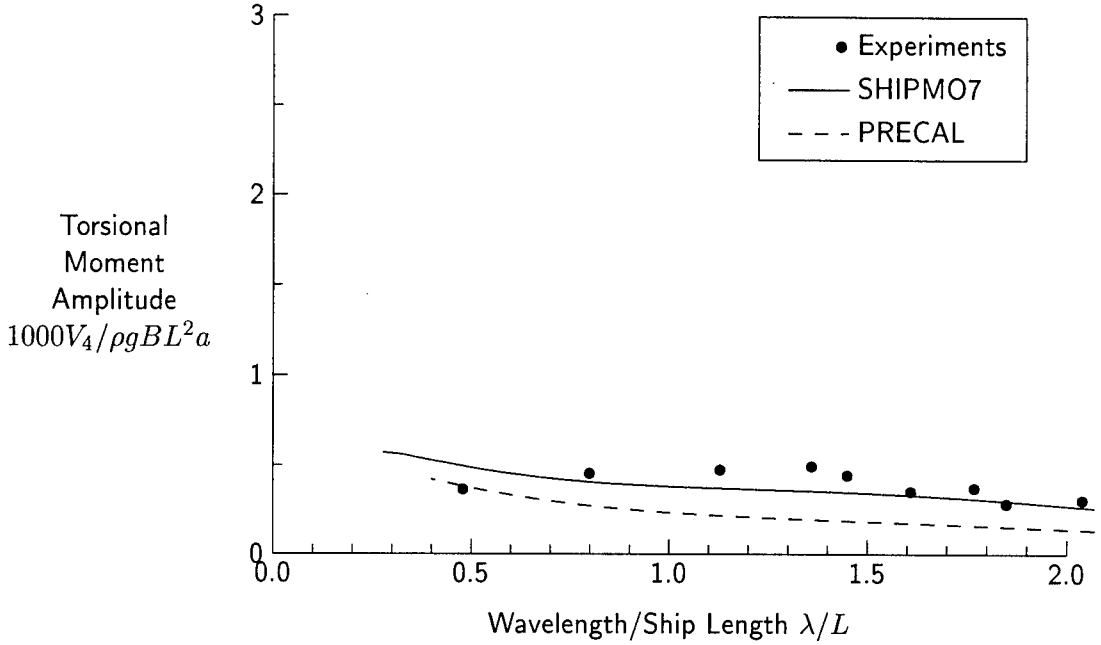

Figure 114: Torsional Moment at Station 5, $Fn = 0.21$, $\beta = 90$ degrees

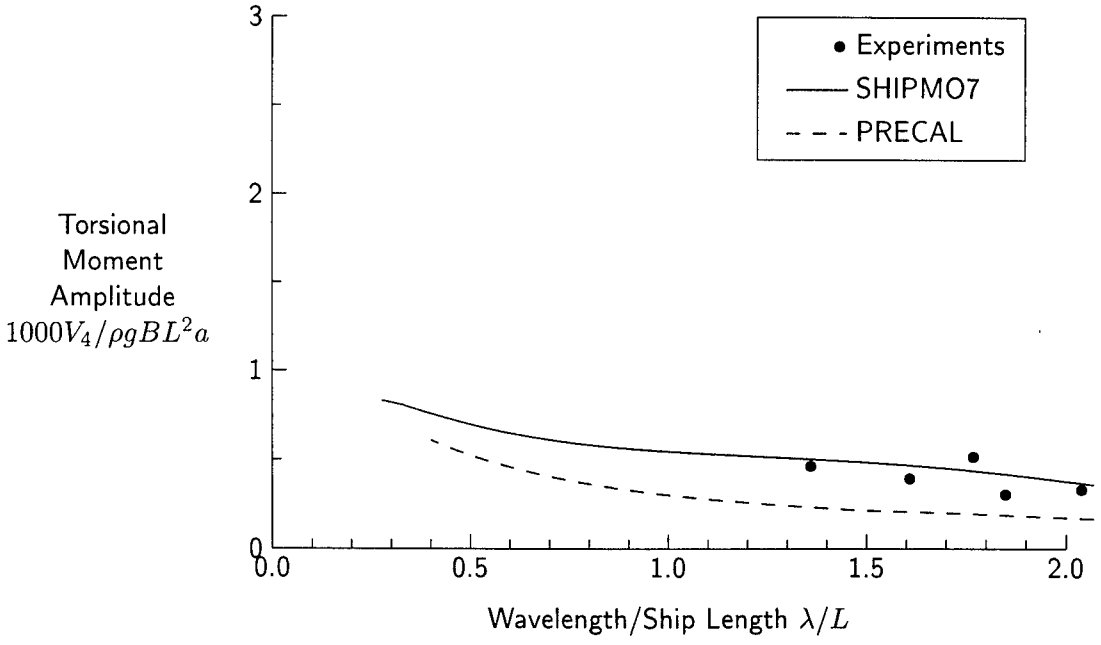

Figure 115: Torsional Moment at Station 10, $Fn = 0.21$, $\beta = 90$ degrees

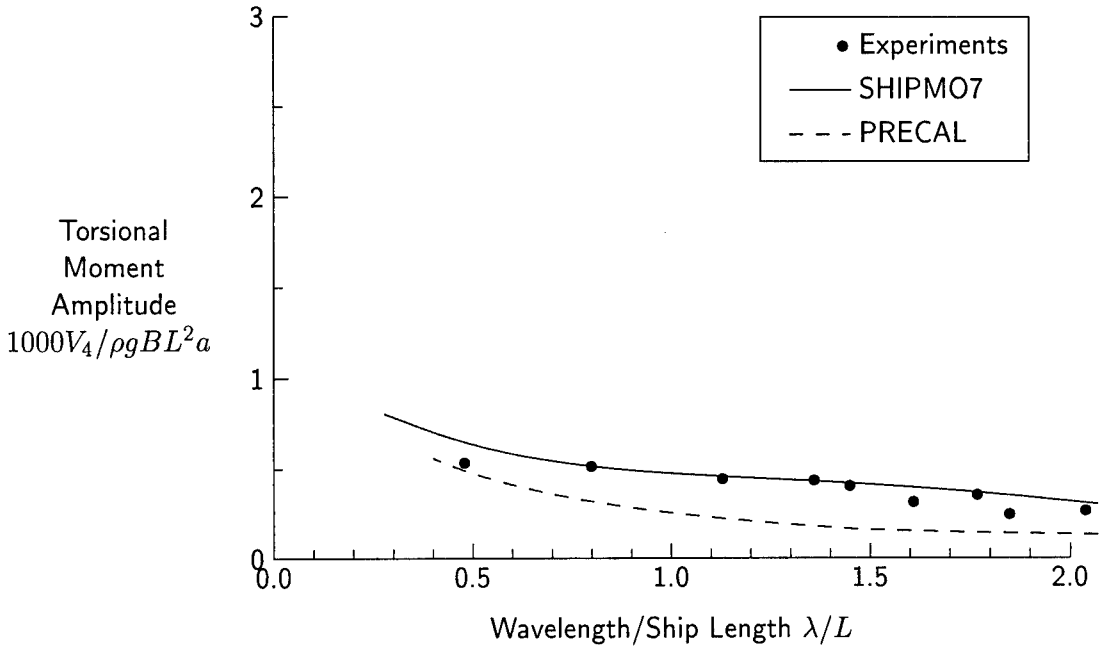

Figure 116: Torsional Moment at Station 13, $Fn = 0.21$, $\beta = 90$ degrees

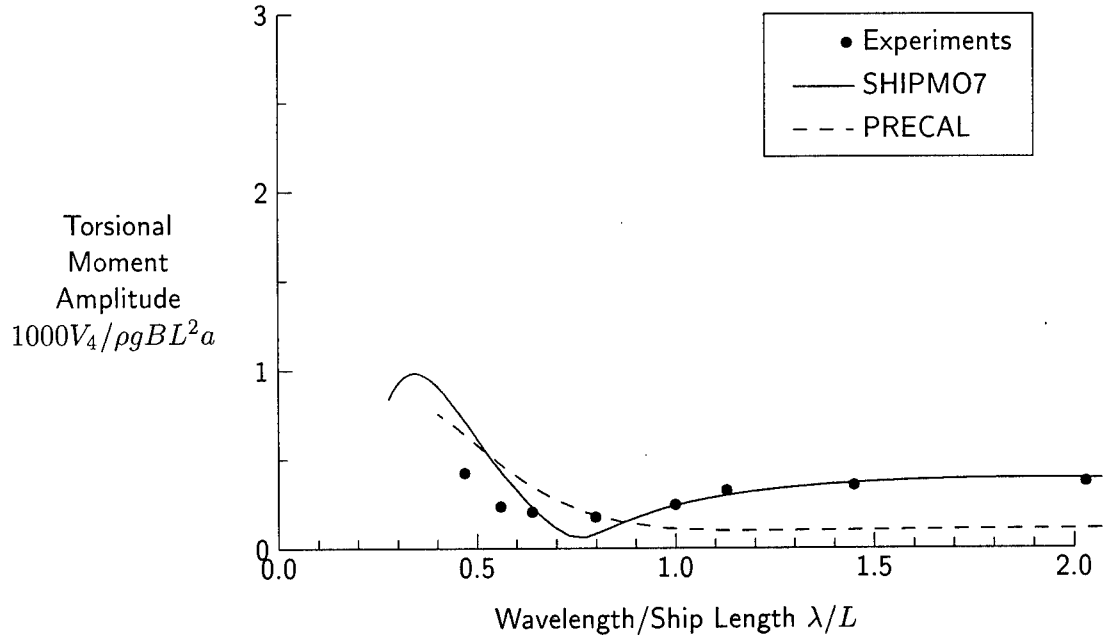

Figure 117: Torsional Moment at Station 5, $Fn = 0.21$, $\beta = 120$ degrees

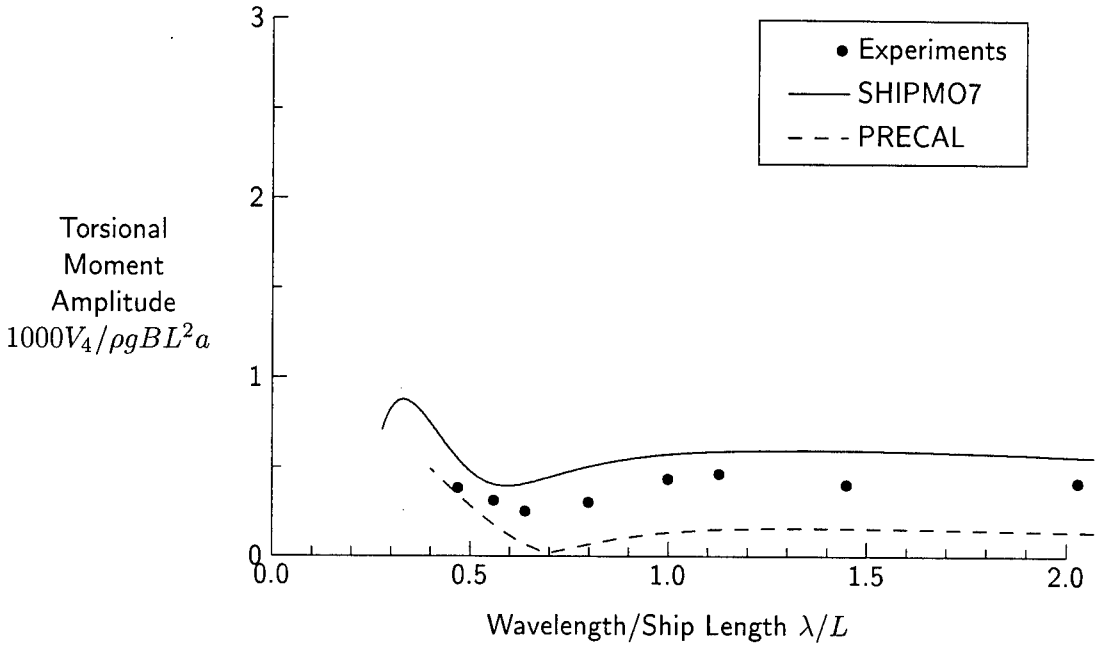

Figure 118: Torsional Moment at Station 10, $Fn = 0.21$, $\beta = 120$ degrees

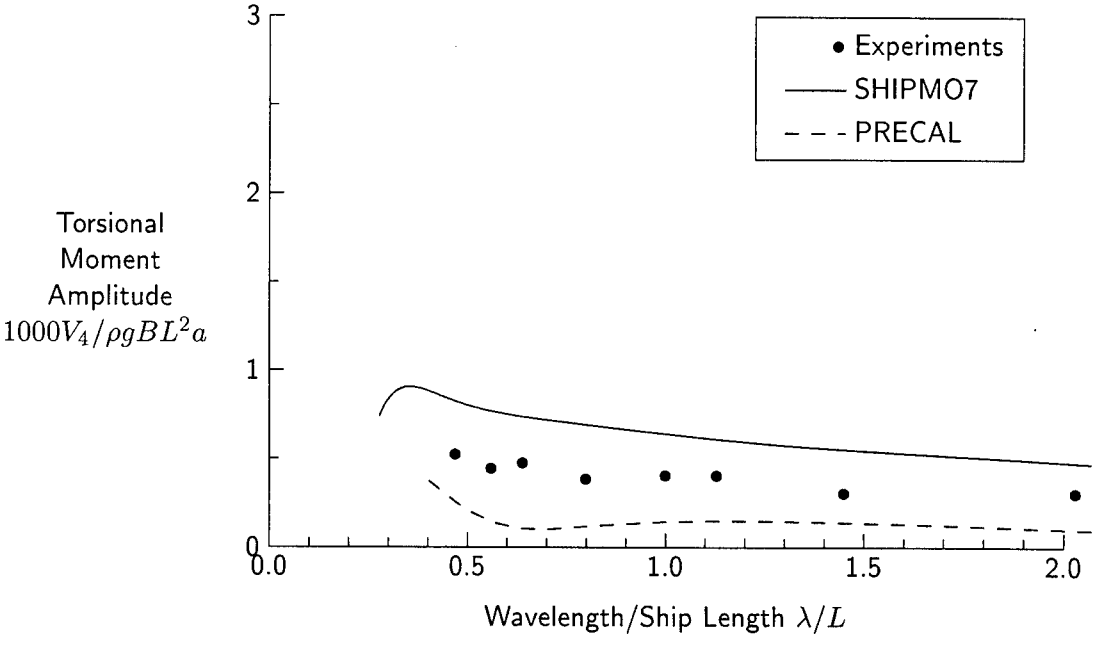

Figure 119: Torsional Moment at Station 13, $Fn = 0.21$, $\beta = 120$ degrees

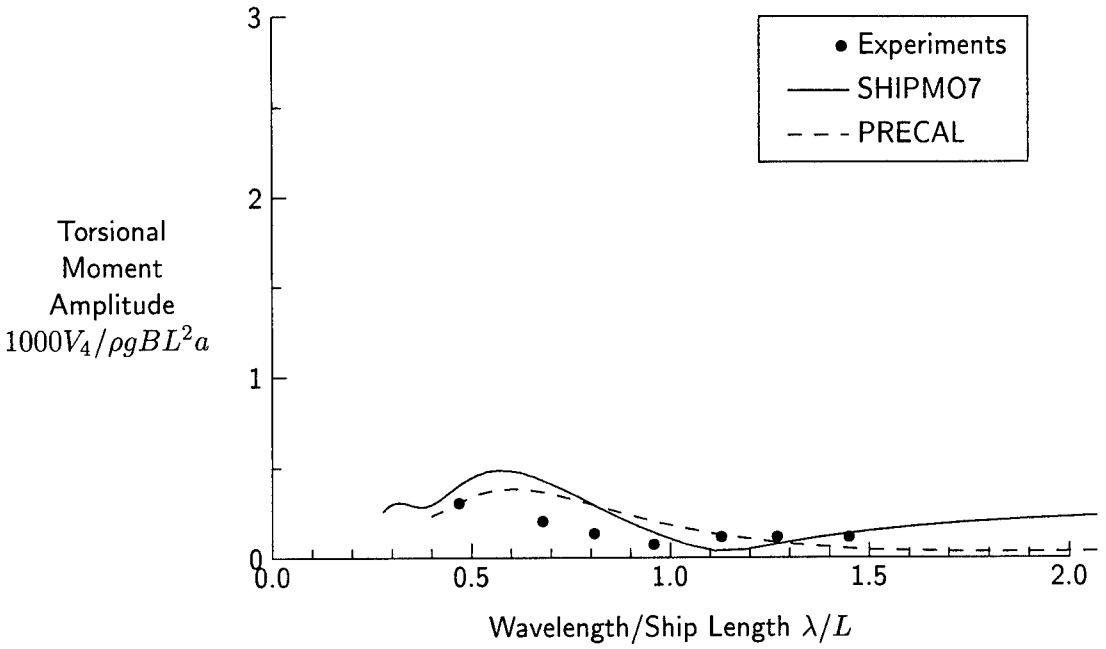

Figure 120: Torsional Moment at Station 5, $Fn = 0.21$, $\beta = 150$ degrees

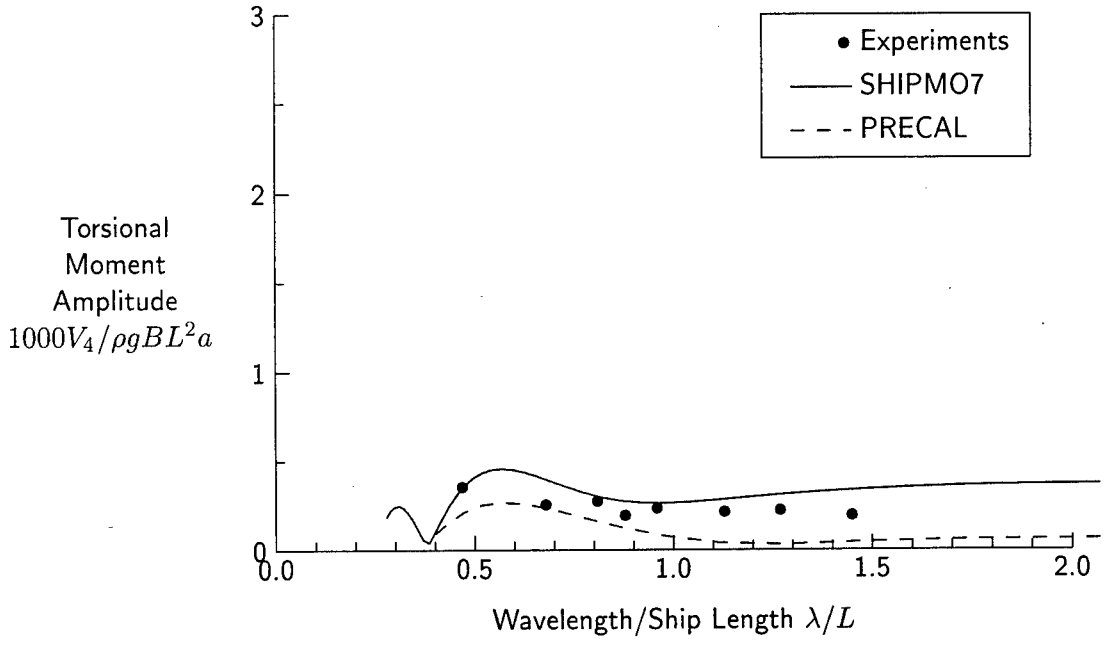

Figure 121: Torsional Moment at Station 10, $Fn = 0.21$, $\beta = 150$ degrees

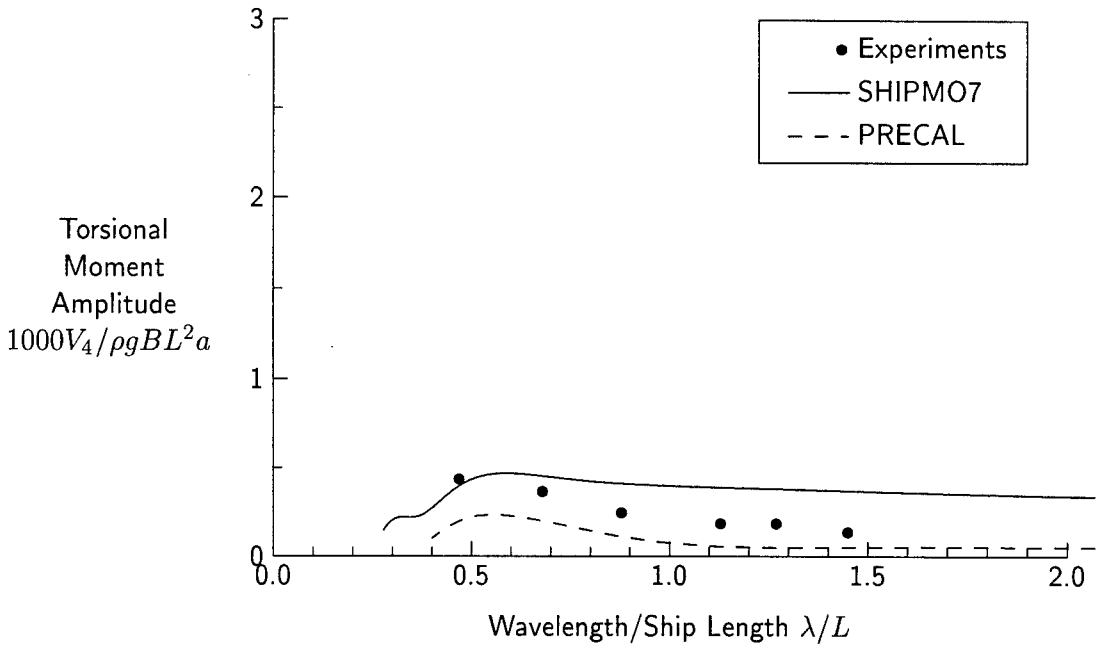

Figure 122: Torsional Moment at Station 13, $Fn = 0.21$, $\beta = 150$ degrees

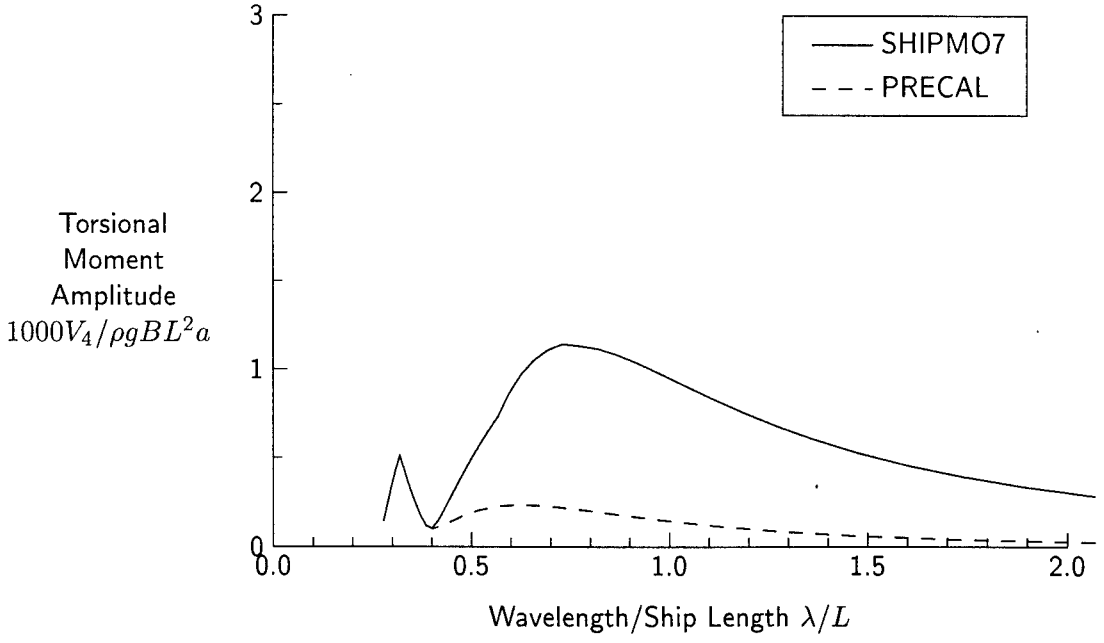

Figure 123: Torsional Moment at Station 5, $Fn = 0.29$, $\beta = 30$ degrees

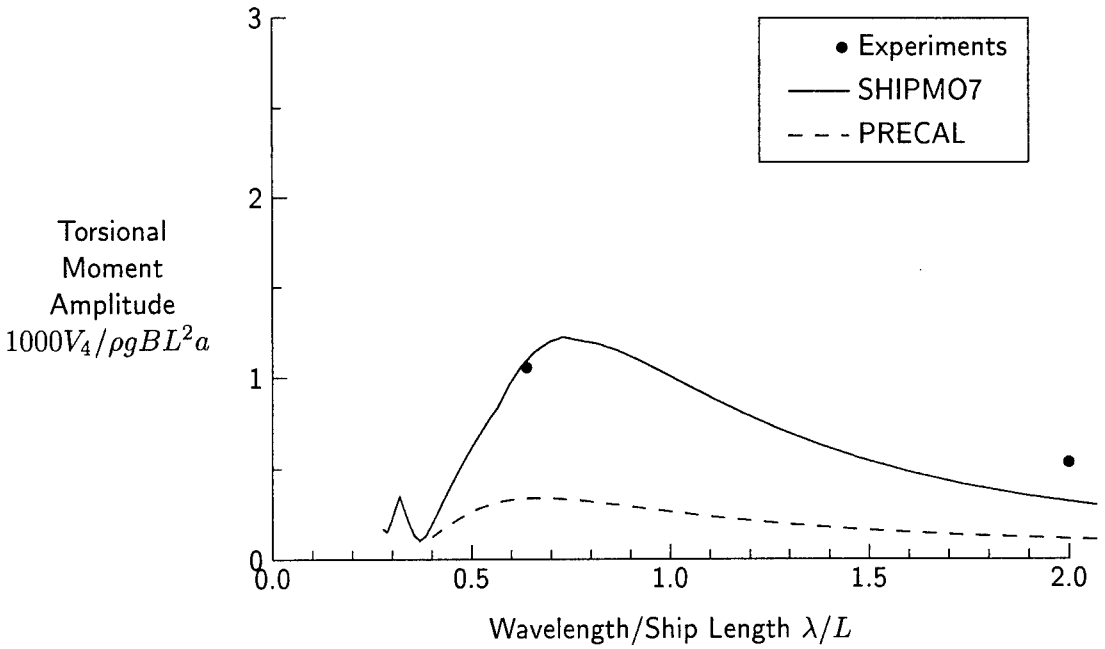

Figure 124: Torsional Moment at Station 10, $Fn = 0.29$, $\beta = 30$ degrees

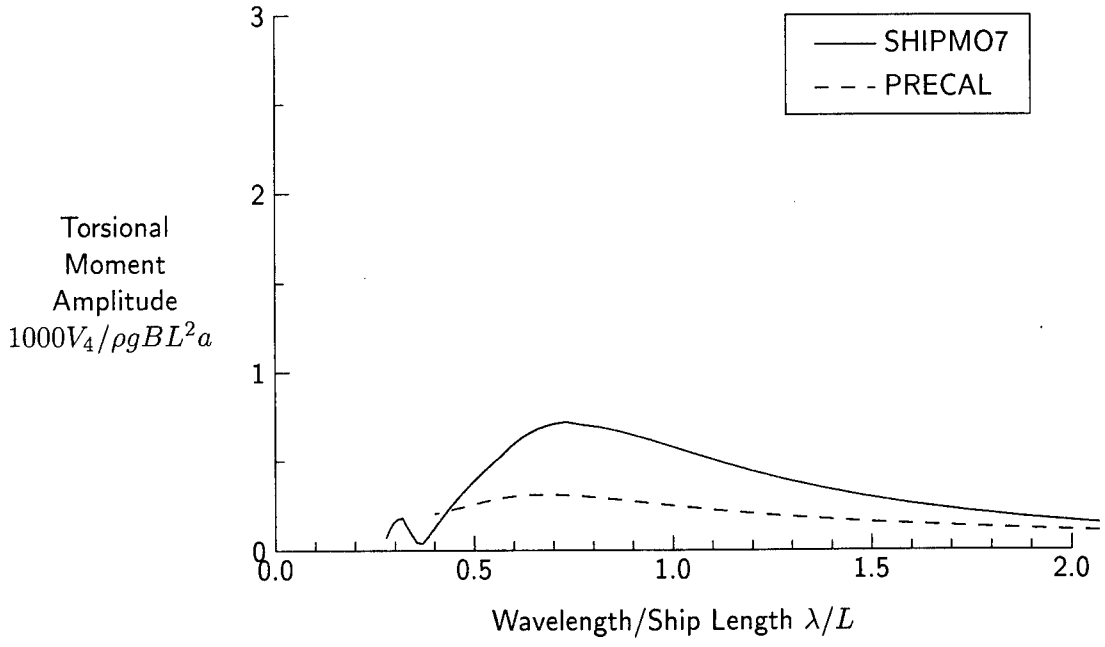

Figure 125: Torsional Moment at Station 13, $Fn = 0.29$, $\beta = 30$ degrees

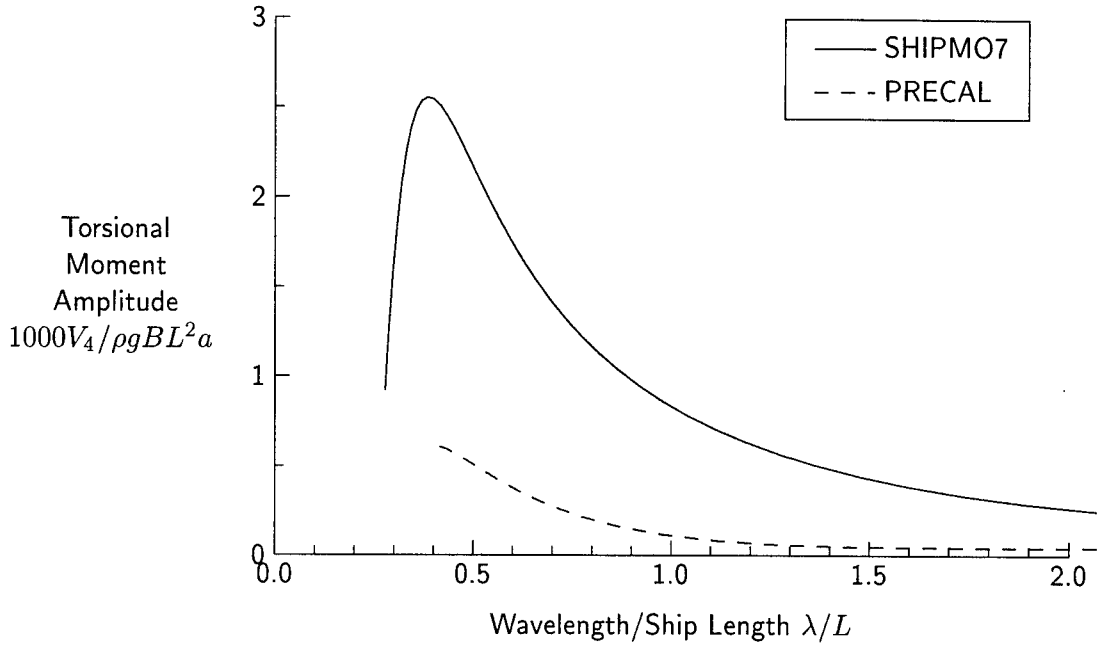

Figure 126: Torsional Moment at Station 5, $Fn = 0.29$, $\beta = 60$ degrees

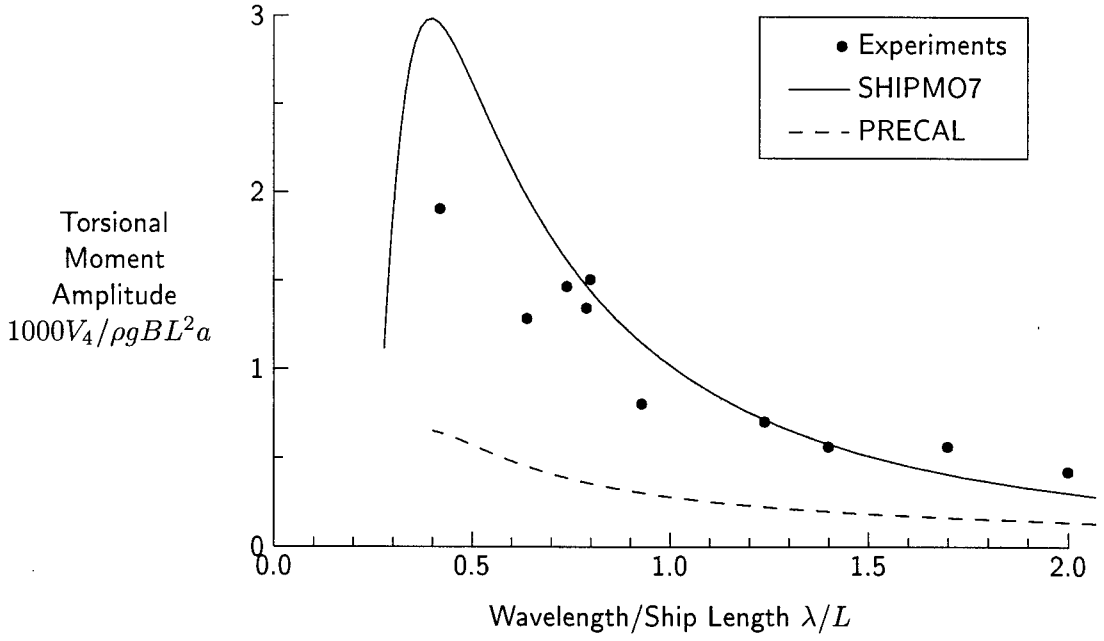

Figure 127: Torsional Moment at Station 10, $Fn = 0.29$, $\beta = 60$ degrees

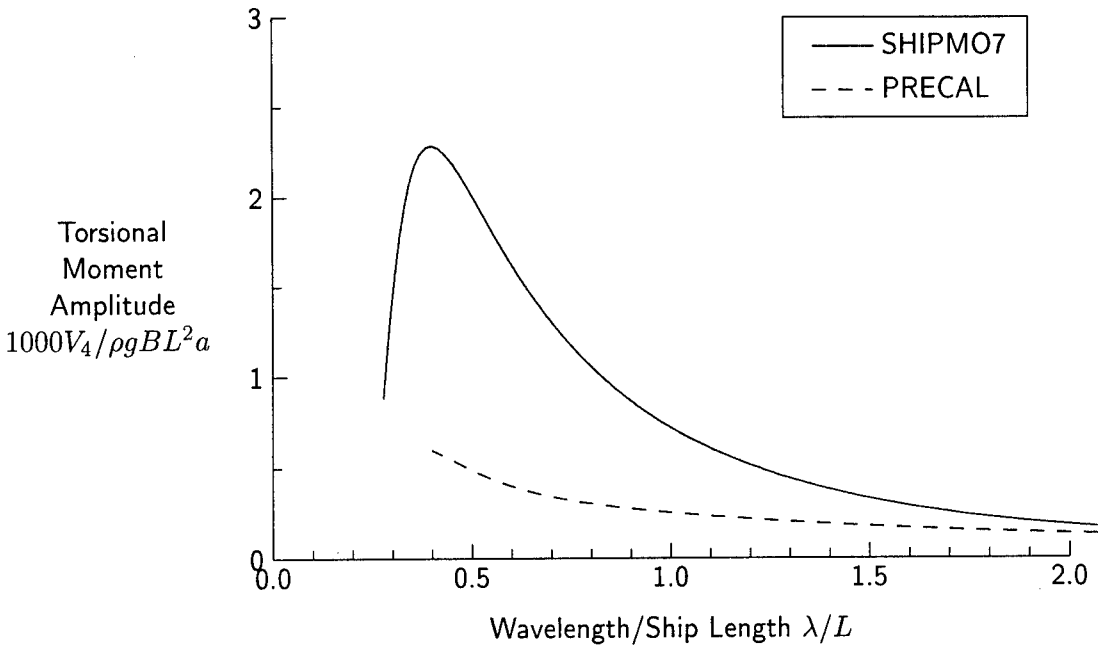

Figure 128: Torsional Moment at Station 13, $Fn = 0.29$, $\beta = 60$ degrees

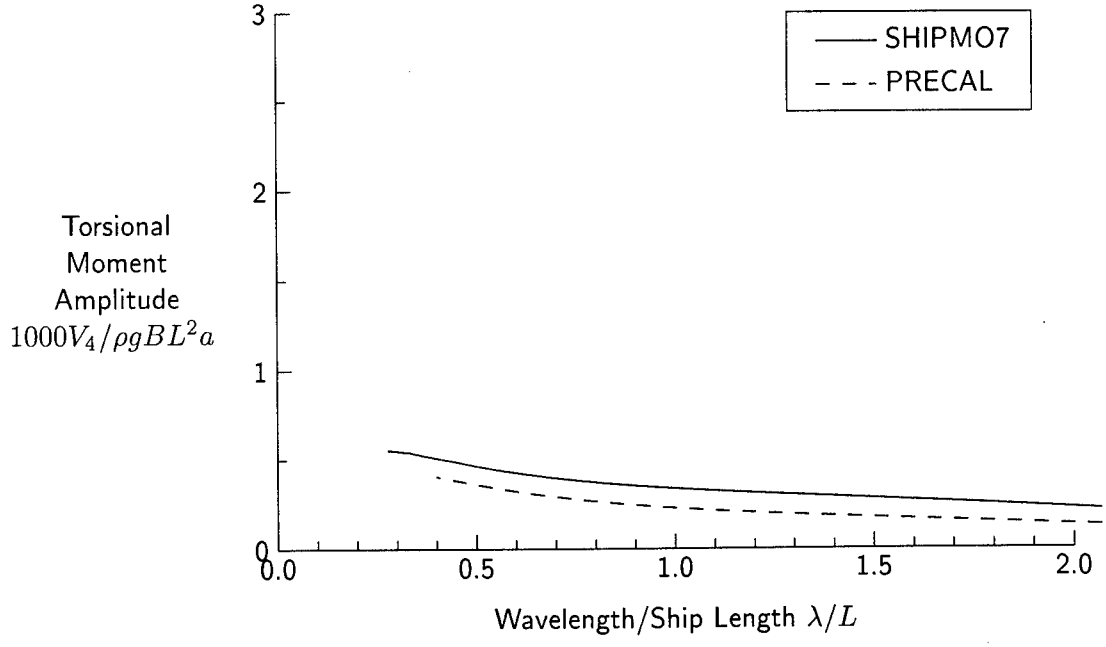

Figure 129: Torsional Moment at Station 5, $Fn = 0.29$, $\beta = 90$ degrees

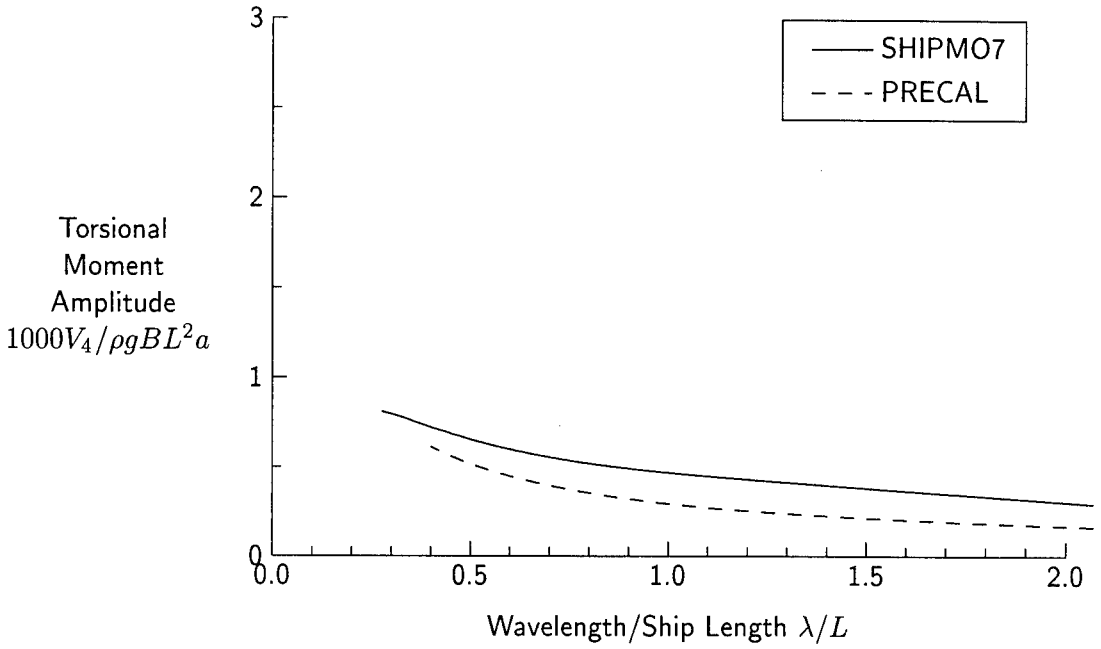

Figure 130: Torsional Moment at Station 10, $Fn = 0.29$, $\beta = 90$ degrees

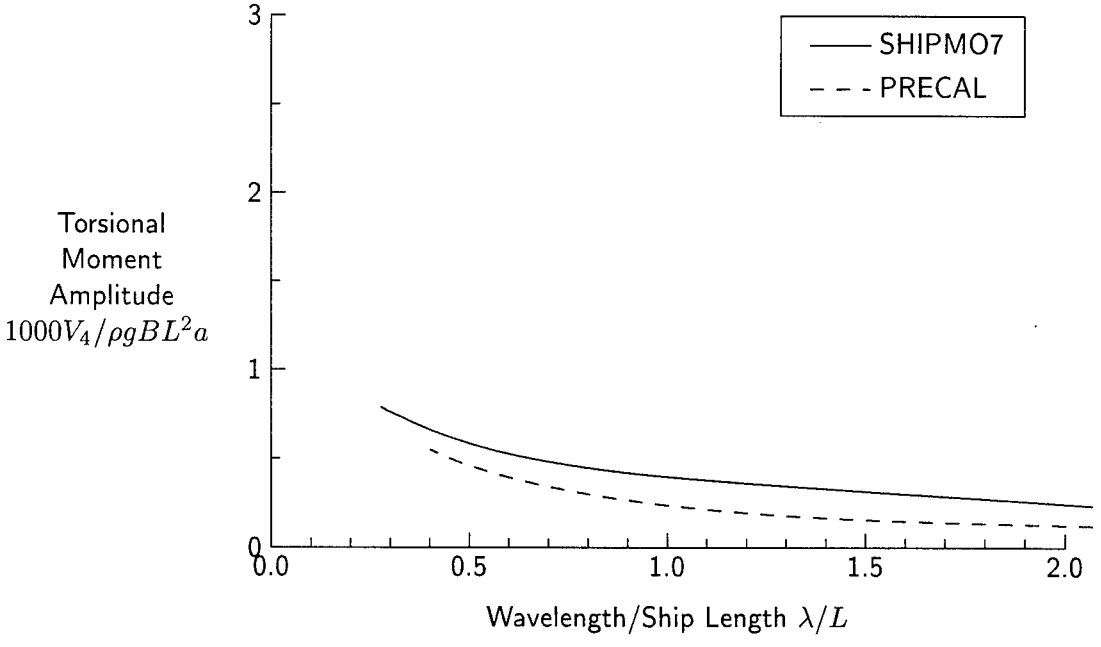

Figure 131: Torsional Moment at Station 13, $Fn = 0.29$, $\beta = 90$ degrees

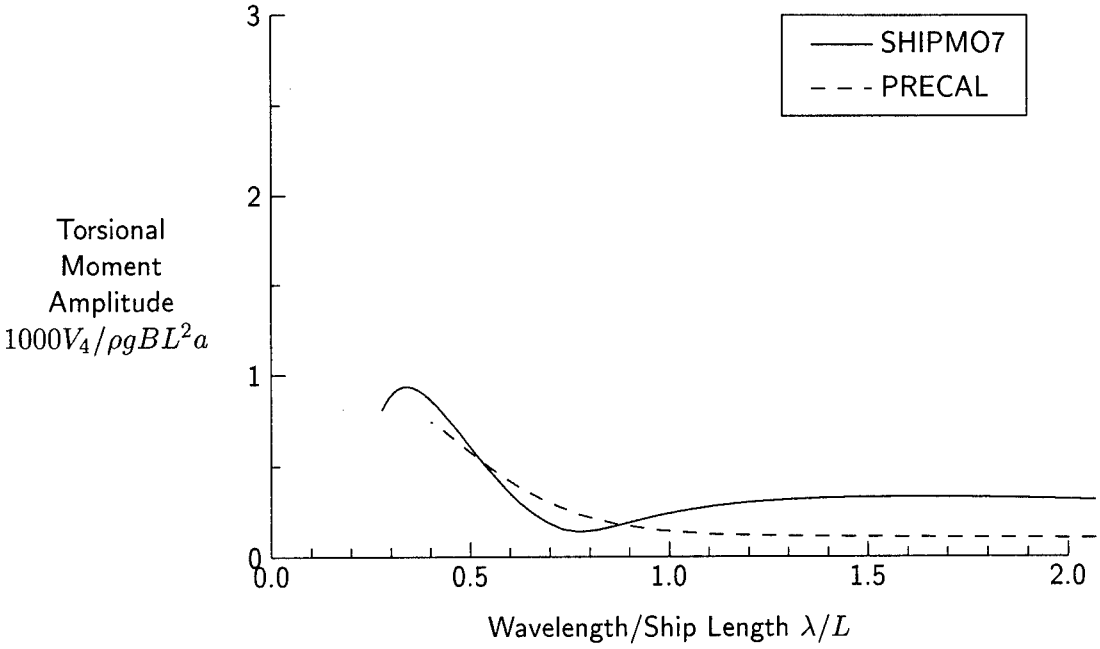

Figure 132: Torsional Moment at Station 5, $Fn = 0.29$, $\beta = 120$ degrees

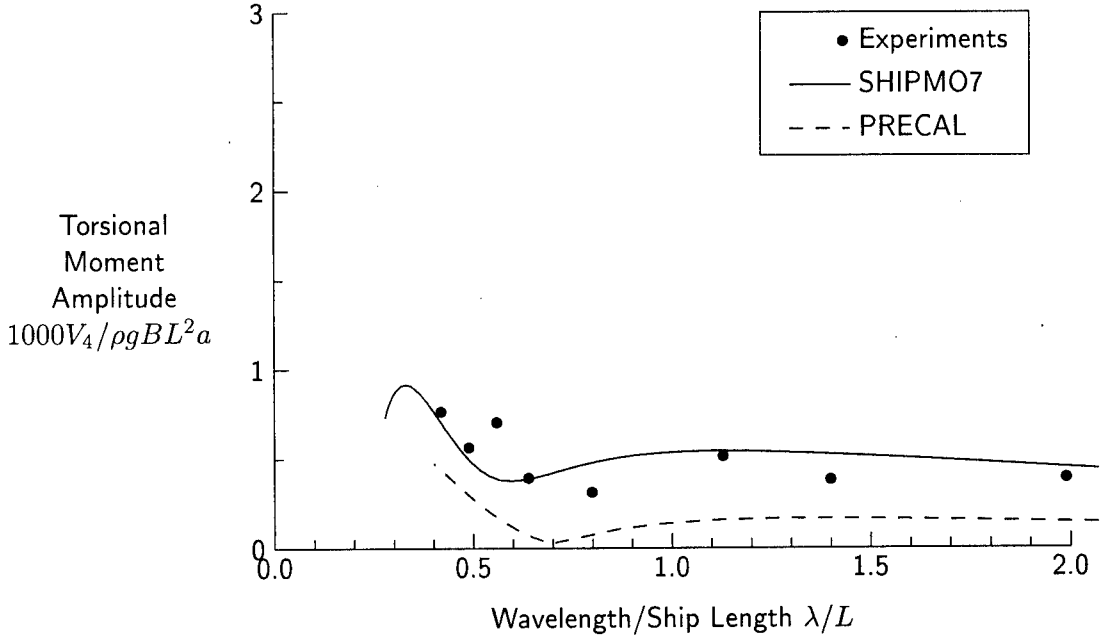

Figure 133: Torsional Moment at Station 10, $Fn = 0.29$, $\beta = 120$ degrees

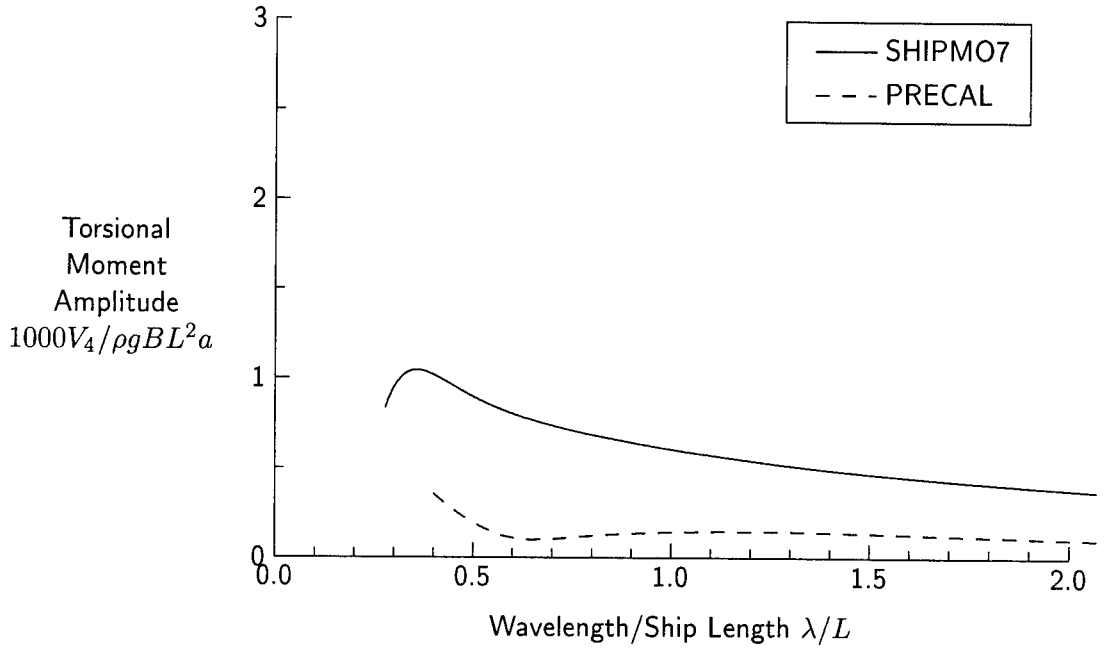

Figure 134: Torsional Moment at Station 13, $Fn = 0.29$, $\beta = 120$ degrees

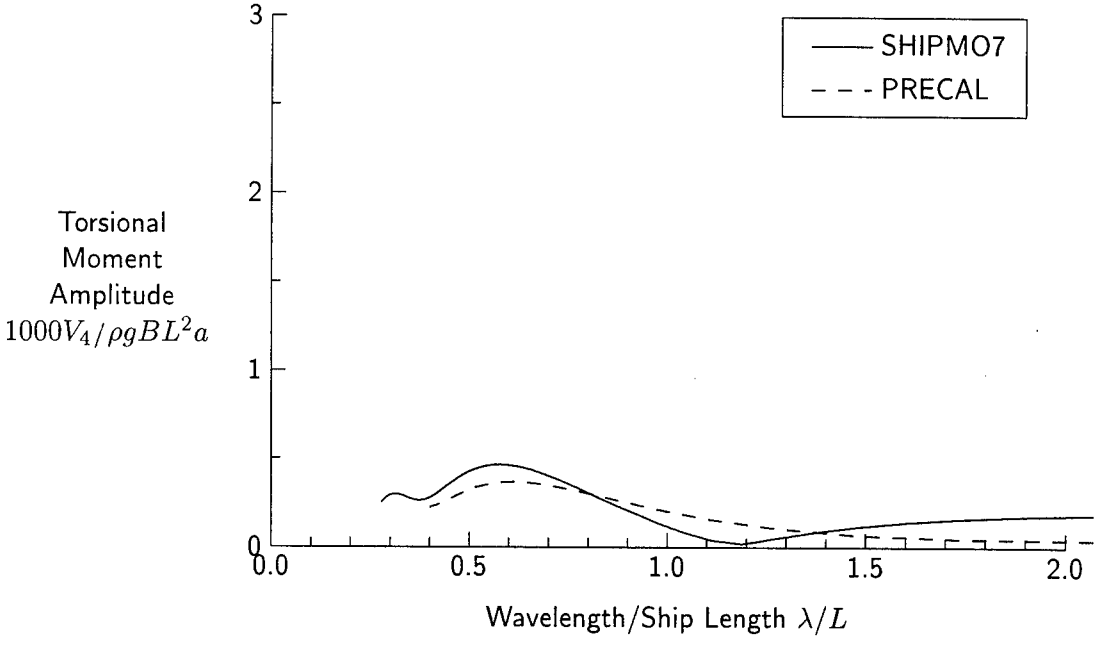

Figure 135: Torsional Moment at Station 5, $Fn = 0.29$, $\beta = 150$ degrees

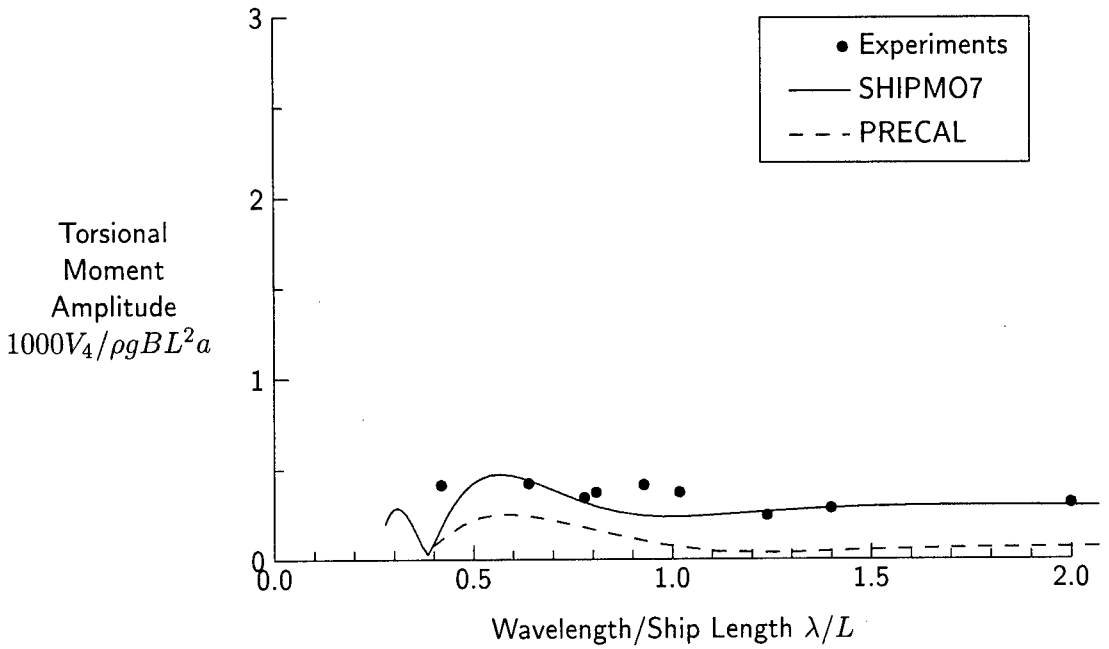

Figure 136: Torsional Moment at Station 10, $Fn = 0.29$, $\beta = 150$ degrees

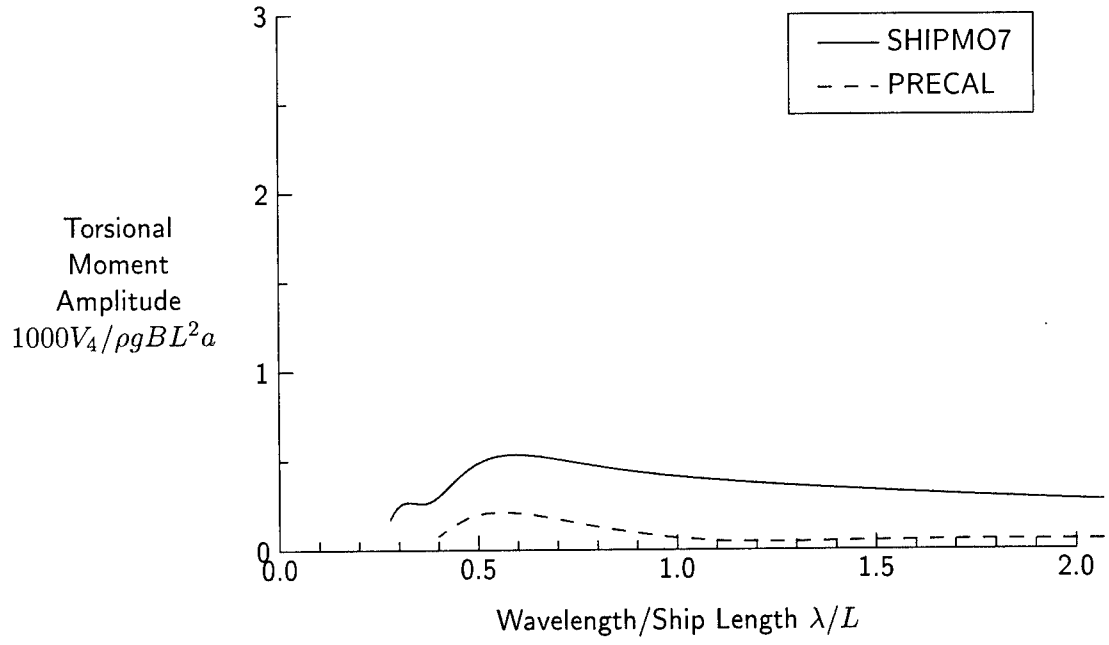

Figure 137: Torsional Moment at Station 13, $Fn = 0.29$, $\beta = 150$ degrees

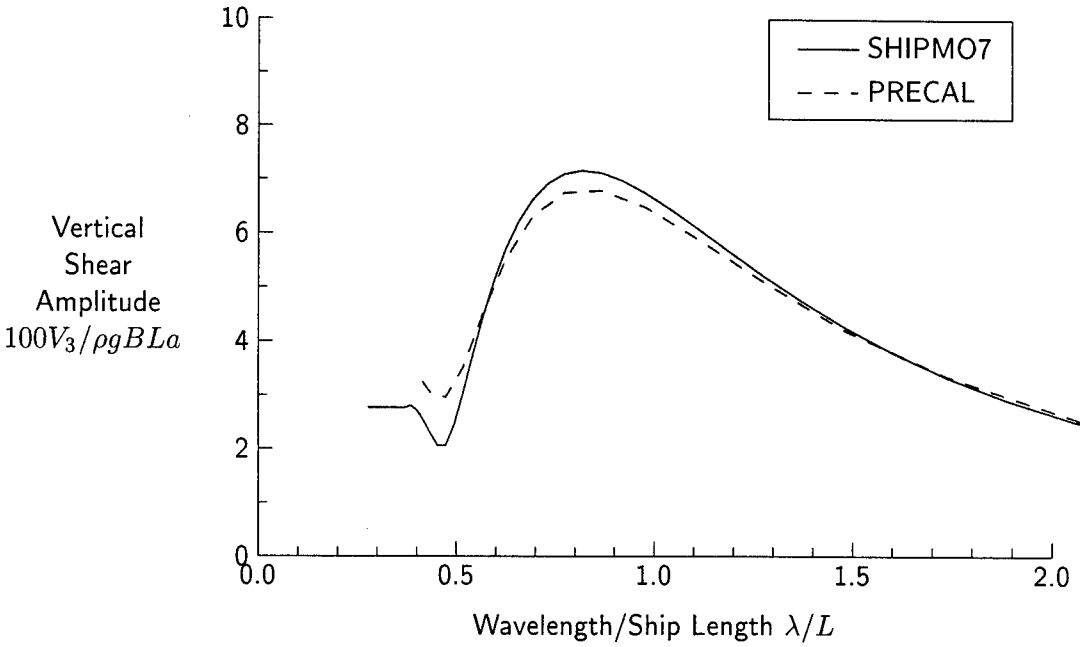

Figure 138: Vertical Shear Force at Station 5, $Fn = 0.21$, $\beta = 0$ degrees

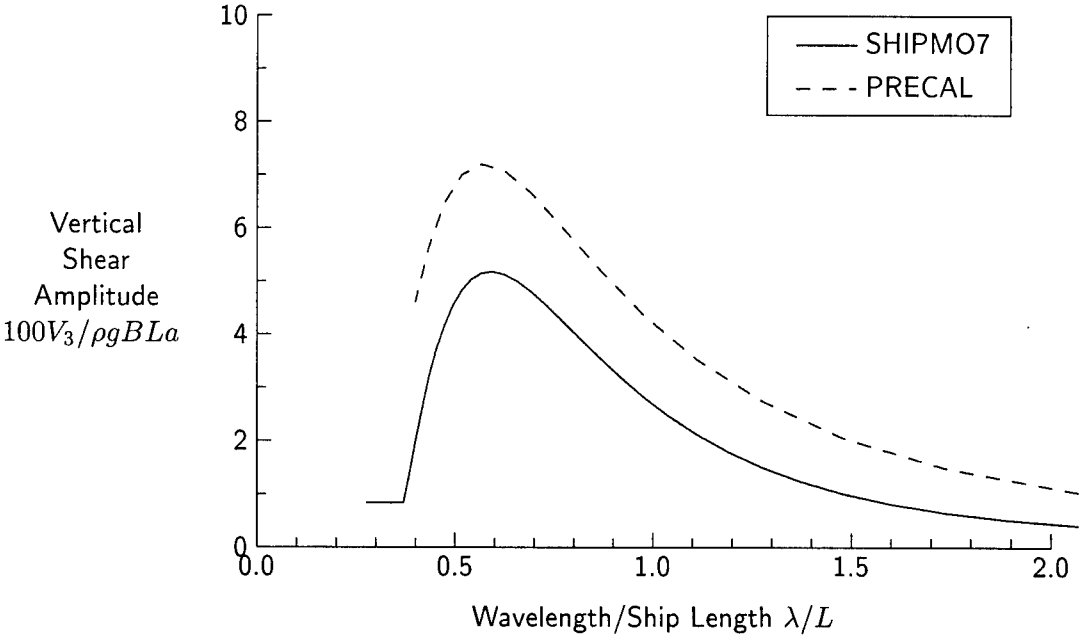

Figure 139: Vertical Shear Force at Station 10, $Fn = 0.21$, $\beta = 0$ degrees

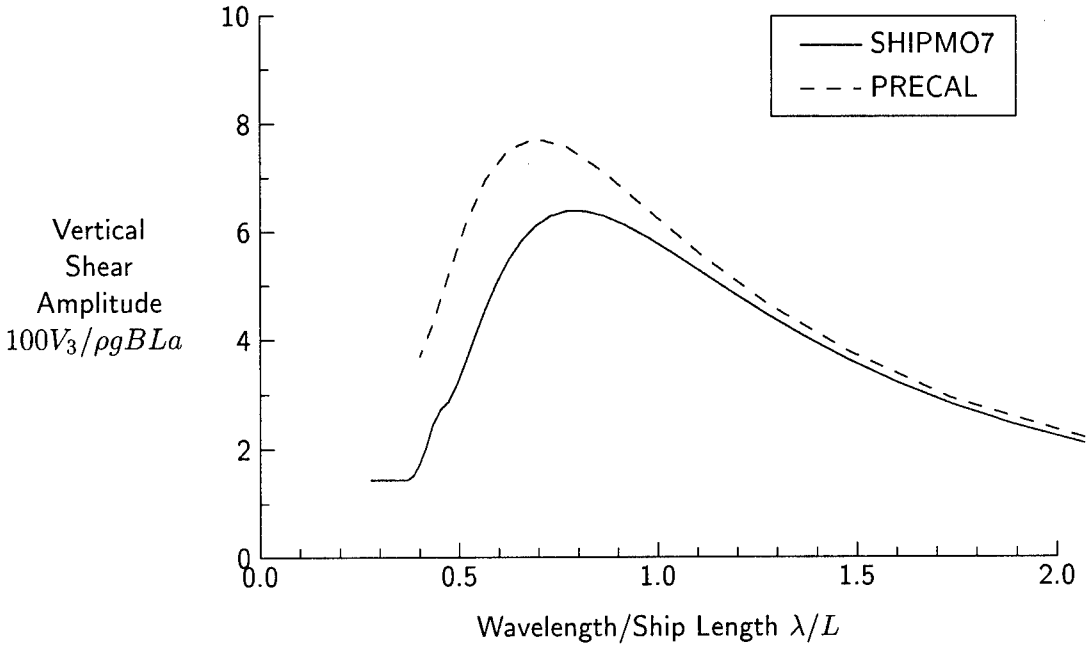

Figure 140: Vertical Shear Force at Station 13, $Fn = 0.21$, $\beta = 0$ degrees

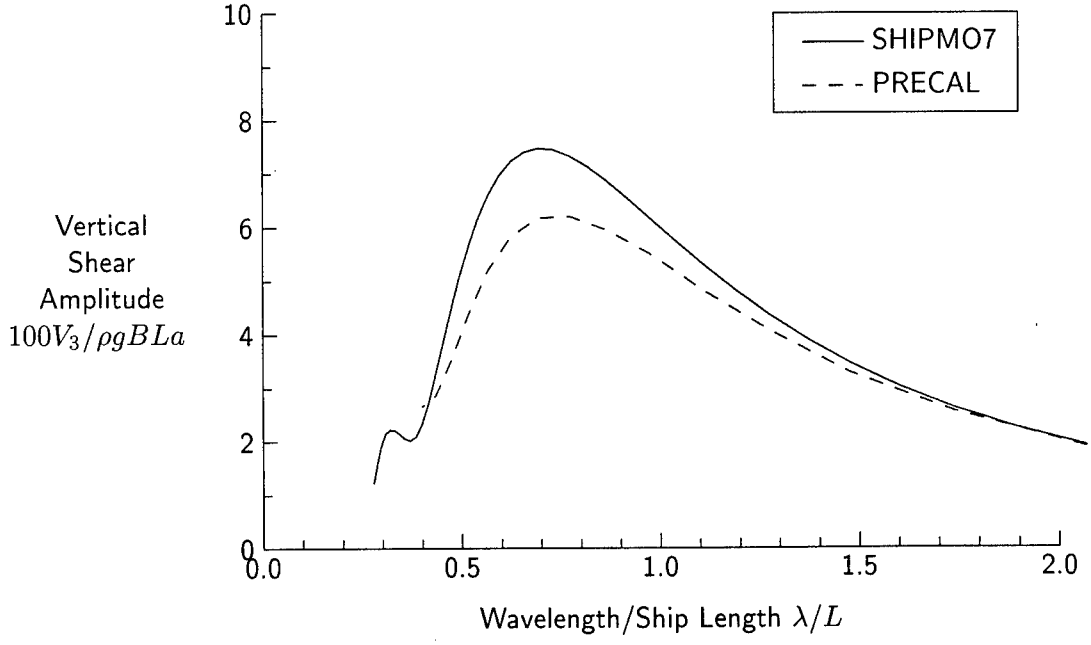

Figure 141: Vertical Shear Force at Station 5, $Fn = 0.21$, $\beta = 30$ degrees

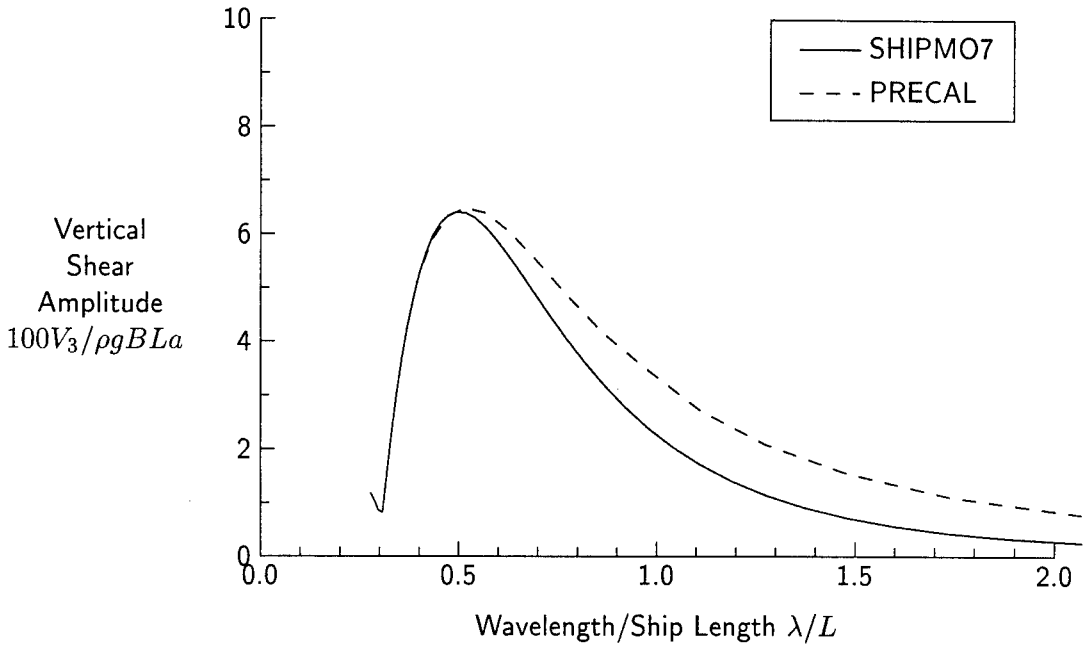

Figure 142: Vertical Shear Force at Station 10, $Fn = 0.21$, $\beta = 30$ degrees

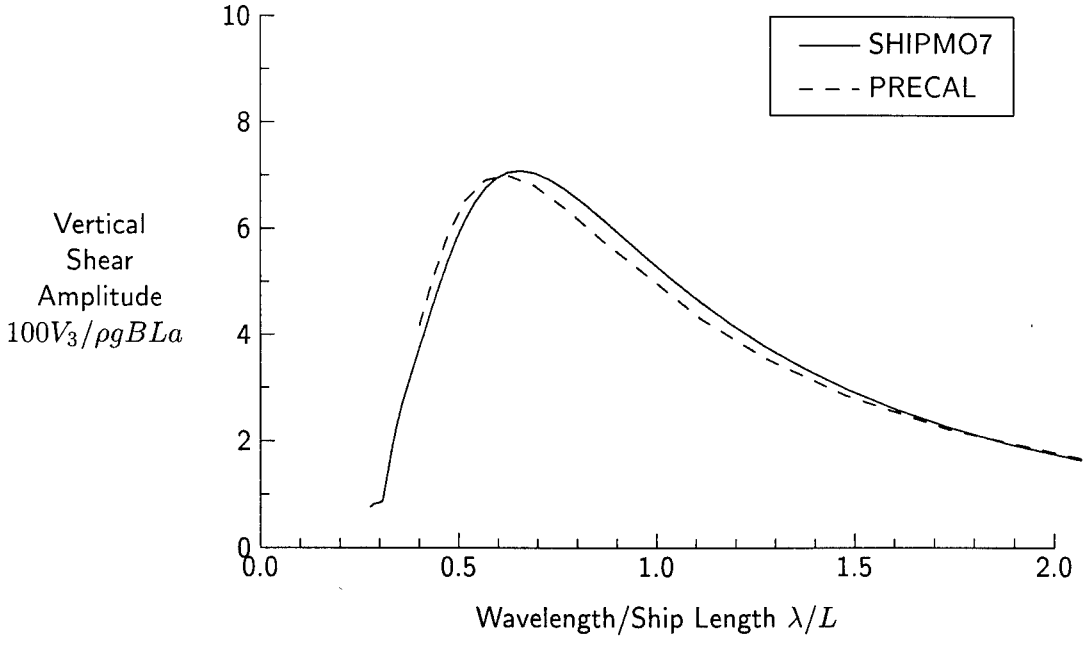

Figure 143: Vertical Shear Force at Station 13, $Fn = 0.21$, $\beta = 30$ degrees

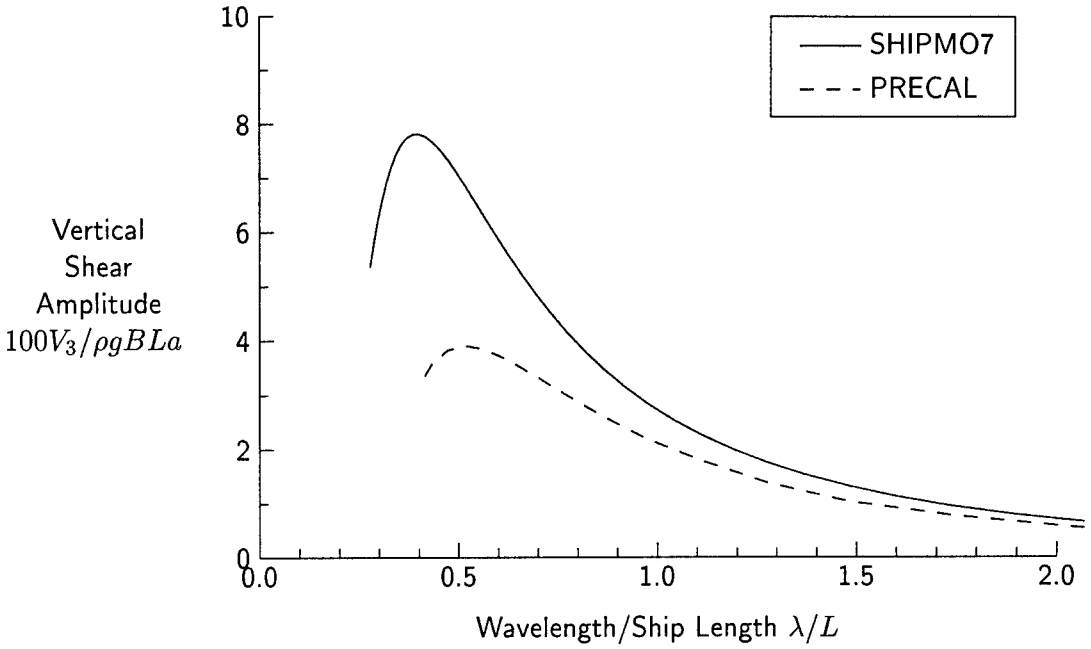

Figure 144: Vertical Shear Force at Station 5, $Fn = 0.21$, $\beta = 60$ degrees

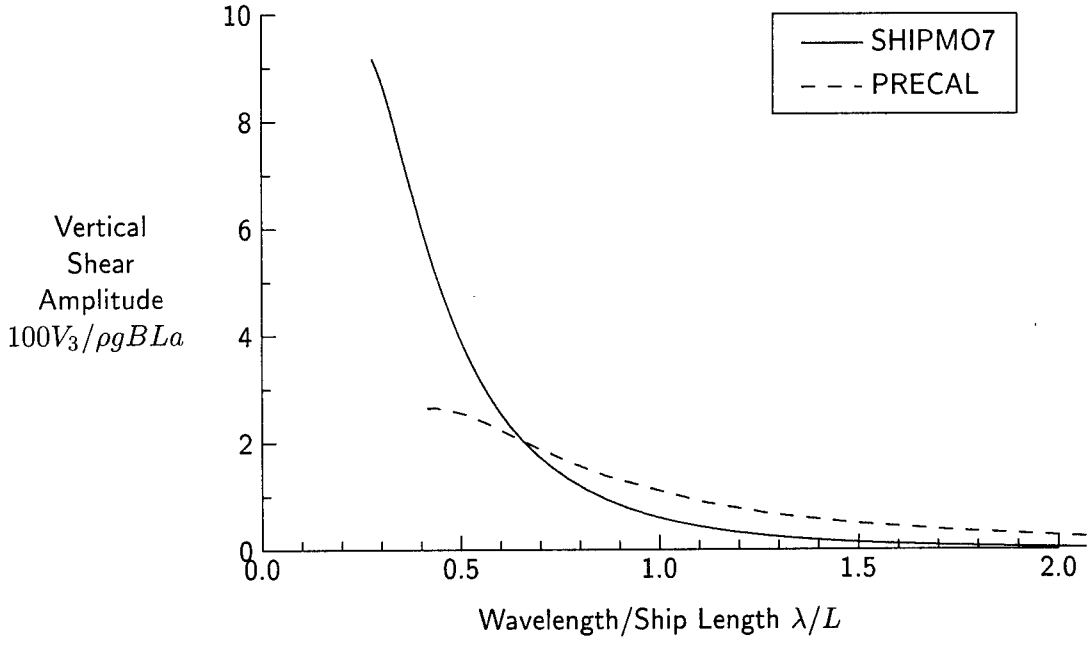

Figure 145: Vertical Shear Force at Station 10, $Fn = 0.21$, $\beta = 60$ degrees

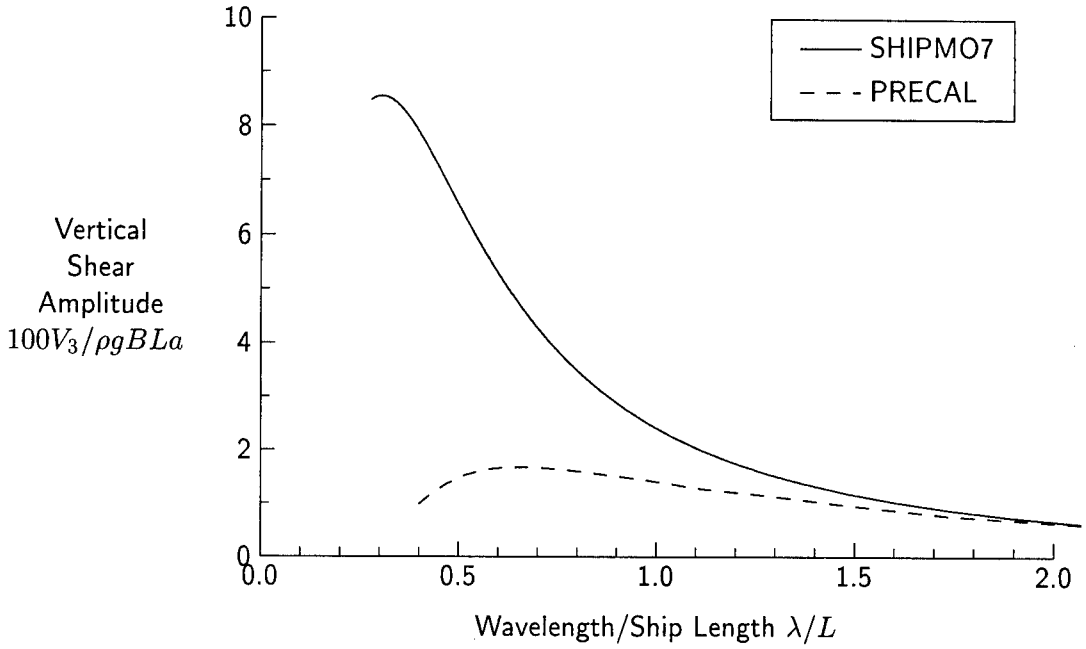

Figure 146: Vertical Shear Force at Station 13, $Fn = 0.21$, $\beta = 60$ degrees

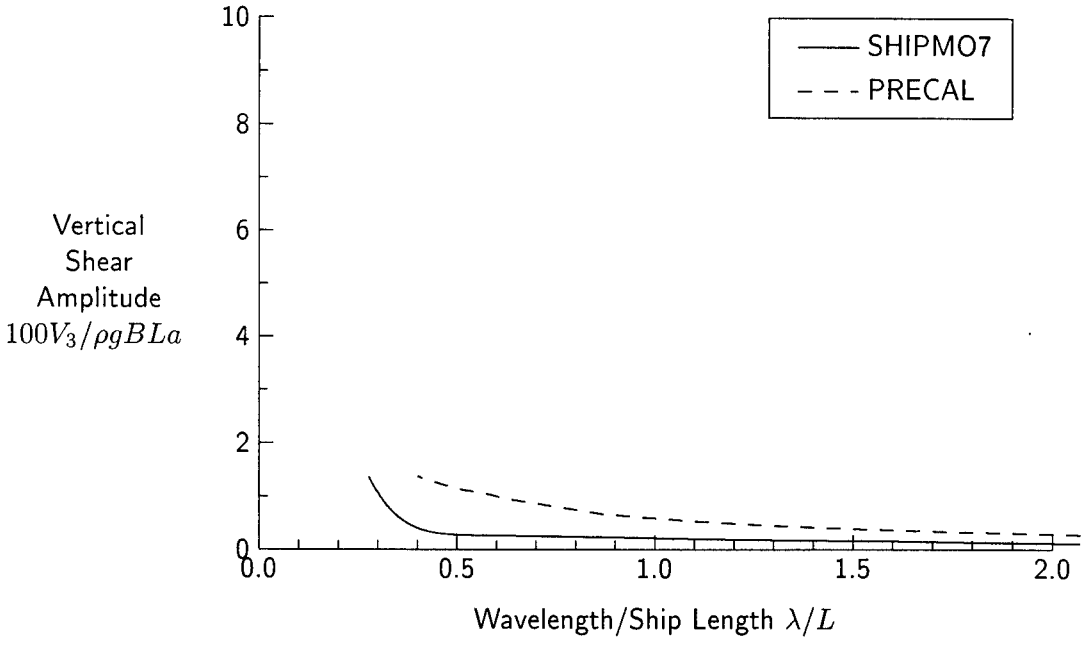

Figure 147: Vertical Shear Force at Station 5, $Fn = 0.21$, $\beta = 90$ degrees

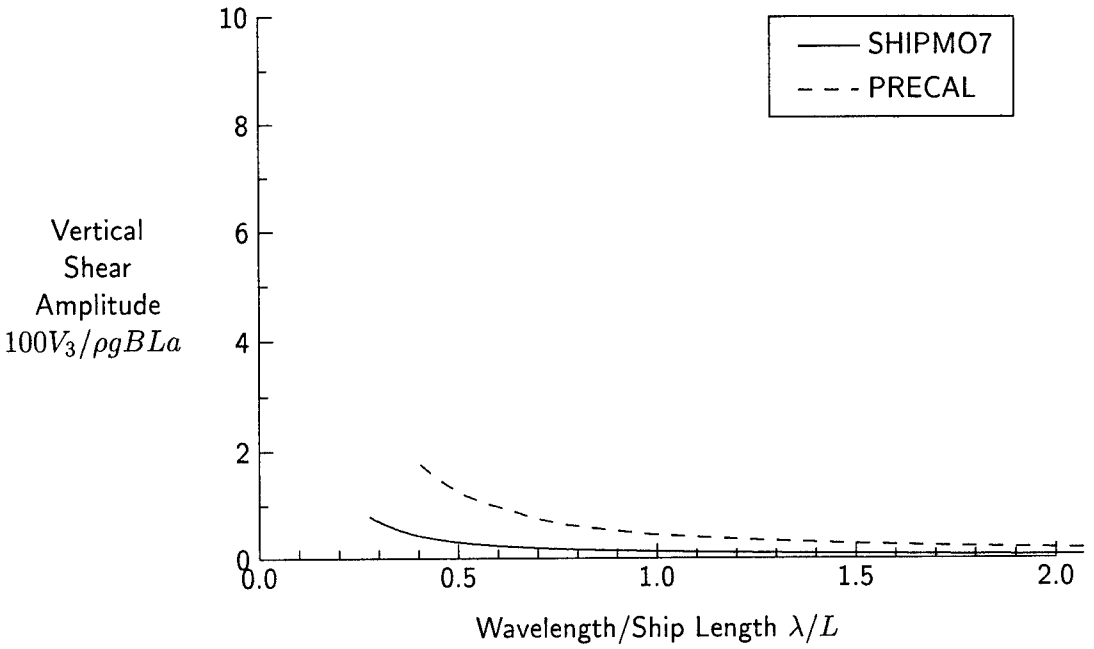

Figure 148: Vertical Shear Force at Station 10, $Fn = 0.21$, $\beta = 90$ degrees

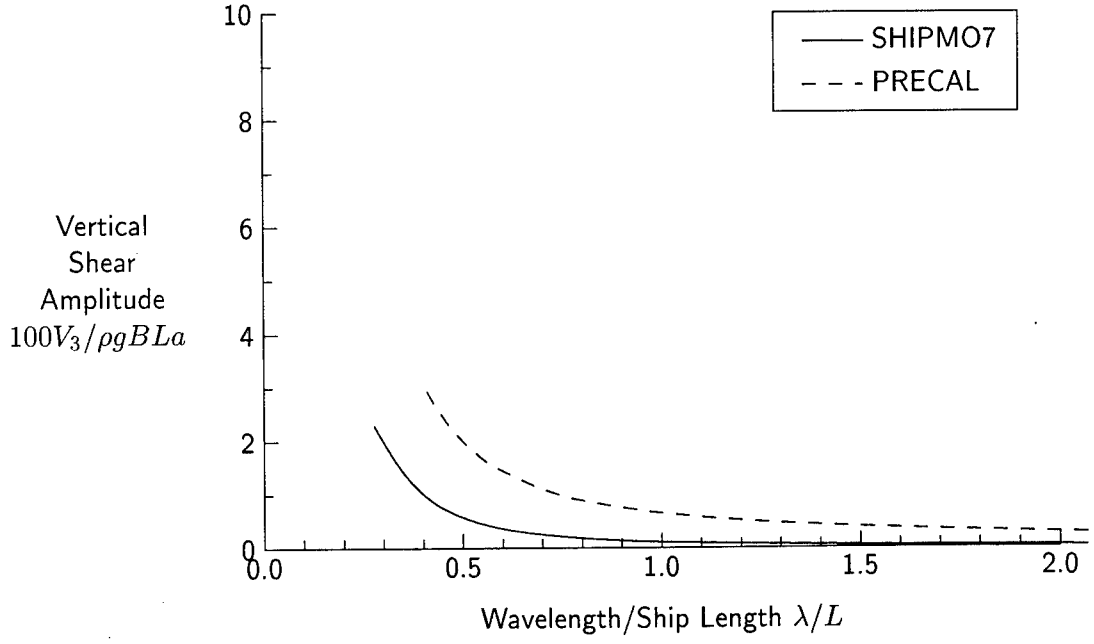

Figure 149: Vertical Shear Force at Station 13, $Fn = 0.21$, $\beta = 90$ degrees

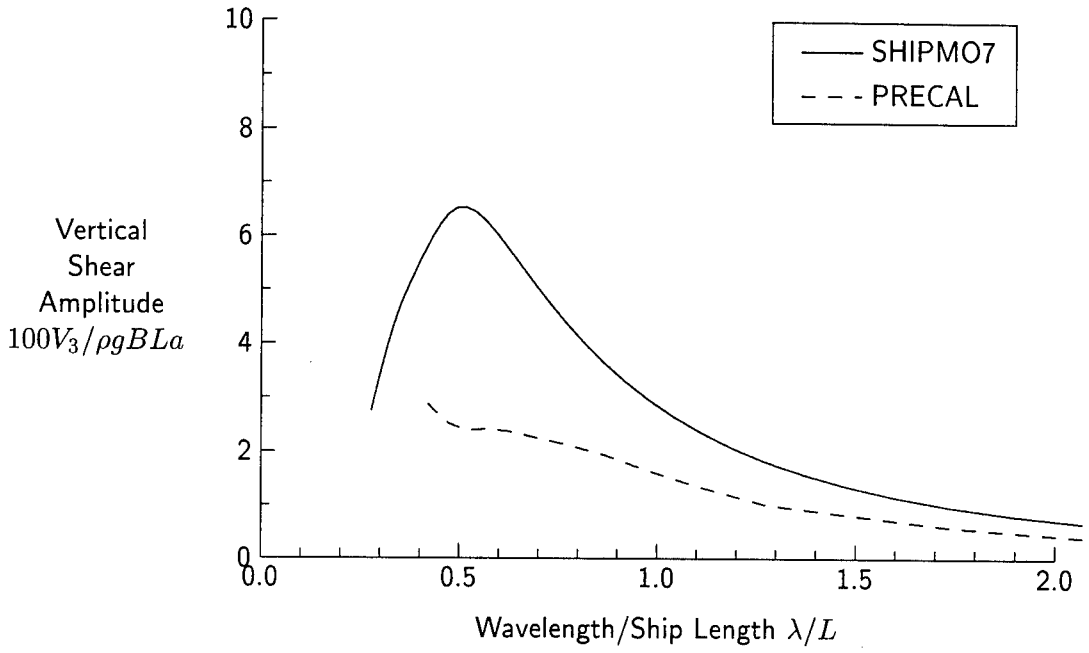

Figure 150: Vertical Shear Force at Station 5, $Fn = 0.21$, $\beta = 120$ degrees

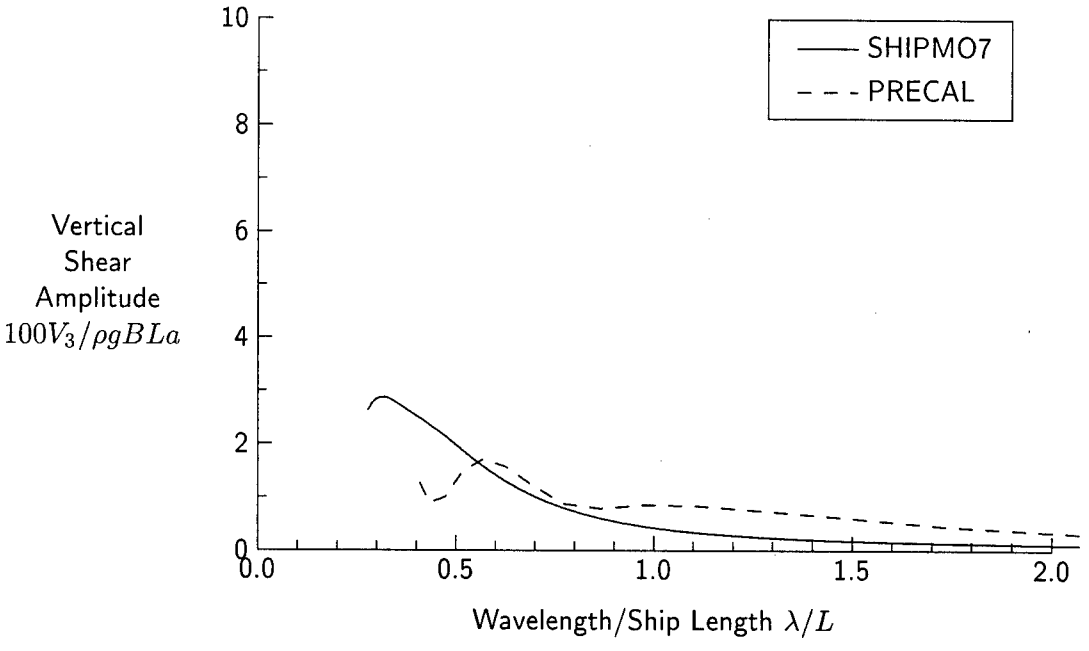

Figure 151: Vertical Shear Force at Station 10, $Fn = 0.21$, $\beta = 120$ degrees

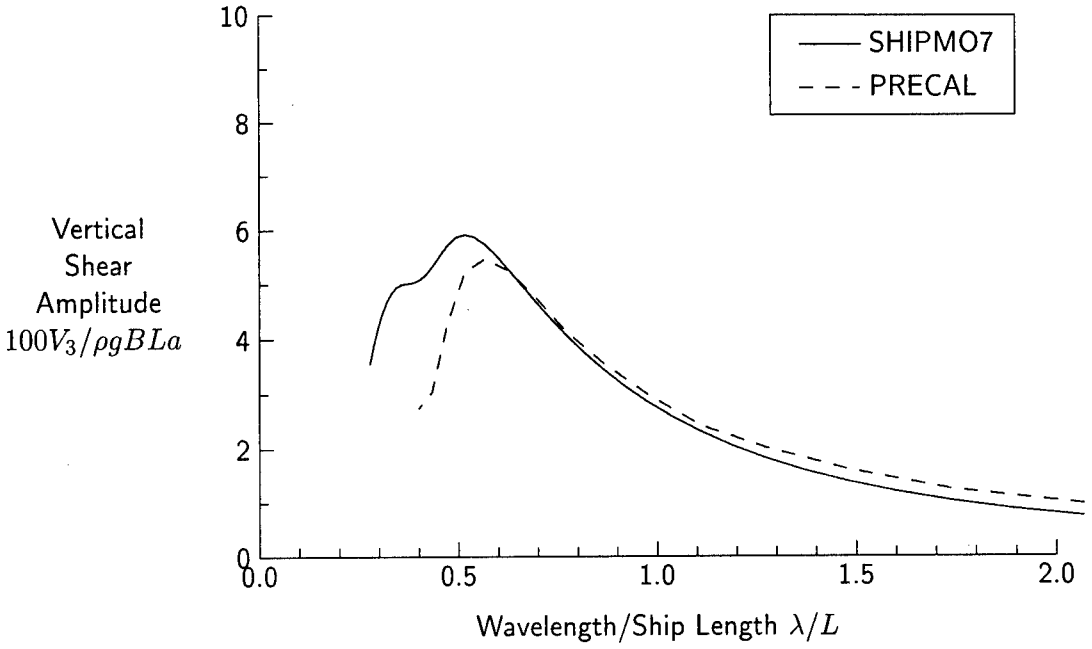

Figure 152: Vertical Shear Force at Station 13, $Fn = 0.21$, $\beta = 120$ degrees

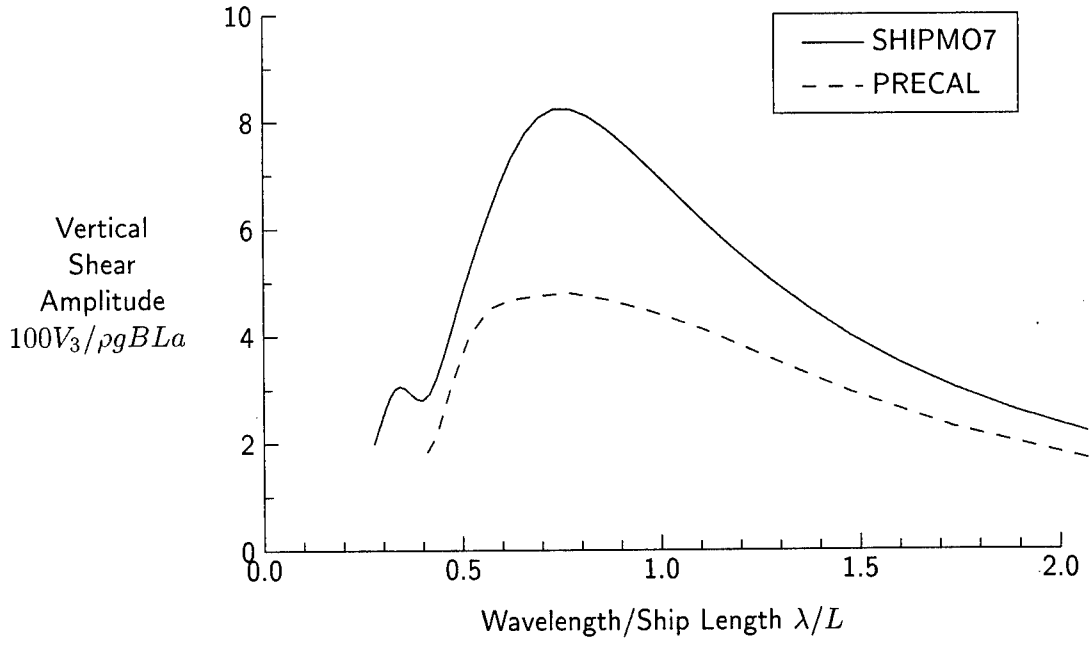

Figure 153: Vertical Shear Force at Station 5, $Fn = 0.21$, $\beta = 150$ degrees

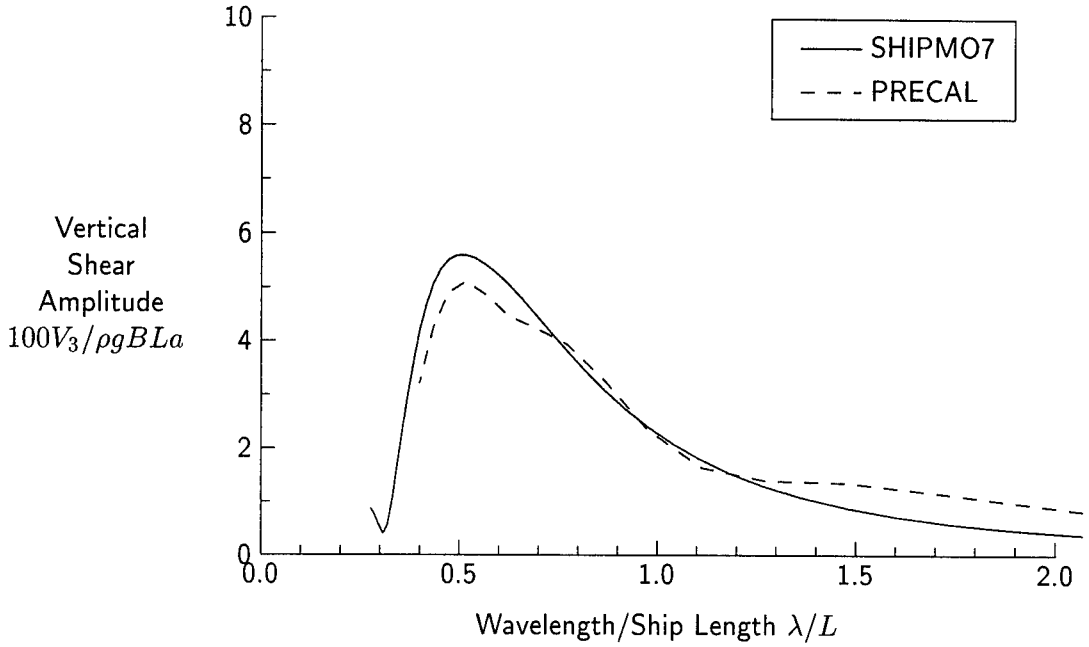

Figure 154: Vertical Shear Force at Station 10, $Fn = 0.21$, $\beta = 150$ degrees

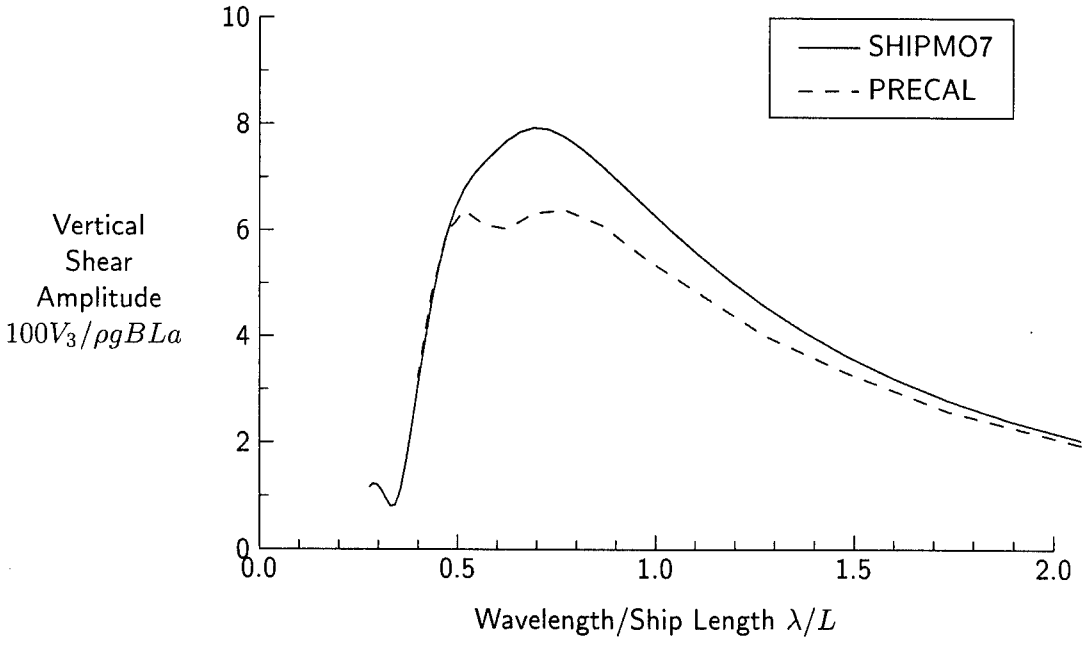

Figure 155: Vertical Shear Force at Station 13, $Fn = 0.21$, $\beta = 150$ degrees

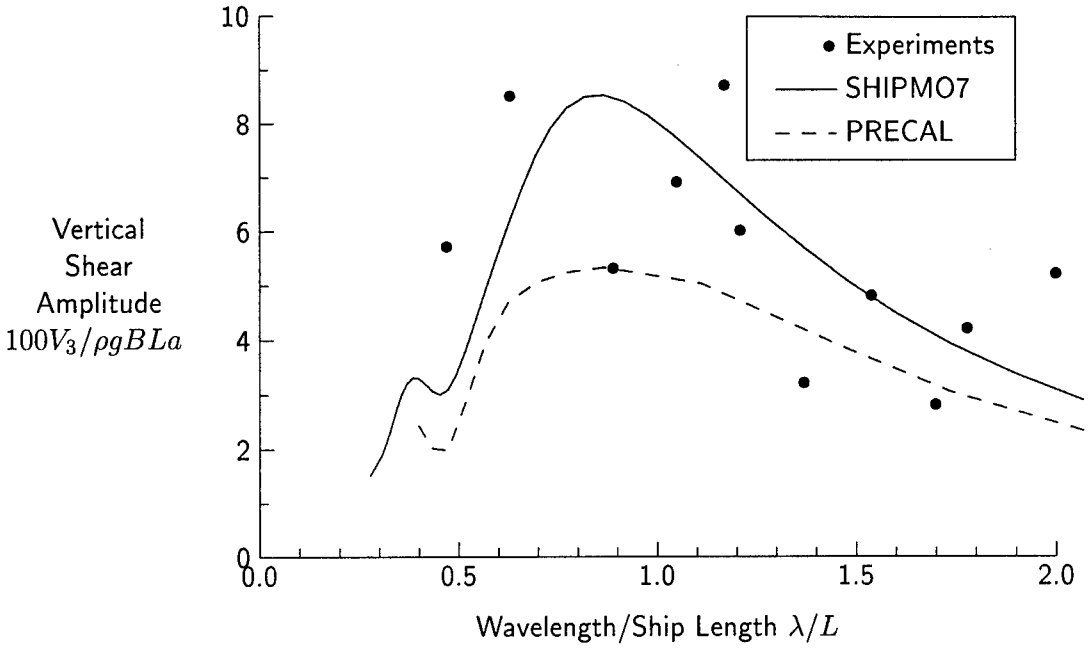

Figure 156: Vertical Shear Force at Station 5, $Fn = 0.21$, $\beta = 180$ degrees

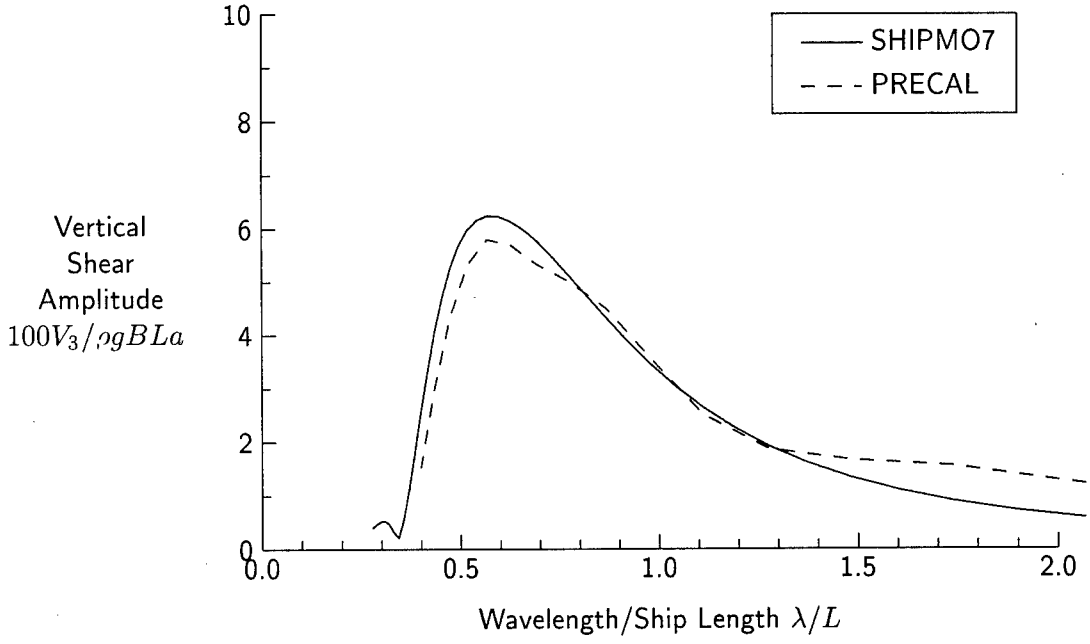

Figure 157: Vertical Shear Force at Station 10, $Fn = 0.21$, $\beta = 180$ degrees

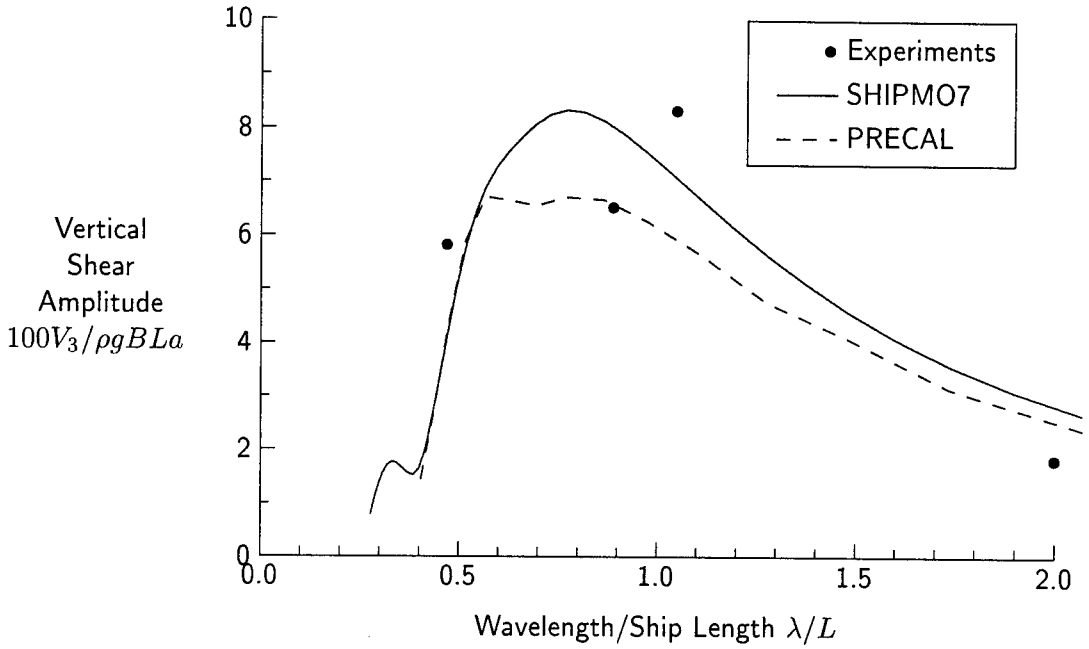

Figure 158: Vertical Shear Force at Station 13, $Fn = 0.21$, $\beta = 180$ degrees

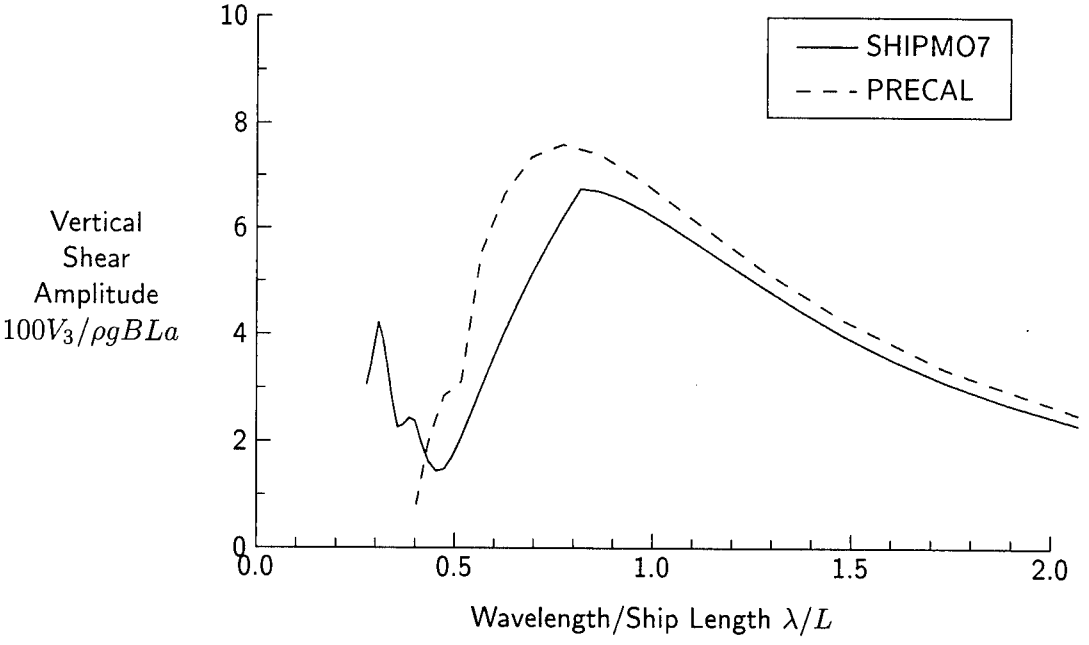

Figure 159: Vertical Shear Force at Station 5, $Fn = 0.29$, $\beta = 0$ degrees

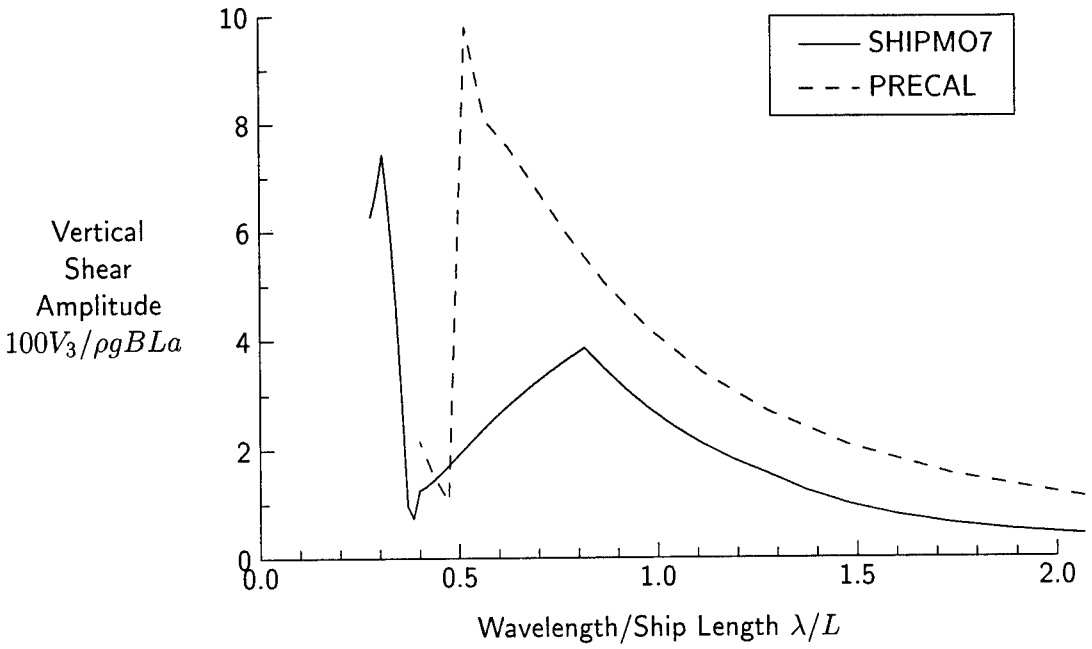

Figure 160: Vertical Shear Force at Station 10, $Fn = 0.29$, $\beta = 0$ degrees

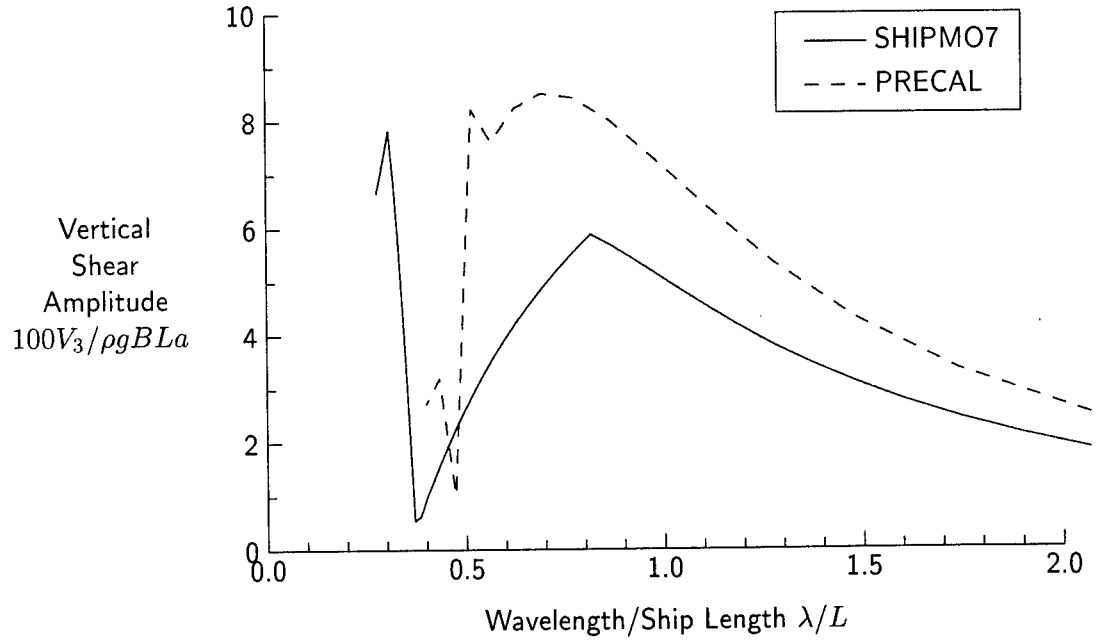

Figure 161: Vertical Shear Force at Station 13, $Fn = 0.29$, $\beta = 0$ degrees

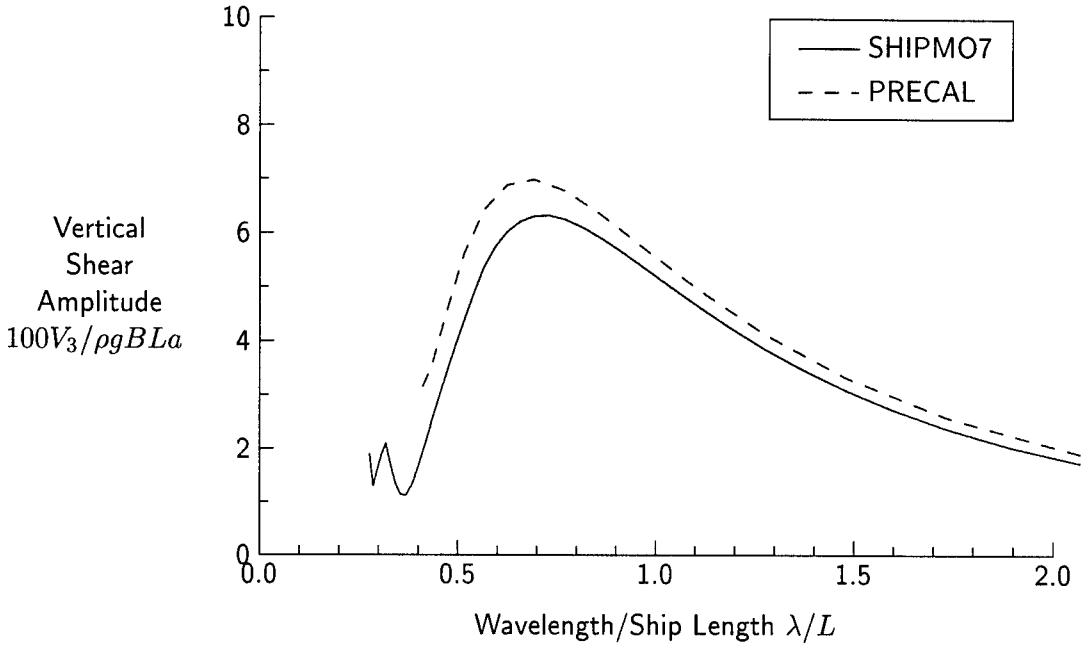

Figure 162: Vertical Shear Force at Station 5, $Fn = 0.29$, $\beta = 30$ degrees

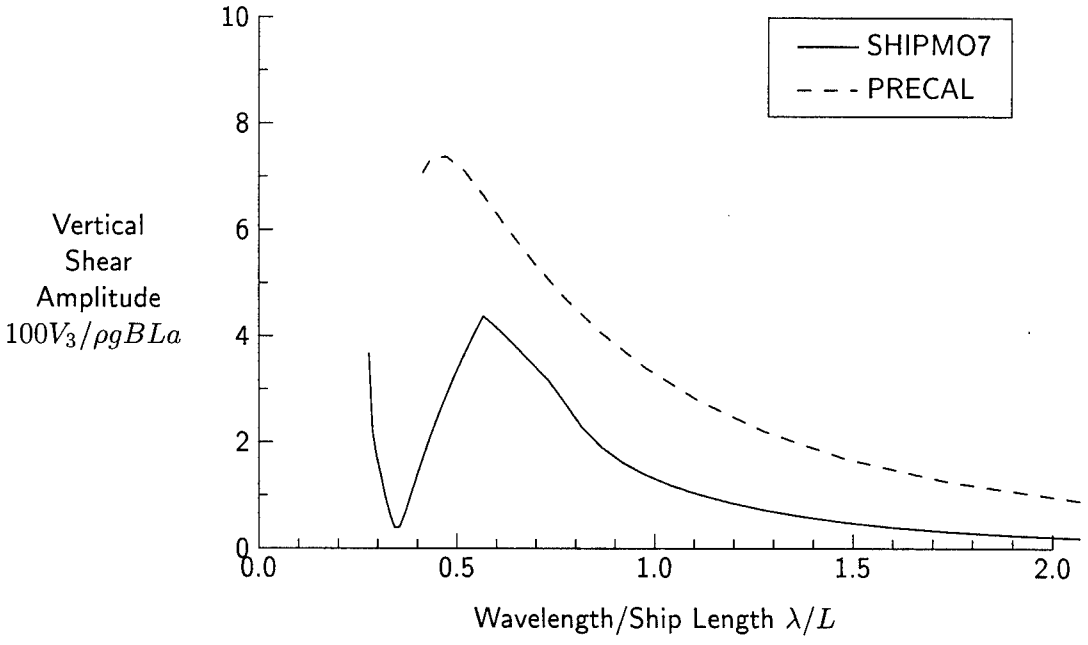

Figure 163: Vertical Shear Force at Station 10, $Fn = 0.29$, $\beta = 30$ degrees

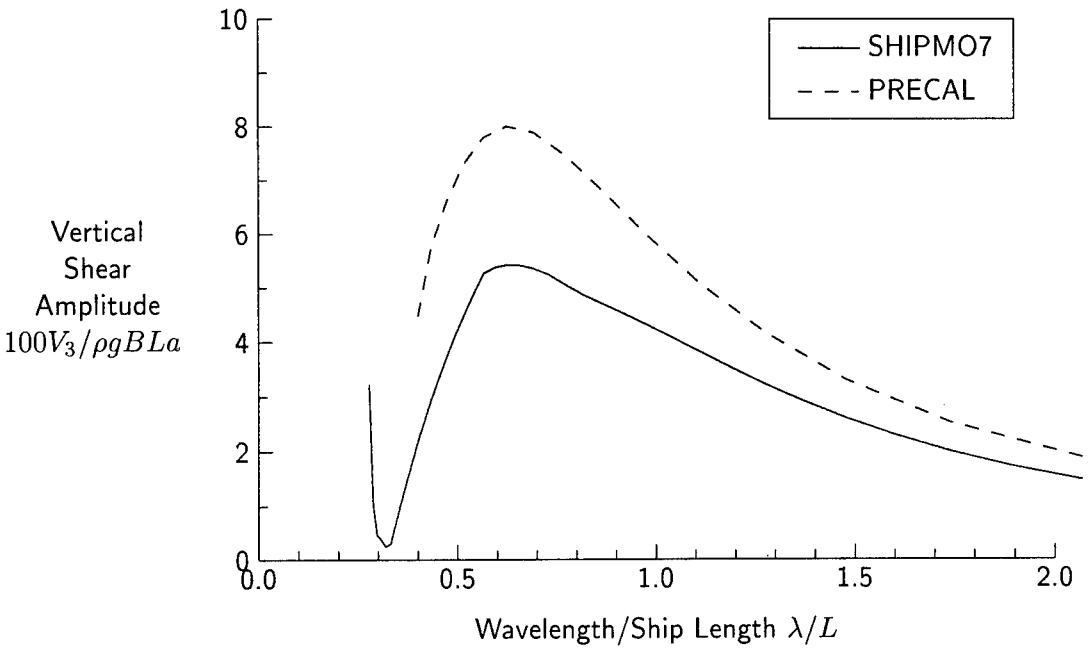

Figure 164: Vertical Shear Force at Station 13, $Fn = 0.29$, $\beta = 30$ degrees

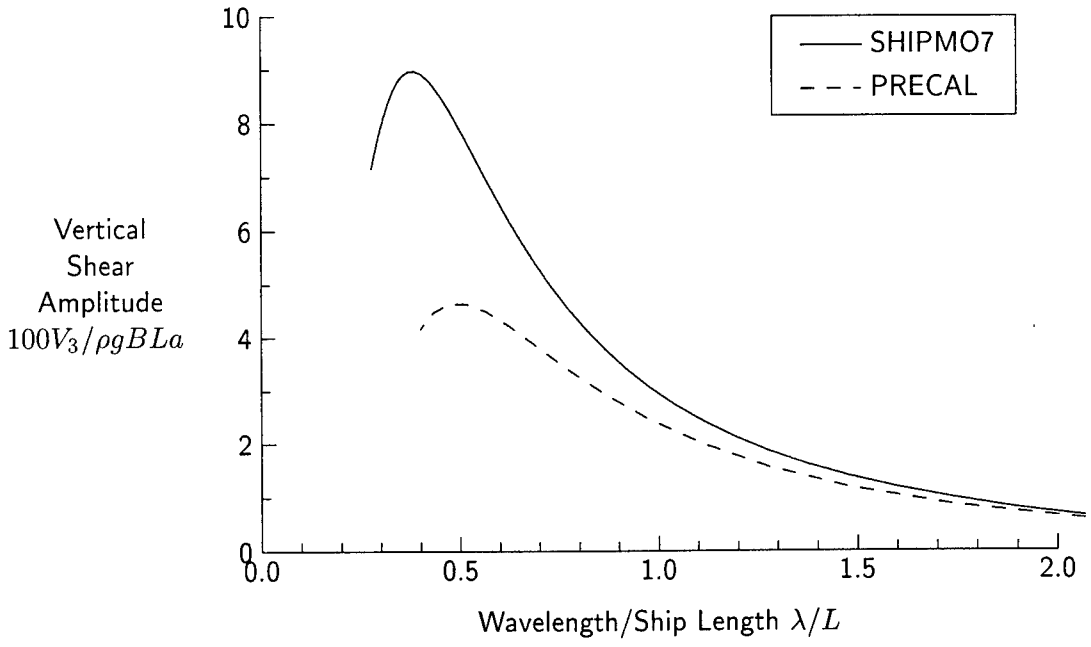

Figure 165: Vertical Shear Force at Station 5, $Fn = 0.29$, $\beta = 60$ degrees

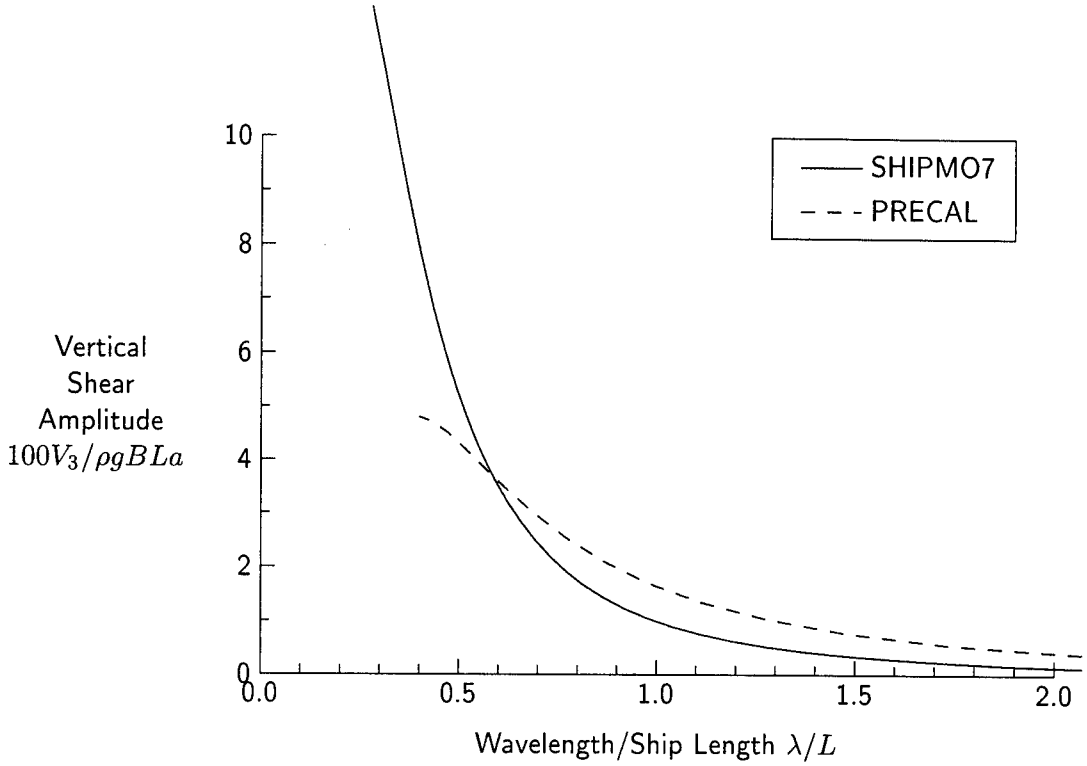

Figure 166: Vertical Shear Force at Station 10, $Fn = 0.29$, $\beta = 60$ degrees

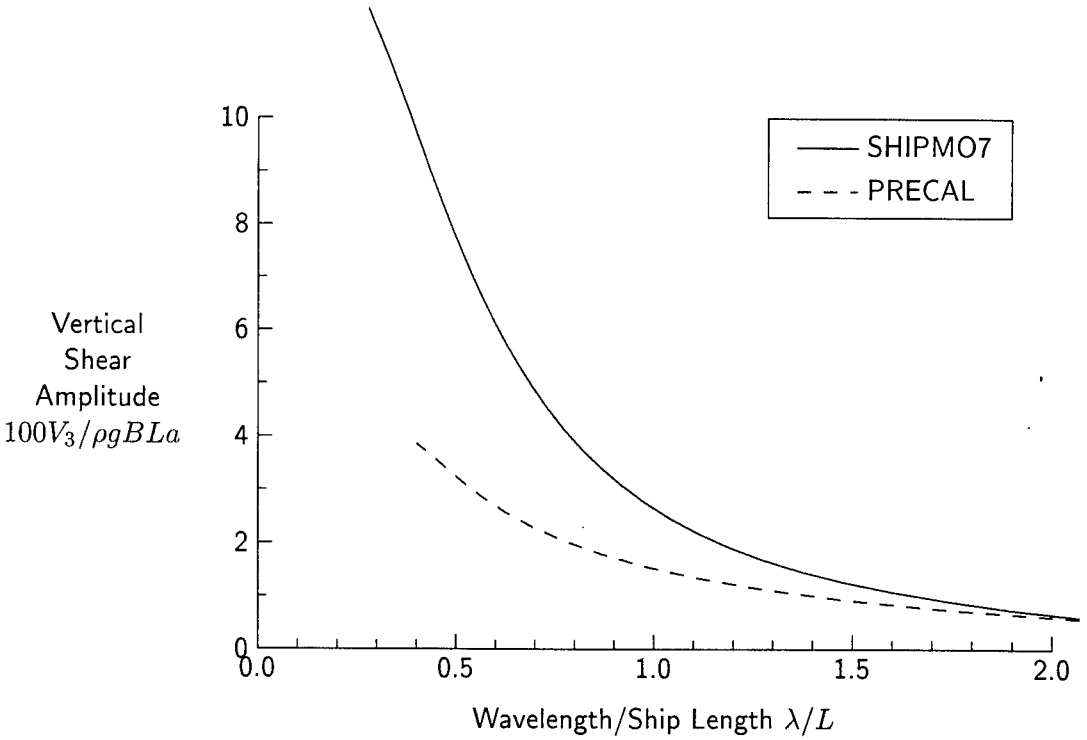

Figure 167: Vertical Shear Force at Station 13, $Fn = 0.29$, $\beta = 60$ degrees

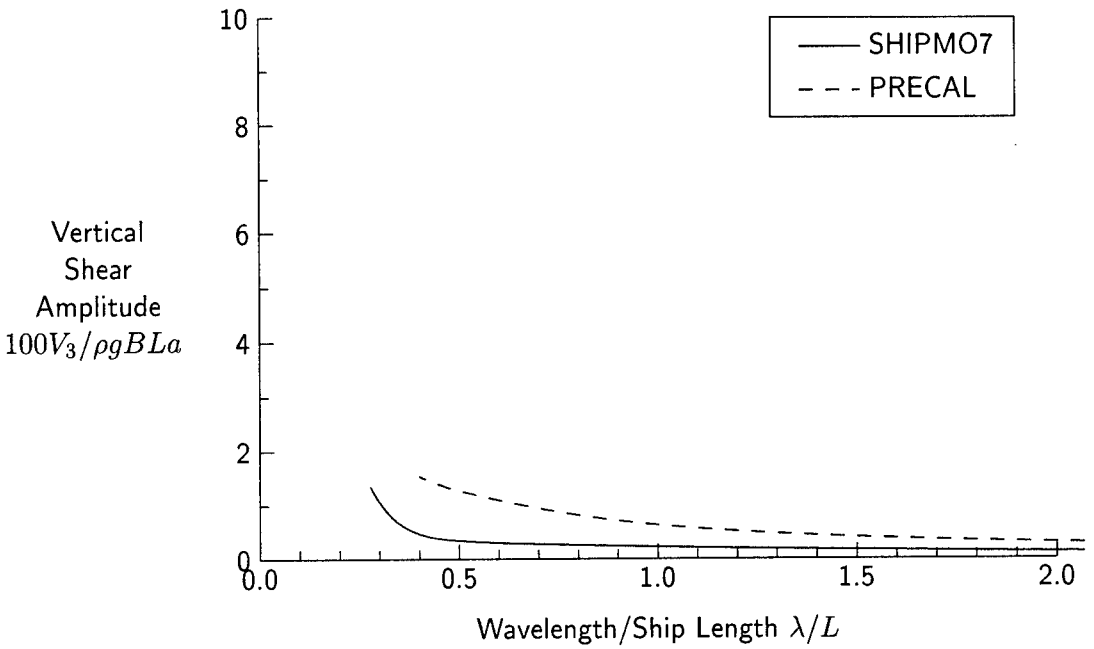

Figure 168: Vertical Shear Force at Station 5, $Fn = 0.29$, $\beta = 90$ degrees

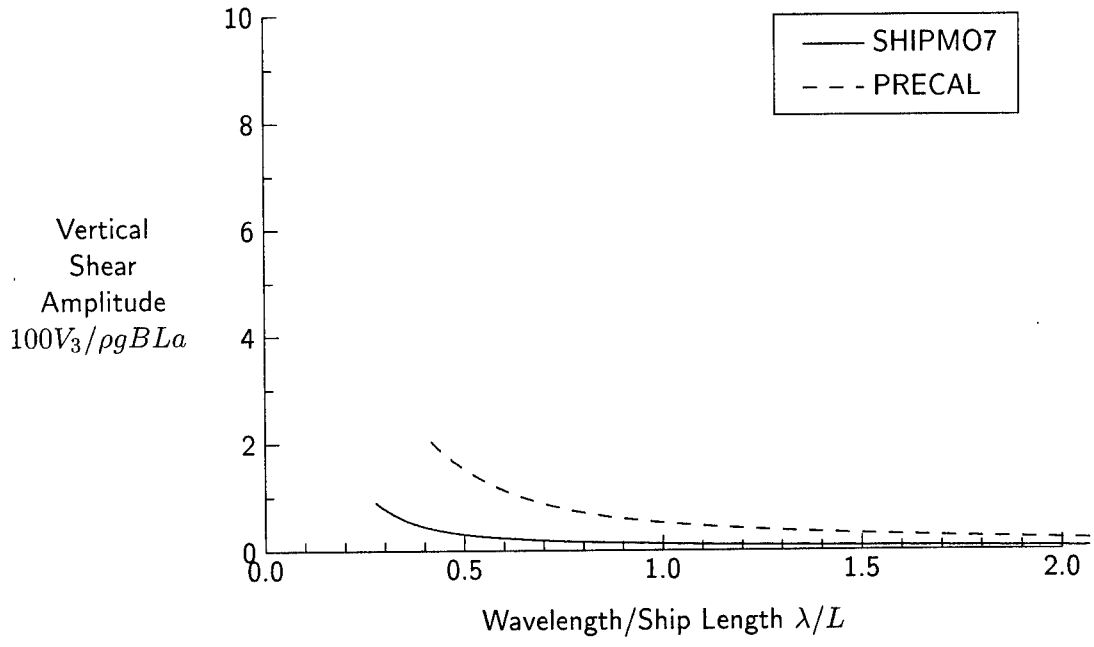

Figure 169: Vertical Shear Force at Station 10, $Fn = 0.29$, $\beta = 90$ degrees

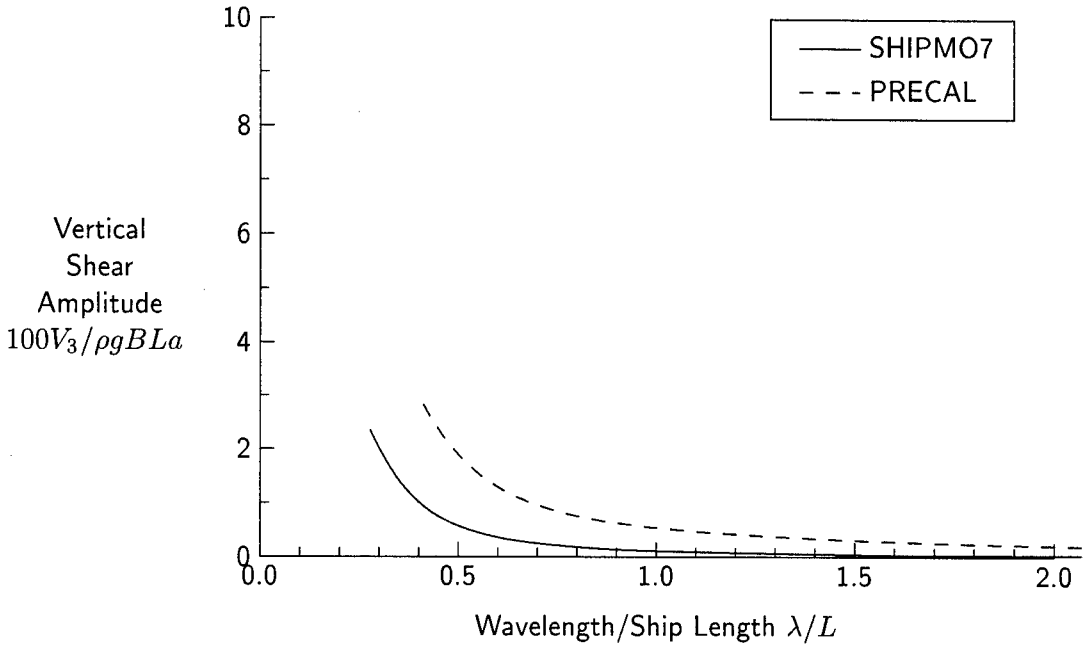

Figure 170: Vertical Shear Force at Station 13, $Fn = 0.29$, $\beta = 90$ degrees

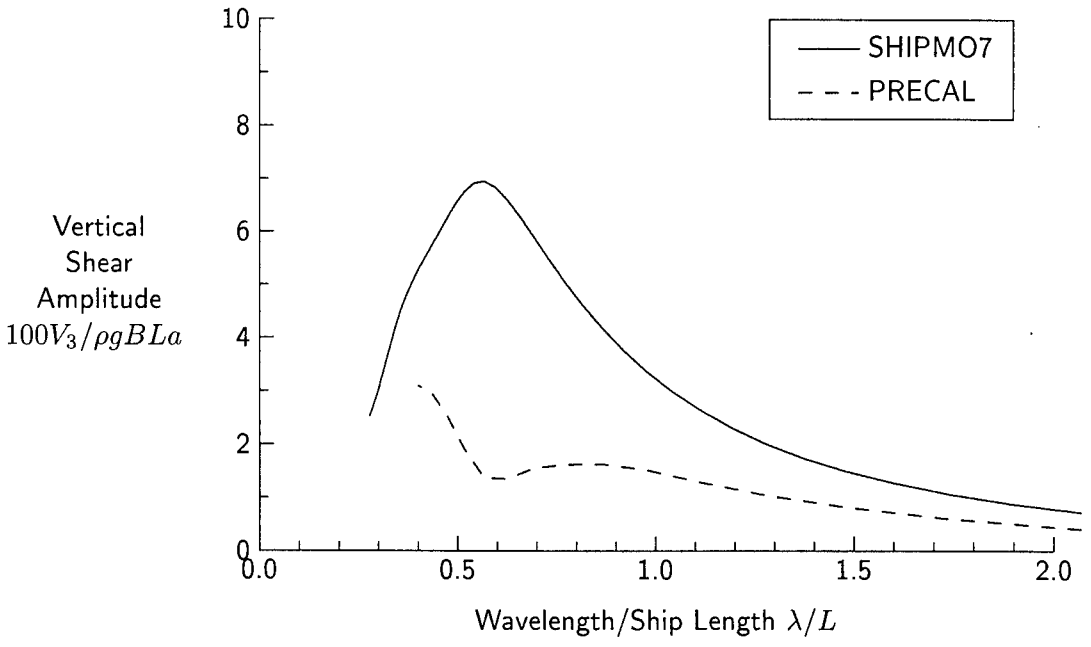

Figure 171: Vertical Shear Force at Station 5, $Fn = 0.29$, $\beta = 120$ degrees

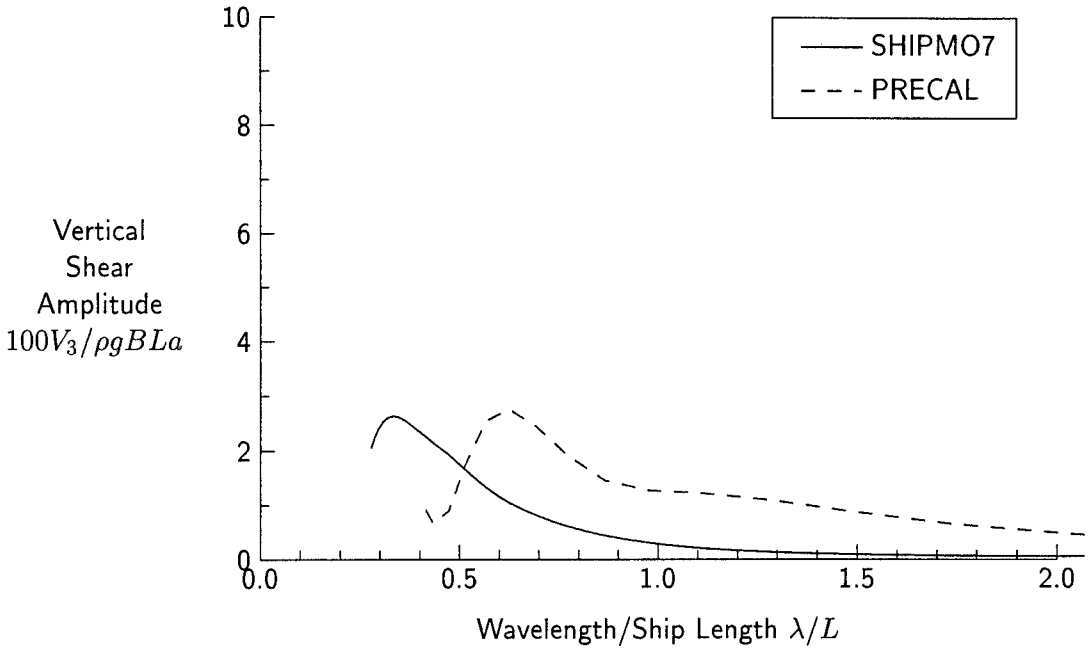

Figure 172: Vertical Shear Force at Station 10, $Fn = 0.29$, $\beta = 120$ degrees

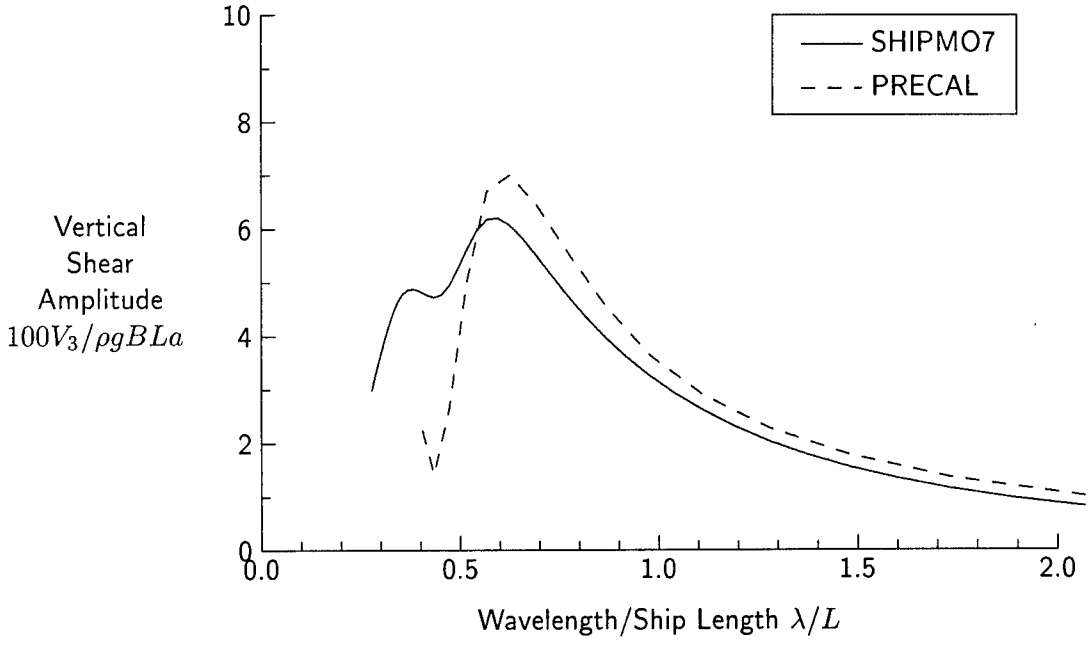

Figure 173: Vertical Shear Force at Station 13, $Fn = 0.29$, $\beta = 120$ degrees

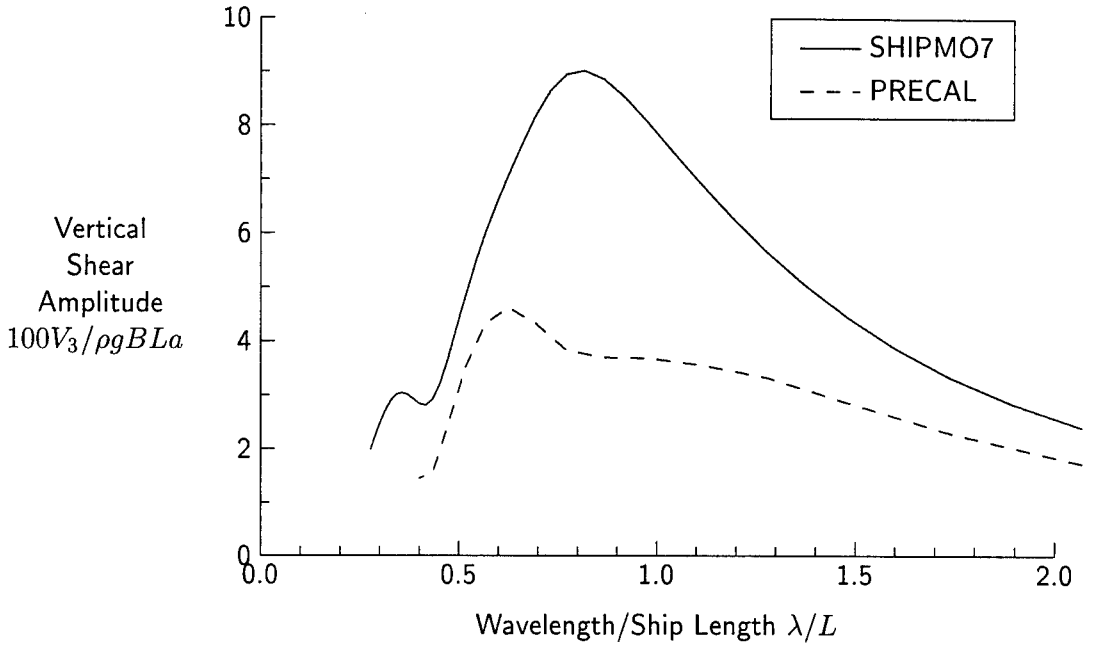

Figure 174: Vertical Shear Force at Station 5, $Fn = 0.29$, $\beta = 150$ degrees

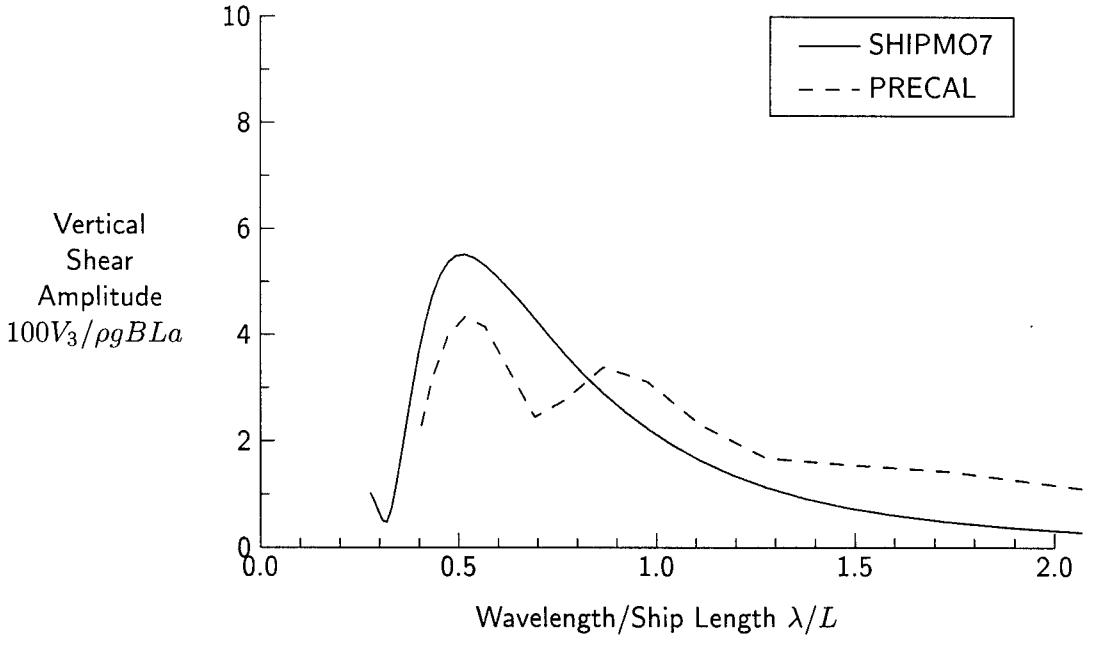

Figure 175: Vertical Shear Force at Station 10, $Fn = 0.29$, $\beta = 150$ degrees

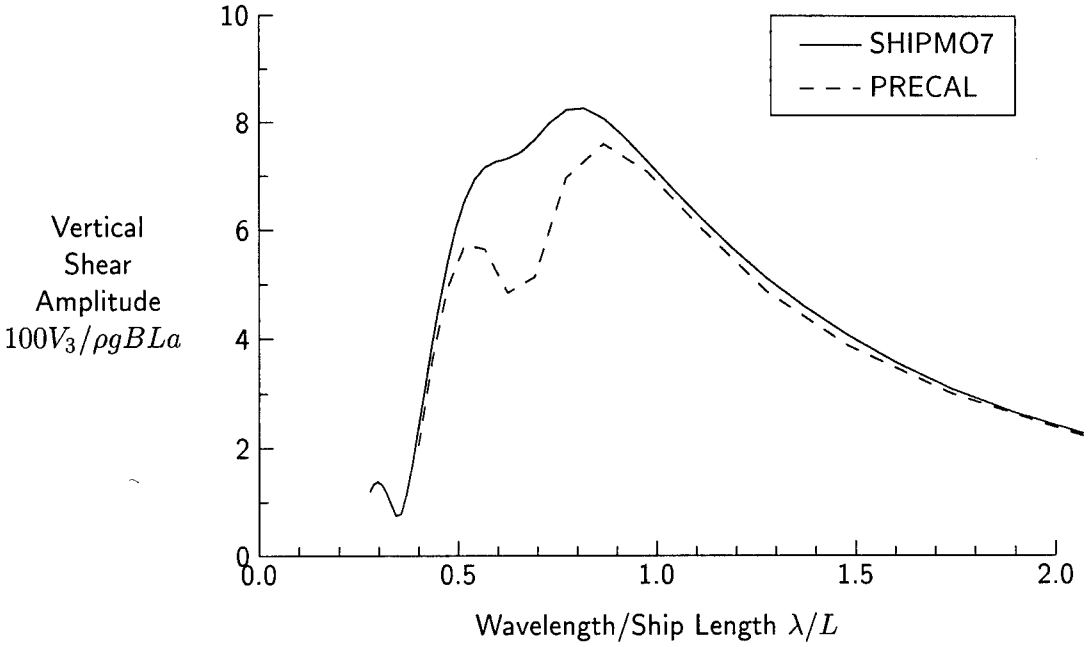

Figure 176: Vertical Shear Force at Station 13, $Fn = 0.29$, $\beta = 150$ degrees

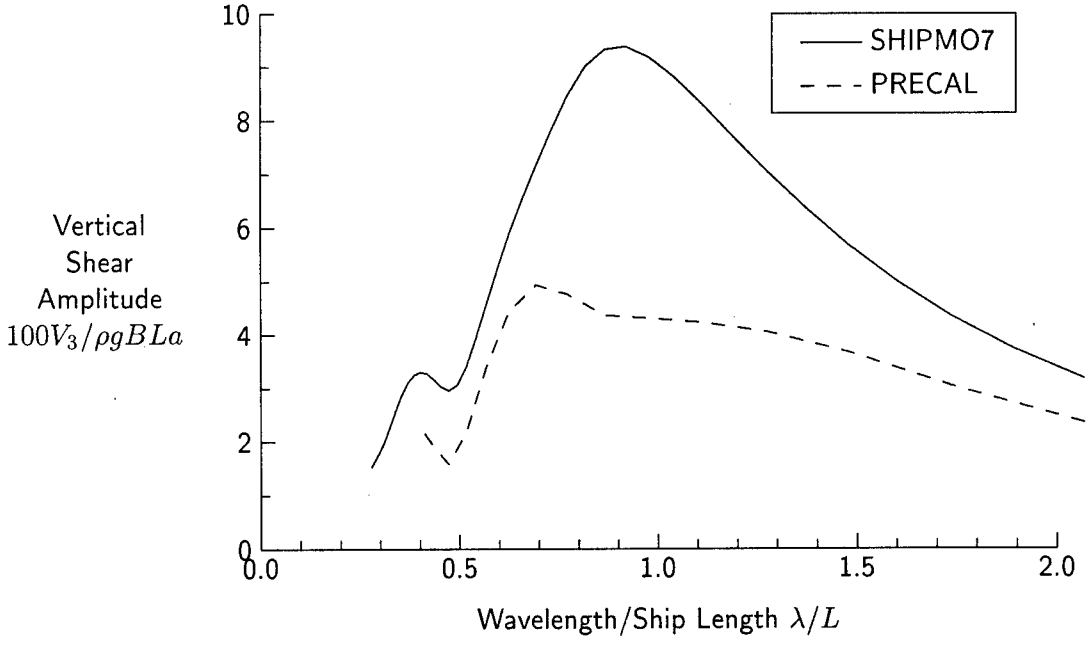

Figure 177: Vertical Shear Force at Station 5, $Fn = 0.29$, $\beta = 180$ degrees

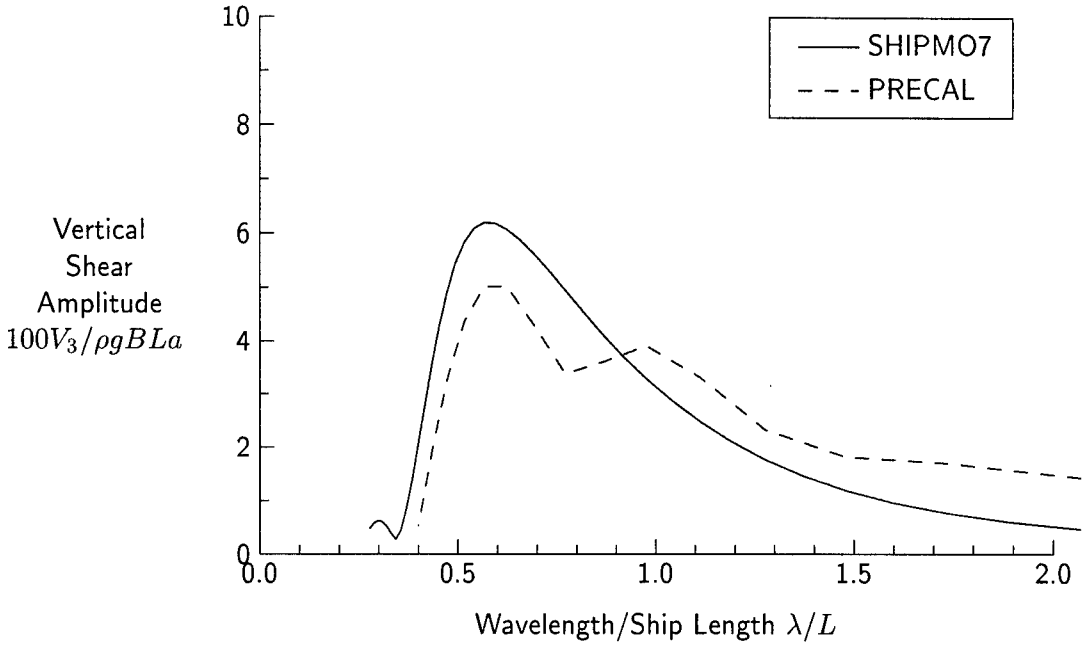

Figure 178: Vertical Shear Force at Station 10, $Fn = 0.29$, $\beta = 180$ degrees

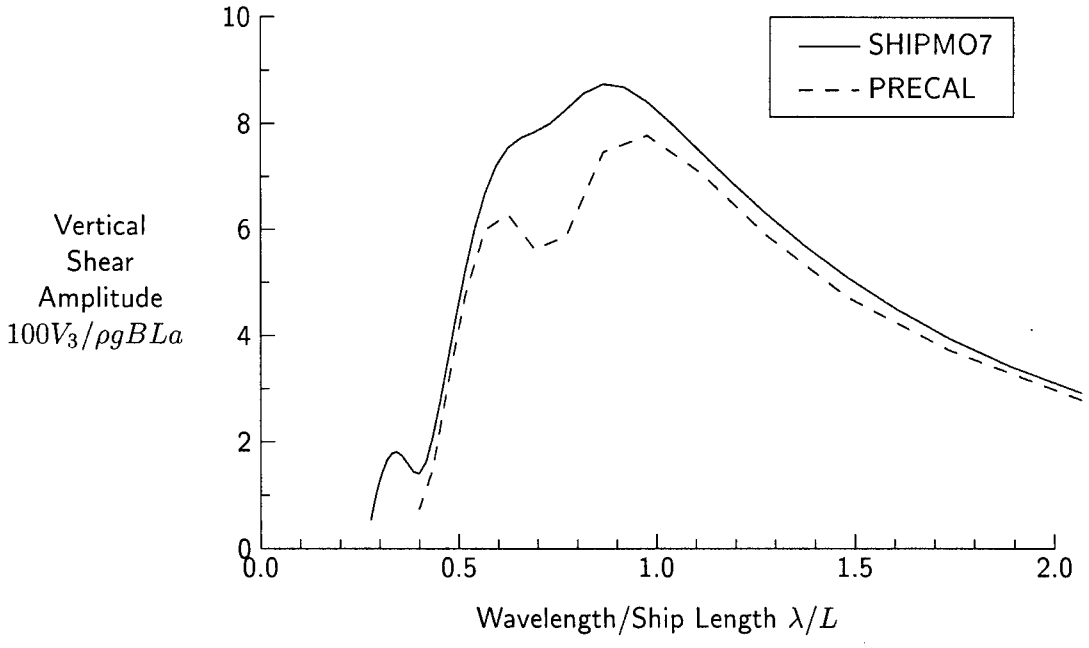

Figure 179: Vertical Shear Force at Station 13, $Fn = 0.29$, $\beta = 180$ degrees

References

[1] A.R.J.M. Lloyd, J.C. Brown, and J.F.W. Anslow, "Motions and Loads on Ship Models in Regular Oblique Waves," *Transactions, Royal Institution of Naval Architects* **122**, 21–43 (1980).

[2] A.R.J.M. Lloyd, J.C. Brown, and J.F.W. Anslow, *Wave Induced Motions and Loads on a Model Warship*, Royal Institution of Naval Architects, Occasional Publication No. 3, 1980.

[3] K.A. McTaggart, "SHIPMO7: An Updated Strip Theory Program for Predicting Ship Motions and Sea Loads in Waves," DREA Technical Memorandum 96/243, March 1997.

[4] S. Ando, "Wave Load Prediction for the SHIPMO Computer Program," DREA Technical Memorandum 82/L, October 1982.

[5] S. Ando, "Correlation of Wave Loads Predicted by the Extended SHIPMO Computer Program and Experiments," DREA Technical Memorandum 85/218, August 1985.

[6] N. Salvesen, E.O. Tuck, and O. Faltinsen, "Ship Motions and Sea Loads," *Transactions, Society of Naval Architects and Marine Engineers* **78**, 250–287 (1970).

[7] R.T. Schmitke, "Ship Sway, Roll, and Yaw Motions in Oblique Seas," *Transactions, Society of Naval Architects and Marine Engineers* **86**, 26–46 (1978).

[8] BMT SeaTech, "User's Manual for Motion, Load and Pressure Program Suite - PRECAL," Technical Report, prepared for NSMB CRS PRECAL Working Group, January 1995. Limited Distribution.

[9] J.M. Toring, Y.S. Shin, and H.H. Chen, "Theoretical Manual for Three-dimensional Hydrodynamic Pressure Calculation Program (PRECAL)," Technical Report RD-88025, American Bureau of Shipping, December 1988. Limited Distribution.

[10] D. Cooper and A.K. Brook, "Hydrodynamic Pressure Project Correlation between HPC-FEM and Experiment," Report W1815 (Parts 1 and 2), BMT, November 1988. Limited Distribution.

[11] S. Ando, "Experimental Validation of PRECAL - Part 1: Responses in Regular Head Waves," DREA Technical Memorandum 95/212, May 1995. Limited Distribution.

UNCLASSIFIED

SECURITY CLASSIFICATION OF FORM
(highest classification of Title, Abstract, Keywords)

DOCUMENT CONTROL DATA

(Security classification of title, body of abstract and indexing annotation must be entered when the overall document is classified)

1. ORIGINATOR (The name and address of the organization preparing the document. Organizations for whom the document was prepared, e.g. Establishment sponsoring a contractor's report, or tasking agency, are entered in section 8.)

Defence Research Establishment Atlantic
P.O. Box 1012, Dartmouth, N.S. B2Y 3Z7

2. SECURITY CLASSIFICATION (Overall security of the document including special warning terms if applicable.)

UNCLASSIFIED

3. TITLE (The complete document title as indicated on the title page. Its classification should be indicated by the appropriate abbreviation (S,C.R or U) in parentheses after the title.)

Validation of SHIPMO7 and PRECAL with a Warship Model

4. AUTHORS (Last name, first name, middle initial. If military, show rank, e.g. Doe, Maj. John E.)

CHOW, Dann L. and McTAGGART, Kevin A.

5. DATE OF PUBLICATION (Month and year of publication of document.)

November 1996

6a. NO. OF PAGES (Total containing information. Include Annexes, Appendices, etc.)

118

6b. NO. OF REFS. (Total cited in document.)

11

6. DESCRIPTIVE NOTES (The category of the document, e.g. technical report, technical note or memorandum. If appropriate, enter the type of report, e.g. interim, progress, summary, annual or final. Give the inclusive dates when a specific reporting period is covered.)

Technical Memorandum

8. SPONSORING ACTIVITY (The name of the department project office or laboratory sponsoring the reseach and development. include the address.)

Defence Research Establishment Atlantic
P.O. Box 1012, Dartmouth, N.S. B2Y 3Z7

9a. PROJECT OR GRANT NUMBER (If appropriate, the applicable research and development project or grant number under which the document was written. Please specify whether project or grant.)

1.g.b

9b. CONTRACT NUMBER (If appropriate, the applicable number under which the document was written.)

10a. ORIGINATOR'S DOCUMENT NUMBER (The official document number by which the document is identified by the originating activity. This number mrst be unique to this document.)

DREA Technical Memorandum 97/203

10b. OTHER DOCUMENT NUMBERS (Any other numbers which may be assigned this document either by the originator or by the sponsor.)

11. DOCUMENT AVAILABILITY (Any limitations on further dissemination of the document, other than those imposed by security classification)

(X) Unlimited distribution
( ) Distribution limited to defence departments and defence contractors; further distribution only as approved
( ) Distribution limited to defence departments and Canadian defence contractors; further distribution only as approved
( ) Distribution limited to government departments and agencies; futher distribution only as approved
( ) Distribution limited to defence departments; further distribution only as approved
( ) Other (please specify):

12. DOCUMENT ANNOUNCEMENT (Any limitation to the bibliographic annoucement of this document. This will normally correspond to the Document Availability (11). However, where futher distribution (beyond the audience specified in 11) is possible, a wider announcement audience may be selected.)

Unlimited

UNCLASSIFIED

SECURITY CLASSIFICATION OF FORM

DCD03 2/06/87

13. ABSTRACT (a brief and factual summary of the document. It may also appear elsewhere in the body of the document itself. It is highly desirable that the abstract of classified documents be unclassified. Each paragraph of the abstract shall begin with an indication of the security classification of the information in the paragraph (unless the document itself is unclassified) represented as (S), (C), (R), or (U). It is not necessary to include here abstracts in both official languages unless the text is bilingual).

This technical memorandum describes a validation study of SHIPMO7 and PRECAL, two frequency domain codes for predicting ship motions and sea loads in waves. SHIPMO7 is a strip theory code while PRECAL is a three-dimensional panel code. Results from the two codes are compared with non-proprietary experimental data for a warship model. In general, SHIPMO7 gives good agreement with motions and sea loads, while PRECAL is slightly inferior. The consistently better results for SHIPMO7 in the lateral plane are likely due to its careful treatment of appendage and viscous forces. Neglecting rudder autopilot motions does not appear to influence significantly predictions from either code. A proposed approximate method for predicting sectional gyradii leads to satisfactory predictions of torsional moment.

14. KEYWORDS, DESCRIPTORS or IDENTIFIERS (technically meaningful terms or short phrases that characterize a document and could be helpful in cataloguing the document. They should be selected so that no security classification is required. Identifiers, such as equipment model designation, trade name, military project code name, geographic location may also be included. If possible keywords should be selected from a published thesaurus. e.g. Thesaurus of Engineering and Scientific Terms (TEST) and that thesaurus-identified. If it not possible to select indexing terms which are Unclassified, the classification of each should be indicated as with the title).

seakeeping
ship motions
strip theory
panel methods
sea loads
heave
roll
pitch
yaw
shear
bending moment
torsion